# THÈSE POUR OBTENIR LE GRADE DE DOCTEUR DE L'UNIVERSITÉ DE MONTPELLIER

**En Biologie des Populations et Écologie**

**École doctorale GAIA**

**Unité de recherche ISEM (UMR 5554)**

# ECO-EVOLUTIONARY DYNAMICS IN ECOSYSTEMS UNDER STRESS


**Présentée par Sirine BOUCENNA**


**le 26 Septembre 2024**


**Sous la direction de Vasilis DAKOS**

**et Gaël RAOUL**


**Devant le jury composé de**

| | |
|---|---|
| Jean-Christophe Poggiale, PR, Aix-Marseille Université | Rapporteur |
| Thomas Lepoutre, CR, INRIA Lyon | Rapporteur |
| Ophélie Ronce, DR, CNRS ISEM | Examinatrice |
| Hélène Leman, CR, ENS Lyon | Examinatrice |
| Lionel Roques, DR, INRAE Avignon | Examinateur |
| Vasilis Dakos, CR, ISEM | Directeur de thèse |

UNIVERSITÉ DE MONTPELLIER

بِسْمِ اللَّهِ الرَّحْمَٰنِ الرَّحِيمِ

*À mes parents et ma mamie.*

# Acknowledgements

Nous y voilà, et à tous ceux qui me répetaient sans cesse au début de cette aventure : "3 ans ca passe vite !", eh bien vous aviez raison.
Je tiens tout d'abord à remercier vivement mes directeurs de thèse qui m'ont si bien encadrée, Vasilis et Gaël. Merci pour cette chance inouïe, pour votre bienveillance et votre écoute. Merci aussi pour vos précieux conseils, votre patience et surtout pour votre temps. Ce fut un honneur et un plaisir de travailler sous votre direction.
Je souhaite vivement remercier mes rapporteur; Jean-Christophe Poggiale et Thomas Lepoutre, ainsi que tous les membres de mon jury qui ont accepté d'accoder de leur temps et évaluer mon travail.
Aux membres de mon comité de suivi de thèse; Sepideh Mirahimmi, Nicolas Galtier, Luis-Miguel Chevin et Nicolas Loeuille, merci pour votre écoute et vos conseils.

Je remercie aussi les gens du CMAP et tous les chercheurs et doctorants que j'ai pu croiser, notamment Madeleine Kubasch, Josué Tchouanti, Ignacio Madrid, Ana Fernandez et tous les autres. Merci à Nicolas Loeuille, Ophélie Ronce, Sepideh Mirahimmi, Isabelle Chuine, Xavier Morin pour leurs précieux conseils et les discussions fructueuses. À tous ceux que j'ai rencontrés pendant les diverses conférences et principalement aux écoles d'Aussois où j'ai passé de merveilleux moments en joignant l'utile à l'agréable.

To my Montpellier people, Alejandro, thank you for your weird questions, for cantine time, for all the conversations and for your precious friendship. Berta *obbiously*, to our nights and our coffee breaks. Kikii, I will never get bored of you ! You guys made Montpellier feel like home <3. To brunch ISEM people, Jhelam, Vandana, Lila, Alba and Peter, it was such a pleasure meeting you guys ! Thank you for everything and I wish you all a great career.

À la best team BioDicee, Sonia et son sourire, Vince et ses blagues et discours philo, Claire et ses

récits et débats, Mathieu et ses belles photos et ses poissons, Maëlys et ses passions sportives, Ismaël, ses taquineries et son cholocolat UK, Guim, gracias por todo, Nathan, Hsiao, Lydie, Minya, Raphael, Alexis, merci à vous tous ! Un spécial merci à Bichon, pour tes relecture, nos sessions ciné, tes gâteaux et pour la piscine !! Je suis si ravie d'avoir passé cette année parmi vous. Merci pour votre accueil et votre bonne humeur.

Des milliers de mercis particuliers à mes amis. Jasmine, il faudrait tout un livre pour raconter tout ce qu'on a vécu. Merci pour les fou-rires qui ont egayé mes moments de doute et de stress. Ishak mon binome, merci pour ton humour et tes mots durs mais efficaces ! Love you guys. À ma tendre Mariem, si tu savais comme m'est chère. Merci pour tes conseils et pour les heures passées au télephone ! We made it dude. À ma chère Ines, merci d'être toujours là, à nos années de licence et celles à venir.

À mes petits frères, mes protégés, Simou mon confident et mon pilier, merci pour ces belles années à mes côtés, pour ton amour et ton soutien. Ramissou, my forever baby boy, merci d'être toi et d'être aussi unique. Vous avez grandi si vite !!!!
À mes parents qui ont toujours cru en moi et à qui je dois tout. Merci pour vos sacrifices, votre confiance, votre soutien inépuisable et votre amour inconditionnel.

Quelle aventure, certes dure mais passionante et indélébile. Et pour finir je souhaite vous dédier à tous ce poème :

*Hier encore je n'étais qu'une enfant,*
*âgée d'à peine six ou sept ans.*
*Quand la curiosité envahissait tous mes sens*
*et fleurissaient en moi des rêves teintés d'innocence.*
*Des rêves naissant d'impétueuses passions,*
*pour un univers fait de chiffres et d'équations.*
*Aspirant à faire des calculs pour toujours,*
*en ésperant un jour compter.*
*Cet âge où se mêlent naïve fragilité et infinies possibilités.*
*Et puis un jour on grandit et on perd le leurre,*

*contre cette réalité qui affleure.*

*Cette vérite qui nous rattrape et l'absurde qui nous frappe.*

*Dans cet exile on peine à garder le fil*

*qui nous relie à ces rêves d'enfance, quoiqu'elle fut brève.*

*Mais quand on songe à renoncer et que le doute nous ronge,*

*il suffit de se tourner vers ces êtres avec qui le rêve se prolonge.*

*Ces parents et amis qui consolent par leur seule présence.*

*Qui nous aiment et nous soutiennet avec véhémence.*

*Ceux qui ont embelli nos jours lugubres,*

*et ont éclairé nos chemins semés d'embûches.*

*À la vie et ses vicissitude je déclare ma gratitude.*

*Il y a dans le labeur une certaine saveur,*

*qui nous envahit en repensant à toutes ces heures.*

*Une saveur au goût de fierté et d'honneur*

*d'être devenue un jour docteure.*

*Chose qui ne s'accomplit que grâce aux directeurs,*

*qui misent sur nous et nous poussent vers l'excellence.*

*À jamais je leurs dois ma reconnaissance.*

*À ce pays qui m'a accueillie je dis merci.*

*À ma mère et ses prières qui m'ont permis d'être ici.*

*À son amour*

*qui me berce depuis toujours.*

*Je remercie mon cher père,*

*qui pour nous a remué ciel et terre.*

*À nos amis qui sont la famille que l'on choisit.*

*Qui nous ont connu sous toutes nos couleurs,*

*et ont partagé nos rires et nos pleurs.*

*C'est avec des gens autour que l'absurde s'écroule.*

*C'est votre présence qui donne à la vie tout son sens.*

*Et comme ont dit les anciens ... le meilleur pour la fin.*

*Et ce n'est guère sans chagrin*

*que je dédie tout ce que je suis à ma tendre mamie.*

*Ô hélas trop tôt partie ...*

*Dans mon coeur ou dans les plaines éternelles elle est immortelle.*

*Pour te décrire mon amour et le manque qui m'entoure,*

*Il n'y a pas sur terre assez d'encre.*

*Alors c'est ici que je jette l'ancre.*

*Hier encore je n'étais qu'une enfant,*

*et depuis chaque jour j'apprends,*

*en attendant ardemment ce précieux moment.*

*Sirine*

# Contents

**Abstract** i

**Résumé en francais** 4

**Introduction** 5

0.1 Context : The Threat of Global Change on Ecosystems . . . 5

0.1.1 A brief Overview of Population dynamics models : Eco without Evo . . . 7

0.2 Ecological Responses to Global Change . . . 9

0.2.1 Sudden Ecological Shifts in Response to Gradual Environmental Changes . . . 9

0.2.2 Ecological Responses to Sudden Environmental Changes . . . 13

0.3 Can Evolutionary Dynamics Save the Day? . . . 14

0.3.1 Understanding Evolution: A Fundamental Biological Process . . . 16

0.3.2 Adaptation to Environmental Changes in Lakes and Phenology . . . 18

0.4 Current Theories and Models in Evolutionary Dynamics . . . 20

0.4.1 Population Genetics Models : Evo without Eco . . . 20

0.4.2 Adaptive Dynamics : Eco-Evo . . . 21

0.4.3 Quantitative Genetics . . . 25

0.5 Chapters and Questions . . . 27

0.5.1 Chapter 1 : Evolutionary Outcomes Arising from Bistability in Ecosystem Dynamics . . . 28

0.5.2 Chapter 2 : Derivation of a macroscopic model in a tree population . . . 30

0.5.3 Chapter 3 : Modeling Phenotypic Structure and Plasticity in a Tree Population 31

**Bibliography** 33

**1 Chapter 1: Evolutionary outcomes arising from bistability in ecosystem dynamics** 45

1.1 Introduction . . . 2

1.2 Materials and methods . . . 6
1.2.1 Model description . . . 6
1.2.2 Co-evolution of Submerged and Floating macrophytes . . . 13
1.2.3 Numerical methods . . . 15
1.3 Results . . . 17
1.3.1 Ecological dynamics . . . 17
1.3.2 Evolutionary asymptotic analysis . . . 19
1.3.3 Co-evolution of submerged and floating macrophytes . . . 24
1.4 Discussion . . . 28
1.4.1 Evolution of the submerged macrophytes can lead to evolutionary branching, oscillations and evolutionary suicide . . . 29
1.4.2 Co-evolution of the floating macrophytes prevents evolutionary cycles and delays evolutionary suicide of submerged macrophytes . . . 31
1.4.3 Conclusion . . . 33
1.5 Data Availability . . . 33
1.6 Supplementary information . . . 34
1.6.1 SI A. Effect of nutrient diffusion on total nutrient concentration . . . 34
1.6.2 SI B. Bifurcation diagrams under different parameter conditions . . . 35
1.6.3 SI C. Steady states of the submerged macrophytes for very low nutrient diffusion rates . . . 36
1.6.4 SI D. Distribution of the submerged macrophytes population from the structured population model . . . 36
1.6.5 SI E. Comparison of the final mean traits from the structured population model with and without mutations . . . 37
1.6.6 SI F. An example of nutrient diffusion rate $u = 5.7$ : Only S evolution vs co-evolution . . . 38
1.6.7 SI G. An example of nutrient diffusion rate $u = 5.9$ : Only S evolution vs co-evolution . . . 39
1.6.8 SI H. An example of nutrient diffusion rate $u = 6.8$ at the beginning of the cycle region . . . 40
1.6.9 SI I. The example of nutrient diffusion rate $u = 6.8$ in case of co-evolution . . . 41
1.6.10 SI J. Bifurcation diagrams in $(z_s, z_f)$-plane for different nutrient diffusion rates 42

1.6.11 SI K. Distribution and fitness of the floating macrophytes population in case of evolution when $u = 7$ . . . 43

**Bibliography** **44**

**2 Chapter 2: Derivation of a Macroscopic Model in a Tree Population** **49**

2.1 Introduction . . . 2

2.2 Models, asymptotic limits and main results . . . 4

2.2.1 The annual structured model . . . 4

2.2.2 Asymptotic limit to the continuous structured model . . . 9

2.2.3 Derivation of the macroscopic model . . . 12

2.3 Proofs of the main results . . . 15

2.3.1 Preliminaries . . . 16

2.3.2 Proof of Theorem 2.1 - Existence and uniqueness of the solution of the annual structured model . . . 19

2.3.3 Proof of Theorem 2.2 - Existence and uniqueness of the solution of the continuous structured model . . . 21

2.3.4 Proof of Theorem 2.3 - asymptotic limit from the annual structured model to the continuous structured model . . . 25

2.4 Discussion . . . 28

2.5 Approximation of the population by a normal distribution . . . 30

2.6 Heuristic derivation of the macroscopic model (2.2.20)-(2.2.21) . . . 32

**3 Chapter 3: Modeling Phenotypic Structure and Plasticity under Climate Shifts in a Tree Population** **39**

3.1 Introduction . . . 2

3.2 Models and methods . . . 5

3.3 Numerical methods . . . 7

3.4 Results . . . 11

3.4.1 Initialisation : Evolution of number of seeds $X$ and dormancy temperature $Y$ before a climate change . . . 11

3.4.2 Evolution of number of seeds $X$ and dormancy temperature $Y$ with climate change : Temperature shift . . . 19

3.4.3 Evolution of number of seeds $X$ and dormancy temperature $Y$ with climate change : Precipitation shift . . . 23
3.4.4 Evolution of number of seeds $X$ and dormancy temperature $Y$ under climate change : Temperature increase and precipitation decrease . . . 27
3.5 Discussion . . . 30
3.6 Appendix . . . 35
3.6.1 Co-evolution of $X$ and $Y$ before and after a temperature shift with intrinsic mortality . . . 35

**Bibliography** **36**

**4 Discussion** **43**
4.1 Main Results . . . 43
4.1.1 Evolution is Double-Edged . . . 43
4.1.2 Impact of Co-evolution on Species Stability and Adaptation . . . 45
4.1.3 Making Sense of Mechanistic Eco-Evolutionary Models . . . 47
4.2 Limitations and Perspectives . . . 48
4.2.1 The Need for Empirical Validation . . . 48
4.2.2 Considering Adaptive Phenotypic Plasticity . . . 50
4.2.3 Including Stochasticity . . . 51
4.3 Conclusion . . . 52

**Bibliography** **54**

**French Synthesis** **57**

# Abstract

In the dawn of global change, many ecosystems are facing increasing threat due to environmental stressors. Ecosystems may respond abruptly to gradual environmental changes, leading to significant shifts in their structure and function, known as regime shifts. Alternatively, they can face sudden and severe environmental changes, which can have fatal consequences for many species. Evolutionary dynamics play a crucial role in determining how species respond to these challenges and shape ecosystem dynamics. Understanding the underlying evolutionary processes is crucial for predicting how ecosystems will respond to these challenges. Eco-evolutionary models provide a powerful framework for studying these dynamics, offering insights into how species adapt, evolve, and interact within their changing environments. In this thesis, we study eco-evolutionary dynamics using well established mathematical models and frameworks in ecosystems facing environmental stress. Specifically, we explore the evolutionary outcomes of competitive species in an ecosystem exhibiting ecological regime shifts. Moreover, we investigate the adaptive capacities of an ecosystem facing abrupt environmental shifts.

In chapter 1, we explore the impact of rapid trait evolution on ecosystem dynamics and stability in shallow lakes exhibiting alternative stable states. Using a competition model between floating and submerged macrophytes, and employing Adaptive Dynamics (AD) and Quantitative Genetics (QG) approaches, the results reveal complex evolutionary outcomes, including oscillations and evolutionary suicide, where the evolved trait lead to species extinction. This underscores the potential for evolution to destabilize ecosystems and leading species to extinction. However, the research also highlights the stabilizing role of co-evolution, showing that it can prevent oscillations and delay evolutionary suicide, thereby promoting temporary stability, illustrating the nuanced impact of evolutionary processes on ecosystem dynamics.

Chapter 2 introduces a mechanistic model describing the dynamics of dormancy and seed production in tree populations. The model accounts for sexual reproduction and environmental factors such as temperature and water availability. This chapter presents a simplification process that involves

deriving a macroscopic model from a detailed mechanistic one, using a typical QG result that under weak selection the trait distribution closely resembles a Gaussian centered around the mean traits of the population. The macroscopic model captures the essential dynamics of the system, revealing how trees may respond to abrupt environmental changes through the evolution of mean traits.

In chapter 3, we focus on the evolutionary dynamics of seed production and dormancy under climate change, using the macroscopic model derived in Chapter 2 and conducting numerical simulations. The primary questions addressed include the impact of environmental changes, particularly shifts in temperature and precipitation, on the evolutionary strategies of these traits. The study reveals that phenotypic plasticity in dormancy timing can hinder adaptation to temperature shifts, as it prevents reproduction. However, the results also emphasize the importance of the amplitude of precipitation shifts in driving adaptive responses. The co-evolution of seed production and dormancy is shown to enable adaptation to significant environmental shifts. This chapter underscores the complex interplay between temperature and precipitation shifts and highlights the necessity of considering co-evolution and phenotypic plasticity to understand and predict adaptive capacities.

# Résumé en français

À l'ère du changement global, de nombreux écosystèmes font face à une menace croissante due aux stress environnementaux. Les écosystèmes peuvent réagir brusquement aux changements environnementaux graduels, entraînant des modifications significatives de leur structure et de leur fonction, connues sous le nom de changements de régime. Alternativement, ils peuvent être confrontés à des changements environnementaux soudains et sévères, ayant des conséquences fatales pour de nombreuses espèces. Les dynamiques évolutives jouent un rôle crucial dans la façon dont les espèces répondent à ces défis et façonnent la dynamique des écosystèmes. Comprendre les processus évolutifs sous-jacents est essentiel pour prédire comment les écosystèmes réagiront à ces défis. Les modèles éco-évolutifs fournissent un cadre puissant pour étudier ces dynamiques, offrant des perspectives sur la manière dont les espèces s'adaptent, évoluent et interagissent au sein de leurs environnements changeants. Dans cette thèse, nous étudions les dynamiques éco-évolutives à l'aide de modèles mathématiques et de cadres bien établis dans des écosystèmes confrontés au stress environnemental. Plus précisément, nous explorons les résultats évolutifs des espèces en compétition dans un écosystème présentant des changements de régime écologiques. De plus, nous étudions les capacités adaptatives d'un écosystème face à des changements environnementaux brusques.

Dans le chapitre 1, nous explorons l'impact de l'évolution rapide des traits sur la dynamique et la stabilité des écosystèmes dans les lacs peu profonds présentant des états stables alternatifs. En utilisant un modèle de compétition entre macrophytes flottants et submergés, et en utilisant des approches de Dynamique Adaptative (AD) et de Génétique Quantitative (QG), les résultats révèlent des résultats évolutifs complexes, y compris des oscillations et un suicide évolutif, où le trait évolué conduit à l'extinction des espèces. Cela souligne le potentiel de l'évolution pour déstabiliser les écosystèmes et conduire à l'extinction des espèces. Cependant, la recherche met également en lumière le rôle stabilisateur de la co-évolution, montrant qu'elle peut prévenir les oscillations et retarder le suicide évolutif, favorisant ainsi une stabilité temporaire, illustrant l'impact nuancé des processus évolutifs sur la dynamique des écosystèmes.

Le chapitre 2 introduit un modèle mécaniste décrivant la dynamique de la dormance et de la production de graines dans les populations d'arbres. Le modèle tient compte de la reproduction sexuée et de facteurs environnementaux tels que la température et la disponibilité en eau. Ce chapitre présente un processus de simplification qui implique la dérivation d'un modèle macroscopique à partir d'un modèle mécaniste détaillé, en utilisant un résultat typique de la Génétique Quantitative selon lequel, sous une sélection faible, la distribution des traits ressemble étroitement à une gaussienne centrée autour des traits moyens de la population. Le modèle macroscopique capture les dynamiques essentielles du système, révélant comment les arbres peuvent répondre aux changements environnementaux brusques par l'évolution des traits moyens.

Dans le chapitre 3, nous nous concentrons sur les dynamiques évolutives de la production de graines et de la dormance face au changement climatique, en utilisant le modèle macroscopique dérivé dans le chapitre 2 et en réalisant des simulations numériques. Les questions principales abordées incluent l'impact des changements environnementaux, en particulier les variations de température et de précipitations, sur les stratégies évolutives de ces traits. L'étude révèle que la plasticité phénotypique dans le timing de la dormance peut entraver l'adaptation aux changements de température, car elle empêche la reproduction. Cependant, les résultats soulignent également l'importance de l'amplitude des variations de précipitations dans la stimulation des réponses adaptatives. La co-évolution de la production de graines et de la dormance est montrée comme permettant une adaptation aux changements environnementaux significatifs. Ce chapitre met en évidence l'interaction complexe entre les changements de température et de précipitations, et souligne la nécessité de considérer la co-évolution et la plasticité phénotypique pour comprendre et prédire les capacités adaptatives.

# Introduction

## 0.1 Context : The Threat of Global Change on Ecosystems

It is now widely recognized, though not universally accepted, that global change is a reality. For decades, many indicators and scientific research have underscored the evidence of global change. Early measurements of atmospheric CO2 concentrations, such as those establishing the Keeling Curve, provided unequivocal evidence of rising CO2 levels attributable to human activities (Keeling 1960). Further documentation includes the accelerating ice loss from Greenland and Antarctica, which has significantly contributed to global sea level rise (Rignot et al. 2011). Analyses of global surface temperatures also demonstrate a consistent warming trend over the past century (Hansen et al. 2010). Numerous studies have highlighted the potential threats to biodiversity and ecosystems. For instance, a study provides globally coherent evidence of climate change impacts across various natural systems, linking observed changes directly to global warming (Parmesan and Yohe 2003).

These studies emphasize the urgent need for awareness and action to address these changes. While not all environmental factors are equally predictable, the fact remains that these changes are occurring at alarming rates (Comiso et al. 2008; Velicogna 2009; J. Liu and Curry 2010). For instance, various studies have documented the consistent rise in global temperatures (Vinnikov et al. 1999; D. W. Thompson and Wallace 2001; Brohan et al. 2006) and the increasing frequency and severity of droughts (Chiang, Mazdiyasni, and AghaKouchak 2021; Trenberth et al. 2014; Dai 2011).

Environmental changes are not only confined to natural and climate-related phenomena. Human activities play a significant role in altering environmental conditions (Nelson et al. 2006). One clear consequence of the Anthropocene is pollution, which exacerbates the already precarious state of ecosystems (Eriksen et al. 2014; Steffen, Broadgate, et al. 2015; Steffen, Crutzen, McNeill, et al. 2007). For instance, a study investigates the spatiotemporal variations in nitrogen and phosphorus levels in a large man-made lake, and explores their relationships with human activities. The findings highlight

the significant impact of human activities on nutrient enrichment and water eutrophication in the lake (Zhou et al. 2020).

The alterations in environmental conditions due to global change carry significant consequences. There is concerning evidence that the impacts of global change on ecosystems, species, and biodiversity are severe. Numerous studies have highlighted the global decline in biodiversity, pointing to the alarming rates of species extinction and population decline (Rosenberg et al. 2019; Stork 1997; Sala and Knowlton 2006; Malcolm and Markham 2000). Beyond the threat of extinction, global change also leads to alterations in ecological behavior (Steffen, Crutzen, McNeill, et al. 2007; Rockström et al. 2009) and the reorganization of species interactions and system structures (Marten Scheffer 2020; Solé and Bascompte 2012). Increased environmental stress often results in more frequent migrations and invasions, changes in species dominance, and shifts in certain species activities.

Moreover, examples that will be central in this work, are related to the fact that rising temperatures can lead to earlier flowering times in plants, disrupting the timing of interactions with pollinators (Raju 2018). Or also to how temperature shifts hasten the evolution of seed dormancy in tree populations,and lead to an impact on dormancy (Y. Liu et al. 2017; Cheddadi et al. 2016). Similarly, changes in precipitation patterns can affect the availability of water resources, impacting plant growth and survival (Zeppel, Wilks, and Lewis 2014; Miranda et al. 2009).

The complex interplay of these factors shows the importance of understanding the impacts of global change on ecosystems and biodiversity. By studying the dynamics of species and their interactions in response to changing environmental conditions, we can develop strategies to promote the conservation of biodiversity. This thesis aims to contribute to this understanding by exploring the evolutionary dynamics within populations under varying environmental conditions, providing insights into the adaptive capacities and potential responses of these species to global change.

In light of the aforementioned global changes and their impacts on ecosystems and ecological dynamics, it is crucial to comprehend the various mechanisms that dictate and characterize ecological responses to environmental factors. This endeavor carries significant importance, as it enables the anticipation or prediction of ecological outcomes within ecosystems, thereby facilitating better preparedness to address the consequences of such changes, or ideally, to prevent them altogether. A deeper under-

standing of these underlying mechanisms can also enhance decision-making in ecological management.

One of the most effective tools available for this purpose is mathematical modeling. Throughout history, humans have employed mathematical language to capture phenomena observed and deduced from the natural world. This approach serves to explain and validate hypotheses, establish connections between variables, and ultimately predict outcomes within a structured framework grounded in rationality and logic. By leveraging mathematical models, we can systematically analyze complex ecological systems, offering insights that are critical for both immediate and long-term ecological management and conservation strategies.

### 0.1.1 A brief Overview of Population dynamics models : Eco without Evo

In this introduction, I will provide a selective historical overview of some important models in population dynamics. These models aim to describe temporal variations in species populations within specific ecosystems under certain assumptions that govern these variations. Our focus will be on deterministic continuous-time models, particularly ordinary and partial differential equations, as these are the types of models employed in this thesis. Additionally, deterministic population dynamics models, described by differential equations, are appropriate when population sizes are large enough to avoid the risk of accidental extinction (Wissel and Stöcker 1991; Bürger 2000).

One of the earliest models in population dynamics was proposed by Malthus in 1798 (Malthus 1798), known as the Malthusian growth model. This model describes exponential population growth based on the principle that populations grow at a rate proportional to their size, expressed by the differential equation

$$\frac{dN}{dt} = rN$$

where $N$ represents the population size and $r$ is the intrinsic growth rate. Several decades later, another scientist (Verhulst 1838) refined this model by introducing the concept of carrying capacity, which limits population growth. This modification led to the logistic growth model, defined by the equation

$$\frac{dN}{dt} = rN\left(1 - \frac{N}{K}\right) \tag{0.1.1}$$

where $K$ denotes the carrying capacity.

These models describe the dynamics of a single population. In 1926, two researchers, Lotka and Volterra (Lotka 1925; Volterra 1927), expanded this approach by incorporating interactions between two different species, specifically in a predator-prey context. This led to the development of the renowned Lotka-Volterra model, formulated as a system of differential equations to capture the dynamics between predators and their prey.

Later, in 1945, P.H. Leslie (Leslie 1945) introduced a model that used matrix methods to describe age-structured population dynamics. This approach provided a more detailed understanding of how different age groups within a population contribute to overall population changes. This model paved the way for structured population models in general. For instance, stage-strcutured models extend the age-structured approach to include other characteristics such as size or developmental stage. Moreover, the Lotka-Volterra equations were also extended to include phenotypic variation among individuals. I will discuss more in details this type of models in the evolutionary models section.

A crucial concept in differential equations is stability. Under certain assumptions, systems tend to evolve towards an equilibrium point, when the population does not experience a net growth, satisfying the condition

$$\frac{dN}{dt} = 0$$

This equilibrium can be either stable, meaning that the population converges back to it after a small perturbation, or unstable, if it goes away from it. If $N' = F(N)$, the stability condition relies on derivative of $F$ at the equilibrium value of $N$. For instance, in the logistic growth model 0.1.1, we know that the system has two different equilibria; $N = 0$ which is unstable because $F'(0) > 0$, and $N = K$ which is stable because $F'(K) < 0$. This indicate that in the logistic growth model, the population will eventually stabilize at the carrying capacity $K$ even if it is perturbed. The zero population size is an unstable equilibrium, meaning any small positive population will grow away from this point.

This concept is fundamental in mathematical modeling as it allows for the prediction of long-term behavior of systems and their outcomes following perturbations. Dynamical system models have significantly enhanced our understanding of population trajectories and the impact of various hypotheses and parameters (Pielou 1981), allowing better ecological predictions that can inform ecosystem

management and conservation (Fer et al. 2021; J. S. Clark et al. 2001; Bodner et al. 2021). Moreover, these theoretical tools have been validated and gained credibility through various experimental work (Mayer and Butler 1993; Tedeschi 2006).

In our context, these models have also been applied to study the effects of environmental changes on ecological dynamics. For instance, (Ives 1995) showed that competitive interactions may increase the detrimental effects of environmental changes on species population size. A more recent work (Rinnan 2018) explores the impacts of climate change on ecosystems through mathematical modeling. It focuses on how shifts in climate alter species interactions and population dynamics, affecting biodiversity and ecosystem stability. The study emphasizes the importance of understanding these dynamics to predict and mitigate ecological consequences of climate change.

There are several ways to model environmental variations, including gradual and abrupt changes, generally referred to as press and pulse perturbations. Fig.0.1.1 illustrates different types of environmental perturbations with real-world examples.

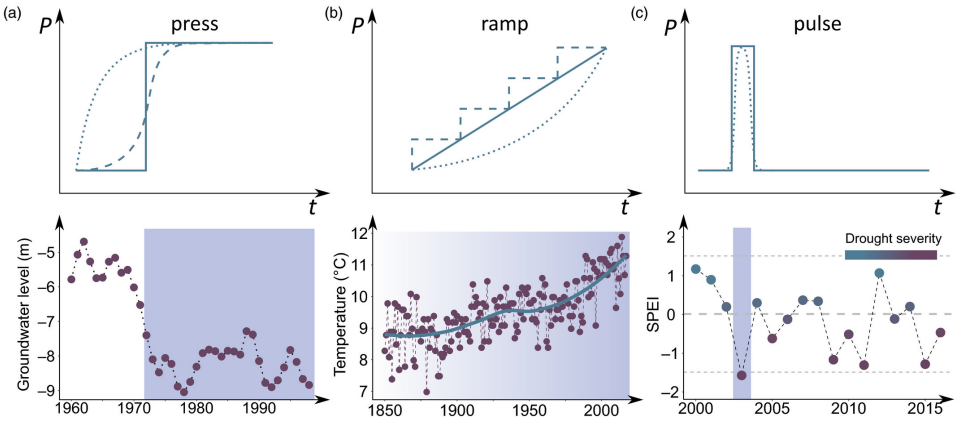



Figure 0.1.1: Different types of perturbations that change system parameters (P) over time (t), that is, press, ramp and pulse perturbations (top row), with real-world examples from Belgium (bottom row) (Van Meerbeek, Jucker, and Svenning 2021).

## 0.2 Ecological Responses to Global Change

### 0.2.1 Sudden Ecological Shifts in Response to Gradual Environmental Changes

Population models have been extensively used since their introduction in the field of ecology. They allowed to study ecosystems dynamics including state transitions, known as regime shifts, in response to environmental parameters. These regime shifts can be gradual and are usually described using

simple deterministic equations, such as the logistic equation. But these equations can also include other interactions, such as positive feedbacks described through non-linear terms, which alter the linear growth rates and from which emerges the concept of multiple equilibria (Villa Martín et al. 2015). A notable example of this is when exactly two stable equilibria exist, a phenomenon known as bistability. Positive feedbacks are the key ingredient of multistability, and possibly so-called abrupt shifts (or critical/catastrophic transitions).

Research by (Holling 1973a; May 1977a) has demonstrated that under specific conditions, an ecosystem can abruptly transition from one stable state to another alternative stable state in response to gradual (press) environmental changes. This transition occurs when an external input exceeds a certain threshold, causing the ecosystem to shift to a different stable state. This critical threshold, known as a tipping point, mathematically corresponds to a bifurcation point. Studies by (Erbach, Lutscher, and Seo 2013; Russo and Spiliotis 2016) have shown that most tipping points manifest as pitchfork, subcritical Hopf, or saddle-node (fold) bifurcations.
Conversely, when the environmental stressor is reduced or reversed, the ecosystem does not immediately return to its original state. Instead, it remains in the alternative stable state until the stressor reaches another tipping point, which is typically further from the initial one. These insights are crucial in understanding ecosystem dynamics, as they highlight the potential for significant and seemingly chaotic ecological transitions resulting from small, gradual changes in environmental factors. Importantly, these findings emphasize the potential irreversibility of such transitions (Marten Scheffer and Stephen R Carpenter 2003a; Suding and Hobbs 2009).
The reversibility of these transitions largely depends on the distance between the two different tipping points, a measure known as hysteresis (Holling 1973a) and represents the difference between the degradation and restoration trajectories. This concept allows to quantifying the resilience of an ecosystem (ecosystem's ability to absorb changes and disturbances without shifting to an alternative stable state) and underscores the importance of understanding and predicting critical thresholds to manage and preserve ecological stability.

Well known examples of regime shifts include freshwater eutrophication, wherein lakes transition from a clear water state to a turbid water state, resulting in decreased fishing productivity and the occurrence of toxic algal blooms (Marten Scheffer, Hosper, et al. 1993; Stephen R Carpenter and Kinne 2003). Another famous example is dryland degradation, where dry forests and savannas

transform into deserts and bare soils, reducing ecosystem services such as agricultural production and water cycling (Geist and Lambin 2004). Additionally, a speculative regime shift is the melting of the Greenland ice sheet, where the frequency and intensity of warm events may shift the ice sheet from a permanent to an occasional state (Greene et al. 2008). Early developments in understanding regime shifts were initially criticized for a lack of empirical evidence; however, by the early 2000s, sufficient evidence had accumulated from systems such as coral reefs and lakes, confirming the existence of regime shifts (Marten Scheffer and Stephen R Carpenter 2003a; Marten Scheffer, S. Carpenter, et al. 2001a; Folke et al. 2004a).

An example of bistable ecosystems studied in the first part of this thesis is shallow lakes, where eutrophication can trigger a transition from a clear water state (illustrated in Fig. 0.2.1), characterized by dominance of submerged vegetation, to a turbid water state, dominated by phytoplankton (Marten Scheffer, Hosper, et al. 1993; Marten Scheffer, Szabo, et al. 2003a; Ibelings et al. 2007). The regime shift in this case results from the following positive feedback : The presence of vegetation stabilizes the clear water state by reducing nutrient availability and enhancing sediment stability, whereas the absence of vegetation promotes a turbid state through increased nutrient cycling and sediment resuspension. When nutrient concentration exceeds a threshold, microalgea growth explodes creating algal blooms. These reduce light penetration to the bottom of the lake, which reduces the ability of submerged plants to grow and this in turn diminishes the vegetation. This feedback is illustrated in Fig. 0.2.1. The primary driver for eutrophication is typically the accumulation of nutrients such as nitrogen and phosphorus (Stephen R Carpenter and Kinne 2003; Stephen R Carpenter, Ludwig, and Brock 1999), although climate change alone has also been reported as a potential cause (Winder 2012).

The abruptness of regime shifts in shallow lakes is not only hypothetical. An observed regime shift occurred in the Veluwe lake (The Netherlands) in the 1960s from a clear state with extensive cover of charophytes to a turbid state in response to increasing nutrient loads Fig. 0.2.2. The state of the lake showed a clear abrupt sudden shift to an alternative state in response to the increased nutrient loading (Van Meerbeek, Jucker, and Svenning 2021).

Regime shifts can greatly affect the provision of ecosystem services (Stephen R Carpenter, Mooney, et al. 2009) and they present a significant challenge for ecological management due to their unpredictability (Hastings and Wysham 2010) and difficult reversibility (Suding and Hobbs 2009; Søndergaard et al. 2007). There is thus an urgent need of understanding the underlying mechanisms and patterns of causation of this phenomena.

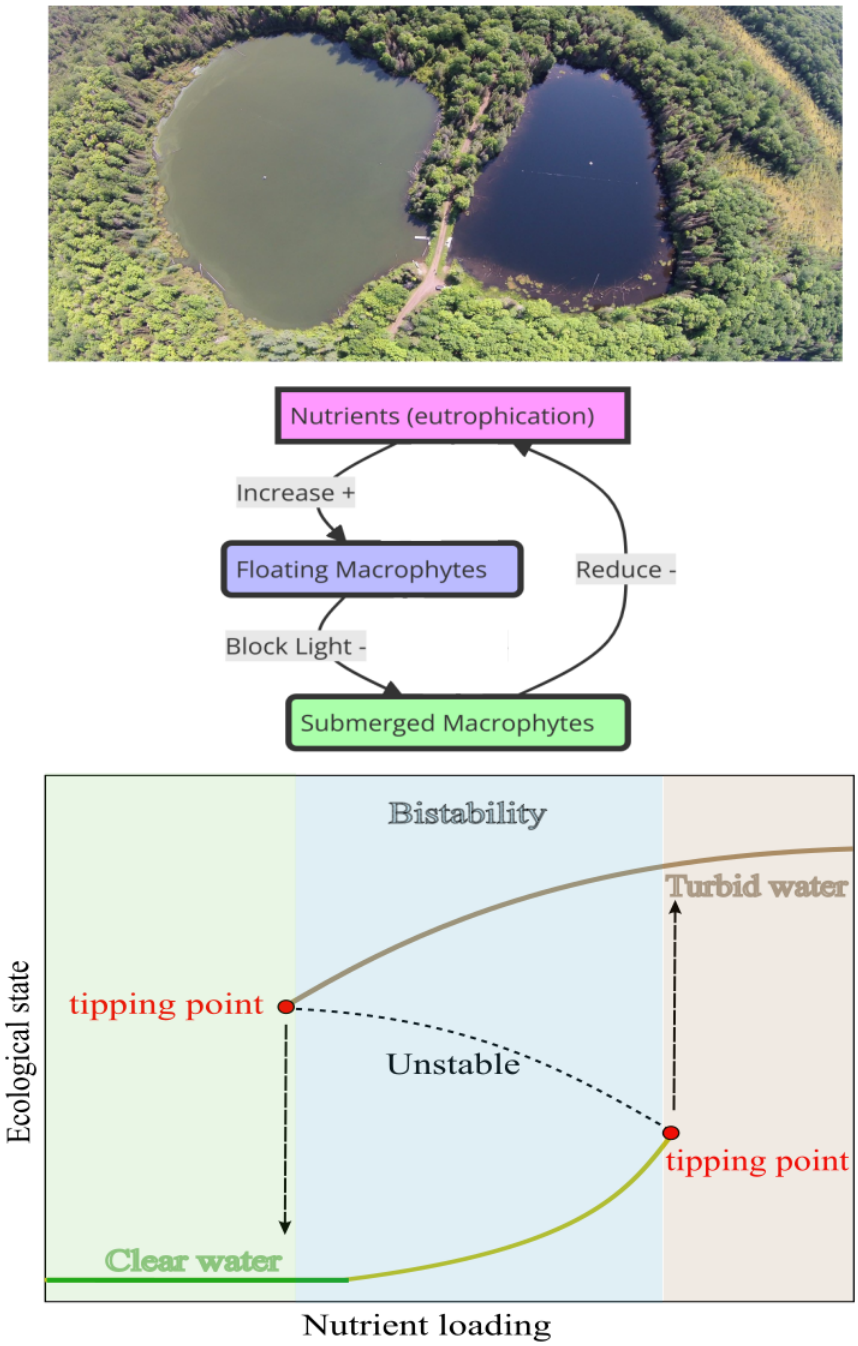



Figure 0.2.1: a) Side by side example of (alternative) stable states in shallow lakes. An example of two lakes where one has transitioned to a turbid, cyanobacteria dominated state while the other remains in a clear-water state. Photo by Dr. Stephen R. Carpenter.
b) Illustration of the positive feedback loop resulting in bistability in shallow lakes.
c) Bifurcation diagram : Starting from lower branch : the ecosystem is in a clear water stable state, where solid lines potentially represent the free floating plants biomass, until the nutrient input reaches a first tipping point (right) where it shifts to the alternative stable state of turbid water state. When the nutrient loading decreases, the system remains in the turbid state, until reaching the second tipping point (left), where it switches back to the original state. In the blue range area, ecosystem can be found in either of the two alternative stable states (bistability).

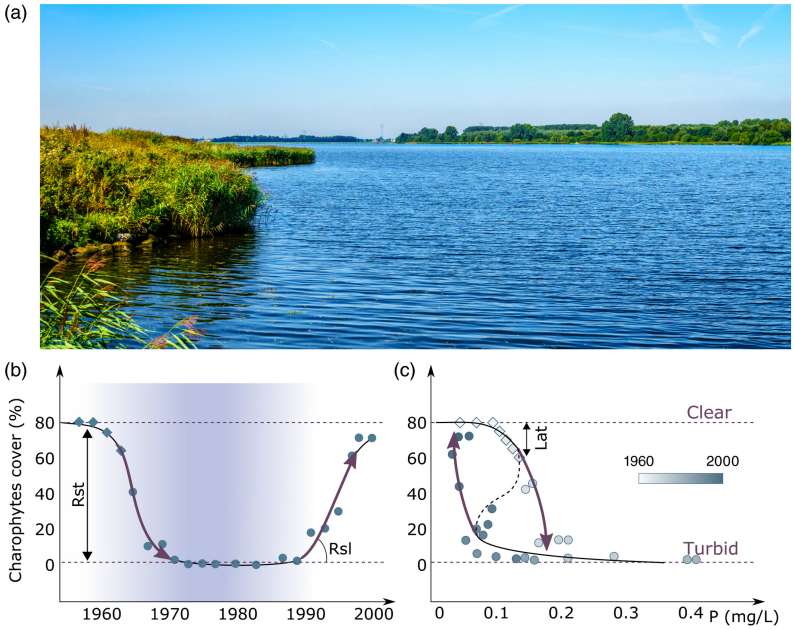



Figure 0.2.2: (a) The Veluwe lake in the Netherlands, created in 1957 as a result of land reclamation (Picture: Harry Beugelink). (b) A regime shift occurred in the Veluwe lake (The Netherlands) in the 1960s from a clear state with extensive cover of charophytes to a turbid state in response to increasing nutrient loads. Recovery occurred in the 1990s after reducing nutrient input and biomanipulation. (c) The state of the lake shows a sudden dramatic shift to an alternative state in response to the increased nutrient load. The resilience of the lake system showed hysteresis (Van Meerbeek, Jucker, and Svenning 2021).

### 0.2.2 Ecological Responses to Sudden Environmental Changes

Sudden (pulse) environmental perturbations are short-term, intense disturbances that can have significant impacts on ecosystems. For example, hurricanes are a type of pulse perturbation that can dramatically alter coastal ecosystems. The immediate impact includes physical destruction of habitats, such as mangroves and coral reefs, but the aftermath can lead to changes in species composition and nutrient cycling as the ecosystem recovers (Patrick et al. 2020). Another example is wildfire, which acts as a pulse perturbation in forest and grassland ecosystems. Wildfires can rapidly change the landscape by removing vegetation, altering soil properties, and releasing large amounts of carbon into the atmosphere. The ecological effects of wildfires include shifts in species dominance, with fire-adapted species often gaining an advantage in the post-disturbance environment (Brown and J. K. Smith 2000). Additionally, volcanic eruptions represent another form of pulse perturbation, where the sudden deposition of ash and lava can devastate local flora and fauna. However, these areas often become sites of rapid ecological succession, leading to the establishment of new ecological communities over time (Dale et al. 2005).

Sudden environmental shifts can also profoundly impact phenology, another important notion studied

in this work, which is the study of cyclic and seasonal natural phenomena, especially in relation to climate and plant and animal life. These shifts can alter the timing of key phenological events, such as flowering, fruiting, and migration. For instance, an increase in temperature might cause plants to flower earlier than usual, potentially leading to mismatches with the availability of pollinators. This can result in reduced pollination success and subsequent declines in plant reproductive output, ultimately affecting plant populations and the species that rely on them (Dalpasso et al. 2023).

Similarly, sudden changes in precipitation patterns can affect the timing of seed germination and growth in plants, disrupting established ecological relationships. For example, a shift to earlier or later germination times can lead to competition mismatches among plant species, altering community composition and potentially leading to shifts in species distributions. This has been observed in various ecosystems where precipitation changes significantly impact plant life cycles (Li et al. 2023).

Furthermore, phenological shifts can have various negative effects throughout ecosystems. For instance, changes in the phenology of one species can affect the timing and behavior of other species that interact with it, leading to broader ecological impacts. A study reveled that phenological shifts can disrupt the synchrony between plants and their pollinators, leading to altered seasonal structures of pollinator assemblages (Duchenne et al. 2020). An illustration of potential scenarios of plant phenology responses to environmental change in presented in Fig. 0.2.3.

In the second part of this thesis, the focus is on studying the impacts of temperature and precipitation shifts on the phenology of tree populations. Given their long lifespans, often spanning several decades to centuries, trees may perceive environmental changes that seem gradual on a human timescale as abrupt. For instance, a rapid shift in climate patterns, such as an increase in average temperatures or changes in precipitation over a few decades, can be perceived by trees as an abrupt change. This perceived abruptness can induce significant stress on tree populations, potentially leading to shifts in species composition and forest structure, as some tree species may be unable to adapt rapidly to the new conditions (Stanke et al. 2021).

## 0.3 Can Evolutionary Dynamics Save the Day?

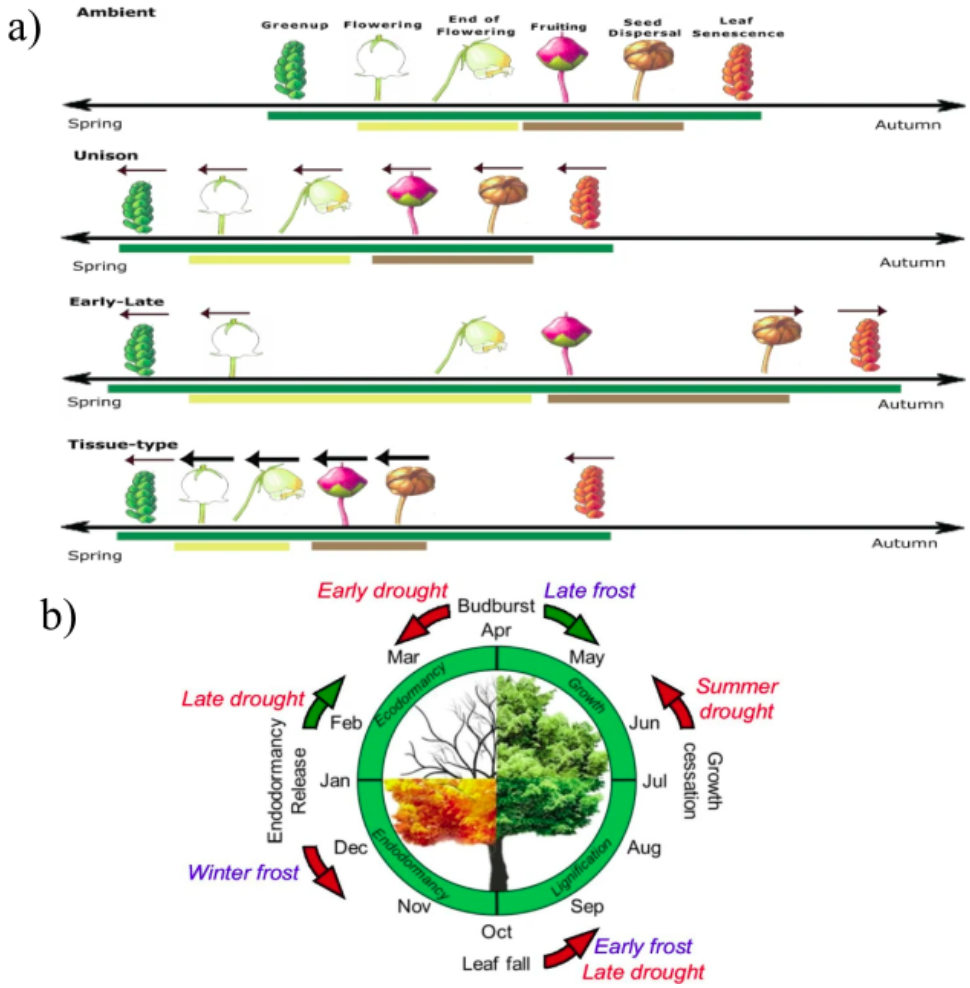



Figure 0.2.3: a) Potential scenarios of plant phenology responses to warming: The arrows above images show the direction and magnitude (arrow thickness) of changes in timing for each phenophase in response to warming. Green, yellow, and brown horizontal bars reflect the length (duration) of the growth, flowering, and fruiting periods, respectively. Ambient signifies no warming (C. G. Collins et al. 2021).
b) Hastening (brown arrow) or delaying (green arrow) phenological stages in response to drought and frost events. At the center is presented the typical seasonal phenological stages in a deciduous tree in the Northern Hemisphere and outside the potential effects of drought and frost stress depending on their timing (Charrier et al. 2021).

### 0.3.1 Understanding Evolution: A Fundamental Biological Process

We have highlighted the increasing risk that many ecosystems face due to global changes and the urgent need to understand the mechanisms behind this environmental impact. However, if we limit our approach to merely using ecological modeling and observations of interactions and dynamics of ecosystems only, we find ourselves in a worthwhile but ultimately insufficient endeavor. This is because, first, these changes and their consequences are occurring at an accelerating pace, and they will not slow down until we figure out how they are happening or how to stop them. Second, despite the relentless work and effort of the scientific community and the myriad of answers and potential solutions they suggest, there remains a significant challenge in influencing and convincing decision-makers to implement these actions, especially when their personal interests are at stake. But nature has a potentially powerful yet often neglected ally: Evolution.

But one might first wonder, what is evolution? According to Charles Darwin, the founding father of evolutionary theory, evolution is the process by which species of organisms change over time through the mechanism of natural selection. Darwin stated, "Natural selection acts only by taking advantage of slight successive variations; she can never take a great and sudden leap, but must advance by short and sure, though slow steps" (Darwin 1859). This provides a foundational understanding, but given the rapid and significant environmental changes we mentioned earlier, this gradual process may seem inadequate.

Fortunately, our understanding of evolution has advanced significantly since 1859. Today, we recognize that natural selection acts on phenotypic variation, causing adaptive evolutionary changes. Such phenotypic variation often arises from mutational processes that generate heritable genetic variation. Contrasting with Darwin's traditional view of evolution as a slow and gradual process occurring over long geological time scales, we now understand that rapid evolution is also possible. Rapid evolution refers to significant evolutionary changes occurring over relatively short periods, often observable within a few generations, driven by intense selective pressures.

One of the earliest and most well-documented examples of rapid evolution is the case of the peppered moth. During the Industrial Revolution in England, the prevalence of dark-colored moths increased dramatically due to pollution darkening tree bark and providing a camouflage advantage against predators. This shift occurred over just a few generations, illustrating how environmental pressures can drive rapid evolutionary change (Kettlewell 1955; Cook and Saccheri 2013). Moreover, a study

highlights that *Spartina densiflora*'s ability to adapt to changing abiotic conditions, such as increasing salinity and temperatures driven by global climate change, underscores its potential for rapid evolution and successful invasion in new environments (Bora, Thomaz, and Padial 2020).

Although many species have the potential to adapt rapidly, this is not always the case. For instance, this study demonstrates that the rates of genetic evolution in flowering plants are positively correlated with species numbers, providing insights relationship between evolutionary rates and species diversity in plants (Barraclough and Savolainen 2001). Another paper reveals that limited genetic diversity and asexual patterns imply a slow rate of genetic evolution in the studied species (Ahrens and James 2015).

An important mechanism of adaptation, which occurs at the phenotypic scale rather than the genetic scale and can sometimes be mistaken for rapid evolution, is phenotypic plasticity. Phenotypic plasticity is a concept with broad significance as it integrates various aspects of biology, including genetics, development, ecology, and evolution, and extends to physics, physiology, and behavioral science. Phenotypic plasticity is commonly defined as "the environmentally sensitive production of alternative phenotypes by given genotypes" (Stearns 1989). This definition allows considerable flexibility in determining which traits exhibit plasticity, as the term "phenotype" can be interpreted in diverse ways. The risk of a too broad definition is that all biological processes are influenced by the environment to some extent, potentially putting everything within the domain of plasticity. Consequently, it is recommended that researchers draw the line where they see fit while remaining open to insights from those who delineate differently (Dercole and Sergio Rinaldi 2008).
Although the concept of phenotypic plasticity was for long controverted and neglected, there is today a great amount of evidence that is undeniable. For instance, in response to low-quality, fibrous food, one species of grasshopper develops larger mandibles and mandibular muscles (D. B. Thompson 1992), while another species develops a larger gut (Yang and Joern 1994). Additionally, a different grasshopper species adjusts the number of chemosensilla on its antennae based on the variety of plant chemicals it encounters (Chapman and Lee 1991).

Another aspect of evolution that will be central to the results of this thesis is co-evolution. The co-evolution of different species and traits plays a crucial role in maintaining the stability and functionality of ecosystems. Co-evolution involves reciprocal evolutionary changes between interacting species, leading to highly specialized relationships and mutual adaptations. This process is fundamental to

the structure of ecological communities, influencing species diversity, resilience, and the provision of ecosystem services. For example, the relationship between pollinators and flowering plants exemplifies co-evolution, with specific traits in flowers and pollinators evolving in response to each other, thereby enhancing pollination efficiency and plant reproduction (John N. Thompson 1994). Similarly, the evolutionary arms race between predators and prey, where adaptations in predators' hunting strategies and prey's defensive mechanisms drive each other's evolution, contributes to the dynamic balance of ecosystems (Brodie III and Brodie Jr 2014). Furthermore, mutualistic relationships, such as those between mycorrhizal fungi and plant roots, underscore the importance of co-evolution in nutrient exchange and plant growth, which are essential for the productivity of terrestrial ecosystems (S. E. Smith and Read 2003). Therefore, co-evolution not only fosters biodiversity but also underpins ecosystem stability and resilience amidst environmental changes.

This modern understanding of evolution as both a gradual and potentially rapid process provides a more comprehensive framework for addressing the challenges posed by environmental changes. Evolution provides a dynamic framework through which species and ecosystems can adapt to changing conditions. The evolutionary dynamics are crucial as they offer a complementary approach to traditional ecological models methods. Integrating evolutionary with ecological modeling could enhance our understanding of ecosystem responses to global change and improve our predictive capacities, potentially enabling the protection of our planet's biodiversity.

### 0.3.2 Adaptation to Environmental Changes in Lakes and Phenology

Now that we have introduced evolution into our framework and highlighted the importance of incorporating this dimension in the study of ecosystems, I will further justify this need by providing substantial examples and evidence of species adaptation to changing environments. These adaptations can occur through genetic changes, phenotypic plasticity, and behavioral modifications.

In the case of aquatic plants in lakes, their evolution is influenced by a variety of environmental factors, such as water depth, nutrient availability, light penetration, and competition with other species. Macrophytes may develop adaptations to specific conditions in their environment, such as evolving different leaf structures, root systems, or reproductive strategies to better survive in their particular habitat (Castellani et al. 2023; Tóth et al. 2017).

A seed bank, defined as the reserve of viable seeds embedded within the sediment of aquatic environments, is instrumental in the evolutionary dynamics of macrophytes' growth depths in shallow lakes (McFarland and Rogers 1998). This seed bank functions as a genetic repository, significantly influencing the population dynamics, genetic diversity, and adaptive capacity of macrophyte species. It enables these species to thrive across various depth conditions over time. Since the rate of evolution is generally proportional to the genetic variance within a population, seed banks have the potential to facilitate rapid evolutionary changes in aquatic species, thereby enhancing their ability to swiftly adapt to changing environmental conditions. For instance, studies has demonstrated that seed banks in crayfish-invaded lakes exhibit limited potential for macrophyte recovery, characterized by reduced seed quantity and diversity compared to those in non invaded lakes (Baldridge and Lodge 2014).

An important example of phenotypic plasticity, which will be further developed in this work, is plant phenology—the study of the timing of periodic biological events such as flowering, seed dormancy, and leaf-out. Traits related to phenology are highly plastic, meaning the timing of these events can vary depending on environmental factors. This plasticity is particularly crucial in the context of climate change, where shifts in temperature and precipitation patterns can significantly impact the timing of biological events. Species with high phenotypic plasticity are more likely to cope with and adapt to these changes, potentially conferring a survival advantage in rapidly changing ecosystems (Cleland et al. 2007; Peñuelas, Rutishauser, and Filella 2009).

Tree phenology also provides clear examples of adaptation. A European beech has exhibited shifts in the timing of leaf-out in response to rising temperatures (Menzel, Sparks, Estrella, Elvira Koch, et al. 2006). Similarly, the Japanese cherry tree (Prunus serrulata) is known for its sensitivity to temperature changes, with historical data showing that the timing of cherry blossom flowering in Japan has advanced significantly due to warmer spring temperatures, aligning reproductive phases with favorable conditions (Aono and Kazui 2008). Trees like Norway spruce and silver birch have shown flexibility in the timing of bud dormancy and bud break in response to temperature fluctuations, breaking dormancy earlier in warmer winters and springs (Heide 2003). In arid and semi-arid regions, trees such as mesquite and certain eucalyptus species exhibit drought-induced dormancy, conserving resources during water stress periods to survive prolonged dry conditions (Huxman et al. 2004). As climate change intensifies droughts, these adaptive responses are vital for tree survival and ecosystem stability.

However, despite these positive adaptations, evolution can be double-edged. Evolutionary rescue occurs when populations at risk of extinction due to environmental stressors adapt rapidly through genetic changes, ensuring their survival and continued evolution (Bell 2017). Conversely, evolution to extinction can occur when short-term advantageous traits become detrimental over time, leading to population collapse. This phenomenon is called evolutionary suicide (Ferriere 2000), but it is also called Darwinian extinction (Webb 2003a), and evolution to extinction (Dieckmann, Marrow, and Law 1995).

Thus, understanding both evolutionary rescue and evolutionary suicide is essential for developing effective conservation strategies. By recognizing the conditions that lead to either adaptation and survival or extinction, we can better predict and manage the impacts of environmental changes on biodiversity. Eco-evolutionary models provide a helpful tool to this aim. These models integrate ecological and evolutionary processes, providing a comprehensive framework to simulate and analyze the interactions between populations and their different responses to changing environments.

## 0.4 Current Theories and Models in Evolutionary Dynamics

### 0.4.1 Population Genetics Models : Evo without Eco

Since the emergence of the theory of evolution, mathematical models have flourished with the aim of understanding the mechanisms of evolutionary processes such as natural selection, genetic drift, mutations, and gene flow. These models also aim to predict the outcomes of evolutionary changes over time and to test hypotheses in a controlled and systematic manner. Here, I provide a brief overview of some foundational evolutionary models.

The journey began in 1931 with the famous Wright-Fisher model (Wright 1931; Ronald Aylmer Fisher 1930), which describes genetic drift and changes in allele frequencies within a finite population. This model was independently developed by Sewall Wright and Ronald Fisher. The previous year, Fisher had developed Fisher's fundamental theorem of natural selection (1930) (Ronald Aylmer Fisher 1930), which states that the rate of increase in fitness of any organism at any time is equal to its genetic variance in fitness at that time. In 1932, J.B.S. Haldane introduced a model of selection that describes how selection acts on alleles (Haldane 1932). In 1958, Patrick Moran introduced a model of genetic drift in a finite population, which, unlike Fisher's model, assumes overlapping generations

and constant population size (Moran 1958).

Population genetic models are used to predict how genetic changes occur within a population over time in different situations. These models simplify the dynamics by focusing on a small number of major genetic alleles, such as coding for eye color (Bürger 2020), instead of considering all alleles at once. Classical population genetics studies changes in genotypic distribution over short demographic timescales but doesn't consider ecological dynamics. However, if the genotype-phenotype map is known, it is possible to link demography to evolutionary dynamics (Crow 2017).
Using a stochastic demographic model, we can describe how birth, death, and migration processes change population abundances, with phenotypic variability arising from random genetic mutations and recombinations. This approach leads to the well-known individual-based models, where each individual is represented by its genotype. These models are at the forefront of modern population genetics, offering a detailed and realistic framework for describing demography and evolutionary change.

Due to the complexity of genetics and the need for simpler mathematical models, researchers have developed alternative approaches. One such method considers phenotypes controlled by many genes with small effects.

### 0.4.2 Adaptive Dynamics : Eco-Evo

A landmark paper by (Champagnat, Ferrière, and Méléard 2006) used a birth-death stochastic individual-based model for asexually reproducing populations and accounted for various biological phenomena driving individual life, such as natural selection, non-local interactions including competition for resources, and non-faithful gene transmissions involving mutations. The authors proved that, in the limit of large populations, their renormalized stochastic process converges to a deterministic partial differential equation (PDE) describing the dynamics of trait distribution. A generic example of such a PDE is:

$$\partial_t n(t,z) = \mathcal{B}[n](t,z) - \mathcal{D}[n](t,z)$$

where $\mathcal{B}[n]$ (resp. $\mathcal{D}[n]$) represents a birth (resp. death) term of individuals with continuous trait $z \in \mathbf{R}^d$ at time $t > 0$, which can also depend non-locally on the whole trait distribution $n$.

Moreover, in the same study, authors (Champagnat, Ferrière, and Méléard 2006) obtained another mathematical limit when simultaneously taking large population and rare mutation limits: a jump process model. This model reflects the heuristic that the occurrence of mutations is so rare that after a mutation appears and the number of mutant reaches a certain threshold, the ecological dynamics of the resident and the variant with the mutation are deterministic and reach a steady state before another mutation occurs. This trait substitution process, modeled by the so-called canonical equation, is a fundamental object of adaptive dynamics. I will detail this framework as it has been used in the first chapter of my thesis.

Adaptive dynamics, an approach developed by (Dieckmann and Law 1996a; Metz and S. A. H. Nisbet a. G. 1996; Geritz et al. 1997), finds its origins in evolutionary game theory where the concept of an evolutionarily stable strategy was introduced by (G. R. Price 1973; J. M. Smith 1974). This approach simplifies genetic details by using a time scale separation argument, which justifies the use of asexual demographic models. In adaptive dynamics, the competition between resident and mutant populations is explicitly described by a resident-mutant model. This model, an ODE system, details the population densities of resident and mutant populations for any given trait value, incorporating frequency and density-dependent effects.

The notion of a fitness landscape is central to this framework. The long-term evolutionary dynamics of a continuous trait $x$ can be visualized as an ascent on a fitness landscape $s(x)$, where peaks on the landscape represent optimal trait combinations with high fitness, while valleys represent low fitness (Wright 1931; Dieckmann and Law 1996a). This suggests a simplified view where the evolutionary rate of change $\dot{x}$ is determined by the fitness gradient $\frac{\partial s}{\partial x}$

The evolutionary dynamics described by this equation suggest a continuous increase in fitness, potentially reaching a local maximum on the fitness landscape.

In the adaptive dynamics framework, mutations occur randomly, and evolutionary changes are represented as a sequence of trait substitutions, depicted as random walks in trait space. For continuous traits, these random walks align with the trajectories of an ODE system in a well chosen asymptotics involving rare mutations, large population and small mutation effects. The selection gradient is crucial, and (Dieckmann and Law 1996a) called their ordinary differential equation (ODE) the canonical equation of adaptive dynamics. This equation describes the evolutionary trajectory of a

continuous trait under the influence of mutation and selection :

$$\dot{x} = \nu(x)\frac{\sigma^2}{2}n(x)\frac{\partial s}{\partial x}$$

where $\nu(x)$ is the probability that a birth from an individual with trait $x$ gives rise to a mutation, $\sigma^2$ denotes the variance of the distribution of a mutant and $n(x)$ is the equilibrium population size (Champagnat, Ferričre, and Ben Arous4 2002).

An evolutionary equilibrium (or singular point) is defined as a constant solution of the canonical equation, i.e., a trait $\bar{x}$ at which the selection gradient vanishes:

$$\frac{\partial}{\partial y}s(\bar{x}, y)\Big|_{y=\bar{x}} = 0,$$

where $s(x, y$ is the fitness function defined as the long term population growth rate of a mutant population with trait $y$ under the conditions set by the resident population with trait $x$. Then if

$$\frac{\partial^2}{\partial y^2}s(\bar{x}, y)\Big|_{y=\bar{x}} < 0 \tag{0.4.1}$$

the evolutionary equilibrium is protected against invasion and therefore correspond to a so-called *evolutionary stable strategy* (ESS). This corresponds to a steady-state for Adaptive Dynamics.
Then $\bar{x}$ is called *Convergence Stable Strategy*, meaning that successful invaders would be closer to $\bar{x}$, if

$$\frac{\partial^2}{\partial x^2}s(x, y)\Big|_{y=x=\bar{x}} > \frac{\partial^2}{\partial y^2}s(\bar{x}, y)\Big|_{y=\bar{x}} \tag{0.4.2}$$

This corresponds to a local attractor for Adaptive Dynamics. If the opposite inequality holds, then $\bar{x}$ is a repellor.
If $\bar{x}$ is both Convergent Stable and ESS, then it is called a CSS (*Continuously Stable Strategy).*
We note that the Adaptive Dynamics canonical equations can lead to a branching point, which is a critical point in the trait space where a single evolutionary lineage can split into two distinct lineages. This phenomenon occurs when disruptive selection favors the divergence of traits. At this branching point, new variants can invade and coexist with previously established traits. This occurs when a singular point is Convergent stable (inequality 0.4.2 holds) but not ESS (inequality 0.4.1 doesn't hold).
When studying the evolutionary dynamics of one-dimensional strategies in Adaptive Dynamics

framewok, a pairwise invasibility plot (Matsuda 1985; Van Tienderen and De Jong 1986) is a valuable graphical tool. These plots illustrate the invasion fitness based on resident and mutant strategies. Dark gray regions in the plots usually signify combinations of resident and mutant traits where mutants can successfully invade (positive invasion fitness. Conversely, light gray regions indicate combinations where invasion fitness is negative, suggesting deleterious mutants. One possible evolutionary outcome is evolutionary suicide, where evolution can (with small mutations) take the strategy of the population sufficiently close to the extinction boundary, that a mutant with a strategy outside the feasibility region can invade, moving the dynamics out of the resident attractor with as a result in the extinction of the whole population, resident and mutant alike (Parvinen 2005). This scenario can be illustrated thanks to the invasibility plot in Fig. 0.4.1.

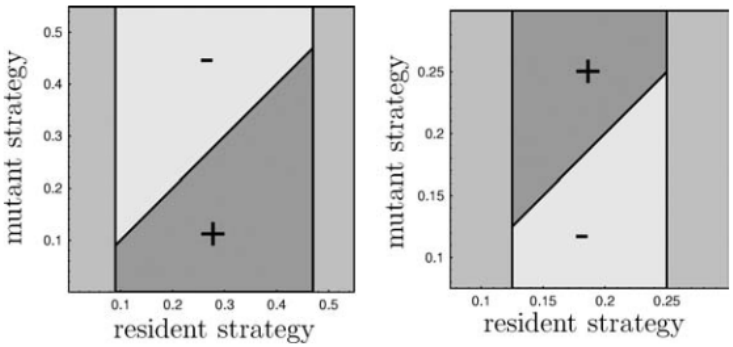



Figure 0.4.1: Typical pairwise invasibility plots in the case of evolutionary suicide. The medium gray rectangles on the left and right side of each panel corresponds to values of the resident strategy for which the population is not viable (Parvinen 2005).

Overall, Adaptive Dynamics provide a framework for studying the long-term selective pressures that determine the success of mutations within ecological contexts. It incorporates ecological interactions and population dynamics, aiming to predict evolutionary outcomes and understand the emergence of complex traits. However, it presents considerable limitations, we will cite only a few ones. First, he separation of time scales of AD assuming that evolutionary dynamics are much slower than population dynamics can be irrelevant in many cases, especially since evidence for rapid evolution is accumulating (John N Thompson 1998; Hendry et al. 2000). Moreover, AD only considers asexual populations while the majority of species reproduce sexually, although if if mutations are rare on a demographic timescale and observations are made over a long evolutionary timescale, using asexual demographic models for sexually reproducing populations can be justified (Lang, Botstein, and Desai 2011). Genetic variation is also considered to be small, and there's no clear justification for limiting the use of fitness-gradient models to scenarios where evolution happens through rare, minor-effect mutations replacements (Abrams 1992).

### 0.4.3 Quantitative Genetics

Given the limitations of the adaptive dynamics framework including its simplified assumptions, limited genetic detail and non applicability to sexual populations, in this thesis, I also employ a comparative approach : quantitative genetics. Quantitative genetics models the effects of inheritance, natural selection, and evolutionary factors on the phenotypic distribution of populations. These phenotypes are almost continuously distributed and can be measured on a metric scale. Therefore, a quantitative trait $x$ can be described by a continuous probability distribution $p(t,x)$ across the population at generation $t$ (Lande 1976; Taper and Case 1992; Case and Taper 2000). Assuming all possible genetic variability is always present in the population, mutations can be neglected, allowing the evolution of trait distribution to be governed solely by inheritance and natural selection (Lande 1976).

In one part of this work, the quantitative genetics framework is used to consider sexual reproduction in the study of tree populations. Considering sexual reproduction, is relevant for many reasons. Firstly, it is more realistic and applicable to a wide range of species. Indeed, many species, including most plants, animals, and many microorganisms, reproduce sexually. Additionally, it maintains more genetic variation, due to genetic shuffling according to Mendelian laws.
The basic assumption in the inheritance of quantitative traits is that within each family, offspring' breeding values follow a normal distribution with a constant variance, and a mean that equals the average of the breeding values of their two parents (Michael George Bulmer 1981), as illustrated in Fig. 0.4.2. This model is known as the *infinitesimal model*, reflecting its derivation from the cumulative effects of an infinite number of unlinked genes contributing to the trait (Ronald A Fisher 1919; Michael George Bulmer 1981; Barton, Etheridge, and Véber 2017; Turelli and Barton 1994). The infinitesimal model is a fundamental cornerstone of both population and quantitative genetics and was used for many applications (Verrier, Colleau, and Foulley 1991; Martinez, Bünger, and Hill 2000).

Mathematical analysis of differential equations with sexual reproduction operators is a relatively recent development in the field, presenting several challenges due to added complexity. Fisher's seminal work demonstrated that the additive effects of multiple genes, each following Mendelian inheritance, could explain continuous variation in traits.

Among his several previous contributions, Fisher's seminal work demonstrated that the additive effects

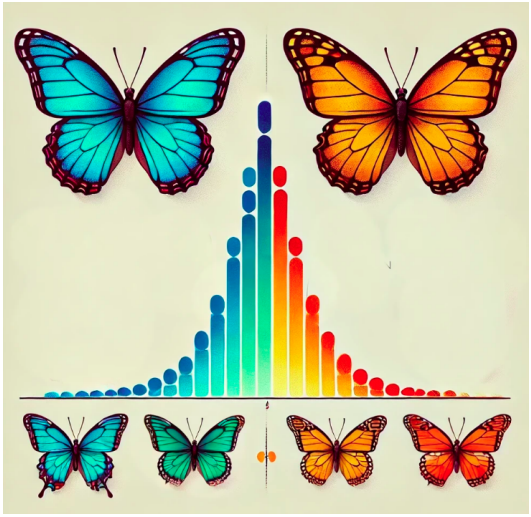


Figure 0.4.2: Illustration of the trait inheritance process with sexual reproduction according to the infinitesimal model. The variance of the Gaussian distribution represents the segregational variance ($\sigma^2$) and is constant parameter.

of multiple genes, each following Mendelian inheritance, could explain the continuous variation in traits. By applying the central limit theorem, Fisher showed that the distribution of polygenic traits would be approximately normal (Gaussian) around the mean of the parental traits. Half and century later in 1971, Bulmer (Michael G. Bulmer 1971) provided a detailed and rigorous treatment of the topic. Bulmer's work significantly advanced the mathematical theory and understanding of quantitative genetics.

Under the infinitesimal model, the assumption of linkage equilibrium is often made to simplify the genetic architecture of the trait. Linkage equilibrium means that alleles at different loci are inherited independently of each other. When this assumption holds (which is commom in quantitative genetics), the model assumes a Gaussian distribution of the trait. This framework was applied to use macroscopic quantinities to describe the dynamics of the populations (Sepideh Mirrahimi and Raoul 2011; Sepideh Mirrahimi and Raoul 2013; Bourgeron et al. 2017; Calvez, Garnier, and Patout 2019; Calvez, Poyato, and Santambrogio 2023). For instance, in Raoul 2021, the author proposed a method to study the adaptation of well-mixed sexually reproducing populations over time. The main result of this study is the existence and local uniqueness of a stable steady state, which is close to Gaussian distributions under weak selection assumption, where integro-differential equation can asymptotically be described by the dynamics of the mean trait and the population size.

This result relies heavily on an extension of the Wasserstein contractive property of the infinitesimal model operator to when the selection strength is weak. The quadratic Wasserstein distance $W_2$ is the optimal transport metric which can be illustrated by its application on two Dirac distributions : $W_2(\delta_a, \delta_b)^2 = |a-b|^2$, (the cost of moving a Dirac mass between two locations is equal to the Euclidian

distance between them).

These different mathematical frameworks in evolutionary modeling offer various approaches to study evolutionary dynamics and understand species adaptation under different assumptions, particularly in the context of global change. By leveraging these diverse mathematical frameworks, we can better predict species' adaptive responses to climate change, identify potential risks, and develop effective conservation strategies.

## 0.5 Chapters and Questions

Given the increasing threat of global environmental changes on ecosystems and the critical role of evolutionary dynamics in determining different outcomes of these changes, my thesis aims to use various mechanistic eco-evolutionary models, using well-established theoretical frameworks, to explore the potential adaptations of different populations under environmental stress. This research focuses on the ecological and evolutionary responses to two distinct abrupt shifts.

Firstly, I investigate ecosystems characterized by regime shifts (bistability). The objective here is to integrate evolutionary dynamics into models with ecological alternative stable states. This integration aims to enhance our understanding of the effects of phenotypic evolution on species within these systems that experience critical transitions.

Secondly, my goal is to develop a more theoretical approach using a robust mathematical framework. This framework will facilitate the study of evolution and potential adaptations of species facing abrupt environmental changes, particularly shifts in temperature and precipitation.

In both parts of my thesis, I will analyze the phenotypic evolution of various species and traits separately under different adaptive mechanisms. Furthermore, I will investigate the potential role of co-evolution, considering both the evolution of a single trait across different species and the evolution of multiple traits within a single species, in the ecosystems under study. A diagram summarising the work of this thesis is presented in Fig. 0.5.1.

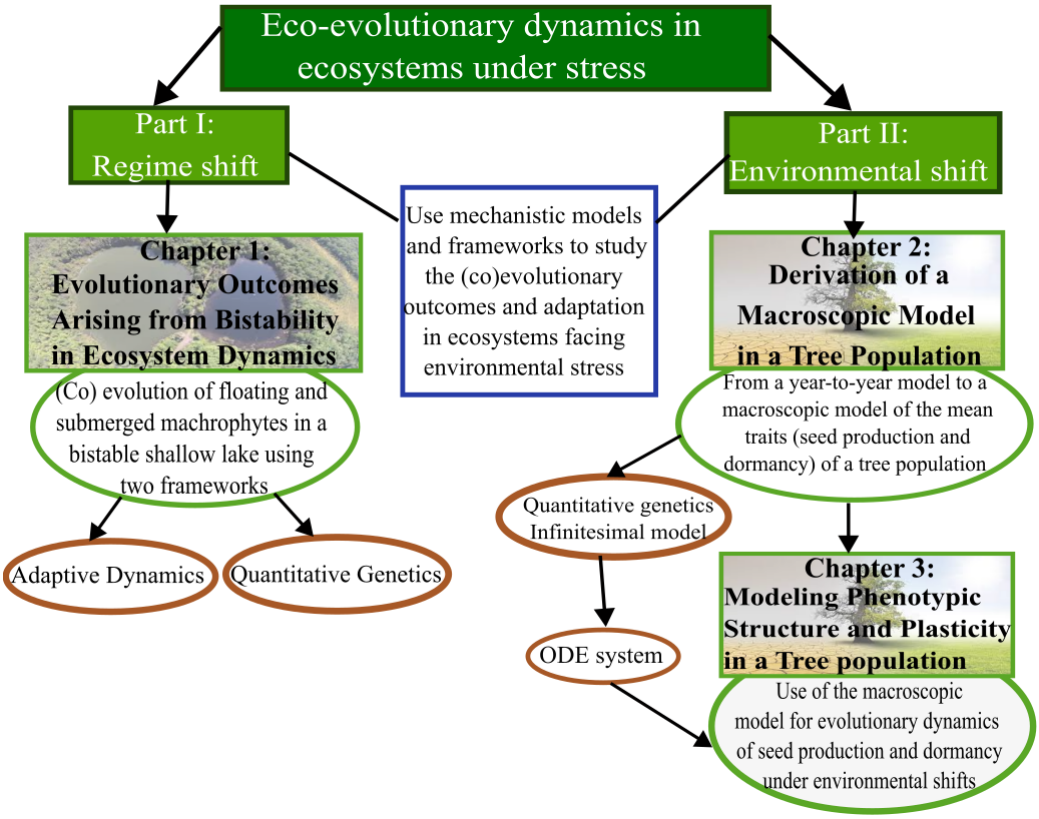



Figure 0.5.1: Diagram summarizing chapters and main purpose of this thesis.

### 0.5.1 Chapter 1 : Evolutionary Outcomes Arising from Bistability in Ecosystem Dynamics

In this chapter, I explore the eco-evolutionary dynamics of submerged and floating macrophytes in bistable shallow lake ecosystems, using a mechanistic competition model for nutrients and light, posing key scientific questions:

- How does rapid trait evolution impact the dynamics and stability of these ecosystems?
- Can eco-evolutionary feedbacks delay or advance ecological tipping points, potentially leading the system towards or outside a bistability zone ?
- What role does co-evolution play in these dynamics?

To answer these questions, I consider an ODE model of competition between floating and submerged macrophytes for nutrients and light, as an extension of a model used in (Marten Scheffer, Szabo, et al. 2003a). These two species are characterized by a phenotypic trait, representing their growth depth in the lake, which underlies their access capacities to both resources. The model presents a positive feedback between the two species, where the floating macrophytes have an advantage for light given their position on the surface from where they exert a shading effect on the submerged

macrophytes and prevent light penetration. In turn, submerged macrophytes have better access to nutrients as they are usually rooted in the bottom, which decreases the quantity of nutrients diffused to the surface for the floating macrophytes. The dynamics of the model is illustrated in Fig. 0.5.2.

I then use Adaptive Dynamics and Quantitative Genetics approaches to study the evolutionary outcomes of the studied phenotypic trait. This provides a comparative approach to study on one hand a resident-mutant population, and on another hand continuous trait distribution across the water column.

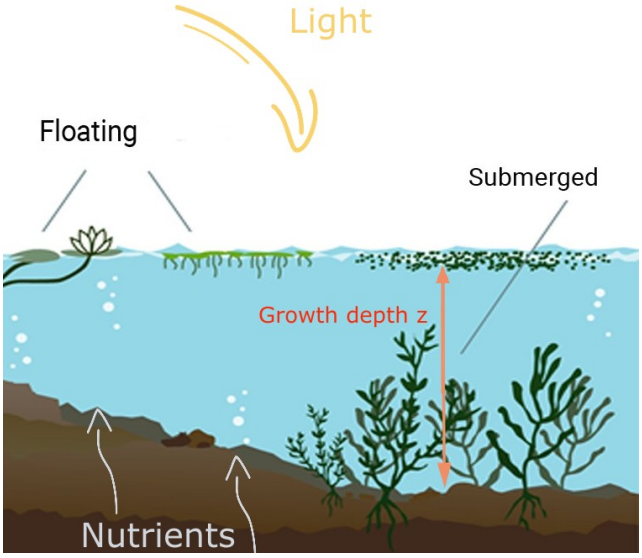



Figure 0.5.2: Illustration of the dynamics of the model studied in chapter 1. The floating and submerged macrophytes compete for nutrients and light and are characterized by their growth depth $z$.

The results show that the evolution of the growth depth of submerged macrophytes can impact the ecological dynamics and stability of the system by promoting diversification and enabling coexistence with competitive floating macrophytes. Moreover, this evolution also leads to complex dynamics, including evolutionary oscillations and evolutionary suicide, where evolved trait results in species extinction. When submerged macrophytes evolve to higher levels crossing bistability regions, they experience increasingly larger oscillations as nutrient diffusion increase, ultimately causing the population to go extinct. The co-evolution of submerged and floating macrophytes provides a stabilizing effect by preventing oscillations, delaying evolutionary suicide and hence promoting temporary stability in the ecosystem. Despite this, co-evolution does not significantly change the overall evolutionary outcomes; ecosystem collapse still occurs under high nutrient diffusion rates.

### 0.5.2 Chapter 2 : Derivation of a macroscopic model in a tree population

In this chapter, I define a mechanistic model to describe the dynamics of dormancy and daily seed production in tree populations, including different feature we believe are important. The model accounts for sexual reproduction, distinguishing between seeds and mature individuals. The population are characterized by two phenotypic traits (breeding values that are determined by the genotypes of individuals only), one is defined as the daily number of seeds produced, denoted as $x \in \mathcal{R}$, and another as the threshold temperature above which individuals become dormant; ceasing to die and reproduce, denoted as $y \in \mathcal{R}$. This latter trait represent the breeding value (latent trait) that determines the plastic trait of annual timing; meaning the moment at which individuals switch to a dormant state. The traits representing the number of seeds produced $x$ and dormancy temperature threshold $y$ are influenced by environmental factors, including annual temperature variations and water availability. For an individual tree with traits $(x, y)$, I assume that it becomes dormant and cease to die and reproduce when the temperature reaches $y$. Bellow this threshold, the mortality is conditioned by the lack of water, meaning that individuals don't die unless all water is consumed. Similarly, reproduction occurs only when there is enough water supply to produce $x$ seeds. The mean traits of the population are denoted as $X(t)$ and $Y(t)$. The dynamics of the model are illustrated in Fig. 0.5.3. In this part, I am interested in the following question :

- How do we derive a macroscopic model describing the dynamics of the mean traits of the population $X(t)$ and $Y(t)$ ?

The simplification process involves deriving from a year-to-year model, an annual limit integro-differential model under the assumption of a low death rate for mature individuals ($\varepsilon \ll 1$). Under weak selection assumptions, this reduced model of traits distribution is close to a Gaussian distribution centered around the mean traits of the population. This provides an approach to describe the overall population dynamics through the dynamics of the mean traits. I then derive a macroscopic model for these quantities, which results in a simple ODE system. By focusing on the mean seed production and the mean dormancy temperature, the macroscopic model captures the essential dynamics of the system.

The chapter details how the complex mechanistic model transitions to a more tractable one. This approach will help reveal the adaptive strategies trees may use to balance seed production and dormancy timing in response to abrupt environmental changes.

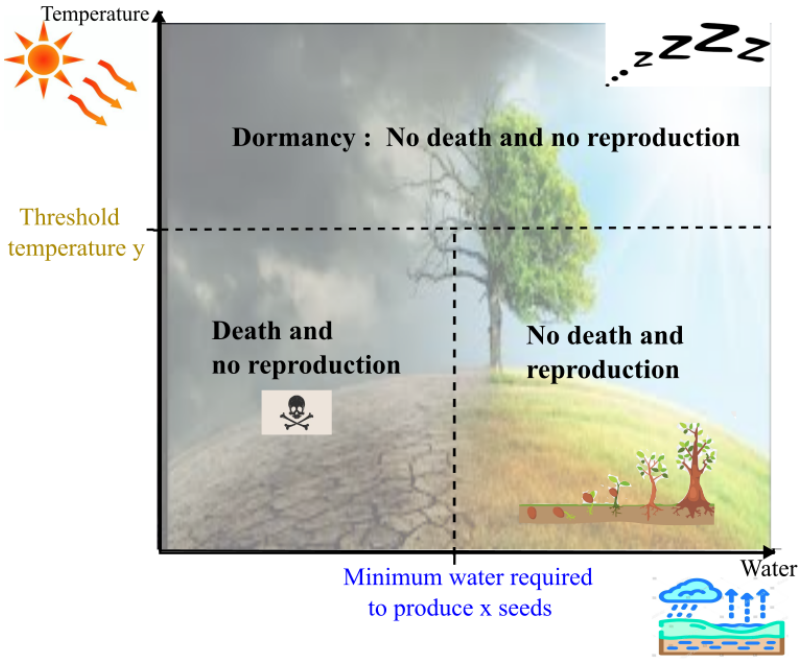



Figure 0.5.3: Illustration of the dynamics of the model studied in chapter 2. The population becomes dormant and cease to die and reproduce when the temperature reaches $y$. Bellow this threshold, the trees produce $x$ seeds providing water is available. When water lacks, the trees cease to reproduce and start dying.

### 0.5.3 Chapter 3 : Modeling Phenotypic Structure and Plasticity in a Tree Population

This chapter presents a detailed investigation into the evolutionary dynamics of tree populations, focusing on seed production and dormancy under the influence of climate change, using the macroscopic model derived in the previous chapter and numerical simulations.

The primary questions addressed are:

- How do environmental changes, particularly shifts in temperature and precipitation, impact the evolutionary strategies of seed production and dormancy in trees?
- What are the adaptive responses of these traits under different climatic scenarios, and how does phenotypic plasticity shape these responses ?

The study reveals that phenotypic plasticity may prevent the adaptation of the traits to temperature shifts through dormancy and due to the absence of intrinsic mortality. However, abrupt changes in precipitation significantly influence both seed production and dormancy, with the magnitude of these shifts determining the extent of the adaptive response. The results also show that while dormancy can adapt to high precipitation shifts, seed production can only adapt adapt up to a certain shift amplitude, above which they evolve to a different biological niche. However, when exploring the co-evolution of seed production and dormancy, I found that under this scenario, both traits could

evolve towards the new optimal strategy even when the precipitation shift is high. This co-evolution leads to two extreme stable strategies depending on the evolutionary rates of the traits: a strategy favoring fewer seeds over a longer period and another favoring rapid seed production followed by early dormancy. The interplay between temperature and precipitation shifts ultimately shapes the evolutionary outcomes, highlighting the complex adaptive responses required for tree populations to cope with multifaceted climate changes. The findings show that while dormancy allows the survival of species during extreme climatic events, it can also hinder rapid adaptation to new environments.

# Bibliography


Abrams, PA (2005). "Adaptive Dynamics' vs.'adaptive dynamics". In: *Journal of Evolutionary Biology* 18.5, pp. 1162–1165.

Abrams, Peter A (1992). "Adaptive foraging by predators as a cause of predator-prey cycles". In: *Evolutionary Ecology* 6, pp. 56–72.

Ahrens, Collin W and Elizabeth A James (2015). "Range-wide genetic analysis reveals limited structure and suggests asexual patterns in the rare forb Senecio macrocarpus". In: *Biological Journal of the Linnean Society* 115.2, pp. 256–269.

Aono, Yasuyuki and Kazuhiko Kazui (2008). "Phenological data series of cherry tree flowering in Kyoto, Japan, and its application to reconstruction of springtime temperatures since the 9th century". In: *International Journal of Climatology: A Journal of the Royal Meteorological Society* 28.7, pp. 905–914.

Baldridge, Ashley K and David M Lodge (2014). "Long-term studies of crayfish-invaded lakes reveal limited potential for macrophyte recovery from the seed bank". In: *Freshwater Science* 33.3, pp. 788–797.

Barraclough, Timothy G and Vincent Savolainen (2001). "Evolutionary rates and species diversity in flowering plants". In: *Evolution* 55.4, pp. 677–683.

Barton, Nicholas H, Alison M Etheridge, and Amandine Véber (2017). "The infinitesimal model: Definition, derivation, and implications". In: *Theoretical population biology* 118, pp. 50–73.

Beckage, Brian and Chris Ellingwood (2008). "Fire feedbacks with vegetation and alternative stable states". In: *Complex Systems* 18.1, p. 159.

Bell, Graham (2017). "Evolutionary rescue". In: *Annual Review of Ecology, Evolution, and Systematics* 48.1, pp. 605–627.

Bodner, Korryn et al. (2021). "Bridging the divide between ecological forecasts and environmental decision making". In: *Ecosphere* 12.12, e03869.

Bora, Leticia Siman, Sidinei Magela Thomaz, and André Andrian Padial (2020). "Evidence of rapid evolution of an invasive poaceae in response to salinity". In: *Aquatic Sciences* 82, pp. 1–16.

Bourgeron, Thibault et al. (2017). "Existence of recombination-selection equilibria for sexual populations". In: *arXiv preprint arXiv:1703.09078*.

Brodie III, Edmund D. and Edmund D. Brodie Jr (2014). "Antagonistic coevolution and the evolution of plant defense". In: *Science* 344.6188, pp. 746–747.

Brohan, Phillip et al. (2006). "Uncertainty estimates in regional and global observed temperature changes: A new data set from 1850". In: *Journal of Geophysical Research: Atmospheres* 111.D12.

Brown, James K and Jane Kapler Smith (2000). "Wildland fire in ecosystems: effects of fire on flora". In: *Gen. Tech. Rep. RMRS-GTR-42-vol. 2. Ogden, UT: US Department of Agriculture, Forest Service, Rocky Mountain Research Station. 257 p.* 42.

Bulmer, Michael G. (1971). *The Mathematical Theory of Quantitative Genetics*. Oxford University Press.

Bulmer, Michael George (1981). *The mathematical theory of quantitative genetics.*

Bürger, Reinhard (2000). *The Mathematical Theory of Selection, Recombination, and Mutation*. Wiley.

— (2020). "Multilocus population-genetic theory". In: *Theoretical Population Biology* 133, pp. 40–48.

Calvez, Vincent, Jimmy Garnier, and Florian Patout (2019). "Asymptotic analysis of a quantitative genetics model with nonlinear integral operator". In: *Journal de l'École polytechnique—Mathématiques* 6, pp. 537–579.

Calvez, Vincent, David Poyato, and Filippo Santambrogio (2023). "Uniform contractivity of the Fisher infinitesimal model with strongly convex selection". In: *arXiv preprint arXiv:2302.12063*.

Carpenter, Stephen R and Otto Kinne (2003). "Regime shifts in lake ecosystems". In.

Carpenter, Stephen R, Donald Ludwig, and William A Brock (1999). "Management of eutrophication for lakes subject to potentially irreversible change". In: *Ecological applications* 9.3, pp. 751–771.

Carpenter, Stephen R, Harold A Mooney, et al. (2009). "Science for managing ecosystem services: Beyond the Millennium Ecosystem Assessment". In: *Proceedings of the National Academy of Sciences* 106.5, pp. 1305–1312.

Case, Madelon F et al. (2019). "Severe drought limits trees in a semi-arid savanna". In: *Ecology* 100.11, e02842.

Case, Ted J and Mark L Taper (2000). "Interspecific competition, environmental gradients, gene flow, and the coevolution of species' borders". In: *The american naturalist* 155.5, pp. 583–605.

Castellani, Maria Beatrice et al. (2023). “Genetic drift versus natural selection affecting the evolution of spectral and functional traits of two key macrophytes: Phragmites australis and Nuphar lutea”. In: *Freshwater Biology* 68.10, pp. 1739–1750.

Chambers, Robert G and Vangelis Tzouvelekas (2013). “Estimating population dynamics without population data”. In: *Journal of Environmental Economics and Management* 66.3, pp. 510–522.

Champagnat, Nicolas, R Ferričre, and G Ben Arous4 (2002). “The canonical equation of adaptive dynamics: a mathematical view”. In: *Selection* 2.1-2, pp. 73–83.

Champagnat, Nicolas, Régis Ferrière, and Sylvie Méléard (2006). “Unifying evolutionary dynamics: From individual stochastic processes to macroscopic models”. In: *Theoretical Population Biology* 69.3, pp. 297–321.

Chaparro Pedraza, P Catalina et al. (2021). “Adaptive evolution can both prevent ecosystem collapse and delay ecosystem recovery”. In: *The American Naturalist* 198.6, E185–E197.

Chapman, RF and JC Lee (1991). “Environmental effects on numbers of peripheral chemoreceptors on the antennae of a grasshopper”. In: *Chemical Senses* 16.6, pp. 607–616.

Charrier, Guillaume et al. (2021). “Interaction of drought and frost in tree ecophysiology: rethinking the timing of risks”. In: *Annals of Forest Science* 78, pp. 1–15.

Cheddadi, Rachid et al. (2016). “Temperature range shifts for three European tree species over the last 10,000 years”. In: *Frontiers in Plant Science* 7, p. 1581.

Chiang, Felicia, Omid Mazdiyasni, and Amir AghaKouchak (2021). “Evidence of anthropogenic impacts on global drought frequency, duration, and intensity”. In: *Nature communications* 12.1, p. 2754.

Clark, James S et al. (2001). “Ecological forecasts: an emerging imperative”. In: *science* 293.5530, pp. 657–660.

Cleland, Elsa E et al. (2007). “Shifting plant phenology in response to global change”. In: *Trends in Ecology & Evolution* 22.7, pp. 357–365.

Collins, Courtney G et al. (2021). “Experimental warming differentially affects vegetative and reproductive phenology of tundra plants”. In: *Nature Communications* 12.1, p. 3442.

Comiso, Josefino C et al. (2008). “Accelerated decline in the Arctic sea ice cover”. In: *Geophysical research letters* 35.1.

Cook, LM and Ilik J Saccheri (2013). “The peppered moth and industrial melanism: evolution of a natural selection case study”. In: *Heredity* 110.3, pp. 207–212.

Crow, James Franklin (2017). *An introduction to population genetics theory*. Scientific Publishers.

Dai, Aiguo (2011). “Drought under global warming: a review”. In: *Wiley Interdisciplinary Reviews: Climate Change* 2.1, pp. 45–65.

Dale, Virginia H et al. (2005). “Effects of modern volcanic eruptions on vegetation”. In: *Volcanoes and the Environment*, pp. 227–249.

Dalpasso, Andrea et al. (2023). “Effects of temperature and precipitation changes on shifts in breeding phenology of an endangered toad”. In: *Scientific Reports* 13.1, p. 14573.

Darwin, Charles (1859). *On the Origin of Species by Means of Natural Selection, or the Preservation of Favoured Races in the Struggle for Life*. London: John Murray.

Dercole, Fabio and Sergio Rinaldi (2008). *Analysis of evolutionary processes: the adaptive dynamics approach and its applications: the adaptive dynamics approach and its applications*. Princeton University Press.

Dieckmann, Ulf and Richard Law (1996). “The dynamical theory of coevolution: a derivation from stochastic ecological processes”. In: *Journal of Mathematical Biology* 34.5-6, pp. 579–612.

Dieckmann, Ulf, Paul Marrow, and Richard Law (1995). “Evolutionary cycling in predator-prey interactions: population dynamics and the red queen”. In: *Journal of theoretical biology* 176.1, pp. 91–102.

Diekmann, Odo et al. (2005). “The dynamics of adaptation: an illuminating example and a Hamilton–Jacobi approach”. In: *Theoretical population biology* 67.4, pp. 257–271.

Doebeli, Michael and Graeme D Ruxton (1997). “Evolution of dispersal rates in metapopulation models: branching and cyclic dynamics in phenotype space”. In: *Evolution* 51.6, pp. 1730–1741.

Donoghue, Michael J., Charles D. Bell, and Hui Li (2014). *Introduction to Plant Taxonomy*. Wiley.

Duchenne, François et al. (2020). “Phenological shifts alter the seasonal structure of pollinator assemblages in Europe”. In: *Nature Ecology & Evolution* 4.1, pp. 115–121.

Ehrenfeld, Joan G (2010). “Ecosystem consequences of biological invasions”. In: *Annual review of ecology, evolution, and systematics* 41, pp. 59–80.

Erbach, Alexandra, Frithjof Lutscher, and Gunog Seo (2013). “Bistability and limit cycles in generalist predator–prey dynamics”. In: *Ecological Complexity* 14, pp. 48–55.

Eriksen, Marcus et al. (2014). “Plastic pollution in the world’s oceans: more than 5 trillion plastic pieces weighing over 250,000 tons afloat at sea”. In: *PloS one* 9.12, e111913.

Fer, Istem et al. (2021). “Capturing site-to-site variability through Hierarchical Bayesian calibration of a process-based dynamic vegetation model”. In: *bioRxiv*, pp. 2021–04.

Ferriere, Régis (2000). “Adaptive responses to environmental threats: evolutionary suicide, insurance, and rescue”. In: *Options Spring* 2000, pp. 12–16.

Fisher, Ronald A (1919). “XV.—The correlation between relatives on the supposition of Mendelian inheritance.” In: *Earth and Environmental Science Transactions of the Royal Society of Edinburgh* 52.2, pp. 399–433.

Fisher, Ronald Aylmer (1930). *The genetical theory of natural selection*. Oxford University Press.

Folke, Carl et al. (2004). “Regime shifts, resilience, and biodiversity in ecosystem management”. In: *Annu. Rev. Ecol. Evol. Syst.* 35, pp. 557–581.

Geist, Helmut J and Eric F Lambin (2004). “Dynamic causal patterns of desertification”. In: *Bioscience* 54.9, pp. 817–829.

Geritz, Stefan A. H. et al. (1998). “Evolutionarily singular strategies and the adaptive growth and branching of the evolutionary tree”. In: *Evolutionary Ecology* 12.1, pp. 35–57.

Geritz et al. (1997). “Dynamics of adaptation and evolutionary branching”. In: *Physical Review Letters* 78.10, pp. 2024–2027.

Greene, Charles H et al. (2008). “Arctic climate change and its impacts on the ecology of the North Atlantic”. In: *Ecology* 89.sp11, S24–S38.

Greenwade, George D. (1993). “The Comprehensive Tex Archive Network (CTAN)”. In: *TUGBoat* 14.3, pp. 342–351.

Haldane, J.B.S. (1932). “The causes of evolution”. In.

Hansen, James et al. (2010). “Global surface temperature change”. In: *Reviews of geophysics* 48.4.

Hastings, Alan and Derin B Wysham (2010). “Regime shifts in ecological systems can occur with no warning”. In: *Ecology letters* 13.4, pp. 464–472.

Heide, Olav M (2003). “Ecological and physiological aspects of photoperiodic control of bud burst in northern deciduous trees”. In: *Tree Physiology* 23.9, pp. 431–442.

Hendry, Andrew P et al. (2000). “Rapid evolution of reproductive isolation in the wild: evidence from introduced salmon”. In: *Science* 290.5491, pp. 516–518.

Holling, Crawford S (1973). “Resilience and stability of ecological systems”. In: *Annual review of ecology and systematics* 4.1, pp. 1–23.

Hu, Huifeng et al. (2017). “Drought impact on forest regeneration in the Southeast USA”. In: *Ecosphere* 8.4, e01772.

Huxman, Travis E et al. (2004). “Convergence across biomes to a common rain-use efficiency”. In: *Nature* 429.6992, pp. 651–654.

Ibelings, Bas W et al. (2007). “Resilience of alternative stable states during the recovery of shallow lakes from eutrophication: Lake Veluwe as a case study”. In: *Ecosystems* 10, pp. 4–16.

Ives, Anthony R (1995). “Predicting the response of populations to environmental change”. In: *Ecology* 76.3, pp. 926–941.

Keeling, Charles D (1960). “The concentration and isotopic abundances of carbon dioxide in the atmosphere”. In: *Tellus* 12.2, pp. 200–203.

Kettlewell, H Bernard D (1955). “Selection experiments on industrial melanism in the Lepidoptera”. In: *Heredity* 9.3, pp. 323–342.

Lacoul, Puspa and Bill Freedman (2006). “Relationships between aquatic plants and environmental factors along a steep Himalayan altitudinal gradient”. In: *Aquatic Botany* 84.1, pp. 3–16.

Lande, Russell (1976). “Natural selection and random genetic drift in phenotypic evolution”. In: *Evolution* 30.2, pp. 314–334.

Lang, Gregory I, David Botstein, and Michael M Desai (2011). “Genetic variation and the fate of beneficial mutations in asexual populations”. In: *Genetics* 188.3, pp. 647–661.

Leslie, Patrick H (1945). “On the use of matrices in certain population mathematics”. In: *Biometrika* 33.3, pp. 183–212.

Li, Xuejian et al. (2023). “Spatiotemporal patterns of remotely sensed phenology and their response to climate change and topography in subtropical bamboo forests during 2001-2017: a case study in Zhejiang Province, China”. In: *GIScience & Remote Sensing* 60.1, p. 2163575.

Liu, Jiping and Judith A Curry (2010). “Accelerated warming of the Southern Ocean and its impacts on the hydrological cycle and sea ice”. In: *Proceedings of the National Academy of Sciences* 107.34, pp. 14987–14992.

Liu, Yang et al. (2017). “Impact of temperature shifts on the joint evolution of seed dormancy and size”. In: *Ecology and Evolution* 7.1, pp. 26–37.

Lotka, Alfred James (1925). *Elements of physical biology*. Williams & Wilkins.

Malcolm, Jay R and Adam Markham (2000). “Global warming and terrestrial biodiversity decline”. In.

Malthus, Thomas (1798). “An essay on the principle of population. Printed for J. Johnson”. In: *St. Paul’s church-yard, London*, pp. 1–126.

Marrow, Paul, Richard Law, and C Cannings (1992). “The coevolution of predator—prey interactions: ESSs and Red Queen dynamics”. In: *Proceedings of the Royal Society of London. Series B: Biological Sciences* 250.1328, pp. 133–141.

Martinez, Victor, Lutz Bünger, and William G Hill (2000). "Analysis of response to 20 generations of selection for body composition in mice: fit to infinitesimal model assumptions". In: *Genetics Selection Evolution* 32.1, pp. 3–21.

Matsuda, Hiroyuki (1985). "Evolutionarily stable strategies for predator switching". In: *Journal of Theoretical Biology* 115.3, pp. 351–366.

May, Robert M (1977). "Thresholds and breakpoints in ecosystems with a multiplicity of stable states". In: *Nature* 269.5628, pp. 471–477.

Mayer, DG and DG Butler (1993). "Statistical validation". In: *Ecological modelling* 68.1-2, pp. 21–32.

McFarland, DG and SJ Rogers (1998). "The aquatic macrophyte seed bank in Lake Onalaska, Wisconsin". In: *Journal of Aquatic Plant Management* 36.JAN. Pp. 33–39.

Menzel, Annette et al. (2006). "Response of leaf phenology to climate change: a case study for Central Europe". In: *Agricultural and Forest Meteorology* 139.1-2, pp. 10–26.

Metz and S. A. H. Nisbet and Geritz (1996). "Adaptive dynamics: a geometrical study of the consequences of nearly faithful reproduction". In: *Stochastic and Spatial Structures of Dynamical Systems* 45, pp. 183–231.

Miranda, Juan de Dios et al. (2009). "Do changes in rainfall patterns affect semiarid annual plant communities?" In: *Journal of Vegetation Science* 20.2, pp. 269–276.

Mirrahimi, Sepideh and Gaël Raoul (2011). "Population structured by a space variable and a phenotypical trait". In: *arXiv preprint arXiv:1105.1936*.

— (2013). "Dynamics of sexual populations structured by a space variable and a phenotypical trait". In: *Theoretical population biology* 84, pp. 87–103.

Moran, Patrick AP (1958). "Random processes in genetics". In: *Mathematical Proceedings of the Cambridge Philosophical Society* 54.1, pp. 60–71.

Nelson, Gerald C et al. (2006). "Anthropogenic drivers of ecosystem change: an overview". In: *Ecology and Society* 11.2.

Otto, Sarah P (2009). "The evolutionary enigma of sex". In: *The American Naturalist* 174.S1, S1–S14.

Pachauri, Rajendra K et al. (2014). *Climate change 2014: synthesis report. Contribution of Working Groups I, II and III to the fifth assessment report of the Intergovernmental Panel on Climate Change*. Ipcc.

Paerl, Hans W and Jef Huisman (2008). "Blooms like it hot". In: *Science* 320.5872, pp. 57–58.

Parmesan, Camille and Gary Yohe (2003). "A globally coherent fingerprint of climate change impacts across natural systems". In: *nature* 421.6918, pp. 37–42.

Parvinen, Kalle (2005). “Evolutionary suicide”. In: *Acta biotheoretica* 53.3, pp. 241–264.

Patrick, CJ et al. (2020). “A system level analysis of coastal ecosystem responses to hurricane impacts”. In: *Estuaries and Coasts* 43, pp. 943–959.

Peñuelas, Josep, This Rutishauser, and Iolanda Filella (2009). “Phenology feedbacks on climate change”. In: *Science* 324.5929, pp. 887–888.

Pielou, Evelyn Chrystalla (1981). “The usefulness of ecological models: a stock-taking”. In: *The Quarterly Review of Biology* 56.1, pp. 17–31.

Price, George R. (1973). “The logic of animal conflict”. In: *Nature* 246.5427, pp. 15–18.

Raju, AJS (2018). “Climate Change: Impacts on Plant-Pollinator Interactions”. In.

Rankin, Daniel J and Andrés López-Sepulcre (2005). “Adaptation as a process: what does it mean for ecologists and evolutionists?” In: *Annales Zoologici Fennici* 42.6, pp. 207–217.

Raoul, Gaël (2021). “Exponential convergence to a steady-state for a population genetics model with sexual reproduction and selection”. In: *arXiv preprint arXiv:2104.06089*.

Rignot, Eric et al. (2011). “Acceleration of the contribution of the Greenland and Antarctic ice sheets to sea level rise”. In: *Geophysical research letters* 38.5.

Rinnan, Darwin Scott (2018). “Modeling population dynamics and species interactions in a changing climate”. PhD thesis.

Rockström, Johan et al. (2009). “A safe operating space for humanity”. In: *nature* 461.7263, pp. 472–475.

Rosenberg, Kenneth V et al. (2019). “Decline of the North American avifauna”. In: *Science* 366.6461, pp. 120–124.

Russo, Lucia and Konstantinos G Spiliotis (2016). “Bifurcation analysis of a forest-grassland ecosystem”. In: 1738.1.

Sala, Enric and Nancy Knowlton (2006). “Global marine biodiversity trends”. In: *Annu. Rev. Environ. Resour.* 31, pp. 93–122.

Schaub, Michael and Fitsum Abadi (2011). “Integrated population models: a novel analysis framework for deeper insights into population dynamics”. In: *Journal of Ornithology* 152, pp. 227–237.

Scheffer, Marten (2020). *Critical transitions in nature and society*. Vol. 16. Princeton University Press.

Scheffer, Marten and Stephen R Carpenter (2003). “Catastrophic regime shifts in ecosystems: linking theory to observation”. In: *Trends in ecology & evolution* 18.12, pp. 648–656.

Scheffer, Marten, Steve Carpenter, et al. (2001). “Catastrophic shifts in ecosystems”. In: *Nature* 413.6856, pp. 591–596.

Scheffer, Marten, S Harry Hosper, et al. (1993). “Alternative equilibria in shallow lakes”. In: *Trends in ecology & evolution* 8.8, pp. 275–279.

Scheffer, Marten, Sándor Szabo, et al. (2003). “Floating plant dominance as a stable state”. In: *Proceedings of the national academy of sciences* 100.7, pp. 4040–4045.

Smith, John Maynard (1974). “The theory of games and the evolution of animal conflicts”. In: *Journal of Theoretical Biology* 47.1, pp. 209–221.

Smith, Sally E and David J Read (2003). “Mycorrhizal symbiosis: potential and impact in tropical agriculture”. In: *Biological Reviews* 78.4, pp. 607–615.

Solé, Ricard and Jordi Bascompte (2012). “Self-Organization in Complex Ecosystems.(MPB-42)”. In: *Self-Organization in Complex Ecosystems.(MPB-42)*. Princeton University Press.

Søndergaard, Martin et al. (2007). “Lake restoration: successes, failures and long-term effects”. In: *Journal of Applied ecology* 44.6, pp. 1095–1105.

Stanke, Hunter et al. (2021). “Over half of western United States’ most abundant tree species in decline”. In: *Nature Communications* 12.1, p. 451.

Staver, A Carla and Simon A Levin (2012). “Integrating theoretical climate and fire effects on savanna and forest systems”. In: *The American Naturalist* 180.2, pp. 211–224.

Stearns, Stephen C (1989). “The evolutionary significance of phenotypic plasticity”. In: *Bioscience* 39.7, pp. 436–445.

Steffen, Will, Wendy Broadgate, et al. (2015). “The trajectory of the Anthropocene: the great acceleration”. In: *The anthropocene review* 2.1, pp. 81–98.

Steffen, Will, Paul J Crutzen, John R McNeill, et al. (2007). “The Anthropocene: are humans now overwhelming the great forces of nature”. In: *Ambio-Journal of Human Environment Research and Management* 36.8, pp. 614–621.

Stork, Nigel E (1997). “Measuring global biodiversity and its decline”. In: *Biodiversity II: understanding and protecting our biological resources* 41, pp. 41–68.

Suding, Katharine N and Richard J Hobbs (2009). “Threshold models in restoration and conservation: a developing framework”. In: *Trends in ecology & evolution* 24.5, pp. 271–279.

Taper, Mark L and Ted J Case (1992). “Models of character displacement and the theoretical robustness of taxon cycles”. In: *Evolution* 46.2, pp. 317–333.

Tedeschi, Luis Orlindo (2006). “Assessment of the adequacy of mathematical models”. In: *Agricultural systems* 89.2-3, pp. 225–247.

Thompson, Daniel B (1992). "Consumption rates and the evolution of diet-induced plasticity in the head morphology of Melanoplus femurrubrum (Orthoptera: Acrididae)". In: *Oecologia* 89, pp. 204–213.

Thompson, David WJ and John M Wallace (2001). "Regional climate impacts of the Northern Hemisphere annular mode". In: *Science* 293.5527, pp. 85–89.

Thompson, John N (1998). "Rapid evolution as an ecological process". In: *Trends in ecology & evolution* 13.8, pp. 329–332.

— (1994). *The coevolutionary process*. University of Chicago Press.

Tomiolo, Sara and David Ward (2018). "Species migrations and range shifts: A synthesis of causes and consequences". In: *Perspectives in plant ecology, evolution and systematics* 33, pp. 62–77.

Tóth, Viktor R et al. (2017). "Morphological and genetic variability of Myriophyllum spicatum in different shallow water bodies of Hungary". In: *Wetlands* 37, pp. 351–362.

Trei, Tiiu and Tiia Pedusaar (2006). "Macroflora in Lake Ülemiste (Estonia)–changes and the impact of environmental factors". In: *Proc. Estonian Acad. Sci. Biol. Ecol* 55, pp. 199–215.

Trenberth, Kevin E et al. (2014). "Global warming and changes in drought". In: *Nature Climate Change* 4.1, pp. 17–22.

Turelli, Michael and Nicholas H Barton (1994). "Genetic and statistical analyses of strong selection on polygenic traits: what, me normal?" In: *Genetics* 138.3, pp. 913–941.

Valpine, Perry de (2012). "Frequentist analysis of hierarchical models for population dynamics and demographic data". In: *Journal of Ornithology* 152.Suppl 2, pp. 393–408.

Van Meerbeek, Koenraad, Tommaso Jucker, and Jens-Christian Svenning (2021). "Unifying the concepts of stability and resilience in ecology". In: *Journal of Ecology* 109.9, pp. 3114–3132.

Van Tienderen, PH and G De Jong (1986). "Sex ratio under the haystack model: polymorphism may occur". In: *Journal of Theoretical Biology* 122.1, pp. 69–81.

Velicogna, Isabella (2009). "Increasing rates of ice mass loss from the Greenland and Antarctic ice sheets revealed by GRACE". In: *Geophysical Research Letters* 36.19.

Verhulst, Pierre-François (1838). "Notice sur la loi que la population suit dans son accroissement". In: *Correspondence mathematique et physique* 10, pp. 113–129.

Verrier, E, J Jacques Colleau, and JL Foulley (1991). "Methods for predicting response to selection in small populations under additive genetic models: a review". In: *Livestock Production Science* 29.2-3, pp. 93–114.

Villa Martín, Paula et al. (2015). “Eluding catastrophic shifts”. In: *Proceedings of the National Academy of Sciences* 112.15, E1828–E1836.

Villani, Cédric (2021). *Topics in optimal transportation*. Vol. 58. American Mathematical Soc.

Vinnikov, Konstantin Y et al. (1999). “Global warming and Northern Hemisphere sea ice extent”. In: *Science* 286.5446, pp. 1934–1937.

Volterra, Vito (1927). *Variazioni e fluttuazioni del numero d’individui in specie animali conviventi*. Vol. 2. Societá anonima tipografica" Leonardo da Vinci".

Webb, Colleen (2003). “A complete classification of Darwinian extinction in ecological interactions”. In: *The American Naturalist* 161.2, pp. 181–205.

Winder, Monika (2012). “Lake warming mimics fertilization”. In: *Nature Climate Change* 2.11, pp. 771–772.

Wissel, C. and H. Stöcker (1991). “Stochastic birth and death processes described by a system of partial differential equations”. In: *Theoretical Population Biology* 39.3, pp. 330–354.

Wright, Sewall (1931). “Evolution in Mendelian populations”. In: *Genetics* 16.2, pp. 97–159.

— (1969). *Evolution and the genetics of populations, Volume 2: The theory of gene frequencies*. University of Chicago Press.

Wu, Xiuchen et al. (2022). “Timing and order of extreme drought and wetness determine bioclimatic sensitivity of tree growth”. In: *Earth’s Future* 10.7, e2021EF002530.

Yang, Y and A Joern (1994). “Gut size changes in relation to variable food quality and body size in grasshoppers”. In: *Functional Ecology*, pp. 36–45.

Zeppel, MJB, Janet V Wilks, and James D Lewis (2014). “Impacts of extreme precipitation and seasonal changes in precipitation on plants”. In: *Biogeosciences* 11.11, pp. 3083–3093.

Zhou, Ligang et al. (2020). “Spatiotemporal variations in nitrogen and phosphorus in a large man-made lake and their relationships with human activities”. In: *Water* 12.4, p. 1106.

CHAPTER 1

# Chapter 1: Evolutionary outcomes arising from bistability in ecosystem dynamics

**Abstract**

While it is known that shallow lakes ecosystems may experience abrupt shifts (ie tipping points) from one state to a contrasting degraded alternative state as a result of gradual environmental changes, the role of evolutionary processes and the impact of trait variation in this context remain largely unexplored. It is crucial to elucidate how eco-evolutionary feedbacks affect abrupt ecological transitions in shallow lakes. These feedbacks can significantly alter the dynamics of aquatic plants competition, community structure, and species diversity, potentially affecting the existence of alternative states or either delay or expedite the thresholds at which these ecological shifts occur. In this paper, we explore the eco-evolutionary dynamics of submerged and floating macrophytes in a shallow lake ecosystem under asymmetric competition for nutrients and light. We use adaptive dynamics and a structured population model to analyze the evolution of the growth depth of the submerged and floating macrophytes population, which influences their competitive ability for the two resources. We show how rapid trait evolution can result in complex dynamics including evolutionary oscillations, extensive diversification and evolutionary suicide. Furthermore, we find that the co-evolution of the two competitive species can play a stabilizing role, while not significantly affecting the overall evolutionary dynamics. Overall, this study shows that evolution can have strong effects in the ecological dynamics of bistable ecosystems.

## 1.1 Introduction

Extensive theoretical work and empirical observations have revealed the potential for ecosystems to undergo abrupt and dramatic transitions, shifting from one stable state to a contrasting degraded alternative state (Holling 1973b; May 1977b; Marten Scheffer, S. Carpenter, et al. 2001b). Some of the best-known examples of ecosystems with alternative stable states include lakes transitioning from a clear to a turbid water state (Marten Scheffer and Stephen R Carpenter 2003b), drylands transitioning from vegetation to desert (Kéfi, Rietkerk, et al. 2007), or coral reefs shifting from a healthy coral dominance to being overgrown by macro-algae (Folke et al. 2004b; T. P. Hughes et al. 2018). These transitions occur when external conditions exceed critical thresholds known as "tipping points" (Lenton et al. 2008; Van Nes et al. 2016). Tipping points come in various forms, such as bifurcations, noise-induced shifts, and rate-dependent transitions (Ashwin et al. 2012). In particular, bifurcation tipping points typically correspond to pitchfork, subcritical Hopf, or saddle-node (fold) bifurcations (Erbach, Lutscher, and Seo 2013) (Russo and Spiliotis 2016). It is important to understand tipping point responses, because tipping points not only lead to abrupt changes but these changes can be hard to reverse. That is, if the conditions change in the opposite direction, the system will remain in the alternative state until it reaches another tipping point. The difference between the two tipping points is known as hysteresis and the existence of multiple alternative states is referred to as bistability (Marten Scheffer et al. 1998). As a result, there is mounting concern regarding the crossing of tipping points in environmental conditions, which can trigger catastrophic and potentially irreversible shifts in ecosystems.

In shallow lakes, alternative stable states refer to different ecological states that a lake system can attain and persist in. These states can be distinguished based on their physical, chemical, and biological characteristics, such as water clarity, phytoplankton biomass, and dominance of different species of aquatic plants and animals. The two most common alternative stable states in shallow lakes are related to a clear-water and a turbid-water state (Marten Scheffer, Hosper, et al. 1993). A clear-water state is characterized by a low nutrient concentration (typically phosphorus and nitrogen), which results in minimal algal growth, a dominant vegetation cover of submerged macrophytes, such as pond weeds or water milfoil, which stabilizes the sediment, provides shelter for phytoplankton consumers and altogether enhances water clarity. A turbid-water state is characterized by a high nutrient concentration that leads to excessive algal growth that shades out submerged macrophytes

and reduces their growth. Loss of submerged macrophytes can lead to increased sediment suspension that further reduces water clarity and further inhibits the growth of submerged macrophytes (Blindow, Hargeby, and Andersson 1998). This chain of events create a strong positive feedback that results in the emergence of alternative stable states in shallow lakes where shifts between clear and turbid water states occur in response to changes in external drivers, such as nutrient input or extreme weather conditions including droughts (Marten Scheffer and Jeppesen 2007; Marten Scheffer, S. Carpenter, et al. 2001b) (Faafeng and Mjelde 1998).

Various models of alternative stable states have been proposed in shallow lakes. The most common case describes the competition between phytoplankton and macrophytes in order to determine the level of nutrient loading at which a transition may occur, showed a highly non-linear response and hysteresis (Janse 1997). An aquatic Lotka-Volterra type food web model in shallow lakes was also used by (Kuiper et al. 2015) and showed the occurrence of alternative stable states. During eutrophication, the macrophyte-dominated clear-water state marked by a low level of chlorophyll-a disintegrates abruptly when the critical phosphorus loading is reached, shifting the system to a phytoplankton-dominated state. Another nutrient–phytoplankton–zooplankton model was used in (Zhang and W. Wang 2012) where discontinuous Hopf bifurcations were found and therefore bistable phenomenon occurred with the presence of a stable equilibrium and a stable limit cycle. In another model of competition between blue-green filamentous cyanobacteria and algae used in (Scheffer, Rinaldi, and Mur 1994; Marten Scheffer, Sergio Rinaldi, Gragnani, et al. 1997), alternative stable states occurred in response to turbidity where a cyanobacteria dominance state was found in shallow lakes. Additionally, a predator-prey model of plankton dynamics describing algae and zooplankton densities (Marten Scheffer, Sergio Rinaldi, and Kuznetsov 2000) showed that switches from one regime to another occur abruptly at a critical fish density. Bistability was also described in a model of competition for nutrients and light between free-floating macrophytes and submerged macrophytes in a shallow lake (Marten Scheffer, Szabo, et al. 2003b). Bistability in this ecosystem is a consequence of a strong positive feedback between free-floating macrophytes and submerged macrophytes, where floating macrophytes take precedence over light on the surface of the water. Dark anoxic conditions beneath dense layers of floating vegetation offer little habitat opportunity for flora and fauna and can have significant adverse effects on fishing and shipping in tropical lakes (Marten Scheffer, Szabo, et al. 2003b). Conversely, submerged macrophytes can thrive at lower nutrient levels, thereby reducing nutrient availability and diffusion to the surface (Hutchinson 1975). Thus, in response to nutrient loading, a shallow

lake can shift from a a coexistence state between submerged and floating macrophytes to a floating macrophytes dominance state.

But while ecological tipping points between alternative states have received extensive attention especially in the case of shallow lakes, there has been a significant neglect of evolutionary dynamics and trait changes, which also play a significant role in shaping the dynamics and stability of ecosystems (Hairston Jr et al. 2005) (Loeuille 2010). Large-scale ecological shifts triggered by tipping points can have profound impacts on species interactions, resource availability, and overall ecosystem functioning. These shifts can create selective pressures that influence the adaptive evolution of species traits. At the same time, trait dynamics, including genetic variation, mutation, and selection, can influence the capacity of populations to respond to ecological shifts (Dakos et al. 2019).

Only little theoretical work exists in studying how trait evolution and trait variation affects of shapes the bistable dynamics of ecosystems. For instance, fast environmental change mediated by high trait variation and eco-evolutionary feedbacks could drive regime shifts in ecosystems even before tipping points are crossed (Chaparro-Pedraza 2021). The introduction of evolutionary process can qualitatively affect the response of ecosystems with alternative stable states to increasing environmental stress and makes these ecological systems also sensitive to the rate at which environmental changes occur. Another study about the influence of evolution on the collapse and recovery pathways in bistable ecosystems using quantitative genetics in shallow lakes found that adaptive evolution has the capacity to either advance or delay thresholds at which a tipping points occur (Chaparro Pedraza et al. 2021). These alterations of trajectories of ecosystem collapse and recovery were proposed as a potential consequence of trait change in a bistable ecosystem (Dakos et al. 2019). Additionally, (Dercole, Ferrière, and Sergio Rinaldi 2002) found that including evolution of a trait that relates to competitive performance in a system where multiple ecological equilibria coexist can lead to adaptive reversals that drive cyclic alternation between alternative stable states. Work on arid ecosystems shows that the evolution of local facilitation does not lead to critically low population densities that would put the population at risk of extinction from random processes, but populations evolve towards trait values that are not viable (Kéfi, Baalen, et al. 2008). Interestingly, these populations consistently exhibit alternative stable states. This finding aligns with the results of (Gyllenberg and Parvinen 2001), where, in the case of a metapopulation model, if the transition to extinction is continuous, the extinction boundary acts as a repellent for evolutionary dynamics. In such cases, there is a very

low population density near the extinction boundary, allowing only mutants that are viable without the resident population to successfully invade. This mechanism keeps the strategy within a viable range, preventing extinction due to adaptation. Thus, a sudden transition to extinction, represented by alternative stable states, is a necessary condition for the evolution towards extinction, although it is not sufficient on its own.

Moreover, other studies have shed light on selection-induced regime shifts and the role of evolution in the occurrence of bistability. We know for example that a small ecological change can set the stage for a future tipping point where significant reduction in mortality rates initiated the evolution of body size, leading to a population shift over the long term (Chaparro-Pedraza and Roos 2020). Furthermore, studies indicated that the results of evolutionary rescue models can be influenced by the choice of fitness function (Osmond and Klausmeier 2017; Klausmeier, Osmond, et al. 2020). They showed that there exist evolutionary tipping points that, when crossed by increasing the rate of environmental change, abruptly lead the population to extinction. This feature (among many others) was also characterized analytically in (Garnier et al. 2023) that investigated more broadly the influence of the selection functions on the adaptation of sexually and asexually reproduction populations to a changing environment. Some other complex frameworks have been shown to lead to tipping points. For example, including an age structure to the population (Cotto and Ronce 2014) (Cotto, Sandell, et al. 2019) allows for feedback loops between the dynamics of the demography and the trait dynamics to create multiple co-existing equilibria that promote evolutionary tipping points. Another recent work (Ardichvili, Loeuille, and Dakos 2023) identified the necessary ecological mechanisms for the evolutionary emergence of alternative stable states using adaptive dynamics to study the evolution and diversification of a population of submerged macrophytes in a shallow lake. It showed that the emergence of different phenotypes and alternative stable states required a trade-off between nutrient availability and light availability, asymmetry in competition among individuals, and the presence of a priority effect. But aside from theses three mechanisms, the occurrence of a tipping point also depends on the relative position of the different phenotypes.

In this paper, we integrate evolutionary dynamics into an ecosystem model exhibiting ecological bistability to gain a deeper understanding of the influence of evolutionary processes on bistable ecosystems. We address two research questions. First, what are the evolutionary outcomes in an ecosystem that exhibits bistability? Particularly, does evolution drive the system towards or away

from regions with alternative stable states, and if so, how does evolution affect the ecological dynamics of the ecosystem? Second, what role does co-evolution play in shaping these evolutionary outcomes, and how does it influence the ecological dynamics of a bistable ecosystem? We investigate these two questions in the context of bistable shallow lakes. Our mathematical framework encompasses competition for light and nutrients between two types of aquatic plants: floating and submerged macrophytes. We extend the model used in (Ardichvili, Loeuille, and Dakos 2023) which explored the conditions under which the diversification of a submerged monomorphic macrophyte population could result in the emergence of alternative states and bistability. While keeping the same conditions, in our work we investigate the implications of introducing a competing (co-evolving) floating macrophyte population. We then use adaptive dynamics and a structured population model to study the evolution of a phenotypic trait of the two plants that characterizes their competitive ability, and to investigate the evolutionary and co-evolutionary behavior of the two types of macrophytes and their effects on the ecological dynamics of a shallow lake ecosystem.

## 1.2 Materials and methods

### 1.2.1 Model description

We describe the eco-evolutionary dynamics of the populations of two dominant plant types: submerged macrophytes **S** and floating macrophytes **F** in a shallow lake that compete for nutrients and light. Both species are characterized by a phenotypic trait $z$ that represents their growth depth and underlies their competitive ability for the two resources. We assumed in the first part of our study that (by definition) the floating macrophytes are fixed at the surface of the lake and have a phenotypic trait $z_f = 0$, while that the submerged macrophytes can grow along the water column with a phenotypic trait $z_s \in [0, z_b]$ where $z_b$ represents the depth of the lake.

We used an ecological model based on (Marten Scheffer, Szabo, et al. 2003b; Ardichvili, Loeuille, and Dakos 2023), defined by the following ordinary differential equations (ODEs):

$$\begin{cases} \frac{dS(t,z)}{dt} = rS\frac{Nu(z)}{Nu(z)+h_s(1+q(z)S+q(0)F)}\frac{1}{1+a(z,z)S+a(z,0)F+W(z)} - L_s(z)S \\ \frac{dF(t)}{dt} = rF\frac{Nu(0)}{Nu(0)+h_f(1+q(z)S+q(0)F)}\frac{1}{1+a(0,0)F} - L_f(0)F \end{cases} \tag{1.2.1}$$

Where $S(t,z) \in \mathbb{R}^+$ denotes the population size of the submerged macrophytes at time $t \geq 0$ with a trait $z \in [0, z_b]$ and $F(t) \in \mathbb{R}^+$ is the population biomass of the floating macrophytes. $r_{max}$ is the maximum growth rate of the two populations. The first parts of the two ordinary differential equations are typical limitation-based growth rates of populations S and F respectively 1.2.1. The first term accounts for nutrient limitation, while the second term for light limitation. Under unlimited nutrients and no shading or light limitation, growth rates would attain their maximum rate, $r_{max}$, but are diminished asymptotically to zero if resources become limited due to the consumption by the two competing macrophytes. Specifically, nutrient limitation is a decreasing function of the biomass of both macrophytes. It is modulated by the function $q(z)$, which characterizes the nutrient absorption rate increasing with the depth trait $z$, under the assumption that deeper macrophytes have greater nutrient accessibility as they are closer or rooted to the sediment. The strength of this priority effect is determined by the parameter $p$.

$$q(z) = q_0 \exp(pz)$$

Nutrient limitation depends also on the concentration of nutrients $Nu$ in the absence of macropyhtes that is diffused from the sediment to the surface of the water column as:

$$Nu(z) = \frac{Nu_0}{u\sqrt{2\pi}} \exp\left(\frac{-(z_b - z)^2}{u^2}\right)$$

with half saturation concentration constants $h_s$/ $h_f$ for the submerged/ floating macrophytes representing their respective competitive abilities.

Light limitation depends on background water turbidity and shading by competing and conspecific macrophytes. Water turbidity $W$ is an exponential function of depth $z$ with light attenuation strength $w$. Shading induced by con-specifics is a sigmoid function $a$, where the intensity of the asymmetry given by parameter $b$ is assumed to be high enough to prevent macrophytes from shading the ones that are above them.

$$W(z) = W_0 \exp(wz) - W_0$$

$$a(z_i, z_j) = \frac{2a_0 \exp(b(z_j - z_i))}{1 + \exp(b(z_j - z_i)))}$$

Lastly, we defined mortality functions $L_s(z)$ (for submerged macrophytes) and $L_f(z)$ (for floating macrophytes) to ensure that the two macrophytes do not grow at the same vertical levels (otherwise they would be indistinguishable) by setting an arbitrary depth threshold $z_{thres}$ above/below which

mortality becomes much higher ($l_{max}$) for submerged/floating macrophytes respectively compared to the default mortality ($l$):

$$L_s(z) = l - (l - l_{max}) \frac{z^i_{thres}}{z^i_{thres} + z^i}$$

$$L_f(z) = l_{max} - (l_{max} - l) \frac{z^i_{thres}}{z^i_{thres} + z^i}$$

Floating macrophytes are found on the water surface with their roots not attached to the sediment of the lake. However, submerged macrophytes completely grow underwater with roots attached to the bottom. This difference makes submerged macrophytes have a priority for access to nutrients, which reduces their availability in shallower depths, while floating macrophytes have an advantage on the access to light due to their position and have a shading effect on deeper submerged macrophytes, which reduces their access to light (Marten Scheffer, Szabo, et al. 2003b) (Ardichvili, Loeuille, and Dakos 2023). Also, we assumed that the submerged macrophytes do not exert a shading effect on the floating macrophytes. Consequently, the competition for light in the population of floating macrophytes is solely intraspecific, meaning it only occurs among individuals of the same species.

Based on the above, attenuation of light followed the Beer-Lambert law as described in $W$ 1.2.1, where $w$ determines the strength of light attenuation with depth $z$. Nutrients stored at the sediment of the lake diffuse to the surface with nutrient diffusion strength determined by $u$. Submerged macrophytes' priority effect on nutrients that negatively impacts floating macrophytes is represented by the function $q$ which increases with the growth depth $z$ according to the value $p$. In turn, the floating macrophytes limit submerged macrophytes growth because of the shading effect, whose steepness is determined by the parameter $b$ which represents the strength of asymmetry in competition for light.

Lastly, we defined the functions $L_s$ and $L_f$ so that the submerged macrophytes do not grow near the surface and to prevent the floating macrophytes from reaching deep levels to keep the two plant types distinct. We set the same inflection point for the two step functions at the trait threshold $z_{thres}$ below/above which the population has a high mortality and cannot survive. In order to tally with previous studies (Marten Scheffer, Szabo, et al. 2003b; Ardichvili, Loeuille, and Dakos 2023), we assumed that the mortality functions had the same minimum value of 0.05.

The parameter functions we used were based on previous work (Marten Scheffer, Szabo, et al. 2003b; Ardichvili, Loeuille, and Dakos 2023). The exponential nutrient diffusion and light attenuation functions capture the opposing that gradient can develop for light (from above) and nutrients (from below) in shallow lakes resembling similar work of modeling plankton dynamics (Klausmeier, Litchman, and Levin 2004). The shading effect accounts for direct asymmetric competition which is typically modeled by a sigmoid function (Kisdi 1999), whereas the exponentially decaying nutrient consumption efficiency (Ardichvili, Loeuille, and Dakos 2023) could have been also modeled linearly but with no difference in the results. Lastly, the mortality functions we introduced were artificially sigmoid only to set the biological difference between the two macrophytes (i.e. floating plants cannot grow where submerged plants grow and vice-versa).

Default parameter values are given in 1.1. Most values are based on previous work (cited in 1.1), while for the rest we made choices that allow for the existence of feasible ecological equilibria and alternative stable states. Specifically, maximum growth rate $r_{max}$ and half-saturation of the floating plants $h_f$ (Marten Scheffer, Szabo, et al. 2003b) fall within the spectrum of values documented in studies concerning duckweed growth (Landolt and Kandeler 1987; Hürlimann-Lüönd 1990). Half-saturation of submerged plants $h_s$ was defined as half of $h_f$ to simulate conditions where sediment-derived nutrient supply is twice as sufficient for submerged macrophytes growth (Marten Scheffer, Szabo, et al. 2003b). Floating macrophytes impact on water nutrient content $q_0$, baseline light attenuation $W_0$, and intra-specific light competition $a_0$ values were taken from (Ardichvili, Loeuille, and Dakos 2023) serving as a standard scenario for reproducing alternative stable states. We chose a weak strength of light attenuation $w = 0.1$, a strong priority effect $p = 0.5$ for the submerged macrophytes, and a high total nutrient concentration in the water $Nu_0 = 50$ to compensate the low light attenuation which provides an advantage to submerged macrophytes with a high nutrient concentration to facilitate the growth of floating macrophytes. The strength of asymmetry in intraspecific competition for light $b$ was set to a high value (=10) in order to prevent shading of lower plants to those above. Mortality functions were strongly sigmoid by setting $i = 10$ to restrict the growth of populations at a given depth threshold $z_{thres} = 2$ by setting the mortality rate $l_{max}$ above/below this threshold double the rate of the default mortality $l = 0.05$ for submerged and floating macrophytes respectively.

Table 1.1: Model variables and parameters, their definition and default values

| Variable/Parameter | Definition | Default value |
|---|---|---|
| $z$ | Growth depth | $\in [0, z_b]$ |
| $z_b$ | Bottom of the lake | 10 |
| $r_{max}$ | Maximum macrophyte growth rate | 0.5 |
| $l_{max}$ | Maximum of the mortality functions of | 0.1 |
| $l$ | Baseline mortality | 0.05 |
| $h_s$ | Submerged macrophyte dependency on water nutrient | 0.1 |
| $h_f$ | Floating macrophytes dependency on water nutrient | 0.2 |
| $Nu_0$ | Total nutrient concentration in the lake | 50 |
| $q_0$ | Floating macrophytes impact on water nutrient content | 0.005 |
| $W_0$ | Baseline light attenuation and light limitation | 1 |
| $a_0$ | Intra-specific light competition coefficient | 0.01 |
| p | Strength of priority effect | 0.5 |
| $z_{thres}$ | Threshold trait and inflection point of the mortality functions | 2 |
| $i$ | Strength of slope of the mortality functions | 10 |
| $w$ | Strength of light attenuation | 0.1 |
| $b$ | Strength of asymmetry in intrapecific competition for light | 10 |
| $\sigma^2$ | Initial phenotypic variance of **S** | |
| $\varepsilon$ | Seeding value | 0.001 |
| $u$ | Nutrient diffusion value | $\in [0, 10]$ |

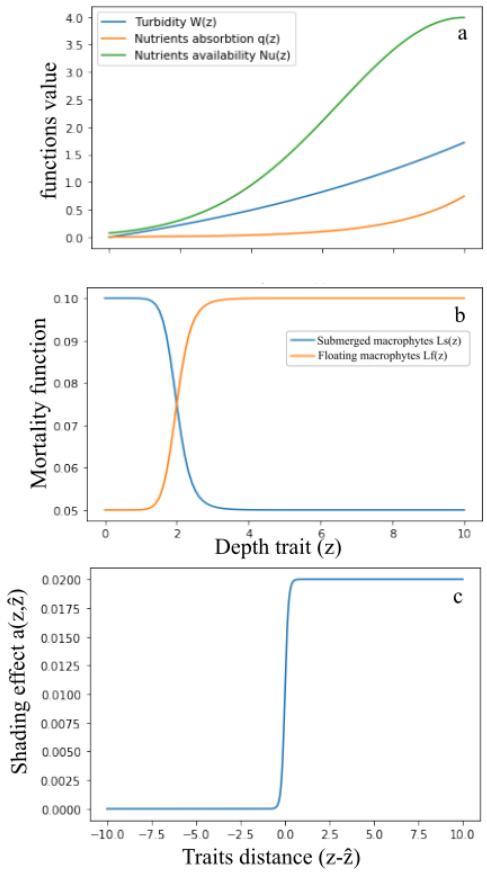



Figure 1.2.1: Mechanism functions : **(a) :** Water turbidity $W$ that increases with the depth. Impact of the plants of nutrient content and priority effect of the submerged macrophytes $q$. Nutrient availability in the water column $Nu$ when the nutrient diffusion $u = 5$. **(b) :** Mortality functions of **S** and **F** that prevent the submerged macrophytes to grow above the inflection point threshold $z_{thre}$ and floating macrophytes to grow below it. **(c) :** Shading effect for light competition according to the distance between conspecifics, where the function is set to 0 when the trait distance is negative, meaning that plants do not shade the other plants that are above them (with smaller trait) in the water column.

### 2.1.1 Adaptive Dynamics - Evolution of Submerged Macrophytes only

We used Adaptive Dynamics (AD) to investigate the evolution of the phenotypic trait $z$ of the submerged macrophyte population (Dieckmann and Law 1996b) (S. A. Geritz et al. 1998) (J. A. Metz, R. M. Nisbet, and S. A. Geritz 1992) (Diekmann et al. 2004). We recall that the floating macrophytes do not evolve and are fixed at the surface of the lake. Initially, the populations **S** and **F** are at their ecological equilibria determined by the external conditions. We define the fitness function of a mutant $S_m$ with trait $z_m$ as its long-time growth rate in an environment set by the resident populations $(S^*, F^*)$ :

$$s(z_m, z) = r\frac{n(z_m, z, S^*, F^*, S_m)}{n(z_m, z, S,^* F^*, S_m) + h}\frac{1}{1 + a(z_m, z)S^* + a(z_m, 0)F^* + W(z_m)} - L_s(z_m) \tag{1.2.2}$$

where $S^*$ and $F^*$ are the ecological equilibria of the populations of the submerged and floating macrophytes, and

$$n(z_m, z, S, F, S_m) = \frac{Nu(z_m)}{1 + q(z)S + q(z_m)S_m + q(0)F}$$

The direction of evolution is determined by the sign of the selection gradient defined as :

$$\frac{\partial}{\partial z_m}s(z, z) = \frac{\partial}{\partial z_m}\Big[s(z_m, z) = r\frac{n(z_m, z, S^*, F^*, S_m)}{n(z_m, z, S^*, F^*, S_m) + h}\frac{1}{1 + a(z_m, z)S^* + a(z_m, 0)F^* + W(z_m)} - L_s(z_m)\Big]_{|z=z_m} \tag{1.2.3}$$

A Singular point $\bar{z}$ is a trait value at which the selection gradient vanishes

$$\frac{\partial}{\partial z_m}s(\bar{z}, \bar{z}) = 0. \tag{1.2.4}$$

In the context of AD (Diekmann et al. 2004), a singular strategy refers to an evolutionary stable strategy (ESS) that cannot be invaded by any alternative strategy in a population. In our model, this means that if the majority of submerged macrophytes have a trait corresponding to the ESS, no rare mutant with a different trait can grow.

In order for $\bar{z}$ to be a local ESS, $\bar{z}$ should be a singular strategy meaning that it should satisfy the condition (Diekmann et al. 2004):

$$\frac{\partial^2}{\partial z_m^2} s(\bar{z}, \bar{z}) < 0 \tag{1.2.5}$$

The last condition is related to the stability of $\bar{z}$ for monomorphic populations. A singular strategy is also Convergence Stable Strategy (CSS) if the resident monomorphic population **S** has a strategy $\tilde{z}$ close to $\bar{z}$ such that successive beneficiary mutations bring the population's trait towards $\bar{z}$ (Diekmann et al. 2004). We consider a singular strategy as a CSS when the selection gradient is positive for $z < \bar{z}$ and negative for $z > \bar{z}$ (Diekmann et al. 2004). Therefore, a strategy $\bar{z}$ is a CSS if it meets the criteria of being a singular strategy and the following conditions :

$$0 > \left[ \frac{\partial}{\partial z} \left( \frac{\partial}{\partial z_m} s(z_m, z) \right)_{z_m = z_m} \right]_{z = \bar{z}} = \left[ \frac{\partial^2 s}{\partial z \partial z_m} + \frac{\partial^2 s}{\partial z_m^2} \right]_{z = z_m = \bar{z}}. \tag{1.2.6}$$

An interesting case occurs when mutants can invade the resident population both for larger and smaller traits. This mutual invasibility case is possible when $\bar{z}$ is CSS but not ESS, resulting in a branching point (BP) where from monomorphic population more than one phenotypes emerge. For a BP to occur, the singular strategy must apply (Diekmann et al. 2004):

$$\frac{\partial^2}{\partial z^2} s(\bar{z}, \bar{z}) > \frac{\partial^2}{\partial z_m^2} s(\bar{z}, \bar{z}) > 0 \tag{1.2.7}$$

### 2.1.2 Structured population model of phenotypic emergence - Evolution of Submerged macrophytes only

AD only allows to estimate long-term evolutionary attractors and their classification (Diekmann et al. 2004), but it does not capture the number and the characteristics of the multiple phenotypes during branching points. Thus, we used a quantitative genetics approach that considers a continuous trait distribution. Specifically, we employed a structured population model for selection, represented by a Partial Differential Equation (PDE), which enables the tracing of the distribution of trait values within a single population. To do this, we assumed a Gaussian distribution centered around the initial mean trait $z_0 = 8$ with minimal phenotypic variance $\sigma = 0.05$. We also neglected mutations, but we allowed different phenotypes to emerge simultaneously by seeding $\varepsilon$ submerged macrophytes across the total water column. In that way, the structured population model allows to explore in detail the emergence and potential coexistence of multiple phenotypes of the submerged macrophyte type.

In that sense, the structured population refers to the emergence and potential coexistence of multiple phenotypes that all belong to the submerged macrophyte type. Since we neglected the mutations in our model, we allow different phenotypes to emerge simultaneously by seeding submerged macrophytes across the water column. In other words, we initially consider a normal distribution of the submerged macrophytes with additional very small phenotypic input uniformly distributed along the trait set. This means that the initial condition resembles a Gaussian distribution with non decaying tails. Thus, model dynamics were generated only by competition and selection for **S** at time $t \geq 0$ with trait $z \in [0, z_b]$ which is a trait continuous version of the previous model :

$$\partial_t S(t,z) = \left( r_{max} \frac{Nu(z)}{Nu(z) + h(1 + \int q(x)S(t,x)dx + q0F)} \frac{1}{1 + \int a(z,x)S(t,x)dx + a(z,0)F + W(z)} - L_s(z) \right) S \tag{1.2.8}$$

We assumed that the floating macrophytes still follow the same dynamics as in 1.2.1:

$$\frac{dF(t)}{dt} = rF \frac{n(0,\bar{S},F)}{n(0,\bar{S},F) + h_f} \frac{1}{1 + a(0,0)F + a(0,\bar{z})\bar{S} + W(0)} - L_f(0)F$$

where $\bar{S}(t) = \int_0^{z_b} S(t,x)dx$ is the total size of the population of the submerged macrophytes and $\bar{z} = \frac{\int_0^{z_b} xS(t,x)dx}{\int_0^{z_b} S(t,x)dx}$ is the mean trait of the population.

Initially the population **S** follows a Gaussian distribution centered around the dominant mean trait $z_0$ with sample seeding along the trait space $[0, z_b]$ introduced through $\varepsilon$ :

$$S(0,z) = S^* \Gamma_{\sigma^2}(z - z_0) + \varepsilon$$

where $S^*$ is the initial ecological steady state (resident population size), $\Gamma_{\sigma^2}(x) = \frac{1}{\sigma\sqrt{2\pi}} \exp \frac{-x^2}{2\sigma^2}$ is the Gaussian Kernel and $z_0$ is the initial mean trait.

We assumed a continuous seed presence of phenotypes throughout the entire water column of the lake, thus we incorporated a sample seeding term $\varepsilon$ to facilitate the emergence of phenotypes even far from the mean dominant phenotype.

### 1.2.2 Co-evolution of Submerged and Floating macrophytes

### 2.2.1 Adaptive Dynamics : Co-evolution of the submerged and floating macrophytes

We also investigated a co-evolutionary scenario involving both floating and submerged macrophytes. In this co-evolutionary scenario, there was a constraint imposed on the growth limits of the two plant types. Specifically, floating macrophytes were restricted from growing at deep levels, while submerged macrophytes were restricted from growing at shallow levels. We implemented this constraint by using step mortality functions 1.2.1.

Following AD, we made the assumption that the two populations of submerged and floating macrophytes , characterized by their initial traits $z_s$ and $z_f$ respectively, are at their ecological equilibrium, denoted as $S^*$ and $F^*$. A mutant submerged plant, denoted as $S_m$, emerges with a trait value of $z_{s_m}$, and a mutant floating plant, denoted as $F_m$, appears with a trait value of $z_{f_m}$. The new system is described as follows:

$$(S')\begin{cases} \frac{dS(t,z_s)}{dt} = rS\frac{n(z_s,z_{sm},z_f,z_{fm})}{n(z_s,z_{sm},z_f,z_{fm})+h_s}\frac{1}{1+a_0S+a(z_s,z_{sm})S_m+a(z_s,z_f)F+a(z_s,z_{fm})F_m+W(z_s)} - L_s(z_s)S \\ \frac{dS_m(t,z_{sm})}{dt} = r_{max}S_m\frac{n(z_{sm},z_s,z_f,z_{fm})}{n(z_{sm},z_s,z_f,z_{fm})+h_s}\frac{1}{1+a(z_{sm},z_s)S+a_0S_m+a(z_{sm},z_f)F+a(z_{sm},z_{fm})F_m+W(z_{sm})} - L_s(z_{sm})S_m \\ \frac{dF(t,z_f)}{dt} = rF\frac{n(z_f,z_{fm},z_s,z_{sm})}{n(z_f,z_{fm},z_s,z_{sm})+h_f}\frac{1}{1+a_0F+a(z_f,z_{fm})F_m+a(z_f,z_s)S+a(z_f,z_{sm})S_m+W(z_f)} - L_f(z_f)F \\ \frac{dF_m(t,z_{fm})}{dt} = r_{max}F_m\frac{n(z_{fm},z_f,z_{sm},z_s)}{n(z_{fm},z_f,z_{sm},z_s)+h_f}\frac{1}{1+a_0F_m+a(z_{fm},z_f)+Fa(z_{fm},z_s)S+a(z_{fm},z_{sm})S_m+W(z_{fm})} - L_f(z_{fm})F_m \end{cases} \tag{1.2.9}$$

where

$$\begin{aligned} n(z_s,z_{s_m},z_f,z_{f_m}) &= \frac{Nu(z_s)}{1+q(z_s)S+q(z_{s_m})S_m+q(z_f)F+q(z_{f_m})} \\ n(z_{s_m},z_s,z_f,z_{f_m}) &= \frac{Nu(z_{s_m})}{1+q(z_s)S+q(z_{s_m})S_m+q(z_f)F+q(z_{f_m})} \\ n(z_f,z_{f_m},z_s,z_{s_m}) &= \frac{Nu(z_f)}{1+q(z_s)S+q(z_{s_m})S_m+q(z_f)F+q(z_{f_m})} \\ n(z_{f_m},z_f,z_s,z_{s_m}) &= \frac{Nu(z_{f_m})}{1+q(z_s)S+q(z_{s_m})S_m+q(z_f)F+q(z_{f_m})} \end{aligned}$$

We defined the respective fitness functions of the mutants $S_m$ and $F_m$ as:

$$\begin{cases} s_s(z_{s_m},z_s) = r\frac{n(z_{sm},z_s,z_f,z_{fm})}{n(z_{sm},z_s,z_f,z_{fm})+h_s}\frac{1}{1+a(z_{sm},z_s)S^*+a(z_{sm},z_f)F^*+W(z_{sm})} - L_s(z_{sm}) \\ s_f(z_{f_m},z_f) = r\frac{n(z_{fm},z_f,z_s,z_{sm})}{n(z_{fm},z_f,z_s,z_{sm})+h_f}\frac{1}{1+a(z_{fm},z_f)F^*+a(z_{fm},z_s)S^*+W(z_{fm})} - L_f(z_{fm}) \end{cases}$$

where the mutants are initially assumed to be rare $S_m = F_m \sim 0$ and the residents are at their ecological equilibrium $S = S^*$ and $F = F^*$.

The respective fitness Gradients are defined by :

$$\begin{cases} \frac{\partial s_s}{\partial z_{sm}}(z_s, z_s)_{|z_s = z_{sm}} \\ \frac{\partial s_f}{\partial z_{fm}}(z_f, z_f)_{|z_f = z_{fm}} \end{cases} \tag{1.2.10}$$

### 2.2.2 Structured population model : Co-evolution of the submerged and floating macrophytes

To assess the final outcome of the co-evolutionary process, we used a structured population model to describe the dynamics of the submerged macrophytes and the floating macrophytes populations:

$$\begin{cases} \partial_t S(t,z_s) = \Big(r_{max}\frac{Nu(z_s)}{Nu(z_s)+h(1+\int q(x)(S(t,x)+F(t,x))dx}\frac{1}{1+\int a(z_s,x)S(t,x)dx+\int a(z_s,x)F(t,x)dx+W(z_s)} - L_S(z_s)\Big)S(t,z_s) \\ \partial_t F(t,z_f) = \Big(r_{max}\frac{Nu(z_f)}{Nu(z_f)+h(1+\int q(x)(S(t,x)+F(t,x))dx)}\frac{1}{1+\int a(z_f,x)F(t,x)dx\int a(z_s,x)S(t,x)dx+W(z_f)} - L_f(z_f)\Big)F(t,z_f \end{cases}$$

Similarly to the analysis of the submerged macrophytes' only evolution (section 2.1.2), we assumed that initially both the submerged macrophytes and the floating macrophytes populations were normally distributed around their respective resident mean traits. Additionally, we assumed a uniform seeding of these populations along the lake. This seeding process ensured that individuals with varying traits were present throughout the lake, allowing for potential evolutionary changes in both populations.

### 1.2.3 Numerical methods

In this section, we explain the numerical methods we followed, as analytical expressions for the eco-evolutionary dynamics of our shallow lake ecosystem were not possible to derive.

The analysis took place in two steps: first, we solved the ODE equations 1.2.1 in order to find the different equilibria of the system and determined the ecological steady states $(S^*, F^*)$ for each nutrient diffusion value $u \in [0, 10]$ and trait $z \in [0, z_b]$ using the python function **odeint** from the

scipy package. This yields the two-dimensional bifurcation analysis where we identified regions of qualitatively different behaviors corresponding to different stable equilibria of the system for each $(u, z)$ combination. The second step used AD for finding the singular strategies (i.e., the roots of the gradient fitness 1.2.4) for different environmental conditions set by the parameter coefficients and the ecological equilibria $(S^*, F^*)$ using the Newton-Raphson method. In the presence of alternative stable states, the ecological equilibria used in the fitness equation 1.2.2 are the states with a positive population size of submerged macrophytes. We did not consider the alternative state of the floating macrophytes dominance since the submerged macrophytes are the evolving species and a resident population is needed. Subsequently, we determined the nature of the distinct singular strategies by assessing the stability and convergence conditions through the evaluation of second derivatives (see equations 1.2.5, 1.2.6, and 1.2.7). We completed the bifurcation analysis by incorporating the different CSS, ESS, and branching points for each nutrient diffusion value $u$.

For the structured population model simulations 1.2.8, we used the explicit Euler method with Neumann boundary condition that specifies the normal derivative at the boundary to be 0 with a numerical discretization of the finite trait space $[0.1, z_b = 10]$ using a step $\Delta z = 0.1$. This analysis allows us to gain insights into the dynamics and trends exhibited by the population over an extended period, providing a holistic perspective on the evolutionary processes and their ultimate consequences. We used arbitrary long simulation times of $N = 30000$, $N = 50000$ and N=70000 for different examples of nutrient diffusion values $u$ and the initial conditions $S(0, z) = S^*\Gamma_{\sigma^2}(z - z_0) + \varepsilon$ and $F(0) = F^*$ where $\varepsilon$ represents the seeding of the submerged macrophytes uniformly distributed across the entire the lake. We assumed $\varepsilon << 1$. This assumption is made because we neglected mutations in our analysis, and our objective was to enable the growth of distinct traits in the submerged macrophyte population.

We used the total population size $\bar{S}(t)$, the emergence of different phenotypes, and the density distribution $\mathbf{S}$ to describe the evolutionary outcome of the population of submerged macrophytes. For each of the 100 nutrient diffusion values $u \in [0.1, 10]$, we ran simulations for a long arbitrary number of iterations $N \in \{30000, 50000, 70000\}$ and considered the final population size and the trait distribution to determine the asymptotic behavior of the population $S$. If the total population size was below the threshold defined as the initial seeding ($< \varepsilon$), then it was considered extinct. The presence of an evolutionary cycle was determined by analyzing the difference between the maximum

and minimum values of the total mass of submerged macrophytes over the last 15000 time steps. If this difference remained relatively large ($> 0.5$) or displayed recurring patterns of oscillation, it indicated the existence of cyclic behavior. Lastly, if the population size stabilized, then we assumed that the submerged macrophytes have evolved towards a monomorphic or polymorphic state according to the final trait distribution of the population.

## 1.3 Results

### 1.3.1 Ecological dynamics

Theoretical and empirical work suggest that shallow lakes may exhibit alternative stable states in response to variations in nutrient concentration -a condition that is strongly related to eutrophication (Marten Scheffer, Szabo, et al. 2003b; Blindow, Hargeby, and Andersson 1998; Janse 1997). In our study, we thus focus on the evolutionary outcomes along a gradient of nutrient diffusion rate $u$ as it is the parameter that significantly influences the distribution of nutrients across the water column (See S1).

Our study focused on a specific scenario characterized by high nutrient concentration ($Nu_0 = 50$), low light attenuation ($w$=0.1), and a strong asymmetry in competition for light ($b$=10). This parameters choice was deliberate because it allowed us to identify a range of ecological equilibrium states and wide regions of bistability (different scenarios are illustrated in SI B. Fig. S2 highlighting less rich ecological equilibria.). These environmental parameter settings give rise to a bifurcation diagram in the (u,z)-plane, where the ecological dynamics of shallow lakes are strongly influenced by nutrient diffusion rate $u$ (Fig. 1.3.1). Figure 1.3.1 illustrates six distinct ecological steady states that differ qualitatively. When nutrient diffusion rate is low, either none of the two populations grows for the non-availability of the resources (I in Fig. 1.3.1) or only the submerged macrophytes invade (III in Fig. 1.3.1), outcompeting the floating macrophytes because of their priority effect on the nutrients. Increasing the level of nutrient diffusion rate ($u > 5$) allows the floating macrophytes to grow (V in Fig. 1.3.1)and even outcompete the submerged macrophytes that are at higher depths (II in Fig. 1.3.1). A coexistence state also emerges for certain ranges of (u,z) (V in Fig. 1.3.1). Higher nutrient diffusion rate generates two additional regions with bistability. In these bistable regions (IV and VI in Fig. 1.3.1), different alternative stable states are present. In the first region (IV), the two alternative states possible are either only floating or only submerged macrophytes presence, whereas

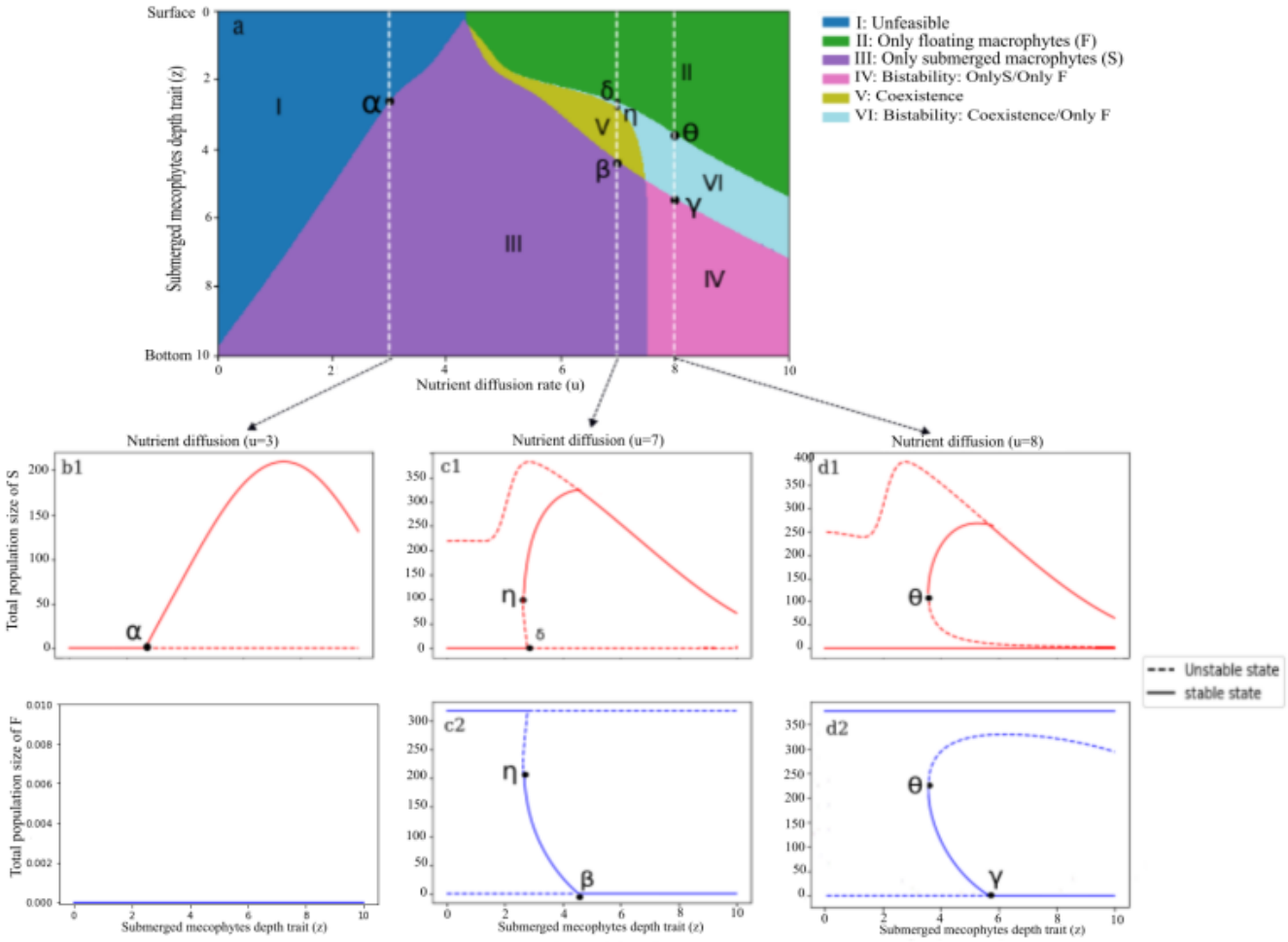



Figure 1.3.1: **Top :** Bifurcation diagram in a (u,z)-plane, where the trait of submerged macrophytes and the nutrient diffusion $z, u \in [0, 10]$, with $z = 0$ being the surface and $z_b = 10$ the bottom of the lake. The different colors represent the different stable equilibria of the system 1.2.1. For low nutrient diffusion, either none of the two populations grows (I) or only the submerged macrophytes are able to invade (III). When $u$ increases, a coexistence state appears (V), a region where the floating macrophytes outcompete the submerged (II), and two different bistability zones emerge. In the region (VI), the two alternative stable states are coexistence or an only **F** state and in the region (IV), the alternative stable states are a floating macrophytes dominance or a submerged macrophytes' dominance. **Bottom:** Equilibrium biomass of the submerged and floating macrophytes (S,F) for specific values of nutrient diffusion $u$ according to the growth depth of the submerged macrophytes $z$. $(a) u = 3$: steady-states for low nutrient diffusion, where only the submerged macrophytes **S** can grow starting from a certain depth $\alpha$. $(b) u = 7$: we observe the different equilibria according to the trait $z$ : when the submerged macrophytes are near the surface, only the floating macrophytes **F** grow while they get outcompeted when **S** are near the bottom. A coexistence stable state is possible when the submerged macrophytes are in intermediate levels, and a small bistable zone (VI) occurs between two tipping points $z \in [\delta, \eta]$ with only **F** and coexistence as alternative stable states.$(c) u = 8$: Another bistability emerges (IV) of either submerged macrophytes dominance or a floating macrophytes' dominance when $z < \gamma$.

in the second bistable region (VI), a coexistence state is possible along with a floating macrophytes dominance alternative state. These alternative stables states result from different mechanisms; a trade-off between nutrients and light, where the parameter of nutrient diffusion rate $u$ determines the distribution of the nutrients in the water column and the decrease of luminosity in deeper levels is determined by light attenuation $w$ (Marten Scheffer, Szabo, et al. 2003b), a priority effect effect of the submerged macrophytes for nutrient access, determined by $p$ and asymmetrical competition for light (Ardichvili, Loeuille, and Dakos 2023).

Bifurcation plots of the submerged and floating macrophytes biomass for specific values of nutrient diffusion rate give more insights on the ecological equilibira of the system. In the case of nutrient diffusion rate $u = 3$ (Fig. 1.3.1 b1, b2), the floating macrophytes never grow and the submerged macrophytes start growing at trait $z = \alpha$. When the nutrient diffusion rate $u = 7$ (Fig. 1.3.1 c1, c2), a coexistence state and a floating dominance alternative state are present (bistable region (VI)) where the submerged macrophytes switch abruptly from a coexistence state to their extinction when their depth trait $z$ approaches the lake surface and crosses the tipping point$z = \eta$. When the trait $z$ of the submerged macrophytes change in the opposite direction and increases from 0, the population **S** shifts from extinction to coexistence at the point $z = \sigma$. When the nutrient diffusion rate increases to $u = 8$ (Fig. 1.3.1 d1,d2), a floating macrophytes dominance is the unique stable state when the trait $z$ is low, but when $z \in [\theta, \gamma]$, a coexistence alternative stable state emerges (bistable region VI). Above that threshold, when $z > \gamma$, the floating macrophytes go extinct and the remaining alternative states are floating macrophytes dominance or submerged macrophytes dominance (bistable region IV).

### 1.3.2 Evolutionary asymptotic analysis

#### 3.2.1 Singular evolutionary strategies from Adaptive Dynamics

For the evolutionary analysis, starting only with the evolution of submerged macrophytes, we show how selection operates in the presence of floating macrophytes fixed to the surface when nutrient diffusion rate $u$ increases and the submerged macrophytes population **S** is precluded from growing near the surface. Figure 1.3.2 shows the singular evolutionary strategies of the evolving submerged macrophytes on top of the underlying ecological states in the (u,z)- plane. When nutrient diffusion rate is $u < 4.5$, floating macrophytes are absent, resulting in a situation akin to the model proposed by (Ardichvili, Loeuille, and Dakos 2023) for the evolution of submerged macrophytes in the absence of

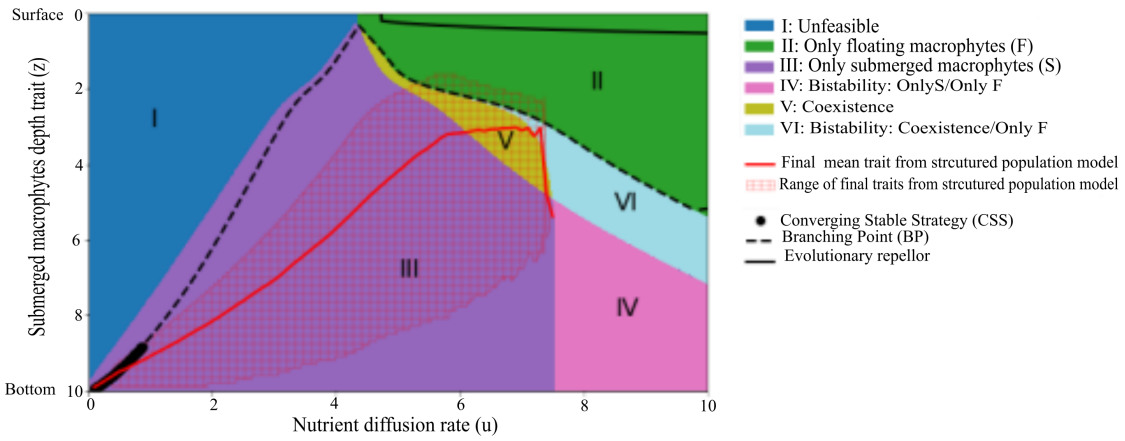



Figure 1.3.2: Bifurcation diagram with singular strategies obtained as roots of the gradient fitness 1.2.4 from the AD framework for each nutrient diffusion rate $u$. The red line represents the final mean trait of the long time distribution of the submerged macrophytes population obtained from the structured population model simulations. The red hatches represent the range of the present phenotypes in the limit distribution of the population of submerged macrophytes **S**, which indicates the trait variation of the submerged macrophytes. The line and the hatches stop when the population **S** doesn't persist and goes extinct.

floating macrophytes . The submerged macrophytes population evolves towards a CSS characterized by a monomorphic population when $u$ is very low $u < 1$. Alternatively, when $1 < u < 4.5$, the population reaches a branching point, leading to the emergence of a polymorphic population with multiple phenotypes (III in Fig. 1.3.2) . When $u$ exceeds 4.5, different ecological scenarios are possible, and the evolutionary strategies appear to lie precisely on the bifurcation points between feasible regions of the submerged macrophytes (V, VI in Fig. 1.3.2) and the extinction state of **S** (II in Fig. 1.3.2). In other words, the population of the submerged macrophytes will evolve towards the surface, crossing either the coexisting region (zone V) when $u < 7.5$ or the bistability region characterized by the alternative states of coexistence or only floating macrophytes (zone VI) when $u > 7.5$.

### 3.2.2 Evolutionary oscillations and evolutionary suicide from the structured population model

While AD allowed us to determine the expected phenotypic trait towards which the population of submerged macrophytes will evolve, simulations of the structured population model provided us with the long-term trait distribution of the submerged macrophytes population in the cases when the singular strategy was a BP. We plotted the final mean trait (red line in Fig. 1.3.1) and the range of all present traits (red hatched area) of the asymptotic distribution of the simulated submerged macrophytes phenotypes in Fig. 1.3.1 (a similar result is found if we consider the median trait

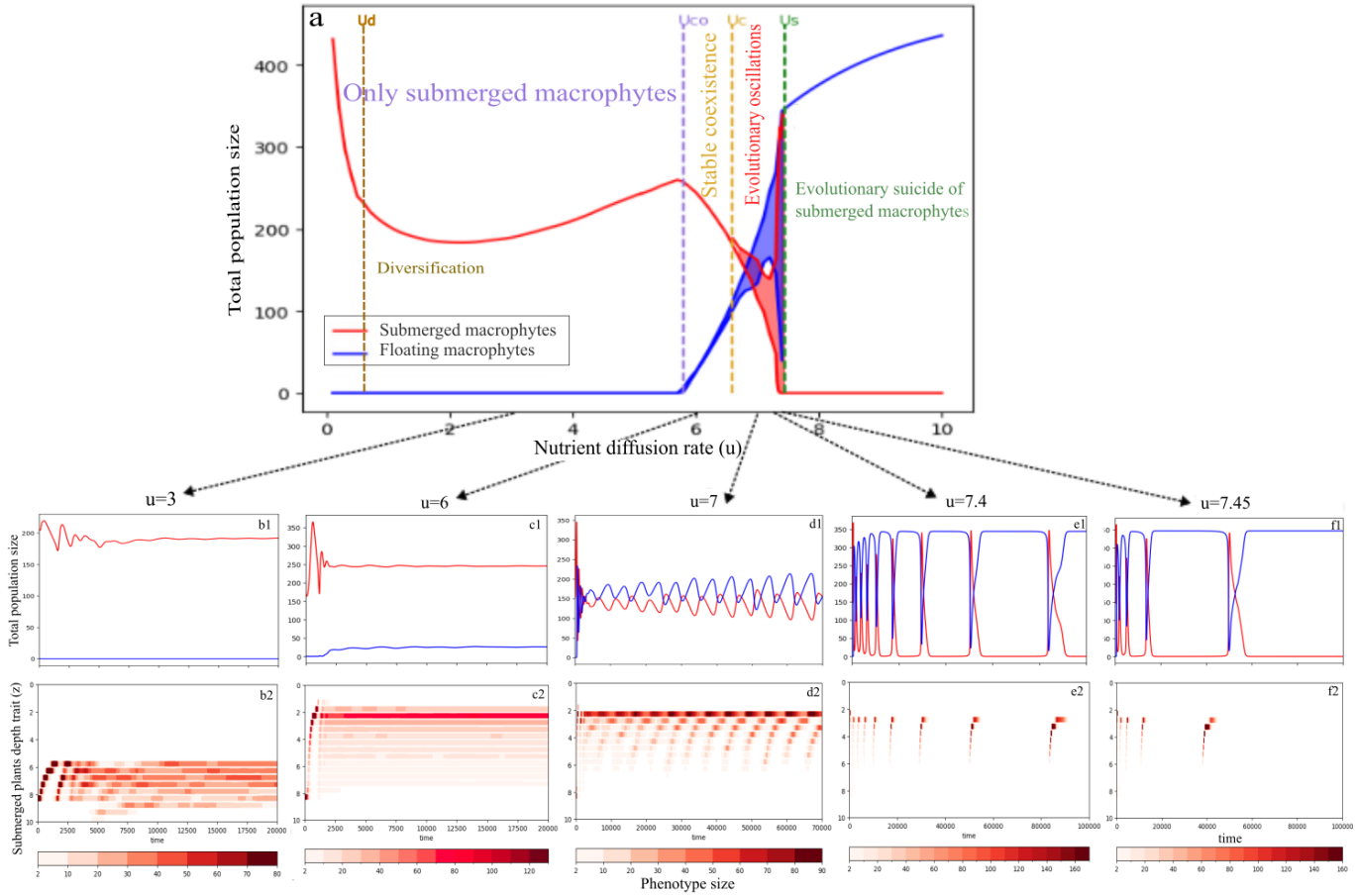



Figure 1.3.3: **top:** $(a)$ : Final total population size of submerged **S** and floating macrophytes **F** from the structured population model simulations as a function of nutrient diffusion rate $u$, where we observe different evolutionary outcomes as $u$ increases and where $U_d = 0.5$ : beginning of diversification, $U_{co} = 5.8$ : beginning of coexistence of the submerged macrophytes with the floating plants, $U_c = 6.78$ : beginning of oscillations and $U_s = 7.45$ : beginning of extinction of the submerged macrophytes. More precisely we observe :
For $u \in [0, U_d[$ **:** Evolution of the submerged macrophytes **S** towards a monomorphic steady-state in the absence of the floating macrophytes. $u \in [U_d, U_{co}[$ **:** Diversification of the submerged macrophytes **S** towards a polymorphic steady-state in the absence of the floating macrophytes. $u \in [U_{co}, U_c[$ **:** Evolution of **S** towards a stable equilibium of coexistence with **F**. $u \in [U_c, U_s = 7.45[$ **:** Beginning of oscillations where is represented the minimum and maximum of the population size during a cycle (amplitude of oscillation). $u \in [U_s, z_b]$ **:** Beginning of evolutionary suicide, where **S** experiences evolutionary suicide.
**bottom:** Total population size of submerged $\int S(t,z)dz$ and floating macrophytes $F(t)$ through time using the structured population model (b1-f1). Emergence of different phenotypes (trait $z$) through time quantified in intervals of 0.5 of the trait as $\int_i^{i+0.5} S(t,z)dz$ using a threshold of detection $\epsilon$ for different nutrient diffusion rate values $u$ (b2-f2). This leads to different evolutionary outcomes: $b1, b2)$ $u = 3$ : Evolution towards an equilibrium of diversification of the population **S** without the presence of the floating macrophytes. $c1, c2)$ $u = 6$ : Evolution towards a steady-state of coexistence between the submerged and the floating macrophytes. $d1, d2)$ $u = 7$ *and* $e1, e2)$ $u = 7.4$ : Emergence of evolutionary oscillations of different amplitude and $f1, f2)$ $u = 7.45$ : Evolution towards the extinction of the submerged macrophytes.

instead of the mean). Interestingly, we found that the adaptive dynamics singular strategies and the evolutionary outcomes from the structured population model approaches are similar only to a certain extent. Specifically, the diversification of the submerged macrophytes population in the structured population model coincides with the predicted branching points from AD (Fig. 1.3.2). However, in the structured population model, the mean trait of the submerged macrophytes population does not match the trait values predicted by AD except for very low nutrient diffusion rates $u < 1$, where the CSS predictions of AD coincided with the single final dominant trait observed in structured population model. Nevertheless, the diversification initiated at lower nutrient diffusion rates compared to the initial branching points predicted by the AD framework. This discrepancy is due to two distinct factors: firstly, the AD approach foresees, for the majority of nutrient diffusion rates, the emergence of branching points, but it does not precisely specify the ultimate positions of the emerged traits (Diekmann et al. 2004). Conversely, AD considers small, rare mutations that we did not incorporate into our structured population model. Instead, we have neglected the effects of mutations but allowed the simultaneous emergence of different traits within the population (see section 2.1.2 ). This assumption can be likened to the scenario of very frequent and substantial mutations (We refer to Fig. S5 in the SI. E for the final mean trait of the population with frequent mutations), or to the presence of a seed bank in the lake (Kaplan and Muer 1990) (McFarland and Rogers 1998), which allowed the rapid emergence of different phenotypes leading to polymorphisms with potential dominant traits. Consequently, these emergent phenotypes influenced fitness through competition, potentially explaining the disparity with AD predictions.

But a closer look at the eco-evolutionary dynamics from the structured population model simulations revealed that the trajectories of the emerged phenotypes were not always stationary but oscillating (panel a in Fig. 1.3.3) In fact, we found that selection towards increased nutrient diffusion rate led to 4 distinct evolutionary behaviors before eventually reaching evolutionary suicide (Fig. 1.3.3). Firstly, there is the convergence towards a stable equilibrium characterized by either a monomorphic or polymorphic population of submerged macrophytes dominance. Secondly, the submerged macrophytes can evolve to a stable equilibrium of coexistence with the floating macrophytes. Thirdly, evolution can manifest as cyclic behavior with the presence of both the submerged and the floating macrophytes oscillating at bigger amplitude as $u$ becomes higher. Finally, the submerged macrophyte population evolves to extinction (evolutionary suicide or Darwinian extinction (Webb 2003b)).

At low nutrient diffusion rate ($u < U_{co} = 5.8$) (Fig. 1.3.3 a), the submerged macrophytes evolve into a submerged macrophytes dominance state. When $u \in [U_{co}, U_c = 6.78[$, the evolution of **S** leads to their coexistence with the floating macrophytes **F**. In panels (Fig. 1.3.3 b1,b2) when the nutrient diffusion rate $u = 3$ and the initial population of submerged macrophytes has a mean trait $z_0 = 8$, the evolution leads to stable equilibrium in the absence of the floating macrophytes (Fig. 1.3.3 b1). The initial seeding allows submerged macrophytes with different traits to grow simultaneously and rapidly, resulting in a large trait variation in the population **S** which leads to a polymorphism with different traits present from 4 to 8 (Fig. 1.3.3 b2).

When the nutrient diffusion rate exceeds $U_{co}$, the floating macrophytes are able to grow and coexist withe submerged macrophytes. In panel (Fig. 1.3.3 c1,c2) when $u = 6$, the population size of **F** increases and the submerged macrophytes evolve towards a coexistence steady-state (Fig.1.3.3 c1). Different phenotypes start growing towards the surface within the population **S**, until reaching the inflection point of the mortality function $L_S$ 1.2.1 $z_{thres} = 2$ level at which the population concentrates with a wide phenotypic variance (Fig. 1.3.3 c2).

At nutrient diffusion rate ($u \geq U_c$), evolutionary oscillations emerge with larger and larger amplitudes as $u$ increases. In panel (Fig. 1.3.3) d1,d2 when $u = 7$, starting from a resident population **S** with initial mean trait $z_0 = 8$ in the absence of the floating macrophytes , these latter grow rapidly and the two population sizes of **S** and **F** start oscillating (Fig. 1.3.3 d1). We observe the rapid emergence of new traits at higher depths up to the turning threshold feature $z_{thres} = 2$ defined by the step mortality function, in which the majority of the population settles down as it has the best access to light, while the rest of the population stays at deeper depths where it grows, increasing the total population size of **S**, and then disappears due to the intrapecific competition for light and shading effect (Fig. 1.3.3 d2).

At nutrient diffusion rate $u = 7.4$ in panel (Fig. 1.3.3 e1,e2), a similar scenario occurs, with evolutionary oscillations resulting from dynamics driven by competition and selection. At this $u$ rate, however, the population of floating macrophytes reaches high total biomass due to higher nutrient diffusion rate, resulting in a strong shadowing effect on the submerged macrophytes which almost die out before being rescued by the emergence of deeper phenotypes, resulting in larger fluctuations in one limit cycle. When the nutrient diffusion rate $u$ ramps up a little more to $U_s = 7.45$ (Fig. 1.3.3 f1,f2), it traverses a homoclinic bifurcation where the limit cycle grows such that the population of submerged macrophytes

eventually transitions to the alternative stable state of extinction due to the bistability present. Then all trajectories belong to the attraction basin of the extinction state of the submerged macrophytes. In other words, selection leads to the evolutionary suicide of the submerged macrophytes population. It is worth noting that in the absence of the floating macrophytes, the submerged macrophytes persist under the same conditions. SI. D (Fig.S4) summarizes the distributions of the submerged macrophytes population at different time steps for the examples of nutrient diffusion rates studied above.

### 1.3.3 Co-evolution of submerged and floating macrophytes

In the previous section we presented the case where only the submerged macrophytes population evolved. In this section, we explored the role of co-evolution by repeating the previous analysis while allowing for the evolution of the floating macrophytes as well. Note that we imposed a step mortality function for both macrophytes types with an arbitrary inflection point at $z_{thres} = 2$ to prevent the submerged macrophytes from growing above the threshold of $z_{thres}$ and to prevent the floating macrophytes from growing below it. We did this because in the absence of such constrain, we would observe each macrophytes type to evolve into its competing type; a situation of reversal that ecologically would be meaningless.

In Figure 1.3.4, we first mapped the ecological equilibria in the $(z_f, z_s)$-plane for two nutrient diffusion rates $u = 7$ and $u = 7.6$ (panels a and b). In both cases, floating macrophytes cannot grow towards the bottom of the lake due to a high mortality rate (II). However, when both traits $z_f$ and $z_s$ are sufficiently low, the floating macrophytes can either outcompete the submerged macrophytes (I) or coexist with them (III), depending on the depth of the submerged macrophytes $z_s$. Relative bistability regions appear (IV) where the two alternative stable states are a coexistence or a floating macrophytes dominance state. Interestingly, the two populations never occupy the same depth. When $z_f$ is set to 0, we revert to the scenario where the floating macrophytes were fixed at the surface, and a bistability zone is observed. In the first case of $u = 7$ (Fig. 1.3.3 a1), this zone widens as the depth of the floating macrophytes increases, until reaching approximately $z_f \sim 2$. In the second scenario $u = 7.6$ (Fig. 1.3.3 b1), we observe a similar result with a bigger bistable region which inversely becomes narrower as $z_f$ increases .

In these specific examples, we did not find any evolutionary equilibria or singular strategies using AD. This implies that there is no combination of traits that results in both the floating and submerged

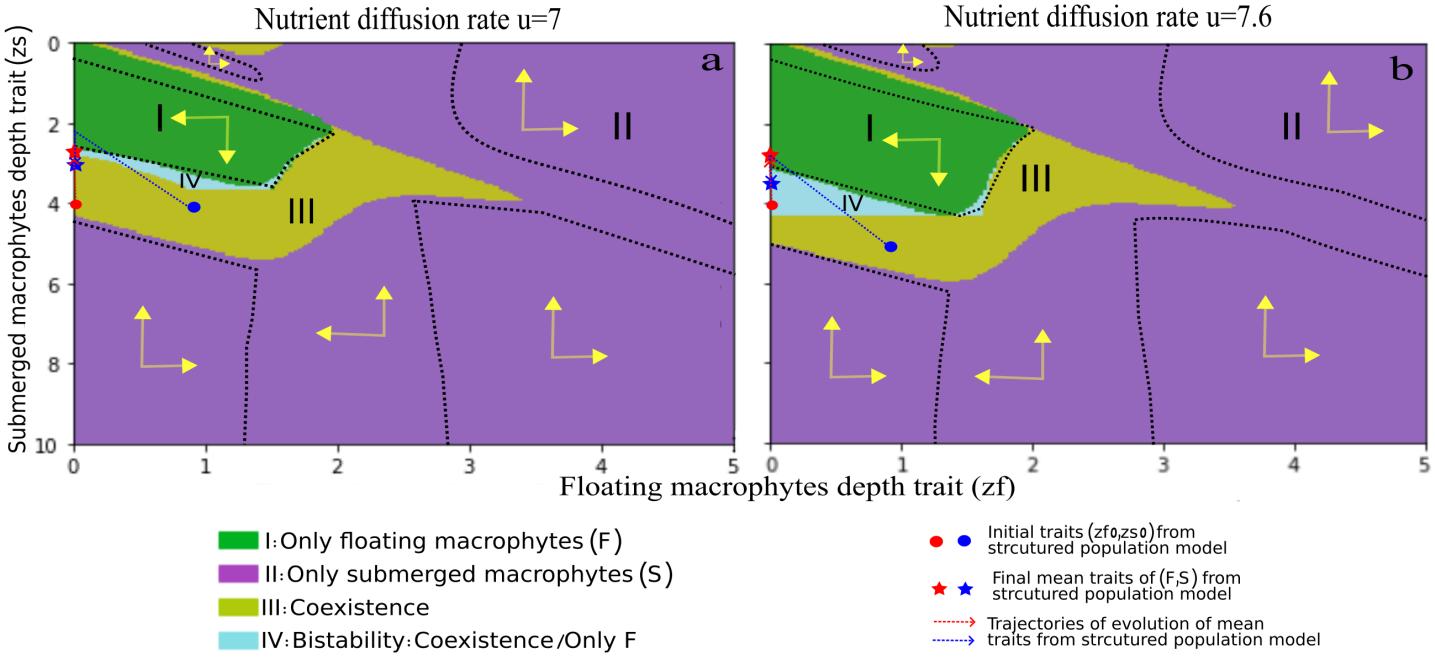



Figure 1.3.4: Bifurcation diagrams for ecological equilibria of **F** and **S** with traits $z_f$ and $z_s$, respectively, when the nutrient diffusion rate $u = 7$ in $(a)$ and $u = 7.6$ in $(b)$. The yellow arrows indicate the direction of evolution of the trait $z_f$ of **F** and trait $z_s$ of **S** in each dotted region, according to the sign of their respective fitness gradients from the AD framework. We used the structured population model under the same set of parameter to simulate the co-evolution of **S** and **F** starting from initial phenotypes $z_{f_0} = 0$ and $z_{s_0} = 4$ (red dots). The results showed that when $u = 7$ in $(a)$, the floating macrophytes population remained at the surface with a final trait of $z_f = 0$, while the submerged macrophytes evolved to greater depths, resulting in diversification with final mean trait of $z_s = 2.56$ (red star) in $(a)$. However, in $(b)$ when $u = 7.6$ the submerged macrophytes evolved to similar depths but didn't persist as this position fell within a bistable region where the extinction of **S** was an alternative stable state (red star).
We used another examples of initial positions $z_{f_0} = 1$ and $z_{s_0} = 4$ (blue dot) when $u = 7$ where the floating macrophytes evolved towards the surface, reaching a final trait $z_f = 0$ while the submerged macrophytes grew at greater depths, later moving deeper again with a final mean trait $z_s = 3.1$ where they coexist with **F** (blue star) in $(a)$. In the case of $u = 7.6$ in $(b)$, we studied the scenario with initial positions $z_{f_0} = 1$ and $z_{s_0} = 5$ where both populations took the same trajectory towards a final position of the floating macrophytes $z_f = 0$ which outcompeted the submerged macrophytes which evolved towards the surface and then went back to deeper depths in the bistability region (blue star) in $(b)$.

macrophytes having zero fitness gradients simultaneously (equations 1.2.10). Instead, we only used the direction of selection based on the signs of the fitness gradients, which indicate the trajectory towards which floating and submerged macrophytes are likely to co-evolve (yellow arrows in Fig. 1.3.4). To find the actual co-evolutionary trajectory, we used the structured population model. For example, by initially setting the traits of the submerged and floating macrophytes to ($z_{s_0} = 4, z_{f_0} = 0$) (red dots in Fig. 1.3.4, we estimated the evolutionary simulated trajectory (red dashed line) showing that the floating macrophytes stayed at the surface while the submerged macrophytes diversified towards a mean trait of $z_s = 2.56$ when $u = 7$ (red cross in a in Fig. 1.3.4) while in panels b1,b2 when $u = 7.6$, the submerged macrophytes evolved towards a mean trait $z_s = 3.01$ which lies within the bistable region (IV) where the population **S** went extinct. In another example when the nutrient diffusion rate $u = 7$, we set the initial populations at initial mean traits $z_{s_0} = 4$ and $z_{f_0} = 1$ (blue dot in panels a1,a2), the floating macrophytes evolved towards the surface and the submerged macrophytes grew at higher depths until reaching a mean trait of $z_s \sim 2.5$ before evolving back to deeper levels with a final mean trait of $z_s = 3$ (blue star in a). Similarly, in the case of $u = 7.6$, we studied the evolution of **S** and **F** initially set at $z_{s_0} = 5$ and $z_{f_0} = 1$ (blue dot in panels b in Fig. 1.3.4) where the two populations adopted a similar trajectory but in this case leading to the suicide of the submerged macrophytes (blue star in b).

Using the structured population model, we simulated the co-evolution of the submerged macrophytes and the floating macrophytes considering the final population sizes of **S** and **F** ($\int S(t_f, z)dz$ and $\int F(t_f, z)dz$ respectively) Fig. 1.3.5. On first sight, the co-evolutionary outcomes were similar to case when only submerged macrophytes evolved (panel a in Fig. 1.3.3 vs panel a in Fig. 1.3.5). This means that submerged macrophytes transitioned from monomorphic or polymorphic populations to a state of coexistence with floating macrophytes to extinction (panel a in Fig. 1.3.5). Nevertheless, the growth of the floating macrophytes occurred at a slightly smaller nutrient diffusion value compared to when only the submerged macrophytes evolve ($u = U_{c0} = 5.7$ Fig. 1.3.5 vs $u = U_{c0} = 5.8$ Fig. 1.3.3). In the co-evolution scenario when the nutrient diffusion rate was set at $uU_{co} = 5.7$, the floating macrophytes evolved below the surface and diversified into a polymorphic population (Fig. S6 b3,b4) reaching a low but positive total population size (Fig. S6 b1), whereas they remained extinct when fixed to the surface and only the submerge macrophytes evolve (Fig. S6 a1). Strikingly, however, we no longer observed the oscillatory dynamics we observed in the case of only the submerged macrophytes evolution (panel a in Fig. 1.3.5). In addition, the extinction of submerged macrophytes is delayed and occurs for a higher nutrient diffusion rate as both plants co-evolve. To understand the lack of oscillations

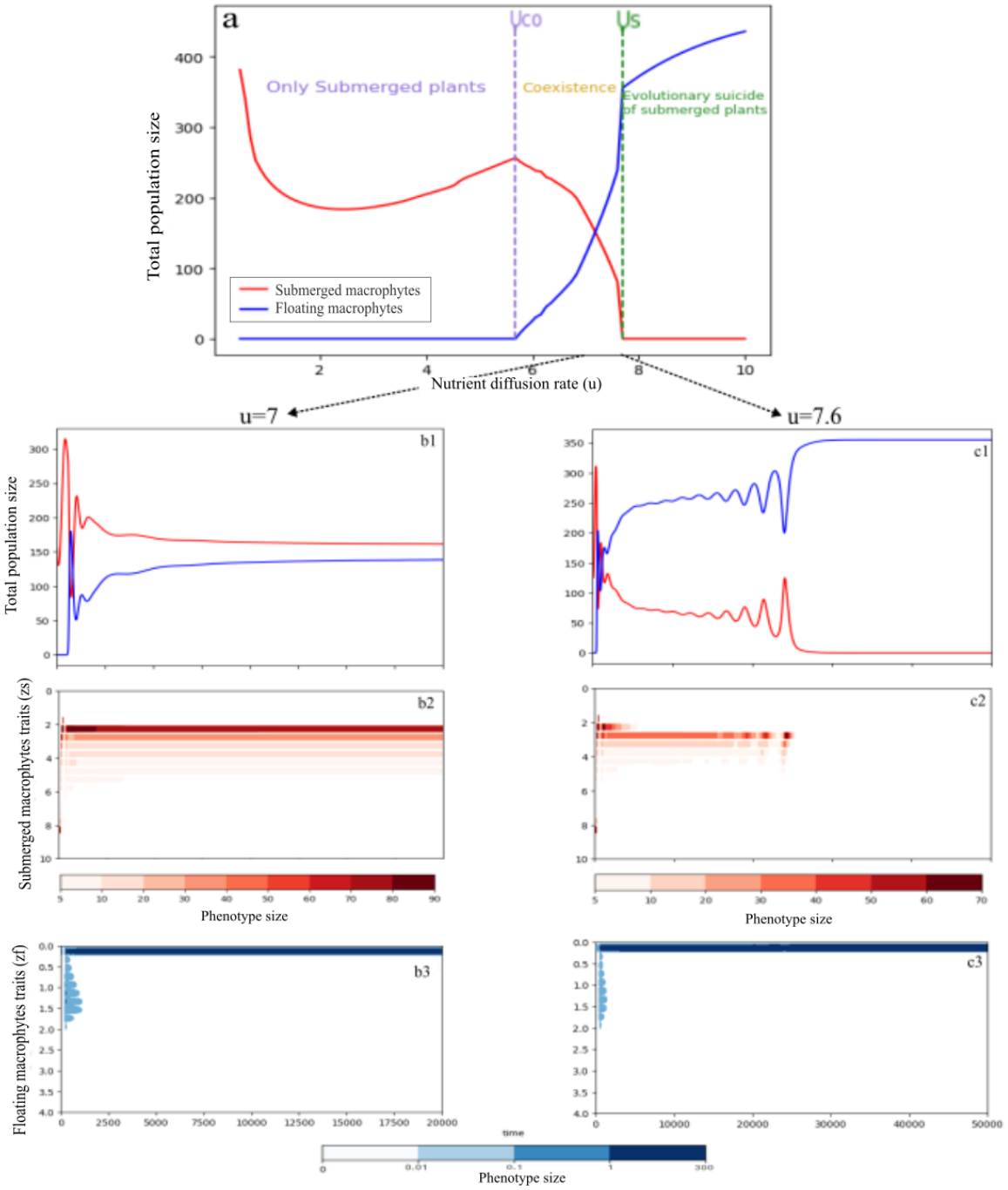



Figure 1.3.5: Results from the structured population model for the co-evolution.
**Top :** $(a)$ : Final total population size, when both **S** and **F** co-evolve, as a function of the nutrient diffusion rate $u$. The oscillations zone disappears and is replaced by a stable equilibrium of coexistence. Moreover, the floating plants start growing at a smaller nutrient diffusion rate $u = U_{co} = 5.7$ evolutionary suicide of the submerged macrophytes is delayed and occurs for a higher $u = U_s = 7.6$.
**Bottom :** Total population size of the submerged **S** and floating macrophytes **F** through time and presence of different phenotypes in the submerged and floating macrophytes populations for different nutrient diffusion rates : $u = 7$ : $b1$): The two population evolve towards a coexistence steady-state. $b2$) the submerged macrophytes population asymptotically concentrate around the inflection point of the mortality function $z_{thres} = 2$ with the presence of other phenotypes bellow. $b3$) While we observe within the floating macrophytes population the emergence of low density population bellow the surface between 0 and 2 during the first time steps but which rapidly disappear leaving only the phenotypes at the surface $z_f = 0$. $u = 7.6$ : $c1$) The floating macrophytes evolve towards a high density population outcompeting the submerged macrophytes that undergo evolutionary suicide. $c2$) The submerged macrophytes diversify with the emergence of different phenotypes at high levels before they get outcompeted by the floating macrophytes and go extinct. $c3$) The floating macrophytes stay at the surface after a few deeper phenotypes appeared and then vanished afterwards.

and the delayed evolutionary suicide of submerged macrophytes, we considered some examples in detail.

When the nutrient diffusion rate $u = 7$ explored in (b1,b2,b3 in Fig. 1.3.5), where evolutionary cycles were observed for when only the submerged macrophytes evolved (panels d2,d2 in Fig. 1.3.3), we extend the analysis to include the evolution of floating macrophytes . Starting from the resident traits ($z_{s_0} = 8, z_{f_0} = 0$), the co-evolutionary dynamics result in stabilized populations without oscillations (panel b1 in Fig. 1.3.3). The submerged plants evolve towards the surface, diversify and stabilize with a concentration around the trait threshold set by the inflection point of the mortality function $z_{thres} = 2$. We observe that individuals of the floating macrophytes population start growing at lower levels that than the surface during the initial time steps $\int_{0.5}^{2} F(t,z)dz > threshold$ (panel b2 in Fig. 1.3.3), as they have positive fitness as can be seen in SI. K Fig. S11). Nonetheless, they do not reach high densities before disappearing. Although the difference is not substantial compared to the scenario where only **S** evolved. The same observation is made for the example of nutrient diffusion rate $u = 6.8$ in SI. G Fig.S8 vs SI. I Fig.S9 where the oscillations disappeared in the co-evolution scenario. These observations suggests that the inclusion of the evolution of floating macrophytes may contribute to the non-replication of the same result without their evolution, which in our study led to evolutionary oscillations. In the co-evolutionary context, floating macrophytes are not confined to the surface alone and can influence the fitness of submerged macrophytes through their shading effect. A similar behavior unfolds within the floating macrophytes population when the nutrient diffusion rate is set to $u = 7.6$ (panels c1,c2,c3 in Fig. 1.3.3). However, in this case, the submerged macrophytes found themselves outcompeted by the floating macrophytes that attained a notably high biomass (panel c1 in Fig. 1.3.3). It's worth noting that the phenomenon of evolutionary suicide among the submerged macrophytes, when considering co-evolution with floating macrophytes, occurred at a higher nutrient diffusion rate. Furthermore, this occurred without the emergence of cyclic behavior, which contrasts with the situation when the submerged macrophytes evolved in isolation.

## 1.4 Discussion

In this study, we explored the effects of evolution and co-evolution in a shallow lake ecosystem exhibiting ecological bistability. The model developed in this study goes beyond the ones proposed by (Marten Scheffer, Szabo, et al. 2003b) and (Ardichvili, Loeuille, and Dakos 2023) as it integrates the competition between floating and submerged macrophytes and their characterisation by a phenotypic

trait in order to describe the eco-evolutionary dynamics of the ecosystem. Bistability arises due to the positive feedback resulting from competition between floating and submerged macrophytes for nutrients and light (Marten Scheffer et al. 1998; Marten Scheffer, Szabo, et al. 2003b; Blindow, Hargeby, and Andersson 1998). Consistent with previous results, we find that ecological alternative stable states occur for high rates of nutrient diffusion, causing shifts from coexistence or exclusive presence of submerged macrophytes to a floating macrophytes dominance. We find that the evolution of a phenotypic trait representing the growth depth of macrophytes in our shallow lake ecosystem leads to evolutionary oscillations and evolutionary suicide. Instead, co-evolution of both macrophyte types stabilises the dynamics but still leads to evolutionary suicide of the submerged macrophytes. Below we discuss our results in detail.

### 1.4.1 Evolution of the submerged macrophytes can lead to evolutionary branching, oscillations and evolutionary suicide

Our analysis shows that submerged macrophytes' growth depth mostly evolves towards the water surface for varying levels of nutrient diffusion rate: basically evolving towards a higher availability of light as light is the limiting resource for the submerged macrophytes. For a range of very low nutrient diffusion rates ($0<u<1.5$ Fig. 1.3.2 red line) when the submerged macrophytes evolve towards the bottom of the lake, we observe an initial decrease in the total population size of the submerged macrophytes (Fig. 1.3.3). This arises because, when the nutrient diffusion rate is very low (near zero), nutrient concentration accumulates at the bottom of the lake, providing an advantage to the deep submerged macrophytes. As the diffusion rate slightly increases (e.g. from 0.1 to 0.2), nutrients disperse to shallower depths, reducing their availability at the bottom. Within this range of nutrient diffusion rates, as the submerged macrophytes evolve toward the bottom, higher nutrient diffusion leads to reduced nutrient access in deep levels, explaining the decrease in the total biomass of the submerged macrophytes population (SI. B Fig. S3).

For a range of intermediate nutrient diffusion rates when the floating macrophytes are absent ($1<u<4.5$, Fig. 1.3.2), submerged macrophytes evolve towards branching points, leading to diversification of the monomorphic population into a polymorphic population as found in (Ardichvili, Loeuille, and Dakos 2023). Diversification can be attributed to the advantageous priority effect held by submerged macrophytes in terms of nutrient access. As nutrient diffusion rate increases,the depth of the singu-

lar strategy decreases (goes towards the surface) since higher diffusion allows shallower depths to experience a significant enrichment in nutrients. However, the evolutionary outcome is not a stable strategy anymore but a branching point. As nutrient availability widens at different depths of the lake, it enables the emergence and almost stable coexistence of different phenotypes within a specific depth range (Fig. 1.3.3).

Interestingly, when the nutrient diffusion rate exceeds a certain value ($u$>4.5, Fig. 1.3.1), the evolutionary equilibria of the submerged macrophytes based on AD (BP in Fig.1.3.2) coincide with the critical depth traits that represent bifurcation points between bistability (VI Fig 1.3.2) and floating macrophytes dominance (II in Fig. 1.3.2). Simulations of the structured population model, though, show that submerged macrophytes evolve to depths where they can either dominate or coexist with the floating macrophytes either in stable coexistence or in oscillations. Especially, for diffusion rates 4.5<$u$<7.5 Fig. 1.3.2, despite the existence of a wide range of phenotypes in which submerged macrophytes could potentially dominate the lake on their own, they still evolve towards depths that enable their competing floating macrophytes to invade and coexist with them.

But what does drive the oscillating evolutionary patterns when nutrient diffusion rate exceeds a specific threshold $u \geq U_c$ (Fig. 1.3.3)? At this threshold of diffusion rate, limitation due to nutrient competition diminishes. Consequently, competition for light becomes the primary driver influencing population dynamics. As we assumed continuous seeding throughout the water column, the emergence of different phenotypes of submerged macrophytes at various depths is possible. Submerged macrophytes evolve to the surface but they cannot be maintained there in high abundance because of the shading effect from the floating macrophytes. Competition for light reduces the population size of submerged macrophytes, and simultaneously increases the population of floating macrophytes as they get more access to nutrients. At the same time though, the reduced size of submerged macrophytes also reduces intraspecific shading of submerged macrophytes and enables the deeper submerged phenotypes to grow again. As a result phenotypes at different depths emerge and then disappear triggering the the oscillating patterns between submerged and floating macrophytes. Similar cycles between high and low abundance has been observed in Antarctic krill populations ((Ryabov et al. 2017)). In that case, intraspecific food competition limits the growth of krill within the same species when krill populations reach a critical abundance, but when krill abundance is low, growth relies more on environmental conditions (Ryabov et al. 2017).

When the nutrient diffusion rate increases the amplitude of the oscillations becomes larger until a threshold ($u \geq U_s$, Fig. 1.3.3), where evolutionary oscillations become so large that the submerged macrophytes cross to the extinction state (Fig. 1.3.3 f1,f2). More in general, at high diffusion rates, the evolutionary trajectory tends towards depth regions where submerged macrophytes face extinction rather than to regions where they can be rescued (or more properly persist). This is due to the fact that at such high range of diffusion rate, nutrient limitation is not anymore present. Instead, the only way to increase fitness is by growing to shallower depths where light is more available, but where the only feasible equilibrium is the one of a dominant floating macrophytes population and an extinct submerged ones. This is a classical case of evolutionary suicide. Evolution to extinction was put forward by (Abrams and Matsuda 1994) in which a prey population went extinct when decreasing foraging activity. Evolutionary suicide through the existence of a catastrophic bifurcation was highlighted by (Gyllenberg and Parvinen 2001) in structured metapopulation models with evolving dispersal. Other examples showed that evolutionary suicide could also occur through non-catastrophic bifurcations, as depicted in a model of pathogen evolution with frequency-dependent transmission in (Boldin and Kisdi 2016). In our simulations of the structured population model, the submerged macrophytes experience a catastrophic collapse as evolutionary oscillations become so large that they cross a homoclinic saddle bifurcation leading to the extinction of the submerged macrophytes. Similar dynamics have been shown in a predator prey model where a sudden ecological shift from a coexistence limit cycle to predator extinction can occur through catastrophic homoclinic bifurcations (Lehtinen 2021).

### 1.4.2 Co-evolution of the floating macrophytes prevents evolutionary cycles and delays evolutionary suicide of submerged macrophytes

Strikingly, co-evolution does not affect the overall qualitative behaviour of the system compared to the evolution of the submerged macrophytes only. One might have expected that, under the influence of co-evolution, the floating macrophytes would start growing at much lower nutrient diffusion values ($u << U_{co} = 5.8$ Fig. 1.3.3), allowing them to establish themselves at deeper depths where the floating macrophytes can grow at levels below the surface. However, the floating macrophytes fail to grow at these low nutrient diffusion rates, because under low nutrient diffusion, floating macrophytes are able to grow at deeper depths only if submerged macrophytes would occupy the

surface. This reversal is unachievable given that the submerged macrophytes are restricted below a certain threshold (i.e. they reside in the deeper depths of the lake, SI. J Fig. S10 b,c,d,e,f). Despite similar evolutionary outcomes, co-evolution triggers floating macrophytes growth at a slightly lower nutrient diffusion value where they diversify at deeper depths (SI. F Fig. S6), compared to scenarios where they are fixed at the surface. The floating macrophytes continue evolving towards phenotypes below the surface for a limited range of nutrient diffusion rates leading to higher total biomass compared to scenarios where floating macrophytes are fixed at the surface (SI G. Fig. S7 a1). However, at sufficiently high nutrient diffusion rates deep traits vanish after a brief period, leaving only surface traits (SI J. Fig. S10). This is due to the fact that nutrients are no longer a limiting resource and staying at the surface becomes the optimal strategy for the floating macrophytes.

Yet, co-evolution of the floating and submerged macrophytes has two more subtle important effects. First, co-evolution prevents the occurrence of evolutionary oscillations, but leads to the establishment of a stable coexistence equilibrium. Comparing dynamics in the nutrient diffusion ranges where evolutionary oscillations disappear (Fig. 1.3.3 d vs (Fig. 1.3.4 b), in the case of co-evolution the floating macrophytes population size is smaller than when floating macrophytes do not evolve. Co-evolution allows the emergence of deeper phenotypes within the floating macrophytes population leading to nutrient competition on the floating macrophytes at the surface. This competition decreases the overall biomass of floating macrophytes and, thus, diminishes their shading impact on submerged macrophytes. In its turn, this results in a higher biomass of submerged macrophytes at shallow depth ($z \sim 2$), which reduces the abundance of deeper phenotypes due to increased shading. As a result the recurrent emergence and decline of submerged macrophytes are no longer possible when the floating macrophytes co-evolve.

Interestingly, this stabilization persists even though there is just a brief emergence of deeper phenotypes within the floating macrophytes populations and asymptotically the floating macrophytes are fixed at the surface. One might question why, in this case, evolutionary oscillations do not occur at a higher nutrient diffusion rate where the floating macrophytes biomass is high enough to trigger oscillatory dynamics as described in the no co-evolution case? This is because deeper phenotypes within the floating macrophytes population appear with lower density and for shorter time as the nutrient diffusion rate increases (SI. I Fig. S9 c and Fig. 1.3.5 b3, c3). By the time their impact fades away, the nutrient diffusion rate becomes that high that the evolutionary suicide

of the submerged macrophytes occurs. This can be seen in the non-persistent oscillations just before the extinction of submerged macrophytes outcompeted by the floating macrophytes (Fig. 1.3.5 c1).

The reduction in floating macrophytes' biomass driven by the emergence of deeper phenotypes is also responsible for the second difference observed in the co-evolution case: the evolutionary suicide of the submerged macrophytes is delayed to a higher nutrient diffusion rate ($u = U_s = 7.45$ Fig. 1.3.3 vs $u = U_s$=7.6 Fig. 1.3.5). The emergence of deeper floating macrophytes phenotypes due to co-evolution suppresses oscillatory dynamics, leads to the growth of the submerged macrophytes to the shallowest possible depth, and allows the submerged macrophytes to persist longer even if only for a narrow additional range of nutrient diffusion rates.

### 1.4.3 Conclusion

Evolution of the growth depth of submerged macrophytes in a bistable shallow lake ecosystem destabilised the stable coexistence between submerged and floating macrophytes. We found an emergence of evolutionary oscillations that eventually lead to the evolutionary suicide of the submerged macrophytes as nutrient diffusion increased and nutrient limitation became weak. Co-evolution of both floating and submerged macrophytes was stabilising by preventing the occurrence of evolutionary oscillations, and delayed, but it did not prevent, the evolutionary suicide of the submerged macrophytes. The fact that evolution ultimately resulted in the submerged macrophytes extinction despite the availability of growth depths where submerged and floating macrophytes could coexist suggests that adaptive evolution does not necessarily prevent collapse in bistable ecosystems.

## 1.5 Data Availability

The codes to reproduce the figures of this artile are available at https://github.com/SirineBoucenna/Eco-evolutionary-model-shallow-lakes

## Aknowledgments

We thank Nicolas Loeuille and Sepideh Mirrahimi their for valuable comments and suggestions. This research was supported in part by the International Centre for Theoretical Sciences (ICTS) for the

program "Tipping Points in Complex Systems " (code: ICTS/tipc2022/9).

## 1.6 Supplementary information

The following subsections gather supplementary figures of the main text.

### 1.6.1 SI A. Effect of nutrient diffusion on total nutrient concentration

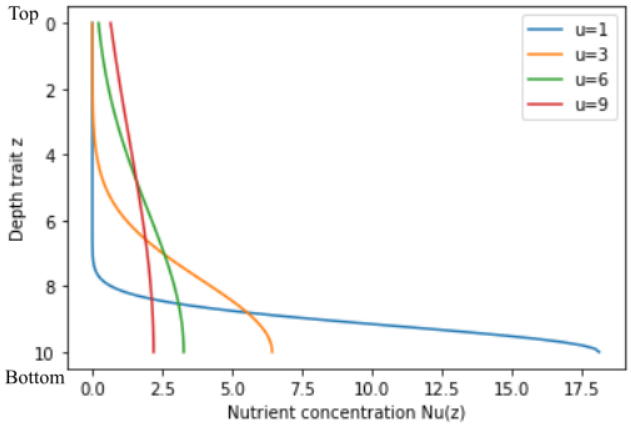



Fig. S1: Nutrient concentration function $Nu(z)$ for varying nutrient diffusion parameter $u$ at different depths $z$.

### 1.6.2 SI B. Bifurcation diagrams under different parameter conditions

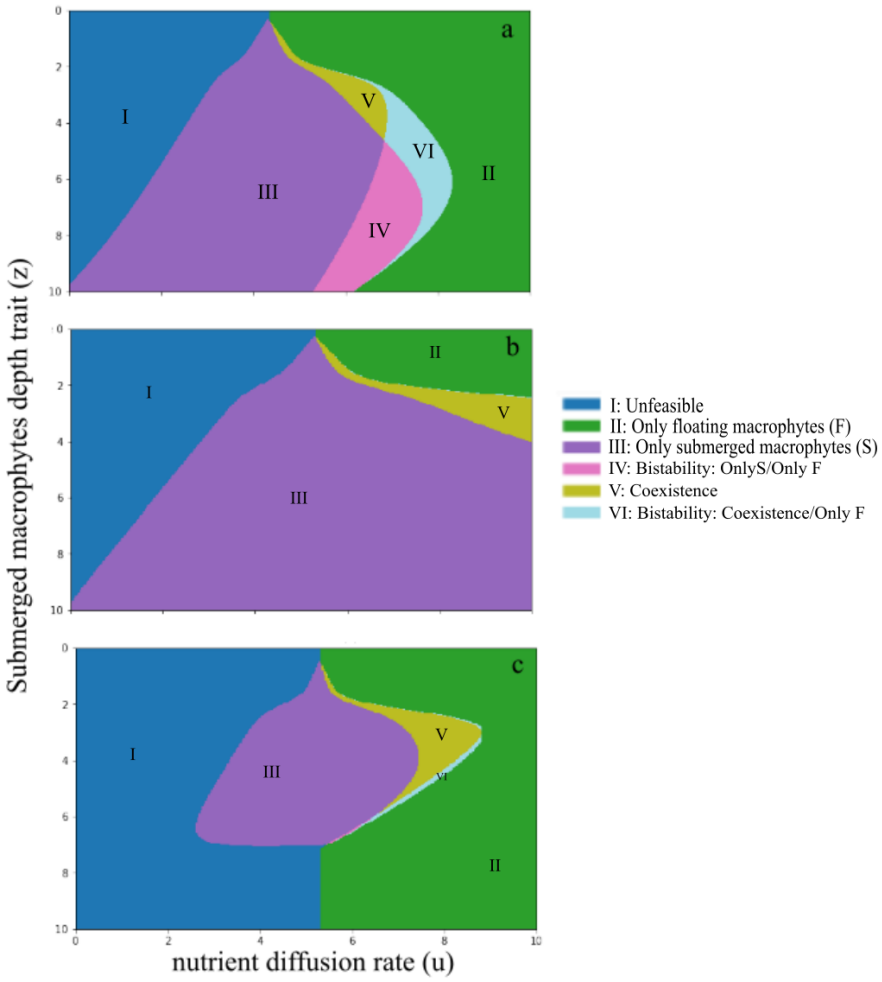



Fig. S2: Bifurcation diagrams for different parameter conditions than used in our study. **a:** Higher light attenuation $w = 0.2$. **b:** Smaller nutrient concentration $Nu_0 = 10$. **c:** Smaller nutrient concentration $Nu_0 = 10$ and higher light attenuation $w = 0.3$.

### 1.6.3 SI C. Steady states of the submerged macrophytes for very low nutrient diffusion rates

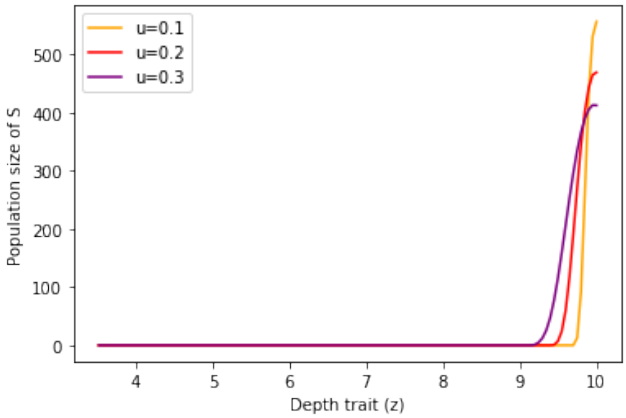
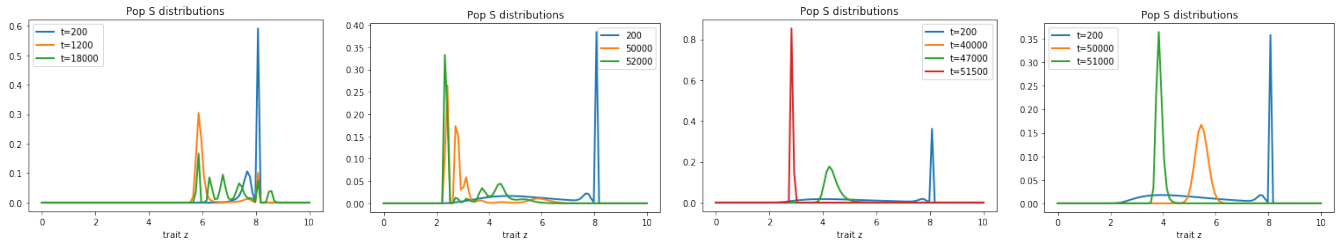



Fig. S3: Ecological equilibria representing the biomass of the submerged macrophytes population for three small nutrient diffusion rates. We can see that the maximum of the the population size decreases as $u$ increases because the higher the diffusion the less the nutrients concentration in the bottom.

### 1.6.4 SI D. Distribution of the submerged macrophytes population from the structured population model




(a) u=3 (b) u=7 (c) u=7.4 (d) u=7.45.

Fig. S4: Density distributions of the submerged macrophytes populations along the trait set of the examples studied in Fig. 1.3.3 at different time steps. In **a)**, we observe the population evolving from a monomorphic population at the depth $z = 8$ to a polymorohism with several trait present. In **b)**, **c)** and **d)** where we observed evolutionary oscillations, we illustrate the distributions of **S** at the exterma in a cycle. In **d)** the population experienced extinction afterwards.

### 1.6.5 SI E. Comparison of the final mean traits from the structured population model with and without mutations

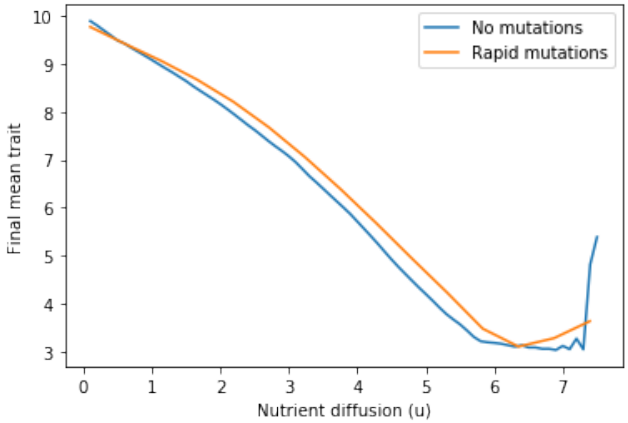



Fig. S5: Final mean traits obtained from the structured population model in the case of neglecting the mutations with initial seeding (from our study in Fig. 1.3.2) and in case of frequent Gaussian mutations with a probability of mutation 0.1 and a variance 0.05 where in this scenario we did not observe oscillations and the final distributions of the submerged macrophytes population were a unique Gaussian with a certain phenotypic variance.

### 1.6.6 SI F. An example of nutrient diffusion rate $u = 5.7$ : Only S evolution vs co-evolution

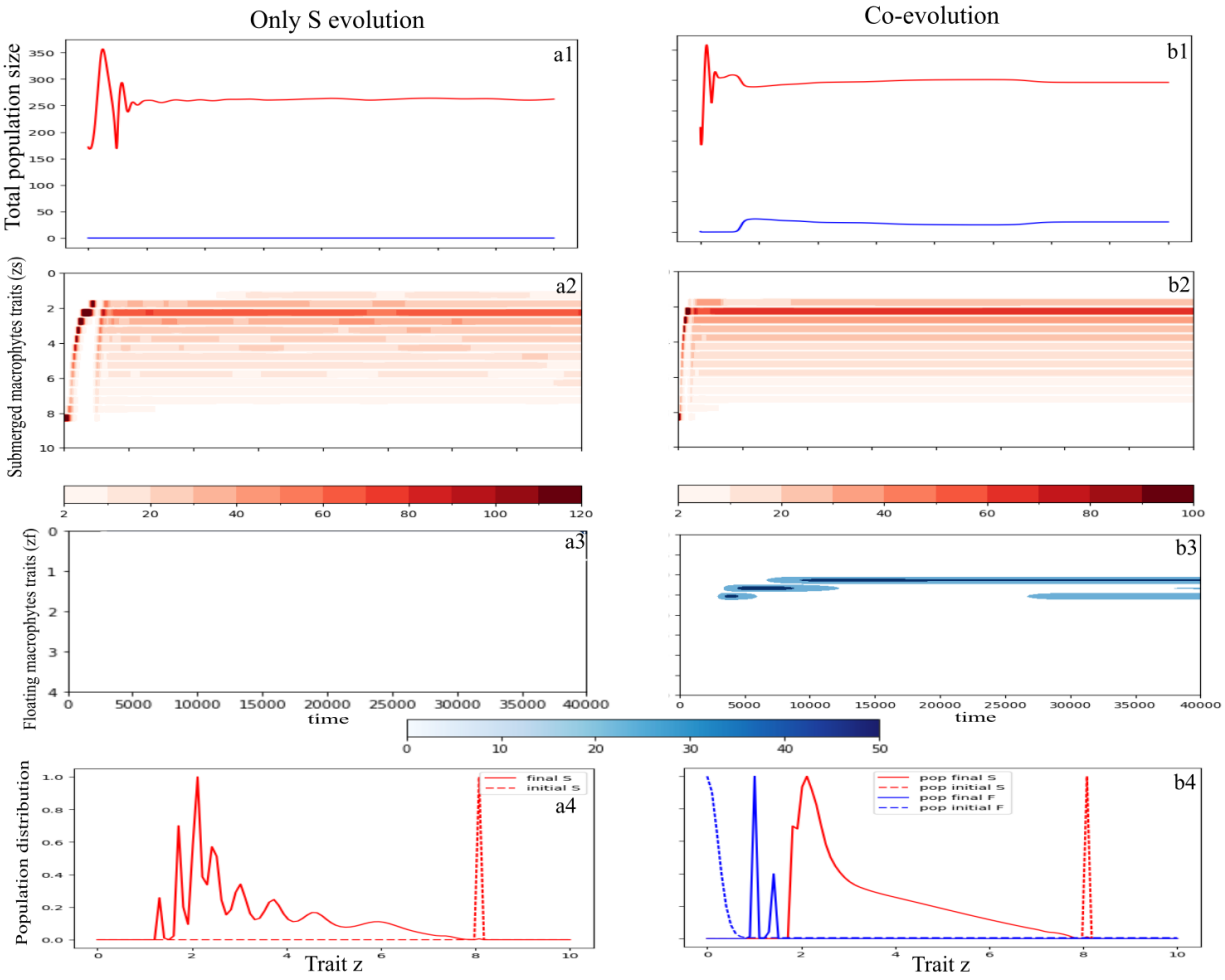



Fig. S6: Comparison of the scenario where only the submerged macrophytes evolve **left** and where the floating and submerged macrophytes co-evolve **right** when the nutrient diffusion rate $u = 5.7$. We observe in panel $(a1)$ that floating macrophytes remain at 0 and don't grow, while in the case of co-evolution the total population size of the floating macrophytes increases in panel $(b1)$ where different phenotypes of the floating macrophytes population emerge $0 < z_f < 2$ in panel $(b3)$ and then the ones closer to the surface disappear. Panels $(a4)$ and $(b4)$ represent the initial and final distributions of the submerged macrophytes population and in case of co-evolution of the floating macrophytes population as well.

### 1.6.7 SI G. An example of nutrient diffusion rate $u = 5.9$ : Only S evolution vs co-evolution

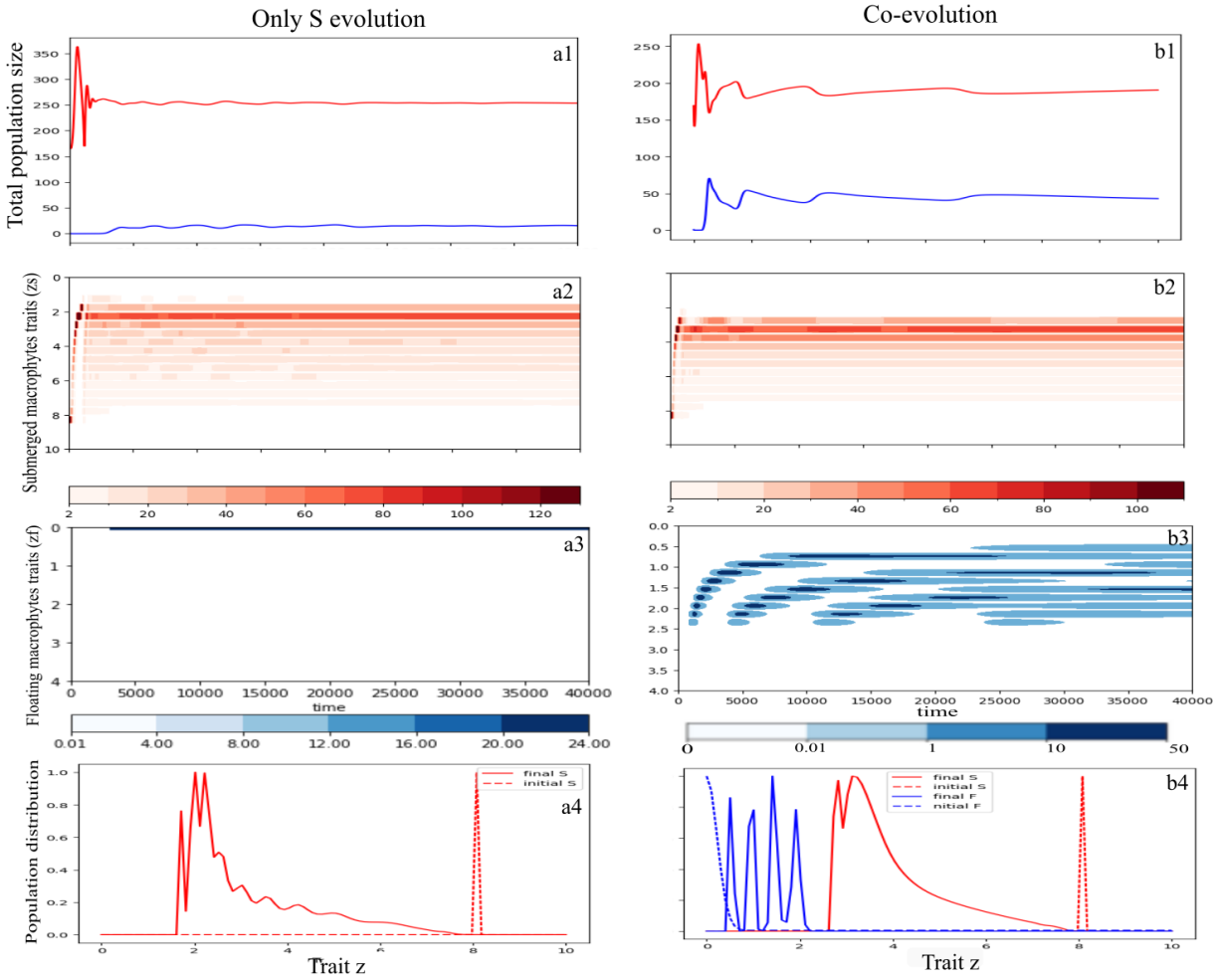



Fig. S7: Comparison of the scenario where only the submerged macrophytes evolve **left** and where the floating and submerged macrophytes co-evolve **right** when the nutrient diffusion rate $u = 5.9$. We observe in panel $(a1)$ that floating macrophytes that are fixed at the surface grow and reach low population size, while in the case of co-evolution the total population size of the floating macrophytes increases and reaches higher values in panel $(b1)$. Different phenotypes of the floating macrophytes population emerge $0.5 < z_f < 2.5$ in panel $(b3)$ whereas they are fixed to the surface when only the submerged macrophytes evolve in panel $(a3)$. Panels $(a4)$ and $(b4)$ represent the initial and final distributions of the submerged macrophytes population and in case of co-evolution of the floating macrophytes population as well.

### 1.6.8 SI H. An example of nutrient diffusion rate $u = 6.8$ at the beginning of the cycle region

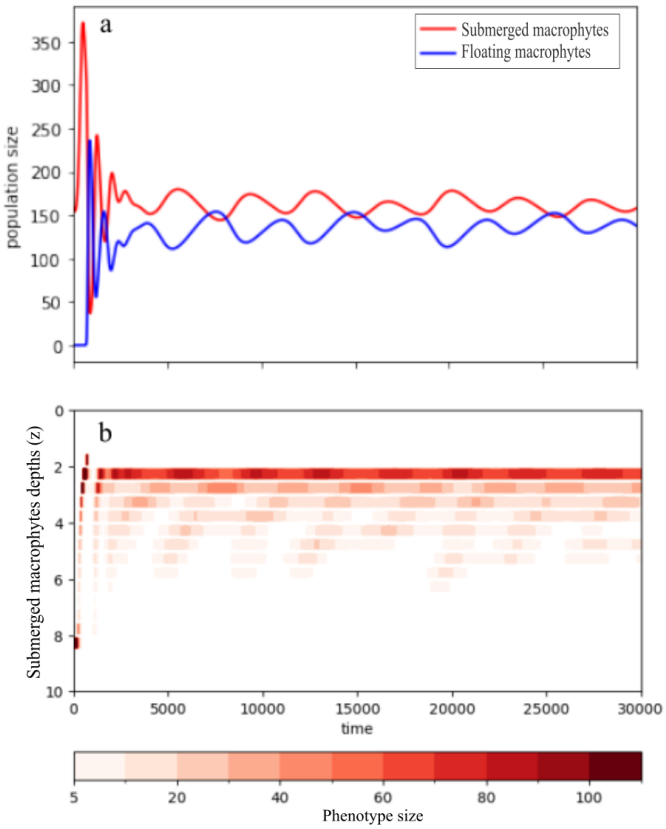



Fig. S8: $(a)$ : Total population size of the submerged macrophytes and the floating macrophytes when only **S** evolve for $u = 6.8$ and $(b)$: the presence of different traits $z$ of the submerged macrophytes, which start from initial depth $z_0 = 8$, with the emergence of small amplitude evolutionary cycles.

### 1.6.9 SI I. The example of nutrient diffusion rate $u = 6.8$ in case of co-evolution

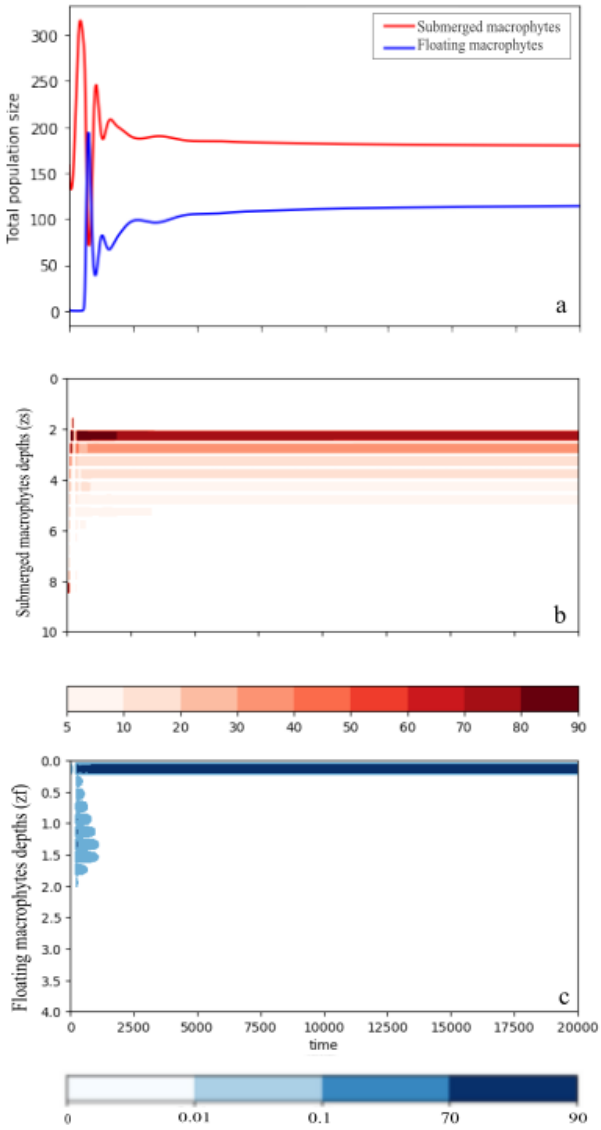



Fig. S9: $(a)$ : Total population size of the submerged macrophytes and the floating macrophytes when **S** and **F** co-evolve for $u = 6.8$. Emergence of different phenotypes of the submerged macrophytes population $z_s$ in $(b)$ and of the floating macrophytes population $z_f$ in $(c)$ through time.

### 1.6.10 SI J. Bifurcation diagrams in $(z_s, z_f)$-plane for different nutrient diffusion rates

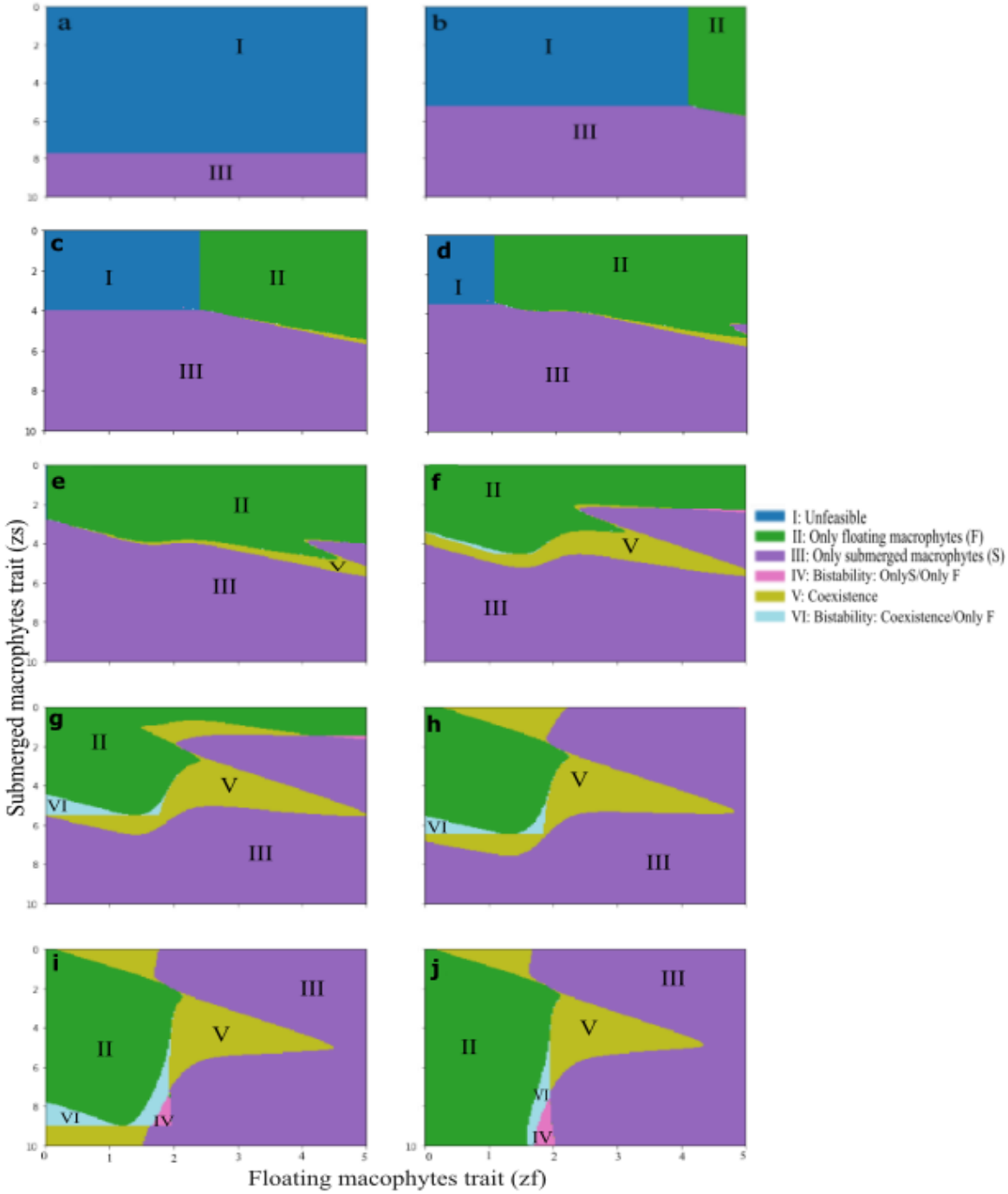



Fig. S10: Bifurcation diagrams in $(z_f, z_s)$-plane with ecological steady-states of the floating and submerged macrophytes when their respective growth depths $z_f \in [0.5]$ and $z_s \in [0.10]$ for different nutrient diffusion rates : $(a)$ : u=1 $(b)$ : u=2 $(c)$ : u=2.5 $(d)$ : u=2.7 $(e)$ : u=3 $(f)$ : u=4 $(g)$ : u=5 $(h)$ : u=6. $(i)$ : u=8 $(j)$ : u=9.

### 1.6.11 SI K. Distribution and fitness of the floating macrophytes population in case of evolution when $u = 7$

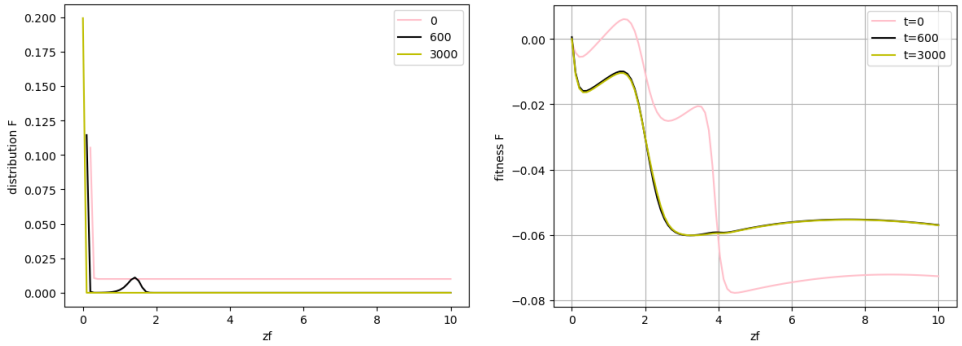



Fig. S11: The example of nutrient diffusion rate $u = 7$ studied in Fig. 1.3.4 when **S** and **F** evolve where were observed the emergence of phenotypes deeper than 0 in the floating macrophytes population which prevented the occurrence of cyclic behaviour. **Left :** Distribution of the floating macrophytes density at different time steps; initially we observe the presence of seeding uniformly distributed along the trait set which disappear at time $t = 600$ except at depth $z_f \sim 1.5$. At a longer time step we can see that only the population at the surface remained. **Right :** fitness of the population **F** at the same time steps for every trait $z_f \in [0, 10]$ which represents their growth rate.

# Bibliography


Abrams, Peter A and Hiroyuki Matsuda (1994). "The evolution of traits that determine ability in competitive contests". In: *Evolutionary Ecology* 8, pp. 667–686.

Ardichvili, Alice Nadia, Nicolas Loeuille, and Vasilis Dakos (2023). "Evolutionary emergence of alternative stable states in shallow lakes". In: *Ecology Letters* 26.5, pp. 692–705.

Ashwin, Peter et al. (2012). "Tipping points in open systems: bifurcation, noise-induced and rate-dependent examples in the climate system". In: *Philosophical Transactions of the Royal Society A: Mathematical, Physical and Engineering Sciences* 370.1962, pp. 1166–1184.

Bernot, Melody J et al. (2006). "Nutrient uptake in streams draining agricultural catchments of the midwestern United States". In: *Freshwater Biology* 51.3, pp. 499–509.

Blindow, Irmgard, Anders Hargeby, and Gunnar Andersson (1998). "Alternative stable states in shallow lakes: what causes a shift?" In: *The structuring role of submerged macrophytes in lakes*. Springer, pp. 353–360.

Boldin, Barbara and Eva Kisdi (2016a). "Evolutionary suicide through a non-catastrophic bifurcation: adaptive dynamics of pathogens with frequency-dependent transmission". In: *Journal of Mathematical Biology* 72, pp. 1101–1124.

— (2016b). "Evolutionary suicide through a non-catastrophic bifurcation: adaptive dynamics of pathogens with frequency-dependent transmission". In: *Journal of Mathematical Biology* 72, pp. 1101–1124.

Chaparro Pedraza, P Catalina et al. (2021). "Adaptive evolution can both prevent ecosystem collapse and delay ecosystem recovery". In: *The American Naturalist* 198.6, E185–E197.

Chaparro-Pedraza, P Catalina (2021). "Fast environmental change and eco-evolutionary feedbacks can drive regime shifts in ecosystems before tipping points are crossed". In: *Proceedings of the Royal Society B* 288.1955, p. 20211192.

Chaparro-Pedraza, P Catalina and André M de Roos (2020). "Ecological changes with minor effect initiate evolution to delayed regime shifts". In: *Nature Ecology & Evolution* 4.3, pp. 412–418.

Cortez, Michael H. and Joshua S. Weitz (2014). "Coevolution can reverse predator–prey cycles". In.

Cotto, Olivier and Ophélie Ronce (Sept. 2014). "Maladaptation as a source of senesence in habitats variables in space and time." In: *Evolution* 68.9, pp. 2481–2493.

Cotto, Olivier, Linnea Sandell, et al. (2019). "Maladaptive shifts in life history in a changing environment". In: *The American Naturalist* 194.4, pp. 558–573.

Dakos, Vasilis et al. (2019). "Ecosystem tipping points in an evolving world". In: *Nature ecology & evolution* 3.3, pp. 355–362.

Dercole, Fabio, Régis Ferrière, and Sergio Rinaldi (2002). "Ecological bistability and evolutionary reversals under asymmetrical competition". In: *Evolution* 56.6, pp. 1081–1090.

Dieckmann, Ulf and Richard Law (1996). "The dynamical theory of coevolution: a derivation from stochastic ecological processes". In: *Journal of Mathematical Biology* 34, pp. 579–612.

Diekmann, Odo et al. (2004). "A beginner's guide to adaptive dynamics". In: *Banach Center Publications* 63, pp. 47–86.

Faafeng, Bjørn A and Marit Mjelde (1998). "Clear and turbid water in shallow Norwegian lakes related to submerged vegetation". In: *The structuring role of submerged macrophytes in lakes*. Springer, pp. 361–368.

Ferriere, Regis and Stephane Legendre (2013). "Eco-evolutionary feedbacks, adaptive dynamics and evolutionary rescue theory". In.

Floreano, Dario, Stefano Nolfi, and Francesco Mondada (1998). "Competitive co-evolutionary robotics: From theory to practice". In: *Proc. of The Fifth International Conference on Simulation of Adaptive Behavior (SAB), From Animals to Animats*. ETH Zürich.

Folke, Carl et al. (2004). "Regime shifts, resilience, and biodiversity in ecosystem management". In: *Annu. Rev. Ecol. Evol. Syst.* 35, pp. 557–581.

Garnier, Jimmy et al. (2023). "Adaptation of a quantitative trait to a changing environment: New analytical insights on the asexual and infinitesimal sexual models". In: *Theoretical Population Biology* 152, pp. 1–22.

Geritz, Stefan AH et al. (1998). "Evolutionarily singular strategies and the adaptive growth and branching of the evolutionary tree". In: *Evolutionary Ecology* 12, pp. 35–57.

Gyllenberg, Mats and Kalle Parvinen (2001). "Necessary and sufficient conditions for evolutionary suicide". In: *Bulletin of Mathematical Biology* 63, pp. 981–993.

Hairston Jr, Nelson G et al. (2005). "Rapid evolution and the convergence of ecological and evolutionary time". In: *Ecology Letters* 8.10, pp. 1114–1127.

Holling, Crawford S (1973). “Resilience and stability of ecological systems”. In: *Annual review of ecology and systematics* 4.1, pp. 1–23.

Hughes, Terry P et al. (2018). “Spatial and temporal patterns of mass bleaching of corals in the Anthropocene”. In: *Science* 359.6371, pp. 80–83.

Hürlimann-Lüönd, Annemarie (1990). “The development of some Lemnaceae under different nutrient conditions”. In: *Folia Geobotanica et Phytotaxonomica* 25, pp. 309–314.

Hutchinson, G Evelyn (1975). “Chapter 32: The algal benthos”. In: *A treatise in limnology III Limnological Botany*, pp. 509–571.

Janse, Jan H (1997). “A model of nutrient dynamics in shallow lakes in relation to multiple stable states”. In: *Shallow Lakes’ 95: Trophic Cascades in Shallow Freshwater and Brackish Lakes*, pp. 1–8.

Jones, Clain A and Eugene B Welch (1990). “Internal phosphorus loading related to mixing and dilution in a dendritic, shallow prairie lake”. In: *Research Journal of the Water Pollution Control Federation*, pp. 847–852.

Kaplan, K and Th Muer (1990). “Beobachtungen zum diasporenreservoir im Bereich ehemaliger Heideweiher”. In: *Floristische Rundbriefe* 24, pp. 38–45.

Kéfi, Sonia, Minus van Baalen, et al. (2008). “Evolution of local facilitation in arid ecosystems”. In: *The American Naturalist* 172.1, E1–E17.

Kéfi, Sonia, Max Rietkerk, et al. (2007). “Spatial vegetation patterns and imminent desertification in Mediterranean arid ecosystems”. In: *Nature* 449.7159, pp. 213–217.

Kisdi, Eva (1999). “Evolutionary branching under asymmetric competition”. In: *Journal of Theoretical Biology* 197.2, pp. 149–162.

Klausmeier, Christopher A, Elena Litchman, and Simon A Levin (2004). “Phytoplankton growth and stoichiometry under multiple nutrient limitation”. In: *Limnology and oceanography* 49.4part2, pp. 1463–1470.

Klausmeier, Christopher A, Matthew M Osmond, et al. (2020). “Ecological limits to evolutionary rescue”. In: *Philosophical Transactions of the Royal Society B* 375.1814, p. 20190453.

Kuiper, Jan J et al. (2015). “Food-web stability signals critical transitions in temperate shallow lakes”. In: *Nature Communications* 6.1, p. 7727.

Landolt, E and R Kandeler (1987). “The family of Lemnaceae a monographic study, Veroffentlchungen Des GeobotanischenInstitutes der ETH”. In: *StiftungRubel* 71.2.

Law, Richard, Paul Marrow, and Ulf Dieckmann (1997). “On evolution under asymmetric competition”. In: *Evolutionary Ecology* 11, pp. 485–501.

Lehtinen, Sami O (2021). “Ecological and evolutionary consequences of predator-prey role reversal: Allee effect and catastrophic predator extinction”. In: *Journal of Theoretical Biology* 510, p. 110542.

Lenton, Timothy M et al. (2008). “Tipping elements in the Earth’s climate system”. In: *Proceedings of the national Academy of Sciences* 105.

Loeuille, Nicolas (2010). “Influence of evolution on the stability of ecological communities”. In: *Ecology Letters* 13.12, pp. 1536–1545.

MATSUDA, H. and P. A. ABRAMS (1994). “Self-extinction due to adaptive change in foraging and anti-predator effort”. In.

May, Robert M (1977). “Thresholds and breakpoints in ecosystems with a multiplicity of stable states”. In: *Nature* 269.5628, pp. 471–477.

Metz, Johan AJ, Roger M Nisbet, and Stefan AH Geritz (1992). “How should we define ‘fitness’ for general ecological scenarios?” In: *Trends in Ecology & Evolution* 7.6, pp. 198–202.

Nonaka, Etsuko, Kalle Parvinen, and Åke Brännström (2013). “Evolutionary suicide as a consequence of runaway selection for greater aggregation tendency”. In: *Journal of theoretical biology* 317, pp. 96–104.

Osmond, Matthew M and Christopher A Klausmeier (2017). “An evolutionary tipping point in a changing environment”. In: *Evolution* 71.12, pp. 2930–2941.

Parker, SMatthew A. (1994). “Pathogens and sex in plants”. In.

Paul R. Ehrlich, Peter H. Raven (1964). “Butterflies and Plants: A Study in Coevolution.” In.

Ryabov, Alexey B et al. (2017). “Competition-induced starvation drives large-scale population cycles in Antarctic krill”. In: *Nature Ecology & Evolution* 1.

Scheffer, M, S Rinaldi, and L Mur (1994). “On the dominance of filamentous blue-green algae in shallow lakes”. In.

Scheffer, Marten et al. (1998). *Ecology of shallow lakes*. Vol. 1. Springer.

Scheffer, Marten and Stephen R Carpenter (2003). “Catastrophic regime shifts in ecosystems: linking theory to observation”. In: *Trends in Ecology & Evolution* 18.12, pp. 648–656.

Scheffer, Marten, Steve Carpenter, et al. (2001). “Catastrophic shifts in ecosystems”. In: *Nature* 413.6856, pp. 591–596.

Scheffer, Marten and Erik Jeppesen (2007). “Regime shifts in shallow lakes”. In: *Ecosystems* 10.1, pp. 1–3.

Scheffer, Marten, Sergio Rinaldi, Alessandra Gragnani, et al. (1997). “On the dominance of filamentous cyanobacteria in shallow, turbid lakes”. In: *Ecology* 78.1, pp. 272–282.

Scheffer, Marten, Sergio Rinaldi, and Yuri A Kuznetsov (2000). “Effects of fish on plankton dynamics: a theoretical analysis”. In: *Canadian Journal of Fisheries and Aquatic Sciences* 57.6, pp. 1208–1219.

Scheffer, Marten, Sándor Szabo, et al. (2003). “Floating plant dominance as a stable state”. In: *Proceedings of the National Academy of Sciences* 100.7, pp. 4040–4045.

Thompson, John N. (2005). “Coevolution: The Geographic Mosaic of Coevolutionary Arms Races”. In.

Van Nes, Egbert H et al. (2016). “What do you mean,‘tipping point’?” In: *Trends in Ecology & Evolution* 31.12, pp. 902–904.

Webb, Colleen (2003). “A complete classification of Darwinian extinction in ecological interactions”. In: *The American Naturalist* 161.2, pp. 181–205.

Witting, Lars (2000). “Population cycles caused by selection by density dependent competitive interactions”. In: *Bulletin of Mathematical Biology* 62.6, pp. 1109–1136.

Zhang, Tianran and Wendi Wang (2012). “Hopf bifurcation and bistability of a nutrient–phytoplankton–zooplankton model”. In: *Applied Mathematical Modelling* 36.12, pp. 6225–6235.

Zu, Jian et al. (2008). “On evolution under symmetric and asymmetric competitions”. In: *Journal of Theoretical Biology* 254.2, pp. 239–251.

CHAPTER 2

# Chapter 2: Derivation of a Macroscopic Model in a Tree Population

**Abstract**

I think it needs here a more general starting point. We model the evolution of two phenotypic traits, seed production and a summer dormancy threshold temperature in a tree population. The two traits are breeding values that impact the phenology of the trees, specifically the time when they encounter water stress and when they enter summer dormancy given some climatic conditions. The phenology itself is plastic, involving the breeding values we consider as well as the meteorological conditions. We assume that the tree population reproduces sexually, which we represent through an infinitesimal reproduction operator. Starting from a detailed year-to-year model, we introduce a first asymptotic limit, considering that the adult trees mortality is low to obtain an integro-differential model. We simplify this model further assuming a small phenotypic variance limit that makes the trait distribution of the population to become almost a Gaussian function. In this way we derive heuristically a system of two ordinary differential equations describing the dynamics of the mean phenotypic traits of the tree population. This simplified model allows us to study the impact of changing climatic conditions on the evolution of seed production and dormancy in our tree population.

**Keywords:** Structured population model, phenotypic trait, integro-differential model, macroscopic limit.

## 2.1 Introduction

As global temperatures rise and precipitation patterns change, the phenological responses of plants can have significant ecological consequences. This is especially true for trees, where earlier leaf budburst or delayed dormancy can alter the competitive dynamics between species, affect the availability of resources, and disrupt the synchrony with pollinators and herbivores. This, in turn, impacts forest composition, carbon sequestration, and overall ecosystem stability (Cleland et al. 2007, Parmesan and Yohe 2003). These phenological responses are not only influenced by inherited genetic factors, which can be represented by breeding values, but also exhibit significant phenotypic plasticity. Evolution of individuals breeding values as well as phenotypic plasticity can allow trees to adjust their developmental processes (eg timing of their phenology) in response to varying environmental conditions. Thus, understanding the role of evolution and plasticity of phenological-related responses of trees under changing climatic conditions is essential to predict their adaptive capacities for informing conservation strategies to maintain biodiversity and ecosystem services (Menzel, Sparks, Estrella, Elisabeth Koch, et al. 2006; Matesanz, Gianoli, and Valladares 2010).

In this manuscript, we are interested in phenotypic adaptation to summer stress related to warm temperatures and lack of water availability. Warm summer temperature associated with water stress may lead to summer dormancy as an adaptive strategy (ref). Typically, the term dormancy refers to winter dormancy, which is the period of inactivity observed in plants and some animals during winter months due to colder temperatures and reduced daylight (ref). More broadly, seasonal dormancy describes an adaptive strategy developed by certain species to endure unfavorable conditions regardless of the season (Vegis 1964), and summer dormancy refers to a strategy developed by plants to cope with hot, dry summers, by slowing down their activity. This plastic adaptation can be triggered by heat but also drought. Mostly described on perennial plants so far, summer dormancy is associated with greater survival rates after severe and repeated summer droughts in many perennial grasses (Volaire and Norton 2006). For instance, it was demonstrated that *Poaceae* enter summer dormancy in the arid summer climate of southern California, even when they were supplied with water throughout the dry season (Laude 1953). Plastic adaptations to heat and/or drought have also been described in

tree populations (Valladares et al. 2000; Ravn et al. 2022; Aspelmeier and Leuschner 2006; Mediavilla et al. 2019). Since extreme conditions like heat and drought are becoming more frequent with climate change, it is important to study plastic adaptation to such climatic conditions(Matesanz, Gianoli, and Valladares 2010).

The starting point of our work is the yearly dynamics of a population of trees structured by two phenotypic traits: seed production (number of seeds) and a threshold temperature inducing dormancy (summer dormancy). We assume a full inheritability of these traits, that are therefore breeding values. With environmental conditions as input, we model the dynamics of a tree population over a long period of time (multiannual). We assume that individuals reproduce sexually, which is represented by a non-linear integral operator. We couple this with an ecological dynamics, where water stress can lead to the death of adult trees. Tree death typically results in freeing up space that allows a rejuvenation process. We therefore consider that deaths are compensated by the maturation of young individuals born from seeds produced the year before. The individual phenotypic traits, as well as plastic effects will affect the life cycle of the trees. Our model should provide an interesting tool to study the resulting evolutionary dynamics on the population and its adaptive capacities. Our focus on relevant environmental input and on phenological aspects should be an asset for future interaction with other approaches existing in forest management and conservation ecology.

An important component of our model is a term representing the effect of sexual reproductions. We use the Fisher's Infinitesimal Model (Ronald A Fisher 1919; Barton, Etheridge, and Véber 2017), which provides a framework for understanding the evolution of continuous quantitative traits in sexually reproducing populations. Structured populations for asexual populations have attracted the attention of the mathematical community (Diekmann et al. 2005; Champagnat and Méléard 2007; Desvillettes et al. 2008; Lorz, Sepideh Mirrahimi, and Perthame 2011), and, more recently, mathematical models for sexual populations have been studied. Heuristic macroscopic limits of sexual structured population models have been proposed (Sepideh Mirrahimi and Raoul 2013; Dekens 2022; Dekens, Otto, and Calvez 2022), and several rigorous framework for such limits have been constructed. In (Calvez, Garnier, and Patout 2019; Patout 2023), a regularity approach was proposed, based on the contraction properties of the infinitesimal operator on regularity functional spaces, while in (Raoul 2017; Calvez, Lepoutre, and Poyato 2024; Frouvelle and Taing 2023; Calvez, Lepoutre, and Poyato 2024) the contraction was expressed in terms of Wasserstein distances. Finally, in (Guerand, Hillairet,

and Mirrahimi 2023), an alternative approach based on and moments has been introduced.

Our manuscript is structured as follows. We first introduce a detailed annual structured model in Section 2.2.1, where we describe precisely the life cycle of individual trees as a function of their phenotypic traits and the environmental conditions. In Section 2.2.2, we take advantage of the low mortality rate of adult trees to derive a simplified continuous structured model. We build an existence and uniqueness setting for solutions of both models and describe the asymptotic limit between these models. The model is simplified further in Section 2.2.3 by a second asymptotic limit, where we assume that the phenotypic variance of the tree population is small. This limit is related to the macroscopic limit mentioned in the last paragraph, and we do not provide a rigorous justification of this limit. This argument however allows us to obtain a simple model describing the dynamics of the mean phenotypic traits of the population through a system of two coupled ordinary differential equations. The analysis of that final model and the biological implications of this model is left for a separate manuscript. In Section 2.3, we prove the results discussed above.

## 2.2 Models, asymptotic limits and main results

### 2.2.1 The annual structured model

In this section we introduce a precise model describing the dynamics of a population of trees. The population of trees is structured by two fully inheritable phenotypic traits: a seed production trait $x \in \mathbb{R}$ which quantifies the speed at which the tree produces seeds during the reproduction season, and a dormancy trait $y \in \mathbb{R}$, describing the temperature above which the individual tree becomes dormant. To model the effect of the two traits precisely, we consider a discrete year structure with $k \in \mathbb{N} \cup \{0\}$ numbering the years. We also consider a season time $s \in [0,1]$: $s = 0$ corresponds to the beginning of the year $k$, and $s = 1$ to the end of year $k$ and the transition to year $k+1$.
The meteorological environment is described through $T_k(s)$, the temperature in year $k$ and seasonal time $s$, and the yearly precipitation quantity $P_k > 0$. We assume moreover that

$$T_k(s) = T_k^M + V_k T^V(s),$$

where $(T_k^M)_k$ is the mean annual temperature and $(T_k^V)_k$ quantifies the variation of the temperature around its yearly mean, and $V(\cdot)$ is the amplitude of yearly temperature variations (we assume

$T^V(0) = T^V(1) = 0$). We assume that $(P_k, T_k^M, V_k)_k$ is a bounded sequence. These environmental data will have an impact of the availability of water, that we denote by $\phi_k^{water}(s,x)$ (the water is lacking for an individual of seed production trait $x \in \mathbb{R}$ at seasonal time $s \in [0,1]$ and year $k \in \mathbb{N} \cup \{0\}$ if $\phi_k^{water}(s,x) = 0$, it is sufficient if $\phi_k^{water}(s,x) = 1$), and the dormancy of individuals (an individual of threshold temperature $y \in \mathbb{R}$ is active at seasonal time $s \in [0,1]$ and year $k \in \mathbb{N} \cup \{0\}$ if $\phi_k^{plast}(s,y) \sim 1$, and is dormant if $\phi_k^{plast}(s,y) \sim 0$). We will define these functions precisely later.

We assume that mature individuals die at a rate proportional to the temperature $T_k(s)$ when the water is lacking (that is when $\phi_k^{water}(s,x) = 0$) and when the individuals are not in dormancy. The individuals are in dormancy if $s \in [0, s_0]$ (this is winter dormancy that we assume fixed), or when $\phi_k^{plast}(s,y) = 1$ (this is summer dormancy). During the year $k \in \mathbb{N}$, the mature population then satisfies, for $s \in [0,1]$

$$\partial_s m_k(s,x,y) = -\varepsilon \phi_k^{plast}(s,y) \gamma (T_k(s))^+ \left(1 - \phi_k^{water}(s,x)\right) 1_{s \geq s_0} m_k(s,x,y). \tag{2.2.1}$$

Note that the notation $x^+$, for $x \in \mathbb{R}$, designates the positive part of $x$, here and throughout this manuscript. When an individual is not in dormancy, its death rate is 0 if enough water is available, and is proportional to the temperature $T_k(s)$ otherwise. Note that the temperature could be an affine function of the Celsius temperature to adapt the model to a specific tree population, and we only consider the positive part of the temperature since our attention in this study is focused on the effect of warm temperatures. Experimental and theoretical work have shown that if the ground water is too limited (that is if $\phi_k^{water}(s,x) = 1$ here), plants evapotranspiration diminishes linearly (Sinclair, Holbrook, and Zwieniecki 2005), and the plan water stress grows linearly (Rizza et al. 2004). The effect of water stress on tree mortality is not fully described yet (see McDowell et al. 2008 for field data analysis) and we decided to use a simple linear relation, leading to the model above. In equation (2.2.1), we have included $\varepsilon > 0$, which is a constant parameter, that we will eventually assume to be small. $\gamma > 0$ quantifies the effect of temperature on mortality. This will represent the fact that only a small fraction of mature individuals die during a given year, which is a reasonable assumption for tree species with a long life expectancy, provided the climatic conditions are not too extreme. This equation on mature individuals is completed by the following equation that provides the initial value of the first equation at the beginning of each year $k \in \mathbb{N}$:

$$m_k(0,x,y) = m_{k-1}(1,x,y) + \frac{1 - \iint_{\mathbb{R}^2} m_{k-1}(\hat{x},\hat{y})\, d\hat{x}\, d\hat{y}}{\iint_{\mathbb{R}^2} s_{k-1}(\hat{x},\hat{y})\, d\hat{x}\, d\hat{y}} s_{k-1}(x,y).$$

The first term on the right hand side of this equation reflects the fact that the mature individuals alive at the end of the previous year are still present. The second term represents the maturation of the seeds $s_{k-1}(x,y)$ (seeds with traits $x$ and $y$) produced during the previous year: we do not consider an intermediate juvenile state between the seed and the mature state. We assume that any space liberated by the death of mature individuals is occupied by new mature individuals, leading to fixed population size at the beginning of each year, $\iint_{\mathbb{R}^2} m_k(x,y)\,dx\,dy = 1$; this explains the factor in front of the last term of the equation.

During the year $k \in \mathbb{N} \cup \{0\}$ and at season time $s \in [0,1]$, an adult with traits $(x,y)$ produces eggs (ie seeds that need fertilization by pollen) at a rate $x^+$ (the positive part of the seed production trait $x \in \mathbb{R}$), provided water is not lacking (that is if $\phi_k^{water}(s,x) = 1$), and provided the individual is not dormant (that is if $\phi_k^{plast}(s,y) \sim 1$). If water is lacking or the plant is dormant, no egg is produced. The number of eggs produced during year $k$ at time $s \in [0,1]$ is then given by the following distribution

$$(x_1,y_1) \mapsto x_1^+ m_k(s,x_1,y_1)\phi_k^{plast}(s,y_1)\phi_k^{water}(s,x_1)1_{s\geq s_0}.$$

Pollen is produced by all mature individuals that do not lack water and are not dormant, so that the quantity of pollen present at season time $s$ is given by the following distribution

$$(x_2,y_2) \mapsto m_k(s,x_2,y_2)\phi_k^{plast}(s,y_2)\phi_k^{water}(s,x_2)1_{s\geq s_0}.$$

We assume that the pollen fertilizing an egg is drawn uniformly among the pollen present at time $s$, and we introduce the parameter $\eta > 0$ to model the fact that if the quantity of pollen production is very low (that is if $\iint m_k(s,\hat{x},\hat{y})\phi_k^{plast}(s,\hat{y})\phi_k^{water}(s,\hat{x})\,d\hat{x}\,d\hat{y} \ll \eta$), the eggs fertilisation fails. More precisely, the probability that an egg is fertilized is

$$(x_2,y_2) \mapsto \frac{\iint_{\mathbb{R}^2} m_k(s,\hat{x},\hat{y})\phi_k^{plast}(s,\hat{y})\phi_k^{water}(s,\hat{x})\,d\hat{x}\,d\hat{y}}{\eta + \iint_{\mathbb{R}^2} m_k(s,\hat{x},\hat{y})\phi_k^{plast}(s,\hat{y})\phi_k^{water}(s,\hat{x})\,d\hat{x}\,d\hat{y}},$$

and if the fertilisation occurs, the law of the traits of the fertilizing pollen is given by

$$(x_2,y_2) \mapsto \frac{m_k(s,x_2,y_2)\phi_k^{plast}(s,y_2)\phi_k^{water}(s,x_2)}{\iint_{\mathbb{R}^2} m_k(s,\hat{x},\hat{y})\phi_k^{plast}(s,\hat{y})\phi_k^{water}(s,\hat{x})\,d\hat{x}\,d\hat{y}}.$$

If we consider a seed produced by an egg of traits $(x_1,y_1)$ and a pollen of traits $(x_2,y_2)$, the traits of

the seed is given by a normal law of covariance

$$\begin{pmatrix} \sigma_x^2 & 0 \\ 0 & \sigma_y^2 \end{pmatrix},$$

centered in the average traits of the parents. We assume that $\sigma_x, \sigma_y > 0$. This is the so-called infinitesimal model (Ronald A Fisher 1919; Barton, Etheridge, and Véber 2017), which represents the effect of sexual reproductions on phenotypic traits. The law of the seed's traits is then

$$(x,y) \mapsto \Gamma_{\sigma_x^2}\left(\frac{x_1+x_2}{2} - x\right)\Gamma_{\sigma_y^2}\left(\frac{y_1+y_2}{2} - y\right). \tag{2.2.2}$$

We also assume a constant immigration of seeds at rate $\nu > 0$, and we the traits of these immigrant seeds are normally distributed around $(0,0)$, with the covariance matrix $\begin{pmatrix} 2\sigma_x^2 & 0 \\ 0 & 2\sigma_y^2 \end{pmatrix}$. Bringing all these assumptions together, the seeds produced during the year $k$, structured by the traits $(x,y)$, is given by

$$\begin{aligned} s_k(x,y) &= \nu\Gamma_{2\sigma_x^2}(x)\Gamma_{2\sigma_y^2}(y) \\ &+ \int_0^1 \iint_{\mathbb{R}^2}\iint_{\mathbb{R}^2} \Gamma_{\sigma_x^2}\left(x - \frac{x_1+x_2}{2}\right)\Gamma_{\sigma_y^2}\left(y - \frac{y_1+y_2}{2}\right) x_1^+ m_k(s,x_1,y_1)\phi_k^{plast}(s,y_1)\phi_k^{water}(s,x_1) \\ &\qquad \frac{m_k(s,x_2,y_2)\phi_k^{plast}(s,y_2)\phi_k^{water}(s,x_2)1_{s\geq s_0}}{\eta + \iint_{\mathbb{R}^2} m_k(s,\hat{x},\hat{y})\phi_k^{plast}(s,\hat{y})\phi_k^{water}(s,\hat{x})\,d\hat{x}\,d\hat{y}}\,dx_1\,dx_2\,dy_1\,dy_2\,ds, \end{aligned}$$

and as mention earlier, a fraction of these seeds will turn into mature individuals at the beginning of year $k+1$.

We will now define the function $\phi_k^{water}(s,x) \geq 0$, that represents the availability of water for an adult individual of seed production trait $x \in \mathbb{R}$ in year $k \in \mathbb{N}\cup\{0\}$, at the season time $s \in [0,1]$. We assume that each individual receives an annual quantity of water $P_k$. After the end of the winter dormancy of the trees, that we consider fixed at season time $s_0 \geq 0$, this water is consumed the mature individuals at a fixed rate 1, plus an additional water consumption rate proportional to the quantity of eggs produced, that is a consumption rate of $1+\alpha x^+$. Moreover, we assume that heat induces an additional consumption of water (for each adult individual) proportional to the temperature. Indeed, a large part of a plant's water consumption is related to its evapotranspiration, which can be modeled as a linear function of the temperature (see Penman 1948; Thornthwaite 1948), provided enough ground water is available to the plant. These assumptions lead to a total water consumption between the

beginning of the year $k \in \mathbb{N} \cup \{0\}$ and the time $s \geq s_0$ given by $(1+\alpha x^+)(s-s_0)+\beta \int_{s_0}^{s} T_k(\tau)\, d\tau$, while no water is consumed for $s \in [0, s_0]$. To see if the water is available at season time $s$ (that is to see if $\phi_k^{water}(s,x) = 1$) or if it is lacking (that is $\phi_k^{water}(s,x) = 0$), we compare the water consumption to the precipitations that occur during year $k$, that is $P_k$. We obtain:

$$\phi_k^{water}(s,x) = \begin{cases} 0 \text{ if } s \geq s_0 \text{ and } (1+\alpha x^+)(s-s_0)+\beta \int_{s_0}^{s} (T_k(\tau))^+ \, d\tau > P_k, \\ 1 \text{ otherwise.} \end{cases} \tag{2.2.3}$$

We should also define the function $\phi_k^{plast}(s,y) \geq 0$, that describes if the individual of threshold temperature trait $y$ is active (that is $\phi_k^{plast}(s,y) \sim 1$) or dormant (that is $\phi_k^{plast}(s,y) \sim 0$). In the definition below, we will actually consider $s \sim \phi_k^{plast}(s,x)$ as a Lipschitz function valued in $[0,1]$. We assume that the dormancy is heat triggered: when the temperature $T_k^0(s)$ is higher than the threshold temperature trait $y$, individuals become dormant with a given rate $\beta$. Then,

$$\phi_k^{plast}(s,y) = e^{-\beta \int_{s_0}^{s} 1_{T_k(\tau)>y}\, d\tau}. \tag{2.2.4}$$

Note that the population $m_k(t,x,y)$ is structured by the phenotypic traits $(x,y) \in \mathbb{R}$ that are actually breeding values: the value of these traits is determined at birth, and are fully inherited. On the contrary, the phenological trait determining when an individual of traits $(x,y)$ becomes dormant, which we can define as the first season time $s \in (0,1)$ such that $T_k(\tau) \geq y$ is a plastic trait that depends on the trait $y$ and the temperature of year $k$, that is $T_k$. Similarly, this adult individual will face a positive death probability if $\phi_k^{plast}(s,y)\left(1-\phi^{water}\right) > 0$ for some $s \in (0,1)$; the existence of such death events and the seasonal time period when that happens are both plastic traits that depend on the phenotypic traits $(x,y)$ of the individual as well as the environmental conditions $T_k$ and $P_k$.

The annual structured model, for $\varepsilon > 0$, is then

$$\begin{cases} \partial_s m_k(s,x,y) = -\varepsilon \phi_k^{plast}(s,y)\gamma(T_k(s))^+ \left(1-\phi_k^{water}(s,x)\right) 1_{s\geq s_0} m_k(s,x,y), \text{ for } (k,s,x,y) \in (\mathbb{N}\cup\{0\})\times\mathbb{R}_+\times \\ \\ m_k(0,x,y) = m_{k-1}(1,x,y) + \frac{1-\iint_{\mathbb{R}^2} m_{k-1}(1,\hat{x},\hat{y})\,d\hat{x}\,d\hat{y}}{\iint_{\mathbb{R}^2} s_{k-1}(\hat{x},\hat{y})\,d\hat{x}\,d\hat{y}} s_{k-1}(x,y), \text{ for } (k,x,y) \in \mathbb{N}\times\mathbb{R}^2, \\ \\ m_0(0,x,y) = m^0(x,y), \text{ for } (x,y)\in\mathbb{R}^2, \\ \\ s_k(x,y) = \nu \Gamma_{2\sigma_x^2}(x)\Gamma_{2\sigma_y^2}(y) \\ \quad + \int_0^1 \iint_{\mathbb{R}^2}\iint_{\mathbb{R}^2} \Gamma_{\sigma_x^2}\left(x-\frac{x_1+x_2}{2}\right)\Gamma_{\sigma_y^2}\left(y-\frac{y_1+y_2}{2}\right) x_1^+ m_k(s,x_1,y_1)\phi_k^{plast}(s,y_1)\phi_k^{water}(s,x_1) \\ \qquad \frac{m_k(s,x_2,y_2)\phi_k^{plast}(s,y_2)\phi_k^{water}(s,x_2)1_{s\geq s_0}}{\eta+\iint_{\mathbb{R}^2} m_k(s,\hat{x},\hat{y})\phi_k^{plast}(s,\hat{y})\phi_k^{water}(s,\hat{x})\,d\hat{x}\,d\hat{y}}\,dx_1\,dx_2\,dy_1\,dy_2\,ds, \text{ for } (k,x,y)\in(\mathbb{N}\cup\{0\})\times\mathbb{R}^2, \end{cases} \tag{2.2.5}$$

where $\phi_k^{plast}$, $\phi_k^{water}$ are defined by (2.2.4), (2.2.3) respectively. This system does define the population $m_k(x,y)$, in the sense of the existence and uniqueness setting given by the following theorem. In that theorem, we denote by $L^1((1+e^x)\,dx\,dy,\mathbb{R}_+)$ the set of non-negative functions on $\mathbb{R}^2$ that are integrable against a weight $(x,y)\mapsto(1+e^x)\,dx\,dy$:

**Theorem 2.1.** Assume $m^0 \in L^1((1+e^x)\,dx\,dy,\mathbb{R}_+)$, with $\iint_{\mathbb{R}^2} m^0(x,y)\,dx\,dy = 1$. There exist a unique global non-negative solution $(m_k,p_k) \in \left(L^\infty([0,1],L^1((1+e^x)\,dx\,dy))\right)^2$ to the annual structured model (2.2.5), for $k\in\mathbb{N}\cup\{0\}$. Moreover, for $k\in\mathbb{N}\cup\{0\}$,

$$\iint_{\mathbb{R}^2} m_k(0,x,y)\,dx\,dy = 1. \tag{2.2.6}$$

### 2.2.2 Asymptotic limit to the continuous structured model

The annual structured model (2.2.5) involves a parameter $\varepsilon > 0$, which quantifies the death rate of adult individuals: the life expectancy of adults trees in our model is of the order of $1/\varepsilon$. For numerous species of trees, year-to-year mortality is low for adults (typically of the order of 1%, see (Das, Stephenson, and Davis 2016)), and we take advantage of this to propose an asymptotic limit of the model. We first perform a heuristic limit of the model (2.2.5): when $\varepsilon > 0$ is small , (2.2.5) implies that $m_k(s,x,y) = m_k(0,x,y) + \mathcal{O}(\varepsilon)$ for $(k,s,x,y)\in\mathbb{N}\times[0,1]\times\mathbb{R}\times\mathbb{R}$. Therefore

$$m_k(1,x,y) = (1-\varepsilon a_k(1,x,y))\,m_k(0,x,y) + \mathcal{O}(\varepsilon^2),$$

where

$$a_k(s,x,y) = \int_0^s \phi_k^{plast}(\tau,y)\gamma(T_k(\tau))^+ \left(1-\phi_k^{water}(\tau,x)\right) 1_{s\geq s_0}\, d\tau. \tag{2.2.7}$$

Then,

$$\begin{aligned} m_{k+1}(0,x,y) \sim\ & e^{-\varepsilon a_k(1,x,y)} m_k(0,x,y) \\ & + \frac{1-\iint_{\mathbb{R}^2} e^{-\varepsilon a_k(1,\hat{x},\hat{y})} m_k(0,\hat{x},\hat{y})\, d\hat{x}\, d\hat{y}}{\iint_{\mathbb{R}^2} s_k(\hat{x},\hat{y})\, d\hat{x}\, d\hat{y}} \\ & \left( \int_0^1 \iint_{\mathbb{R}^2} \iint_{\mathbb{R}^2} \Gamma_{\sigma_x^2}\left(x-\frac{x_1+x_2}{2}\right) \Gamma_{\sigma_y^2}\left(y-\frac{y_1+y_2}{2}\right) x_1^+ e^{-\varepsilon a_k(s,x_1,y_1)} m_k(0,x_1,y_1) \phi_k^{water}(s,x_1) \phi_k^{plast}(s,y_1) \right. \\ & \left. \frac{e^{-\varepsilon a_k(s,x_2,y_2)} m_k(0,x_2,y_2) \phi_k^{water}(s,x_2) \phi_k^{plast}(s,y_2) 1_{s\geq s_0}}{\eta + \iint_{\mathbb{R}^2} e^{-\varepsilon a_k(s,\hat{x},\hat{y})} m_k(0,\hat{x},\hat{y}) \phi_k^{water}(s,\hat{x}) \phi_k^{plast}(s,\hat{y})\, d\hat{x}\, d\hat{y}}\, dx_1\, dx_2\, dy_1\, dy_2\, ds + \nu \Gamma_{2\sigma_x^2}(x) \Gamma_{2\sigma_y^2}(y) \right). \end{aligned} \tag{2.2.8}$$

To pass to the limit in the integral term above, we assume that the environmental parameters $T^{M,\varepsilon}, V^\varepsilon, P^\varepsilon$ change gradually from one year to another. More precisely, for $t \geq 0$ and $\varepsilon \to 0$,

$$(T^{M,\varepsilon}, V^\varepsilon, P^\varepsilon)_{\lfloor t/\varepsilon \rfloor} = (\bar{T}^M, \bar{V}, \bar{P})(t) + \mathcal{O}(\varepsilon), \tag{2.2.9}$$

which corresponds to a situation where the climate changes on a time scale of $1/\varepsilon$, which is the time scale of the life expectancy of the trees. It could be interesting to consider faster environmental dynamics in future work, as we propose in the discussion. We assume that the functions $\bar{T}^M$, $\bar{V}$, $\bar{P}$ are Lipschitz continuous. Then, for $s \in [0,1]$,

$$T^\varepsilon_{\lfloor t/\varepsilon \rfloor}(s) = \bar{T}(t,s) + \mathcal{O}(\varepsilon), \tag{2.2.10}$$

where $\bar{T}(t,s) := \bar{T}^M(t) + \bar{V}(t) T^V(s)$. We may then define

$$\bar{\phi}^{plast}(t,s,y) = e^{-\beta \int_0^s 1_{\bar{T}^o(t,\sigma)>y} 1_{s\geq s_0}\, d\sigma}$$

$$\bar{\phi}^{water}(t,s,x) = \begin{cases} 0 \text{ if } s \geq s_0 \text{ and } (1+\alpha x^+)(s-s_0) + \beta \int_{s_0}^s (\bar{T}(t,\tau))^+\, d\tau > \bar{P}(t), \\ 1 \text{ otherwise,} \end{cases}$$

and the population $m_k$ then satisfies

$$\begin{aligned}\frac{m_{\lfloor t/\varepsilon\rfloor+1}(0,x,y)-m_{\lfloor t/\varepsilon\rfloor}(0,x,y)}{\varepsilon} &\sim -a_{\lfloor t/\varepsilon\rfloor}(1,x,y)m_{\lfloor t/\varepsilon\rfloor}(0,x,y)+\mathcal{O}(\varepsilon^2)\\ &+\left(\iint_{\mathbb{R}^2} a_{\lfloor t/\varepsilon\rfloor}(1,x,y)m_{\lfloor t/\varepsilon\rfloor}(0,x,y)+\mathcal{O}(\varepsilon^2)dx\,dy\right)\\ &\frac{1}{\bar R_{\lfloor t/\varepsilon\rfloor}[m]+\nu}\Bigg[\iint_{\mathbb{R}^2}\iint_{\mathbb{R}^2}\Gamma_{\sigma_x^2}\left(x-\frac{x_1+x_2}{2}\right)\Gamma_{\sigma_y^2}\left(y-\frac{y_1+y_2}{2}\right)x_1^+ m_{\lfloor t/\varepsilon\rfloor}(0,x_1,y_1)m_{\lfloor t/\varepsilon\rfloor}(0,x_2,y_2)\\ &\qquad\rho_{\lfloor t/\varepsilon\rfloor}[m](x_1,y_1,x_2,y_2)\,dx_1\,dx_2\,dy_1\,dy_2\,ds+\nu\Gamma_{2\sigma_x^2}(x)\Gamma_{2\sigma_y^2}(y)\Bigg],\end{aligned} \tag{2.2.11}$$

where

$$Q_{\lfloor t/\varepsilon\rfloor}[m]=\iint_{\mathbb{R}^2} m_{\lfloor t/\varepsilon\rfloor}(0,\hat x,\hat y)\int_0^1 \bar\phi^{water}(t,s,\hat x)\bar\phi^{plast}(t,s,\hat y)1_{s\geq s_0}\,ds\,d\hat x\,d\hat y,$$

$$\begin{aligned}R_{\lfloor t/\varepsilon\rfloor}[m]=\iint_{\mathbb{R}^2}\iint_{\mathbb{R}^2}\hat x^+ m_{\lfloor t/\varepsilon\rfloor}(0,\hat x,\hat y)m_{\lfloor t/\varepsilon\rfloor}(0,\tilde x,\tilde y)\\ \int_0^1\bar\phi^{water}(t,s,\hat x)\bar\phi^{plast}(t,s,\hat y)\frac{\bar\phi^{water}(t,s,\tilde x)\bar\phi^{plast}(t,s,\tilde y)1_{s\geq s_0}}{\eta+Q_{\lfloor t/\varepsilon\rfloor}[m]}\,ds\,d\hat x\,d\hat y\,d\tilde x\,d\tilde y,\end{aligned}$$

$$\rho_{\lfloor t/\varepsilon\rfloor}[m](x_1,y_1,x_2,y_2)=\int_0^1\frac{\bar\phi^{plast}(t,s,y_1)\bar\phi^{plast}(t,s,y_2)\bar\phi^{water}(t,s,x_1)\bar\phi^{water}(t,s,x_2)1_{s\geq s_0}}{\eta+Q_{\lfloor t/\varepsilon\rfloor}[m]}\,ds.$$

We therefore expect the population to converge to a limit when $\varepsilon>0$ is small:

$$m_{\lfloor s/\varepsilon\rfloor}(0,x,y)\to_{\varepsilon\to 0} n(s,x,y),$$

where $n$ is the solution of the following continuous structured model:

$$\begin{aligned}\partial_t n(t,x,y)&=-\bar a(t,x,y)n(t,x,y)\\ &+\frac{\iint_{\mathbb{R}^2}\bar a(t,\hat x,\hat y)n(t,\hat x,\hat y)\,d\hat x\,d\hat y}{\nu+\bar R[n](t)}\Bigg[\iint_{\mathbb{R}^2}\iint_{\mathbb{R}^2}\Gamma_{\sigma_x^2}\left(x-\frac{x_1+x_2}{2}\right)\Gamma_{\sigma_y^2}\left(y-\frac{y_1+y_2}{2}\right)x_1^+ n(t,x_1,y_1)n(t,x_2,y_2)\\ &\qquad\bar\rho[n(t,\cdot,\cdot)](t,x_1,y_1,x_2,y_2)\,dx_1\,dx_2\,dy_1\,dy_2+\nu\Gamma_{2\sigma_x^2}(x)\Gamma_{2\sigma_y^2}(y)\Bigg],\end{aligned} \tag{2.2.12}$$

with

$$\bar a(t,x,y)=\int_0^1\bar\phi^{plast}(t,s,y)\gamma(\bar T(t,s))^+\left(1-\bar\phi^{water}(t,s,x)\right)1_{s\geq s_0}\,ds, \tag{2.2.13}$$

$$\bar Q[n](t)=\iint_{\mathbb{R}^2} n(t,\hat x,\hat y)\int_0^1\bar\phi^{water}(t,s,\hat x)\bar\phi^{plast}(t,s,\hat y)1_{s\geq s_0}\,ds\,d\hat x\,d\hat y,$$

$$\bar{R}[n](t) = \iint_{\mathbb{R}^2}\iint_{\mathbb{R}^2} \hat{x}^+ n(t,\hat{x},\hat{y})n(t,\tilde{x},\tilde{y})\bar{\rho}[n(t,\cdot,\cdot)](t,\hat{x},\hat{y},\tilde{x},\tilde{y})\,d\hat{x}\,d\hat{y}\,d\tilde{x}\,d\tilde{y},$$

$$\bar{\rho}[n(t,\cdot,\cdot)](t,x_1,y_1,x_2,y_2) = \int_0^1 \frac{\bar{\phi}^{plast}(t,s,y_1)\bar{\phi}^{plast}(t,s,y_2)\bar{\phi}^{water}(t,s,x_1)\bar{\phi}^{water}(t,s,x_2)1_{s\geq s_0}}{\eta+\bar{Q}[n](t)}\,ds.$$

We introduce an existence and uniqueness setting for solutions $n$ of (2.2.12) in the following theorem, where $L^1((1+e^x)\,dx\,dy,\mathbb{R}_+)$ designates the set of non-negative functions on $\mathbb{R}^2$ that are integrable against a weight $(x,y)\mapsto(1+e^x)\,dx\,dy$:

**Theorem 2.2.** Assume $n^0 \in L^1(\mathbb{R}^2,\mathbb{R}_+)\cap W^{1,\infty}(\mathbb{R}^2)$. There exists a unique solution $n \in L^\infty(\mathbb{R}_+,L^1(\mathbb{R}^2,\mathbb{R}_+))$ of 2.2.12 with initial data $n^0$. If $n^0 \in L^\infty(\mathbb{R}^2,\mathbb{R}_+)$, then the solution $n$ is bounded locally in time:

$$\|n(t,\cdot,\cdot)\|_{L^\infty(\mathbb{R}^2)} \leq C(1+t),$$

for some $C>0$. Moreover, if $n^0$ is Lipschitz continuous, there is $C>0$ such that for $t\geq 0$, $x,x',y,y' \in \mathbb{R}$ satisfying $y'\leq y$,

$$n(t,x,y)-n(t,x',y') \leq C(1+t^2)\left(|x-x'|+|y-y'|\right). \tag{2.2.14}$$

Finally, there exists $C>0$ such that

$$\iint_{\mathbb{R}^2} x^2 n(t,x,y)\,dx\,dy \leq Ce^{Ct}. \tag{2.2.15}$$

We can also build a rigorous connection between the annual structured model (2.2.5) and the continuous structured model (2.2.12) when $\varepsilon>0$ is asymptotically small, thanks to the following result:

**Theorem 2.3.** Assume $n^0 \in L^1(\mathbb{R}^2,\mathbb{R}_+)\cap W^{1,\infty}(\mathbb{R}^2)$. For $\varepsilon>0$, let $(m_k^\varepsilon,s_k^\varepsilon) \in L^1([0,1],\mathbb{R}^2\times L^\infty(\mathbb{R}^2)$the solution of (2.2.12) in the sense of Theorem 2.1, with initial data $m^0 := n^0$. Let $n_\varepsilon \in L^1(\mathbb{R}_+\times\mathbb{R}^2)$ the solution of 2.2.12 in the sense of Theorem 2.2, with initial data $n^0$. For any $T\geq 0$, we have

$$\lim_{\varepsilon\to 0}\|n(t,x,y)-m^\varepsilon_{\lfloor t/\varepsilon\rfloor}(0,x,y)\|_{L^\infty([0,T],L^1(\mathbb{R}^2))}=0.$$

### 2.2.3 Derivation of the macroscopic model

The model (2.2.5) was constructed the using life cycle processes of individual trees. The drawback of this derivation is the complexity of the model, which was reduced thanks to an asymptotic limit

leading to the continuous structured model (2.2.12). That second model remains complex and in this chapter we simplify it further. Our idea is to use the asymptotic limit where the phenotypic variance of the population is small, that is $\sigma_x^2 > 0$ and $\sigma_y^2 > 0$ small. This assumption correspond to the weak selection that is often used in population genetics (Wakeley 2005), and which has been used in many mathematical studies involving the infinitesimal model (Patout 2023; Raoul 2017). We refer to the discussion for the potential limitations of this approach. Specifically, we assume:

$$(\sigma_x^2, \sigma_y^2) = \sigma^2(\bar{\sigma}_x^2, \bar{\sigma}_y^2),$$

for some parameter $\sigma > 0$ small. We also assume $\nu = \eta = 0$ to simplify the notations in this section.

We define $(X(t), Y(t))$ as the mean phenotypic traits of the population: $X(t)$ is the mean of the trait $x$ - the seed production trait; $Y(t)$ is the mean of the trait $y$ - the threshold temperature trait. Since $\iint_{\mathbb{R}^2} n(t,x,y)\,dx\,dy \equiv 1$,

$$X(t) := \iint_{\mathbb{R}^2} x\, n(t,x,y)\,dx\,dy, \quad Y(t) := \iint_{\mathbb{R}^2} y\, n(t,x,y)\,dx\,dy. \tag{2.2.16}$$

When $\sigma > 0$ is small, the solution $n$ will be distributed as a normal distribution with covariance

$$\sigma^2 \begin{pmatrix} \bar{\sigma}_x^2 & 0 \\ 0 & \bar{\sigma}_y^2 \end{pmatrix},$$

centered around $(X(t), Y(t))$, that is

$$\tilde{n}(t,x,y) \sim \Gamma_{2\sigma^2\bar{\sigma}_x^2}(x - X(t))\,\Gamma_{2\sigma^2\bar{\sigma}_y^2}(y - Y(t)). \tag{2.2.17}$$

We explain why $\sigma > 0$ small leads to this approximation in Section 2.5. Thanks to this approximation formula, we simply need to describe the time dynamics of the mean phenotypic traits $X(t)$ and $Y(t)$, which, thanks to their definition (2.2.16) and to the model (2.2.12), satisfy

$$\begin{aligned}\frac{d}{dt}X(t) = &- \iint_{\mathbb{R}^2} x\bar{a}(t,x,y)n(t,x,y)\,dx\,dy \\ &+ \frac{\iint_{\mathbb{R}^2} \bar{a}(t,x,y)n(t,x,y)\,dx\,dy}{\iint_{\mathbb{R}^2}\iint_{\mathbb{R}^2} x_1^+ n(t,x_1,y_1)n(t,x_2,y_2)\bar{\rho}[n(t,\cdot,\cdot)](t,x_1,y_1,x_2,y_2)\,dx_1\,dy_1\,dx_2\,dy_2} \\ &\iint_{\mathbb{R}^2}\iint_{\mathbb{R}^2} \frac{x_1+x_2}{2} x_1^+ n(t,x_1,y_1)n(t,x_2,y_2)\bar{\rho}[n(t,\cdot,\cdot)](t,x_1,y_1,x_2,y_2)\,dx_1\,dy_1\,dx_2\,dy_2,\end{aligned} \tag{2.2.18}$$

$$\frac{d}{dt}Y(t) = -\iint_{\mathbb{R}^2} y\bar{a}(t,x,y)n(t,x,y)\,dx\,dy + \frac{\iint_{\mathbb{R}^2}\bar{a}(t,x,y)n(t,x,y)\,dx\,dy}{\iint_{\mathbb{R}^2}\iint_{\mathbb{R}^2} x_1^+ n(t,x_1,y_1)n(t,x_2,y_2)\bar{\rho}[n(t,\cdot,\cdot)](t,x_1,y_1,x_2,y_2)\,dx_1\,dy_1\,dx_2\,dy_2} \iint_{\mathbb{R}^2}\iint_{\mathbb{R}^2} \frac{y_1+y_2}{2} x_1^+ n(t,x_1,y_1)n(t,x_2,y_2)\bar{\rho}[n(t,\cdot,\cdot)](t,x_1,y_1,x_2,y_2)\,dx_1\,dy_1\,dx_2\,dy_2. \tag{2.2.19}$$

Using the approximation (2.2.17), it is possible to simplify these expressions, as we detail in the appendix (Section 2.6). We obtain:

$$\frac{d}{dt}X(t) \sim 2\sigma^2\bar{\sigma}_x^2\left[-\partial_x\bar{a}(t,X(t),Y(t)) + \frac{\bar{a}(t,X(t),Y(t))}{2X(t)} + \bar{a}(t,X(t),Y(t))\frac{\partial_x(\hat{\rho}[X(t),Y(t)])(t,X(t),Y(t))}{\hat{\rho}[X(t),Y(t)](t,X(t),Y(t))}\right], \tag{2.2.20}$$

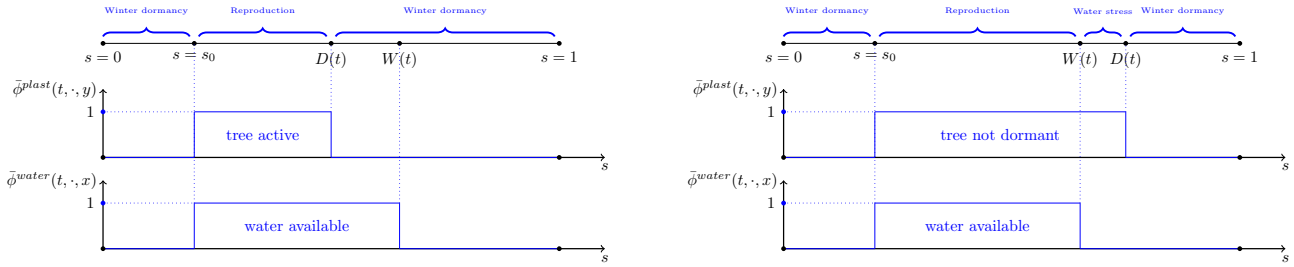
$$\frac{d}{dt}Y(t) \sim 2\sigma^2\bar{\sigma}_y^2\left[-\partial_y\bar{a}(t,X(t),Y(t)) + \bar{a}(t,X(t),Y(t))\frac{\partial_y(\hat{\rho}[X(t),Y(t)])(t,X(t),Y(t))}{\rho[X(t),Y(t)](t,X(t),Y(t))}\right], \tag{2.2.21}$$

where $\bar{a}$ is defined by (2.2.13) and

$$\hat{\rho}[X(t),Y(t)](t,x,y) = \int_0^1 \bar{\phi}^{plast}(t,s,y)\bar{\phi}^{plast}(t,s,Y(t))\bar{\phi}^{water}(t,s,x)\bar{\phi}^{water}(t,s,X(t))1_{s\geq s_0}\,ds.$$

Note that we do not provide a rigorous result for the derivation of (2.2.20)-(2.2.21) from the continuous structured model (2.2.12): our arguments are heuristic only. The ordinary differential equation formed by (2.2.20), (2.2.21) and approximation (2.2.17) provides a simple description of the dynamics of the population. It summarizes the complex biological features taken into account to derive the original model (2.2.5) into a two-dimensional dynamical system. We will analyze the dynamics of this model and its evolutionary ecology predictions a different manuscript. We however briefly discuss the different terms of equations (2.2.20)-(2.2.21):

- The first term on the right hand side of the equation on $X(t)$ comes from the impact of $X(t)$ on the mortality rate $\bar{a}(t,X(t),Y(t))$ and shows that evolution tends to lower the mortality rate of individuals. A similar description can be made on the first term of the equation for $Y(t)$.
- The term $\frac{\bar{a}(t,X(t),Y(t))}{2X(t)}$ in the equation for $X(t)$ results from the definition of the phenotypic trait $x$: it designates the production of (the female part of) seeds, and increasing $X(t)$ therefore has a direct positive contribution on the seed production, which this term represents. The factor $\frac{1}{2}$ appears because the trait $X(t)$ only impacts one of the parents ($X(t)$ has no impact on pollen production), while the factor $\frac{1}{X(t)}$ appears because of our modeling choice of having a regulation




(a) (b)

Fig. S1: Phenology of a typical tree. (a) Cases where $D(t) < W(t)$, trees first face a winter period, until at seasonnal time $s = s_0$ when they start producing seeds, until seasonal time $s = D(t)$ when they become dormant until the next season. Note that in this case, the tree is not using all the available water. (b) Cases where $W(t) < D(t)$, the trees suffer from a lack of water from seasonal time $W(t)$ until they become dormant at seasonal time $D(t)$, this stress results in a positive death rate for trees during that period. Note that in this case, the tree is submitted to water stress for $s \in [W(t), D(t)]$, which induces a positive death rate.

of the population size by birth (new offspring mature only when adults in the population die).

- The last terms in equations for both $X(t)$ and $Y(t)$, involving $\hat{\rho}[X(t),Y(t)]$, represent the effect of preferential mating. For instance, if $\partial_x(\hat{\rho}[X(t),Y(t)])(t,X(t),Y(t)) > 0$, individual trees with a larger trait $x$ engage in more reproduction events and have more offspring. This assortative mating results from the phenological consequences of the traits we consider: at any seasonal time $s \in [s_0, 1]$, reproduction only happens among adults that are not dormant and have sufficient water.

If $\beta > 0$ is large, given $(X(t),Y(t))$, we can recover the seasonal time when individuals become dormant, that we denote $D(t)$, and the seasonal time when individuals run out of water, that we denote by $W(t)$. These plastic traits can indeed be defined as follows:

$$D(t) := \min\left\{s \in (s_0,1); \bar{T}(s,t) \geq Y(t)\right\},$$

$$W(t) := \min\left\{s \in (s_0,1); (1+\alpha X(t))(s-s_0) + \beta \int_{s_0}^{s} (\bar{T}(t,\tau))^+ \, d\tau \leq \bar{P}(t)\right\},$$

with the convention $D(t) = 1$ if the $\bar{T}(s,t) < Y(t)$ for $t \in (0,1)$ (and a similar convention for $W(t)$). At time $t$, the phenology of the population with mean phenotypic traits $(X(t),Y(t))$ can then be summarized using $D(t)$ and $W(t)$, which we represent in Figure S1

## 2.3 Proofs of the main results

### 2.3.1 Preliminaries

We define the application $\mathcal{T}$ below that will be useful to understand the effect of the sexual reproduction term in (2.2.5) and (2.2.12):

$$\begin{aligned}&\mathcal{T}(f,g)(x,y)\\&\quad=\iint_{\mathbb{R}^2}\iint_{\mathbb{R}^2}\Gamma_{\sigma_x^2}\left(x-\frac{x_1+x_2}{2}\right)\Gamma_{\sigma_y^2}\left(y-\frac{y_1+y_2}{2}\right)x_1^+f(x_1,y_1)g(x_2,y_2)\,dx_1\,dy_1\,dx_2\,dy_2.\end{aligned}\tag{2.3.1}$$

$\mathcal{T}$ is actually a quadratic operator over $L^1((1+e^x)\,dx\,dy)$, as shown by the following proposition: The non-linear operator $\mathcal{T}$ is defined on $L^1((1+e^x)\,dx\,dy)$ and there is $C>0$ such that for $f,g\in L^1((1+e^x)\,dx\,dy)$,

$$\|\mathcal{T}(f,g)\|_{L^1((1+e^x)\,dx\,dy)}\leq C\|f\|_{L^1((1+e^x)\,dx\,dy)}\|g\|_{L^1((1+e^x)\,dx\,dy)}.$$

*Remark* 2.4. This Proposition shows that $\mathcal{T}$ is well defined as an operator on $L^1((1+e^x)\,dx\,dy)$. This estimate allows us to define global solution of the annual structured population model (2.2.5), see Theorem 2.1, but since this is a quadratic estimate rather than a linear estimate, it could only lead to a local existence result for the continuous structured population model (2.2.12). To get around this issue and prove Theorem 2.2, we will take advantage of the fact that the total number of seeds produced by an individual tree is limited by the available water (see (2.3.7)), which is a property specific to the model we consider in this manuscript. This will allow us to use a more classical $L^1$ estimate (without weight) on the reproduction term, and the conservation of the total population mass (2.2.6) can then be used to obtain a linear estimate on the reproduction term.

*Proof of Proposition 2.3.1.* For $f,g\in L^1((1+e^x)\,dx\,dy)$, thanks to a change of variable, we can write

$$\begin{aligned}&\mathcal{T}(f,g)(x,y)\\&\quad=\iint_{\mathbb{R}^2}\Gamma_{\sigma_x^2}\left(\frac{1}{2}(2x-X_1)\right)\Gamma_{\sigma_y^2}\left(\frac{1}{2}(2y-Y_1)\right)\\&\qquad\left[\iint_{\mathbb{R}^2}(X_1-x_2)^+f(X_1-x_2,Y_1-y_2)g(x_2,y_2)\,dx_2\,dy_2\right]dX_1\,dY_1,\end{aligned}$$

and using $*$ to represent convolutions over $\mathbb{R}^2$, we notice that $\mathcal{T}(f,g)$ can be seen as a convolution

(see Sepideh Mirrahimi and Raoul 2013 for a similar idea):

$$\mathcal{T}(f,g) = \left[\left((x,y)\mapsto \Gamma_{\sigma_x^2}\left(\frac{x}{2}\right)\Gamma_{\sigma_y^2}\left(\frac{y}{2}\right)\right) * \Big(((x,y)\mapsto xf(x,y)) * g\Big)\right](2x,2y).$$

Therefore

$$\begin{aligned}\iint_{\mathbb{R}^2} \mathcal{T}(f,g)(x,y)\,dx\,dy &\le \left\|(x,y)\mapsto \Gamma_{\sigma_x^2}\left(\frac{x}{2}\right)\Gamma_{\sigma_y^2}\left(\frac{y}{2}\right)\right\|_{L^1(\mathbb{R}^2)} \|(x,y)\mapsto x\,f(x,y)\|_{L^1(\mathbb{R}^2)}\|g\|_{L^1(\mathbb{R}^2)}\\ &\le 4\|f\|_{L^1((1+e^x)\,dx\,dy)}\|g\|_{L^1((1+e^x)\,dx\,dy)},\end{aligned}$$

and in particular $\mathcal{T}(f,g)\in L^1(\mathbb{R}^2)$. Moreover,

$$\begin{aligned}&\iint_{\mathbb{R}^2} e^x\mathcal{T}(f,g)(x,y)\,dx\,dy = \iint_{\mathbb{R}^2}\iint_{\mathbb{R}^2}\left(\int e^x\Gamma_{\sigma_x^2}\left(x-\frac{x_1+x_2}{2}\right)dx\right)x_1^+\,g(x_1,y_1)f(x_2,y_2)\,dx_1\,dy_1\,dx_2\,dy_2\\ &\le \iint_{\mathbb{R}^2}\iint_{\mathbb{R}^2}\left(x_1^+\int_{\mathbb{R}} e^{x-\frac{1}{2\sigma_x^2}\left(x-\frac{x_1+x_2}{2}\right)^2}dx\right)g(x_1,y_1)f(x_2,y_2)\,dx_1\,dy_1\,dx_2\,dy_2,\end{aligned}$$

and thanks to a change of variable $\tilde{x} := \frac{1}{\sqrt{2}\sigma_x}\left(x-\frac{x_1+x_2}{2}\right)$,

$$\begin{aligned}&\iint_{\mathbb{R}^2} e^x\mathcal{T}(f,g)(x,y)\,dx\,dy \le \sqrt{2}\sigma_x\iint_{\mathbb{R}^2}\iint_{\mathbb{R}^2}\left(x_1^+\int_{\mathbb{R}} e^{\left(\tilde{x}+\frac{x_1+x_2}{2}\right)-\frac{\tilde{x}^2}{2\sigma_x^2}}d\tilde{x}\right)g(x_1,y_1)f(x_2,y_2)\,dx_1\,dy_1\,dx_2\,dy_2\\ &\le \sqrt{2}\sigma_x\iint_{\mathbb{R}^2}\iint_{\mathbb{R}^2}\left(x_1^+e^{\frac{x_1+x_2}{2}}\int_{\mathbb{R}} e^{\tilde{x}-\frac{\tilde{x}^2}{2\sigma_x^2}}d\tilde{x}\right)g(x_1,y_1)f(x_2,y_2)\,dx_1\,dy_1\,dx_2\,dy_2\\ &\le C\left(\iint_{\mathbb{R}^2} x_1^+e^{\frac{x_1}{2}}g(x_1,y_1)\,dx_1\,dy_1\right)\left(\iint_{\mathbb{R}^2} e^{\frac{x_2}{2}}f(x_2,y_2)\,dx_2\,dy_2\right)\le C\|g\|_{L^1((1+e^x)\,dx\,dy)}\|f\|_{L^1((1+e^x)\,dx\,dy)}.\end{aligned}$$

□

We prove next the Lipschitz continuity of $t\mapsto \bar{\phi}^{water}(t,\cdot,x)$ for the total variation norm $\|\cdot\|_{TV}$, which we define as

$$\|u-v\|_{TV} := \int_0^1 |u(\tau)-v(\tau)|\,d\tau,$$

for $u,v\in L^1([0,1]))$. We also compare $\bar{\phi}^{water}(t,\cdot,x)$ and $\phi^{water}_{\lfloor t/\varepsilon\rfloor}(\cdot,x)$. These estimates will be used in Section 2.3.4 to prove Theorem 2.3 connecting the annual structured model and the continuous structured model.

**Lemma 2.5.** There is $C>0$ such that for $t,t'\ge 0$, $x,x'\in\mathbb{R}$ and $\varepsilon>0$,

$$\left\|\bar{\phi}^{water}(t,\cdot,x)-\bar{\phi}^{water}(t',\cdot,x')\right\|_{TV} = \int_0^1\left|\bar{\phi}^{water}(t,\tau,x)-\bar{\phi}^{water}(t',\tau,x')\right|d\tau \le C|x-x'|+C|t-t'|.$$

$$\left\|\bar{\phi}^{water}(t,\cdot,x)-\phi^{water}_{\lfloor t/\varepsilon\rfloor}(\cdot,x)\right\|_{TV}=\int_0^1\left|\bar{\phi}^{water}(t,\tau,x)-\phi^{water}_{\lfloor t/\varepsilon\rfloor}(\tau,x)\right|d\tau\le C\varepsilon.$$

*Proof.* We define $\bar{S}^{water}(t,x)\ge s_0$ as the seasonal time when the individual with trait $x$ runs out of water. More precisely, if $(1+\alpha x^+)(1-s_0)+\beta\int_{s_0}^1(\bar{T}(t,\tau))^+\,d\tau-\bar{P}(t)>0$ (that is if the water is exhausted during the season), then $\bar{S}^{water}(t,x)$ is defined by $\bar{\varphi}(t,\bar{S}^{water}(t,x),x)=0$, where

$$\bar{\varphi}(t,\tau,x)=(1+\alpha x^+)(\tau-s_0)+\beta\int_{s_0}^{\tau}(\bar{T}(t,\tau))^+\,d\tau-\bar{P}(t).$$

Othrewise, if $(1+\alpha x^+)(1-s_0)+\beta\int_{s_0}^1(\bar{T}(t,\tau))^+\,d\tau-\bar{P}(t)\le 0$, we let $\bar{S}^{water}(t,x)=1$. To prove the first estimate of the lemma, we notice that the definition 2.2.3 of $\phi^{water}$ implies

$$\int_0^1\left|\bar{\phi}^{water}(t,\tau,x)-\bar{\phi}^{water}(t',\tau,x')\right|d\tau=\left|\bar{S}^{water}(t,x)-S^{water}(t',x')\right|.$$

If $\bar{S}^{water}(t,x)=1=\bar{S}^{water}(t',x')$, the result is proven, so that we may assume $\bar{S}^{water}(t,x)<\bar{S}^{water}(t',x')\le 1$, and then

$$\begin{aligned}
0&\le\left[(1+\alpha x^+)\left(\bar{S}^{water}(t,x)-s_0\right)+\beta\int_{s_0}^{\bar{S}^{water}(t,x)}(\bar{T}(t,\tau))^+\,d\tau-\bar{P}(t)\right]\\
&\quad-\left[(1+\alpha (x')^+)\left(\bar{S}^{water}(t',x')-s_0\right)+\beta\int_{s_0}^{\bar{S}^{water}(t',x')}(\bar{T}(t',\tau))^+\,d\tau-\bar{P}(t')\right]\\
&=-(1+\alpha x^+)\left(\bar{S}^{water}(t',x')-\bar{S}^{water}(t,x)\right)+\alpha((x')^+-x^+)\bar{S}^{water}(t',x')\\
&\quad-\beta\int_{\bar{S}^{water}(t,x)}^{\bar{S}^{water}(t',x')}(\bar{T}(t,\tau))^+\,d\tau+\beta\int_{s_0}^{\bar{S}^{water}(t',x')}|\bar{T}(t,\tau)-\bar{T}(t',\tau)|\,d\tau\\
&\le-\left|\bar{S}^{water}(t,x)-\bar{S}^{water}(t',x)\right|+\alpha|x-x'|+C|t-t'|.
\end{aligned}$$

Therefore $\left|\bar{S}^{water}(t,x)-\bar{S}^{water}(t',x)\right|\le C|x-x'|+C|t-t'|$, which proves the first statement of the lemma. To prove the second result, we introduce $S^{water}_{\lfloor t/\varepsilon\rfloor}(x)\ge s_0$, that is defined by $\varphi(\lfloor t/\varepsilon\rfloor,S^{water}_{\lfloor t/\varepsilon\rfloor}(t),x)=0$ if $(1+\alpha x^+)(1-s_0)+\beta\int_{s_0}^1(T_k(\tau'))^+\,d\tau'-P_k>0$, where

$$\varphi(k,\tau,x)=(1+\alpha x^+)(\tau-s_0)+\beta\int_{s_0}^{\tau}(T_k(\tau'))^+\,d\tau'-P_k,$$

and by $S^{water}_{\lfloor t/\varepsilon\rfloor}(x)=1$ otherwise. If $S^{water}_{\lfloor t/\varepsilon\rfloor}(x)=1=\bar{S}^{water}(t,x)$, the statement is proven. Otherwise,

we may assume w.l.o.g. that $S^{water}_{\lfloor t/\varepsilon\rfloor}(x) < \bar{S}^{water}(t,x)$. Then,

$$\begin{aligned}
0 \leq & \left[(1+\alpha x^+)\left(S^{water}_{\lfloor t/\varepsilon\rfloor}(x)-s_0\right)+\beta\int_{s_0}^{\bar{S}_{\lfloor t/\varepsilon\rfloor}(x)}(\bar{T}_{\lfloor t/\varepsilon\rfloor}(\tau))^+\,d\tau-\bar{P}(\lfloor t/\varepsilon\rfloor)\right] \\
& -\left[(1+\alpha x^+)\left(\bar{S}^{water}(t,x)-s_0\right)+\beta\int_{s_0}^{\bar{S}^{water}(t',x)}(\bar{T}(t,\tau))^+\,d\tau-\bar{P}(t)\right] \\
= & -(1+\alpha x^+)\left(\bar{S}^{water}(t,x)-\bar{S}^{water}_{\lfloor t/\varepsilon\rfloor}(x)\right)-\beta\int_{\bar{S}^{water}_{\lfloor t/\varepsilon\rfloor}(x)}^{\bar{S}^{water}(t,x)}(\bar{T}(t,\tau))^+\,d\tau \\
& +\beta\int_{s_0}^{\bar{S}^{water}_{\lfloor t/\varepsilon\rfloor}(x)}|\bar{T}(t,\tau)-T_{\lfloor t/\varepsilon\rfloor}(\tau)|\,d\tau+\beta\left(\bar{P}(t)-\bar{P}(\lfloor t/\varepsilon\rfloor)\right) \\
\leq & -\left|\bar{S}^{water}(t,x)-\bar{S}^{water}_{\lfloor t/\varepsilon\rfloor}(x)\right|+C\varepsilon,
\end{aligned}$$

and the result unfolds. □

### 2.3.2 Proof of Theorem 2.1 - Existence and uniqueness of the solution of the annual structured model

We will prove this result through an induction on $k \in \mathbb{N}$. Assume that the non-negative function $m_{k-1}(0,\cdot,\cdot)$ satisfies $((x,y)\mapsto m_{k-1}(0,x,y)) \in L^1((1+e^x)\,dx\,dy)$ and (2.2.6). Notice this holds for $k=1$ thanks to the assumptions made on $m^0$ in Theorem 2.1. For any $(x,y)\in\mathbb{R}^2$, the first equation of (2.2.5) is an ordinary differential equation, with the following explicit solution for $s\in[0,1]$:

$$m_{k-1}(s,x,y) = m_{k-1}(0,x,y)e^{-\varepsilon\int_0^s \phi^{plast}_{k-1}(\tau,y)\gamma(T_{k-1}(\tau))^+\left(1-\phi^{water}_{k-1}(\tau,x)\right)1_{s\geq s_0}\,d\tau}, \tag{2.3.2}$$

and since $0 \leq \varepsilon\int_0^s \phi^{plast}_{k-1}(\tau,y)\gamma(T_{k-1}(\tau))^+\left(1-\phi^{water}_{k-1}(\tau,x)\right)1_{\tau\geq s_0}\,d\tau$, we have

$$\|m_{k-1}(s,\cdot,\cdot)\|_{L^1((1+e^x)\,dx\,dy)} \leq \|m_{k-1}(0,\cdot,\cdot)\|_{L^1((1+e^x)\,dx\,dy)}, \tag{2.3.3}$$

for $s \in [0,1]$. Note also that this solution is non-negative, and so is $s_k$ thanks to its definition. We can apply Proposition 2.3.1 to show

$$\begin{aligned}\|s_k\|_{L^1((1+e^x)\,dx\,dy)} &\le \nu \|(x,y) \mapsto \Gamma_{2\sigma_x^2}(x)\Gamma_{2\sigma_y^2}(y)\|_{L^1((1+e^x)\,dx\,dy)} \\ &+ \frac{1}{\eta}\int_0^1 \Bigg\| \iint_{\mathbb{R}^2}\iint_{\mathbb{R}^2} \Gamma_{\sigma_x^2}\left(x - \frac{x_1+x_2}{2}\right)\Gamma_{\sigma_y^2}\left(y-\frac{y_1+y_2}{2}\right) \\ &\qquad\qquad x_1^+ m_k(s,x_1,y_1)m_k(s,x_2,y_2)\,dx_1\,dx_2\,dy_1\,dy_2\Bigg\|_{L^1((1+e^x)\,dx\,dy)} ds \\ &\le C\nu + \frac{C}{\eta}\int_0^1 \|m_k(s,\cdot,\cdot)\|^2_{L^1((1+e^x)\,dx\,dy)}\,ds \le C\nu + \frac{C}{\eta}\|m_k(0,\cdot,\cdot)\|^2_{L^1((1+e^x)\,dx\,dy)}.\end{aligned}$$

We notice next that $m_k(0,\cdot,\cdot)$ is a convex combination of $m_{k-1}(1,\cdot,\cdot)$ and $\frac{s_k}{\iint s_k(x,y)\,dx\,dy}$, with a coefficient $\mathcal{O}(\varepsilon)$ multiplying the latter since $\varepsilon\int_0^s \phi_{k-1}^{plast}(\tau,y)\gamma(T_{k-1}(\tau))^+\left(1-\phi_{k-1}^{water}(\tau,x)\right)1_{\tau\ge s_0}\,d\tau \le C\varepsilon$ and (2.3.2) implies

$$0 \le 1 - \iint_{\mathbb{R}^2} m_{k-1}(\hat{x},\hat{y})\,d\hat{x}\,d\hat{y} \le C\varepsilon.$$

Then $m_k(0,\cdot,\cdot)$ is non-negative and we have

$$\begin{aligned}\|m_k(0,\cdot,\cdot)\|_{L^1((1+e^x)\,dx\,dy)} &\le \|m_{k-1}(1,\cdot,\cdot)\|_{L^1((1+e^x)\,dx\,dy)} + C\varepsilon\|s_k\|_{L^1((1+e^x)\,dx\,dy)} \\ &\le \|m_{k-1}(0,\cdot,\cdot)\|_{L^1((1+e^x)\,dx\,dy)} + C\varepsilon\|m_{k-1}(0,\cdot,\cdot)\|^2_{L^1((1+e^x)\,dx\,dy)} + C\varepsilon.\end{aligned}$$

Therefore,

$$\left(1+\|m_k(0,\cdot,\cdot)\|_{L^1((1+e^x)\,dx\,dy)}\right) \le C\left(1+\|m_{k-1}(0,\cdot,\cdot)\|_{L^1((1+e^x)\,dx\,dy)}\right)^2,$$

and then $\|m_k(0,\cdot,\cdot)\|_{L^1((1+e^x)\,dx\,dy)} \le C^{2^k-1}\left(1+\|m_0(0,\cdot,\cdot)\|_{L^1((1+e^x)\,dx\,dy)}\right)^{2^k}$. We are therefore able to construct $(m_k) \in L^1([0,1], L^1((1+e^x)\,dx\,dy))$ for $k \in \mathbb{N}\cup\{0\}$ recursively, with

$$\|m_k(s,\cdot,\cdot)\|_{L^1((1+e^x)\,dx\,dy)} \le C^{2^k},$$

for $s \in [0,1]$. The solution is well defined, unique, non-negative and we can prove equality (2.2.6) thanks to the definition of $m_k(0,\cdot,\cdot)$:

$$\iint_{\mathbb{R}^2} m_k(0,x,y)\,dx\,dy = \iint_{\mathbb{R}^2} m_{k-1}(1,x,y)\,dx\,dy + \frac{1-\iint_{\mathbb{R}^2} m_{k-1}(1,\hat{x},\hat{y})\,d\hat{x}\,d\hat{y}}{\iint_{\mathbb{R}^2} s_{k-1}(\hat{x},\hat{y})\,d\hat{x}\,d\hat{y}}\iint_{\mathbb{R}^2} s_{k-1}(x,y)\,dx\,dy = 1.$$

### 2.3.3 Proof of Theorem 2.2 - Existence and uniqueness of the solution of the continuous structured model

**Existence and uniqueness of solutions**

We define the operator $\mathcal{G}$ as follows

$$\mathcal{G}[n](t,x,y) = \iint_{\mathbb{R}^2}\iint_{\mathbb{R}^2} \Gamma_{\sigma_x^2}\left(x-\frac{x_1+x_2}{2}\right)\Gamma_{\sigma_y^2}\left(y-\frac{y_1+y_2}{2}\right)x_1^+ n(t,x_1,y_1)n(t,x_2,y_2)$$
$$\bar{\rho}[n(t,\cdot,\cdot)](t,x_1,x_2,y_1,y_2)\,dx_1\,dy_1\,dx_2\,dy_2 + \nu\Gamma_{2\sigma_x^2}(x)\Gamma_{2\sigma_y^2}(y), \tag{2.3.4}$$

and we will show below that this operator is indeed well defined on $L^\infty([0,T],L^1(\mathbb{R}^2))$, for any $T>0$. Solutions of (2.2.12) satisfy $n(t,x,y)=\mathcal{F}[n](t,x,y)$, with

$$\mathcal{F}[n](t,x,y) := n^0(x,y)e^{-\int_0^t \bar{a}(s,x,y)\,ds}$$
$$+\int_0^t \frac{\iint_{\mathbb{R}^2}\bar{a}(s,\hat{x},\hat{y})n(s,\hat{x},\hat{y})\,d\hat{x}\,d\hat{y}}{\nu+\bar{R}[n](s)}\mathcal{G}[n](s,x,y)e^{-\int_s^t \bar{a}(\tau,x,y)\,d\tau}\,ds. \tag{2.3.5}$$

Let $T>0$. The operator maps $L^\infty([0,T],L^1(\mathbb{R}^2,\mathbb{R}_+))$ into itself, since $\mathcal{F}[n](t,x,y)\geq 0$ is $n\geq 0$ and

$$\|\mathcal{F}[n](t,\cdot,\cdot)\|_{L^1(\mathbb{R}^2)} \leq \|n^0\|_{L^1(\mathbb{R}^2)}$$
$$+\frac{T\gamma}{\nu}\|n\|_{L^\infty([0,T],L^1(\mathbb{R}^2))}\left(\frac{\max_{(x_1,x_2,y_1,y_2)\in\mathbb{R}^4}\left(x_1^+\bar{\rho}[n(t,\cdot,\cdot)](t,x_1,x_2,y_1,y_2)\right)}{\eta}\|n\|^2_{L^\infty([0,T],L^1(\mathbb{R}^2))}+\nu\right)$$
$$\leq C\left(1+\|n\|^3_{L^\infty([0,T],L^1(\mathbb{R}^2))}\right), \tag{2.3.6}$$

where we have used that for $(x_1,x_2,y_1,y_2)\in\mathbb{R}^4$,

$$x_1^+\bar{\rho}[n(t,\cdot,\cdot)](t,x_1,x_2,y_1,y_2) = x_1^+\int_0^1 \frac{\bar{\phi}^{plast}(t,s,y_1)\bar{\phi}^{plast}(t,s,y_2)\bar{\phi}^{water}(t,s,x_1)\bar{\phi}^{water}(t,s,x_2)}{\eta+\bar{Q}[n](t)}\,ds$$
$$\leq \frac{x_1^+}{\eta}\int_0^1 \bar{\phi}^{water}(t,s,x_1)\,ds \leq \frac{x_1^+}{\eta}\int_0^1 1_{s_0\leq s}1_{\alpha x_1^+(s-s_0)\leq\|\bar{P}\|_{L^\infty([0,\infty))}}\,ds$$
$$\leq \frac{\|\bar{P}\|_{L^\infty([0,\infty))}}{\eta\alpha}\leq C. \tag{2.3.7}$$

For $n, \tilde{n} \in L^\infty([0,T], L^1(\mathbb{R}^2))$ and $s \in [0,T]$, we have

$$
\begin{aligned}
&\iint_{\mathbb{R}^2} |\mathcal{F}[n] - \mathcal{F}[\tilde{n}]|\,(s,x,y)\,dx\,dy \\
&\quad \le T \max_{t\in[0,T]} \iint_{\mathbb{R}^2} \left| \frac{\iint_{\mathbb{R}^2} \bar{a}(t,\hat{x},\hat{y}) n(t,\hat{x},\hat{y})\,d\hat{x}\,d\hat{y}}{\nu + \bar{R}[n](t)} \mathcal{G}[n](t,x,y) - \frac{\iint_{\mathbb{R}^2} \bar{a}(t,\hat{x},\hat{y}) \tilde{n}(t,\hat{x},\hat{y})\,d\hat{x}\,d\hat{y}}{\nu + \bar{R}[\tilde{n}](t)} \mathcal{G}[\tilde{n}](t,x,y) \right| dx\,dy \\
&\quad \le T \max_{t\in[0,T]} \left\{ \iint_{\mathbb{R}^2} \left( \frac{\iint_{\mathbb{R}^2} \bar{a}(t,\hat{x},\hat{y}) n(t,\hat{x},\hat{y})\,d\hat{x}\,d\hat{y}}{\nu + \bar{R}[n](t)} |\mathcal{G}[n](t,x,y) - \mathcal{G}[\tilde{n}](t,x,y)| \right.\right. \\
&\qquad + \frac{\mathcal{G}[\tilde{n}](t,x,y)}{\nu + \bar{R}[\tilde{n}](t)} \iint_{\mathbb{R}^2} \bar{a}(t,\hat{x},\hat{y})\,|n(t,\hat{x},\hat{y}) - \tilde{n}(t,\hat{x},\hat{y})|\,d\hat{x}\,d\hat{y} \\
&\qquad \left.\left. + \frac{\mathcal{G}[\tilde{n}](t,x,y)}{\nu + \bar{R}[\tilde{n}](t)} \left| \frac{\nu + \bar{R}[\tilde{n}](t)}{\nu + \bar{R}[n](t)} - 1 \right| \iint_{\mathbb{R}^2} \bar{a}(t,\hat{x},\hat{y}) n(t,\hat{x},\hat{y}) d\hat{x}\,d\hat{y} \right) dx\,dy \right\} \\
&\quad \le T\gamma \|\bar{T}\|_{L^\infty} \max_{t\in[0,T]} \left\{ \iint_{\mathbb{R}^2} \left( \frac{1}{\nu + \bar{R}[n](t)} |\mathcal{G}[n](t,x,y) - \mathcal{G}[\tilde{n}](t,x,y)| \right.\right. \\
&\qquad + \frac{\mathcal{G}[\tilde{n}](t,x,y)}{\nu + \bar{R}[\tilde{n}](t)} \iint_{\mathbb{R}^2} |n(t,\hat{x},\hat{y}) - \tilde{n}(t,\hat{x},\hat{y})|\,d\hat{x}\,d\hat{y} + \frac{\mathcal{G}[\tilde{n}](t,x,y)}{\nu + \bar{R}[\tilde{n}](t)} \left| \frac{\bar{R}[\tilde{n}](t) - \bar{R}[n](t)}{\nu + \bar{R}[n](t)} \right| \left.\left. \right) dx\,dy \right\} \\
&\quad \le T \frac{\gamma \|\bar{T}\|_{L^\infty}}{\nu} \max_{t\in[0,T]} \left\{ \iint_{\mathbb{R}^2} |\mathcal{G}[n](t,x,y) - \mathcal{G}[\tilde{n}](t,x,y)|\,dx\,dy \right. \\
&\qquad \left. + C \iint_{\mathbb{R}^2} |n(t,x,y) - \tilde{n}(t,x,y)|\,dx\,dy + \frac{C}{\nu} \left| \bar{R}[\tilde{n}](t) - \bar{R}[n](t) \right| \right\},
\end{aligned} \tag{2.3.8}
$$

where we have used the bound on $|\iint \mathcal{G}[n](t,x,y)\,dx\,dy| \le C\|n(t,\cdot,\cdot)\|^2_{L^1(\mathbb{R}^2)}$ that can be obtained as in (2.3.6). Furthermore,

$$
\begin{aligned}
&\iint_{\mathbb{R}^2} |\mathcal{G}[n](s,x,y) - \mathcal{G}[\tilde{n}](s,x,y)|\,dx\,dy \le \iint_{\mathbb{R}^2} \iint_{\mathbb{R}^2} \iint_{\mathbb{R}^2} \Gamma_{\sigma_x^2}\left(x - \frac{x_1+x_2}{2}\right) \Gamma_{\sigma_y^2}\left(y - \frac{y_1+y_2}{2}\right) \\
&\quad \left| \tilde{n}(s,x_1,y_1)\tilde{n}(s,x_2,y_2) \left( x_1^+ \bar{\rho}[n(s,\cdot,\cdot)](s,x_1,x_2,y_1,y_2) - x_1^+ \bar{\rho}[\tilde{n}(s,\cdot,\cdot)](s,x_1,x_2,y_1,y_2) \right) \right. \\
&\quad \left. + (n(s,x_1,y_1)n(s,x_2,y_2) - \tilde{n}(s,x_1,y_1)\tilde{n}(s,x_2,y_2))\, x_1^+ \bar{\rho}[n(s,\cdot,\cdot)](s,x_1,x_2,y_1,y_2) \right| dx_1\,dy_1\,dx_2\,dy_2\,dx\,dy. \\
&\quad \le \iint_{\mathbb{R}^2} \iint_{\mathbb{R}^2} \tilde{n}(s,x_1,y_1)\tilde{n}(s,x_2,y_2) \\
&\qquad\qquad \left| x_1^+ \bar{\rho}[n(s,\cdot,\cdot)](s,x_1,x_2,y_1,y_2) - x_1^+ \bar{\rho}[\tilde{n}(s,\cdot,\cdot)](s,x_1,x_2,y_1,y_2) \right| dx_1\,dx_2\,dy_1\,dy_2 \\
&\quad + \iint_{\mathbb{R}^2} \iint_{\mathbb{R}^2} \left[ |n-\tilde{n}|\,(s,x_1,y_1)\tilde{n}(s,x_2,y_2) + n(s,x_1,y_1)\,|n-\tilde{n}|\,(s,x_2,y_2) \right] \\
&\qquad\qquad x_1^+ \bar{\rho}[n(s,\cdot,\cdot)](s,x_1,x_2,y_1,y_2)\,dx_1\,dy_1\,dx_2\,dy_2.
\end{aligned}
$$

Since $(s,x_1,x_2,y_1,y_2) \mapsto x_1^+ \bar{\rho}[n(s,\cdot,\cdot)](s,x_1,x_2,y_1,y_2)$ is uniformly bounded, we simply need to estimate

the first term on the right hand side:

$$x_1^+\left|\bar\rho[n(s,\cdot,\cdot)](s,x_1,x_2,y_1,y_2)-\bar\rho[\tilde n(s,\cdot,\cdot)](s,x_1,x_2,y_1,y_2)\right|$$
$$\le\left|x_1^+\int_0^1\bar\phi^{water}(t,s,x_1)\,ds\right|\left|\frac{1}{\eta+\bar Q[n](s)}-\frac{1}{\eta+\bar Q[\tilde n](s)}\right|\le\frac{C}{\eta^2}\|n-\tilde n\|_{L^\infty([0,T],L^1(\mathbb{R}^2))},\tag{2.3.9}$$

estimating $\left|x_1^+\int_0^1\bar\phi^{water}(t,s,x_1)\,ds\right|\le C$ thanks to the argument already employed in (2.3.7). Then,

$$\iint_{\mathbb{R}^2}|\mathcal{G}[n](s,x,y)-\mathcal{G}[\tilde n](s,x,y)|\,dx\,dy\le C\|n-\tilde n\|_{L^\infty([0,T],L^1(\mathbb{R}^2))},\tag{2.3.10}$$

where the constant only depends on a bound on $\|n\|_{L^\infty([0,T],L^1(\mathbb{R}^2))}$ and $\|\tilde n\|_{L^\infty([0,T],L^1(\mathbb{R}^2))}$. Moreover, we notice that $\bar R[n](t)=\iint\mathcal{G}[n](t,x,y)\,dx\,dy-\nu$, therefore

$$|\bar R[n](t)-\bar R[\tilde n](t)|\le\iint_{\mathbb{R}^2}|\mathcal{G}[n](t,x,y)-\mathcal{G}[\tilde n](t,x,y)|\,dx\,dy\le C\|n-\tilde n\|_{L^\infty([0,T],L^1(\mathbb{R}^2))}.$$

This estimate and (2.3.10) can be used to estimate the right hand side of (2.3.8) and obtain

$$\|\mathcal{F}[n]-\mathcal{F}[\tilde n]\|_{L^\infty([0,T],L^1(\mathbb{R}^2))}\le CT\|n-\tilde n\|_{L^\infty([0,T],L^1(\mathbb{R}^2))},\tag{2.3.11}$$

where the constant only depends on a bound on $\|n\|_{L^\infty([0,T],L^1(\mathbb{R}^2))}$ and $\|\tilde n\|_{L^\infty([0,T],L^1(\mathbb{R}^2))}$. If $T>0$ is small enough, this operator is a contraction on $L^\infty([0,T],L^1(\mathbb{R}^2))$. The existence of solutions for a small time interval $[0,T]$, $T>0$, then follows from the Banach contraction Theorem. These solutions are non-negative and an integration of (2.2.12) along $(x,y)\in\mathbb{R}^2$ shows that solutions $n$ satisfy $\iint_{\mathbb{R}^2}n(t,x,y)\,dx\,dy\equiv1$. This property and (2.3.11) prove the existence of solutions for $t\in[0,+\infty)$.

**Regularity of solutions** The boundedness of solutions when $n^0$ is bounded can be seen as follows, using the fact that the kernel $(x,y)\mapsto\Gamma_{\sigma_x^2}(x)\Gamma_{\sigma_y^2}(y)$ appearing in (2.3.4) is bounded:

$$\|n(t,\cdot,\cdot)\|_{L^\infty(\mathbb{R}^2)}\le\|n^0\|_{L^\infty(\mathbb{R}^2)}$$
$$+C\left(\|n\|^2_{L^\infty([0,T],L^1(\mathbb{R}^2))}\int_0^t\left(\max_{(x_1,x_2,y_1,y_2)\in\mathbb{R}^4}x_1^+\bar\rho[n(s,\cdot,\cdot)](s,x_1,x_2,y_1,y_2)\right)ds+C\nu t\right)\le C(t+1).$$

To prove that $n$ satisfies (2.2.14), we notice that thanks to (2.3.5),

$$\begin{aligned}
\left|n(t,x,y)-n(t,x',y')\right| &\le \left|n^0(x,y)-n^0(x',y')\right| e^{-\int_0^t \bar a(s,x,y)\,ds} + n^0(x',y')\left(e^{-\int_0^t \bar a(s,x,y)\,ds} - e^{-\int_0^t \bar a(s,x',y')\,ds}\right)^+ \\
&\quad + \int_0^t \frac{\iint_{\mathbb{R}^2} \bar a(s,\hat x,\hat y) n(s,\hat x,\hat y)\,d\hat x\,d\hat y}{\nu+\bar R[n](s)} \\
&\quad \left(\left|\mathcal{G}[n](s,x,y)-\mathcal{G}[n](s,x',y')\right| e^{-\int_s^t \bar a(\tau,x,y)\,d\tau} + \mathcal{G}[n](s,x',y')\left(e^{-\int_s^t \bar a(\tau,x,y)} - e^{-\int_s^t \bar a(\tau,x',y')\,d\tau}\right)^+\right) ds \\
&\le \|n^0\|_{W^{1,\infty}(\mathbb{R}^2)}\left(|x-x'|+|y-y'|\right) + n^0(x,y)\int_0^t \left(\bar a(s,x',y')-\bar a(s,x,y)\right)^+ ds \\
&\quad + \int_0^t \frac{\iint_{\mathbb{R}^2} \bar a(s,\hat x,\hat y) n(s,\hat x,\hat y)\,d\hat x\,d\hat y}{\nu+\bar R[n](s)} \\
&\quad \left(\left|\mathcal{G}[n](s,x,y)-\mathcal{G}[n](s,x',y')\right| + \|\mathcal{G}[n](s,\dot{;},\dot{;})\|_{L^\infty(\mathbb{R}^2)}\int_s^t \left(\bar a(\tau,x',y')-\bar a(\tau,x,y)\right)^+ d\tau\right) ds.
\end{aligned}$$

We notice that $y \mapsto \bar\phi^{plast}(t,s,y)$ is non decreasing and $x \mapsto \bar\phi^{water}(t,s,x)$ satisfies the regularity estimate provided by Lemma 2.5. Then, if $y' \le y$,

$$\begin{aligned}
\bar a(t,x,y)-\bar a(t,x',y') &= \int_0^1 \bar\phi^{plast}(t,s,y)\gamma(\bar T(t,s))^+\left(\bar\phi^{water}(t,s,x')-\bar\phi^{water}(t,s,x)\right) ds \\
&\quad + \int_0^1 \left(\bar\phi^{plast}(t,s,y)-\bar\phi^{plast}(t,s,y')\right)\gamma(\bar T(t,s))^+\left(1-\bar\phi^{water}(t,s,x')\right) ds \\
&\ge -C|x-x'|.
\end{aligned}$$

Moreover,

$$\begin{aligned}
\left|\mathcal{G}[n](t,x,y)-\mathcal{G}[n](t,x',y')\right| &= \iint_{\mathbb{R}^2}\iint_{\mathbb{R}^2}\Bigg[\left|\Gamma_{\sigma_x^2}\left(x-\frac{x_1+x_2}{2}\right)-\Gamma_{\sigma_x^2}\left(x'-\frac{x_1+x_2}{2}\right)\right|\Gamma_{\sigma_y^2}\left(y-\frac{y_1+y_2}{2}\right) \\
&\qquad \Gamma_{\sigma_x^2}\left(x'-\frac{x_1+x_2}{2}\right)\left|\Gamma_{\sigma_y^2}\left(y-\frac{y_1+y_2}{2}\right)-\Gamma_{\sigma_y^2}\left(y'-\frac{y_1+y_2}{2}\right)\right|\Bigg] \\
&\qquad x_1^+ n(t,x_1,y_1)n(t,x_2,y_2)\bar\rho[n(t,\cdot,\cdot)](t,x_1,x_2,y_1,y_2)\,dx_1\,dy_1\,dx_2\,dy_2 \\
&\le \left(\max_{x_1,x_2,y_1,y_2\in\mathbb{R}}\left(x_1^+\rho[n(t,\cdot,\cdot)](t,x_1,x_2,y_1,y_2)\right)\right)\left(\|\Gamma'_{\sigma_x^2}\|_{L^\infty(\mathbb{R})}|x-x'|+\|\Gamma'_{\sigma_y^2}\|_{L^\infty(\mathbb{R})}|y-y'|\right).
\end{aligned}$$

Therefore, for some $C>0$, if $y' \le y$, $n$ satisfies (2.2.14). To obtain the last inequality of Theorem 2.2, we observe that thanks to (2.2.12),

$$\begin{aligned}
\frac{d}{dt}\iint_{\mathbb{R}^2} x^2 n(t,x,y)\,dx\,dy &\le \left(\max_{x_1,x_2,y_1,y_2\in\mathbb{R}}\left(x_1^+\rho[n(t,\cdot,\cdot)](t,x_1,x_2,y_1,y_2)\right)\right) \\
&\qquad \iint_{\mathbb{R}^2}\iint_{\mathbb{R}^2}\left|\frac{x_1+x_2}{2}\right|^2 n(t,x_1,y_1)n(t,x_2,y_2)\,dx_1\,dx_2\,dy_1\,dy_2 + 2\nu\sigma_x^2 \\
&\le C\iint_{\mathbb{R}^2} x^2 n(t,x,y)\,dx\,dy + 2\nu\sigma_x^2,
\end{aligned}$$

which implies (2.2.15). Notice that to make this last calculation fully rigorous, it would be necessary to introduce a modified model with $x \in [-R, R]$, prove the existence of solutions for this modified model, and then pass to the limit $R \to \infty$ using the calculation above. We omit this very technical argument here.

### 2.3.4 Proof of Theorem 2.3 - asymptotic limit from the annual structured model to the continuous structured model

Using the notation (2.3.4), we have

$$n(t+\varepsilon,x,y) = n(t,x,y)e^{-\int_t^{t+\varepsilon}\bar{a}(s,x,y)\,ds} + \int_t^{t+\varepsilon} \frac{\iint_{\mathbb{R}^2}\bar{a}(s,\hat{x},\hat{y})n(s,\hat{x},\hat{y})\,d\hat{x}\,d\hat{y}}{\nu+\bar{R}[n](s)}\mathcal{G}[n](s,x,y)e^{-\int_s^{t+\varepsilon}\bar{a}(\tau,x,y)\,d\tau}\,ds,$$

and using (2.2.5) we write :

$$\begin{aligned} m_{\lfloor (t+\varepsilon)/\varepsilon\rfloor}(0,x,y) &= m_{\lfloor t/\varepsilon\rfloor}(0,x,y)e^{-\varepsilon a_{\lfloor t/\varepsilon\rfloor}(1,x,y)} \\ &\quad + \frac{1-\iint_{\mathbb{R}^2}e^{-\varepsilon a_{\lfloor t/\varepsilon\rfloor}(1,\hat{x},\hat{y})}m_{\lfloor t/\varepsilon\rfloor}(0,\hat{x},\hat{y})\,d\hat{x}\,d\hat{y}}{\nu+R_{\lfloor t/\varepsilon\rfloor}}\int_0^1 \mathcal{G}[e^{-\varepsilon a}m_{\lfloor t/\varepsilon\rfloor}(0,\cdot,\cdot)](s,x,y)\,ds. \end{aligned}$$

These imply

$$\begin{aligned} \|n(t+\varepsilon,\cdot,\cdot) - m_{\lfloor (t+\varepsilon)/\varepsilon\rfloor}(0,\cdot,\cdot)\|_{L^1(\mathbb{R}^2)} &\le \iint_{\mathbb{R}^2}\left| n(t,x,y)e^{-\int_t^{t+\varepsilon}\bar{a}(s,x,y)ds} - m_{\lfloor t/\varepsilon\rfloor}(0,x,y)e^{-\varepsilon a_{\lfloor t/\varepsilon\rfloor}(1,x,y)}\right| dx\,dy \\ &+ \iint_{\mathbb{R}^2}\left| \int_t^{t+\varepsilon}\frac{\iint_{\mathbb{R}^2}\bar{a}(s,\hat{x},\hat{y})n(s,\hat{x},\hat{y})\,d\hat{x}\,d\hat{y}}{\nu+\bar{R}[n](s)}\mathcal{G}[n(s,\cdot,\cdot)](x,y)e^{-\int_s^{t+\varepsilon}\bar{a}(\tau,x,y)\,d\tau}\,ds \right. \\ &\left. - \frac{1-\iint_{\mathbb{R}^2}e^{-\varepsilon a_{\lfloor t/\varepsilon\rfloor}(1,\hat{x},\hat{y})}m_{\lfloor t/\varepsilon\rfloor}(0,\hat{x},\hat{y})\,d\hat{x}\,d\hat{y}}{\nu+R_{\lfloor t/\varepsilon\rfloor}}\int_0^1 \mathcal{G}[e^{-\varepsilon\bar{a}(s,\cdot,\cdot)}m_{\lfloor t/\varepsilon\rfloor}(0,\cdot,\cdot)](x,y)\,ds\right| dx\,dy. \end{aligned} \tag{2.3.12}$$

To estimate the first term on the right hand side of (2.3.12), we recall the definitions (2.2.7) of $a_k$ and (2.2.13) of $\bar{a}(t,x,y)$. For $s \in [t,t+\varepsilon]$,

$$\begin{aligned} &\left|a_{\lfloor t/\varepsilon\rfloor}(1,x,y) - \bar{a}(s,x,y)\right| \\ &\quad \le \gamma\|T\|_{L^\infty}\left(\int_0^1\left|\phi^{plast}_{\lfloor t/\varepsilon\rfloor}(\tau,y) - \bar{\phi}^{plast}(s,\tau,y)\right|d\tau + \int_0^1\left|\phi^{water}_{\lfloor t/\varepsilon\rfloor}(\tau,x) - \bar{\phi}^{water}(s,\tau,x)\right|d\tau\right) \\ &\quad = C\int_0^1\left|\phi^{plast}_{\lfloor t/\varepsilon\rfloor}(\tau,y) - \bar{\phi}^{plast}(s,\tau,y)\right|d\tau + \mathcal{O}(\varepsilon), \end{aligned} \tag{2.3.13}$$

thanks to Lemma 2.5, while we have

$$\begin{aligned}
&\int_{\mathbb{R}} \left|\phi^{plast}_{\lfloor t/\varepsilon\rfloor}(\tau,y)-\bar\phi^{plast}(s,\tau,y)\right| dy = \int_{\mathbb{R}} \left| e^{-\beta\int_0^\tau 1_{T_{\lfloor t/\varepsilon\rfloor}(\tau')>y}\,d\tau'} - e^{-\beta\int_0^\tau 1_{\bar T(t,\tau')>y}\,d\tau'}\right| dy\\
&\quad\le \beta\int_{\mathbb{R}}\left|\int_0^\tau 1_{T_{\lfloor t/\varepsilon\rfloor}(\tau')>y}\,d\tau' - \int_0^\tau 1_{\bar T(t,\tau')>y}\,d\tau'\right| dy \le \beta\int_0^1\int_{\mathbb{R}}\left|1_{T_{\lfloor t/\varepsilon\rfloor}(\tau')>y}-1_{\bar T(t,\tau')>y}\right| dy\,d\tau'\\
&\quad\le \beta\int_0^1 \left|T_{\lfloor t/\varepsilon\rfloor}(\tau')-\bar T(t,\tau')\right| d\tau' \le \|T_{\lfloor t/\varepsilon\rfloor}-\bar T(t,\cdot)\|_{L^\infty}\le C\varepsilon,
\end{aligned}$$

and then

$$\int_{\mathbb{R}}\left|a_{\lfloor t/\varepsilon\rfloor}(1,x,y)-\bar a(s,x,y)\right| dy \le C\varepsilon, \tag{2.3.14}$$

where the constant $C>0$ is independent from $t\ge 0$, $s\in[t,t+\varepsilon]$ and from $x\in\mathbb{R}$. We can use this estimate to control the first term on the right hand side of (2.3.12):

$$\begin{aligned}
&\iint_{\mathbb{R}^2}\left| n(t,x,y)e^{-\int_t^{t+\varepsilon}\bar a(s,x,y)ds} - m_{\lfloor t/\varepsilon\rfloor}(0,x,y)e^{-\varepsilon a_{\lfloor t/\varepsilon\rfloor}(1,x,y)}\right| dx\,dy\\
&\quad\le \left\| n(t,\cdot,\cdot)-m_{\lfloor t/\varepsilon\rfloor}(0,\cdot,\cdot)\right\|_{L^1(\mathbb{R}^2)} + \iint_{\mathbb{R}^2} n(t,x,y)\left|\int_t^{t+\varepsilon}\bar a(s,x,y)-a_{\lfloor t/\varepsilon\rfloor}(1,x,y)\,ds\right| dx\,dy\\
&\quad\le \left\| n(t,x,y)-m_{\lfloor t/\varepsilon\rfloor}(0,x,y)\right\|_{L^1(x,y)}\\
&\qquad + \left\|\bar a(\cdot,\cdot,\cdot)-a_{\lfloor t/\varepsilon\rfloor}(1,\cdot,\cdot)\right\|_{L^\infty([0,1]\times\mathbb{R}^2)}\left(\int_t^{t+\varepsilon} ds\right)\int_{\mathbb{R}}\int_{x^2\ge 1/\varepsilon} n(t,x,y)\,dx\,dy \qquad (2.3.15)\\
&\qquad + \|n(t,\cdot,\cdot)\|_{L^\infty(\mathbb{R}^2)}\int_{x^2\le 1/\varepsilon}\int_t^{t+\varepsilon}\int_{\mathbb{R}}\left|\bar a(s,x,y)-a_{\lfloor t/\varepsilon\rfloor}(1,x,y)\right| dy\,ds\,dx\\
&\quad\le \left\| n(t,x,y)-m_{\lfloor t/\varepsilon\rfloor}(0,x,y)\right\|_{L^1(x,y)} + 2\varepsilon^2\int_{x^2\ge 1/\varepsilon} x^2 n(t,x,y)\,dx\,dy +\\
&\qquad + \varepsilon\frac{2}{\sqrt{\varepsilon}}\|n(t,\cdot,\cdot)\|_{L^\infty(\mathbb{R}^2)}\max_{|x|\le 1/\sqrt{\varepsilon},s\in[t,t+\varepsilon]}\int_{\mathbb{R}}\left|\bar a(s,x,y)-a_{\lfloor t/\varepsilon\rfloor}(1,x,y)\right| dy\\
&\quad\le \left\| n(t,x,y)-m_{\lfloor t/\varepsilon\rfloor}(0,x,y)\right\|_{L^1(x,y)} + Ce^{Ct}\varepsilon^{3/2}, \qquad (2.3.16)
\end{aligned}$$

where we have used a Chebyshev's inequality, (2.2.15) and (2.3.14). To estimate the last part of

(2.3.12), we notice that for $s \in [t, t+\varepsilon]$,

$$
\begin{aligned}
&\iint_{\mathbb{R}^2} \left| \int_t^{t+\varepsilon} \mathcal{G}[n(s,\cdot,\cdot)](x,y) e^{-\int_s^{t+\varepsilon} \bar{a}(\tau',x,y)\,d\tau'}\,ds - \varepsilon \int_0^1 \mathcal{G}[e^{-\varepsilon a_{\lfloor t/\varepsilon \rfloor}(s,\cdot,\cdot)} m_{\lfloor t/\varepsilon \rfloor}(0,\cdot,\cdot)](x,y)\,ds \right| dx\,dy \\
&\quad = \iint_{\mathbb{R}^2} \left| \int_t^{t+\varepsilon} \mathcal{G}[n(s,\cdot,\cdot)](x,y)\,ds - \varepsilon \int_0^1 \mathcal{G}[m_{\lfloor t/\varepsilon \rfloor}(0,\cdot,\cdot)](x,y)\,ds \right| dx\,dy + \mathcal{O}(\varepsilon^2) \\
&\quad = \mathcal{O}(\varepsilon^2) + \iint_{\mathbb{R}^2} \iint \left( \iint_{\mathbb{R}^2} \Gamma_{\sigma_x^2}\left(x - \frac{x_1+x_2}{2}\right) \Gamma_{\sigma_y^2}\left(y - \frac{y_1+y_2}{2}\right) dx\,dy \right) \\
&\qquad \left| \int_t^{t+\varepsilon} n(s,x_1,y_1) n(s,x_2,y_2) \left( x_1^+ \bar{\rho}[n(t,\cdot,\cdot)](s,x_1,x_2,y_1,y_2) \right) ds \right. \\
&\qquad \left. - \varepsilon \left( \int_0^1 x_1^+ \bar{\rho}[m_{\lfloor t/\varepsilon \rfloor}(0,\cdot,\cdot)](t,x_1,x_2,y_1,y_2)\,ds \right) m_{\lfloor t/\varepsilon \rfloor}(0,x_1,y_1) m_{\lfloor t/\varepsilon \rfloor}(t,x_2,y_2) \right| dx_1\,dy_1\,dx_2\,dy_2 \\
&\quad = \mathcal{O}(\varepsilon^2) + \varepsilon \iint_{\mathbb{R}^2} \iint_{\mathbb{R}^2} \left| n(t,x_1,y_1) n(t,x_2,y_2) \left( x_1^+ \bar{\rho}[n(t,\cdot,\cdot)](t,x_1,x_2,y_1,y_2) \right) \right. \\
&\qquad \left. - m_{\lfloor t/\varepsilon \rfloor}(0,x_1,y_1) m_{\lfloor t/\varepsilon \rfloor}(t,x_2,y_2) \left( x_1^+ \bar{\rho}[m_{\lfloor t/\varepsilon \rfloor}(0,\cdot,\cdot)](t,x_1,x_2,y_1,y_2) \right) \right| dx_1\,dy_1\,dx_2\,dy_2,
\end{aligned}
$$

where we have used the Lipschitz regularity of $n$ in time as a function valued in $L^1(\mathbb{R}^2)$ (we recall that the term $x_1^+ \bar{\rho}[n(t,\cdot,\cdot)](t,x_1,x_2,y_1,y_2)$ is uniformly bounded, see (2.3.7)). Then, using an estimate similar to (2.3.9), we get

$$
\begin{aligned}
&\iint_{\mathbb{R}^2} \left| \int_t^{t+\varepsilon} \mathcal{G}[n(s,\cdot,\cdot)](x,y) e^{-\int_s^{t+\varepsilon} \bar{a}(\tau',x,y)\,d\tau'}\,ds - \varepsilon \int_0^1 \mathcal{G}[e^{-\varepsilon a_{\lfloor t/\varepsilon \rfloor}(s,\cdot,\cdot)} m_{\lfloor t/\varepsilon \rfloor}(0,\cdot,\cdot)](x,y)\,ds \right| dx\,dy \\
&\quad \leq \mathcal{O}(\varepsilon^2) + C\varepsilon \left\| n(t,\cdot,\cdot) - m_{\lfloor t/\varepsilon \rfloor}(0,\cdot,\cdot) \right\|_{L^1(\mathbb{R}^2)}.
\end{aligned} \tag{2.3.17}
$$

Moreover, when $s \in [t, t+\varepsilon]$,

$$
\begin{aligned}
&\left| \frac{\iint_{\mathbb{R}^2} \bar{a}(s,\hat{x},\hat{y}) n(s,\hat{x},\hat{y})\,d\hat{x}\,d\hat{y}}{\nu + \bar{R}[n](s)} - \frac{1}{\varepsilon} \frac{1 - \iint_{\mathbb{R}^2} e^{-\varepsilon a_{\lfloor t/\varepsilon \rfloor}(1,\hat{x},\hat{y})} m_{\lfloor t/\varepsilon \rfloor}(0,\hat{x},\hat{y})\,d\hat{x}\,d\hat{y}}{\nu + R_{\lfloor t/\varepsilon \rfloor}[m]} \right| \\
&\quad = \left| \frac{\iint_{\mathbb{R}^2} \bar{a}(s,\hat{x},\hat{y}) n(t,\hat{x},\hat{y})\,d\hat{x}\,d\hat{y}}{\nu + \bar{R}[n](t)} - \frac{\iint_{\mathbb{R}^2} a_{\lfloor t/\varepsilon \rfloor}(1,\hat{x},\hat{y}) m_{\lfloor t/\varepsilon \rfloor}(0,\hat{x},\hat{y})\,d\hat{x}\,d\hat{y}}{\nu + R_{\lfloor t/\varepsilon \rfloor}[m]} \right| + \mathcal{O}(\varepsilon) \\
&\quad \leq \frac{1}{\nu} \iint_{\mathbb{R}^2} n(t,\hat{x},\hat{y}) \left( \bar{a}(s,\hat{x},\hat{y}) - a_{\lfloor t/\varepsilon \rfloor}(1,\hat{x},\hat{y}) \right) d\hat{x}\,d\hat{y} + \frac{1}{\nu^2} \left| \bar{R}[n](t) - R_{\lfloor t/\varepsilon \rfloor}[m] \right| \\
&\qquad + \frac{1}{\nu} \iint_{\mathbb{R}^2} \left| n(t,\hat{x},\hat{y}) - m_{\lfloor t/\varepsilon \rfloor}(0,\hat{x},\hat{y}) \right| d\hat{x}\,d\hat{y} + \mathcal{O}(\varepsilon) \leq C e^{Ct} \sqrt{\varepsilon} + C \left\| n(t,\cdot,\cdot) - m_{\lfloor t/\varepsilon \rfloor}(0,\cdot,\cdot) \right\|_{L^1(\mathbb{R}^2)},
\end{aligned} \tag{2.3.18}
$$

where we have estimated the first term on the right-hand side with the argument used in (2.3.16). For the second term, we noticed that $\bar{R}[n](t) = \iint_{\mathbb{R}^2} \mathcal{G}[n](t,x,y)\,dx\,dy$ (and a similar formula for $R_{\lfloor t/\varepsilon \rfloor}[m]$), so that (2.3.17) can be used to estimate the term $\left| \bar{R}[n](t) - R_{\lfloor t/\varepsilon \rfloor}[m] \right|$.

Bringing together (2.3.16), (2.3.17) and (2.3.18), the estimate (2.3.12) becomes

$$\begin{aligned}&\|n(t+\varepsilon,\cdot,\cdot)-m_{\lfloor (t+\varepsilon)/\varepsilon\rfloor}(0,\cdot,\cdot)\|_{L^1(\mathbb{R}^2)}\\&\leq \left\|n(t,\cdot,\cdot)-m_{\lfloor t/\varepsilon\rfloor}(0,\cdot,\cdot)\right\|_{L^1(\mathbb{R}^2)}+C\varepsilon\left\|n(t,\cdot,\cdot)-m_{\lfloor t/\varepsilon\rfloor}(0,\cdot,\cdot)\right\|_{L^1(\mathbb{R}^2)}+Ce^{Ct}\varepsilon^{3/2}.\end{aligned}$$

We now consider a fixed time $t\geq 0$. We have

$$\begin{aligned}\left\|n(t,\cdot,\cdot)-m_{\lfloor t/\varepsilon\rfloor}(0,\cdot,\cdot)\right\|_{L^1(\mathbb{R}^2)}&\leq \left\|n(\lfloor t/\varepsilon\rfloor\varepsilon,\cdot,\cdot)-m_{\lfloor t/\varepsilon\rfloor}(0,\cdot,\cdot)\right\|_{L^1(\mathbb{R}^2)}+C\varepsilon\\&\leq \max_{k\leq 1/\varepsilon}\|n(k\varepsilon,\cdot,\cdot)-m_k(0,\cdot,\cdot)\|_{L^1(\mathbb{R}^2)}+C\varepsilon,\end{aligned}$$

while an induction shows

$$\|n(k\varepsilon,\cdot,\cdot)-m_k(0,\cdot,\cdot)\|_{L^1(\mathbb{R}^2)}\leq y(k\varepsilon),$$

where $y'(s)=y(s)+C\sqrt{\varepsilon}e^{Ct}$ and $y(0)=0$, that is $y(s)=C\sqrt{\varepsilon}e^{ct}\left(e^s-1\right)$. Then,

$$\left\|n(t,\cdot,\cdot)-m_{\lfloor t/\varepsilon\rfloor}(0,\cdot,\cdot)\right\|_{L^1(\mathbb{R}^2)}\leq C\sqrt{\varepsilon}e^{ct}\left(e^t-1\right)+C\varepsilon,$$

and $\left\|n(t,\cdot,\cdot)-m_{\lfloor t/\varepsilon\rfloor}(0,\cdot,\cdot)\right\|_{L^1(\mathbb{R}^2)}\to 0$ as $\varepsilon\to 0$, which concludes the proof.

## 2.4 Discussion

In this manuscript, we have introduced a model for a tree population structured by two phenotypic traits: a seed production trait and a threshold temperature trait. These traits are inherited, but they induce phenological traits that are plastic. In particular, the temperature dormancy trait can be seen as a latent trait, while the seasonal time when an individual initiates summer dormancy comprise the temperature dormancy trait as well as environmental components. Note that the activity status of an individual, ie active or dormant, is sometimes considered as a discrete phenotypic trait itself (Reid and Acker 2022). We consider that the individuals become dormant once the temperature of the air around them exceeds their threshold temperature, which is a breeding value. There is then a interplay between these phenotypes and the temperature and precipitations that are input of the model. The phenology of the trees impacts their production of seeds (the production stops when they become dormant), as well as the phenotypes of the seeds produced by the population (dormant trees

do not produce seeds nor pollen). We have tried to consider environmental factors and phenotypic traits that are commonly considered in field studies, to facilitate connection with other approaches in continuations of this work.

We have introduced two successive asymptotic limits to simplify our complex model. The first one is based on the assumption that the yearly death rate of adult trees is low, we believe this is very reasonable for many tree species (Das, Stephenson, and Davis 2016). Note that to use this asymptotic limit, we have assumed that the weather conditions change slowly, but homogenization methods could provide a way to consider more realistic climate conditions. Typically, climate change could induce precipitation levels that are less stable from one year to another. In the amazonian forests, for instance, droughts lasting several years or abnormally intense precipitations are already threatening tree populations (B. M. Flores et al. 2024; ONF 2024). The second asymptotic limit we have used is based on the assumption that at the phenotypic variance of the population is small, which is similar to to the weak selection assumption (Wakeley 2005) commonly used in population genetics, and it is related to assumption that the phenotypic variance of a population is constant (Kirkpatrick and Barton 1997). This limit is a powerful approach to obtain simple macroscopic models. This assumption is well established in the evolutionary biology community, and the mathematical aspects of this asymptotic limit are rapidly strengthening (Raoul 2017; Calvez, Poyato, and Santambrogio 2023). We believe specific models such as the one considered here could bring interesting new mathematical questions. Indeed, the terms of the macroscopic model depends on the life cycles of individuals: the phenotypic traits can affect seed production, pollen production or survival; scarcity of resources can affect either the adult population or the maturation of seeds. It would be interesting to understand how the macroscopic models should be written to take into account such processes. If it is possible to build a unifying framework for macroscopic models, it could be a useful tool.

Coming back to the case of amazonian forests, the lifespan of canopy trees is of the order of hundreds of years (Laurance et al. 2004), so that climate change is a rapid phenomenon on that time scale. This means it would be pertinent to consider a rapid shift of the environmental conditions for our continuous structured population model. In this context, it is not clear that the second asymptotic limit we have used is biologically relevant. That second limit relies on the assumption that the phenotypic variance of the population is small. There is however an important phenotypic diversity observed in natural populations of trees (A. Kremer and Hipp 2020), and this phenotypic diversity,

coupled with adults tolerance to harsh meteorological conditions and to plasticity could allow the populations to evolve on a faster scale that what is described by the approach introduced in this manuscript. An analysis of the dynamics of the continuous structured population model when the phenotypic variance of the population is not small would be a great complement to this manuscript, and could open a fruitful discussion about the effect of plasticity and evolution in tree populations facing the current climate change.

Under the assumption of small phenotypic variance and Gaussian approximation of the population, the macroscopic model we obtain after the two asymptotic limits is a system of two coupled differential equations. The solutions can then be represented in a simple phase plane, and we plan to investigate the dynamics of that model in a forthcoming study. We will take advantage of the simplicity of this final model to describe its evolutionary dynamics thoroughly, and we will discuss its ecological outcomes. Moreover, the approach we have developed could be adapted to describe other phenological traits, such as winter dormancy (that can be plastic and/or driven by a threshold temperature that is under election) or situations where adult trees are more plastic and tolerant than young ones. Finally, the assumption of a population of constant size that we made can be modified to observe ecological consequences of environmental effects. We believe these macroscopic models could be interesting tools to investigate the effect of different forest management practicies.

## 2.5 Approximation of the population by a normal distribution

We want to briefly explain why we expect solutions of (2.2.12) to be well approximated by a normal distribution in the asymptotic limit proposed in Section 2.2.3. More specifically, we believe the population $(x,y) \mapsto n(t,x,y)$ is close to a normal distribution with variance $\sigma^2(\bar{\sigma}_x, \bar{\sigma}_y)$ when $\sigma > 0$ is small. This approximation has been used for simpler models in e.g. (Patout 2023; Raoul 2017), and is related to the assumption that a population is normally distributed with a constant phenotypic variance (*variance at linkage equilibrium*), which is a classical approach in population genetics (Kirkpatrick and Barton 1997).

To explain this idea, assume the population is initially concentrated around $(X(t),Y(t))$. Then, for $t \geq 0$ small and $(x,y)$ in a neighborhood of $(X(t),Y(t)$, that is when $|(x,y)-(X(t),Y(t))| \leq C\sigma$, the

equation (2.2.12) can be roughly approximated as follows:

$$\partial_t n(t,x,y) \sim -\bar{a}(t,X(t),Y(t))n(t,x,y) + \bar{a}(t,X(t),Y(t)) \iint_{\mathbb{R}^2}\iint_{\mathbb{R}^2} \Gamma_{\sigma^2\bar{\sigma}_x^2}\left(x - \frac{x_1+x_2}{2}\right)\Gamma_{\sigma^2\bar{\sigma}_y^2}\left(y - \frac{y_1+y_2}{2}\right) n(t,x_1,y_1)n(t,x_2,y_2)\,dx_1\,dy_1\,dx_2\,dy_2. \quad (2.5.1)$$

The dynamics of (2.5.1) is then dominated on a time scale of order 1 (more precisely for $0 < t \ll 1/\sigma$) by the infinitesimal reproduction operator, defined for $f \in \mathcal{P}_2(\mathbb{R}^2)$ by:

$$\bar{T}[f](\tilde{x}) = \iint_{\mathbb{R}^2} \Gamma_{\bar{\sigma}_x^2}\left(\tilde{x} - \frac{\tilde{x}_1+\tilde{x}_2}{2}\right)\Gamma_{\bar{\sigma}_y^2}\left(\tilde{y} - \frac{\tilde{y}_1+\tilde{y}_2}{2}\right) f(\tilde{x}_1,\tilde{y}_1)f(\tilde{x}_2,\tilde{y}_2)\,d\tilde{x}_1\,d\tilde{x}_2\,d\tilde{y}_1\,d\tilde{y}_2.$$

This reproduction operator does not change the population size (it is coherent with the model (2.2.12) where $\iint_{\mathbb{R}^2} n(t,x,y)\,dx\,dy \equiv 1$ for $t \geq 0$) and it also does not affect the mean phenotypic traits of the population. This operator however contracts solutions exponentially fast to the distribution of the population to the Gaussian function (this can be made rigorous in the sense of the Wasserstein distance, see Raoul 2017):

$$\tilde{n}(t,x,y) \sim \Gamma_{2\sigma^2\bar{\sigma}_x^2}(x - X(t))\,\Gamma_{2\sigma^2\bar{\sigma}_y^2}(y - Y(t)).$$

In particular, this keeps the population density concentrated around its mean phenotypic traits $(X(t),Y(t))$, so that when $\sigma > 0$ is small, the relaxation toward a normal distribution centered around $(X(t),Y(t))$ is propagated in time and (2.2.17) holds for all times $t \geq 0$. Note that the rough approximation (2.5.1) is introduced to explain why $n$ is normally distributed, but that a more precise approach will be necessary to obtain the dynamics of $(X(t),Y(t))$, as we describe in Section 2.2.3.

## 2.6 Heuristic derivation of the macroscopic model (2.2.20)-(2.2.21)

In this section, we simplify the expressions (2.2.18) and (2.2.19) under the approximation (2.2.17).

We have

$$\begin{aligned}
&\iint_{\mathbb{R}^2} x\bar{a}(t,x,y)n(t,x,y)\,dx\,dy \sim \iint_{\mathbb{R}^2} x\bar{a}(t,x,y)\Gamma_{2\sigma_x^2}(x-X(t))\Gamma_{2\sigma_y^2}(y-Y(t))\,dx\,dy\\
&\quad= \iint_{\mathbb{R}^2} x\Big(\bar{a}(t,X(t),Y(t))+(x-X(t))\partial_x\bar{a}(t,X(t),Y(t))+(y-Y(t))\partial_y\bar{a}(t,X(t),Y(t))+\frac{(x-X(t))^2}{2}\partial_{xx}\bar{a}(t,\\
&\qquad+\frac{(y-Y(t))^2}{2}\partial_{yy}\bar{a}(t,X(t),Y(t))+(x-X(t))(y-Y(t))\partial_{xy}\bar{a}(t,X(t),Y(t))+\mathcal{O}(\|(x-X(t),y-Y(t))\|^3)\Big)\\
&\qquad\Gamma_{2\sigma_x^2}(x-X(t))\Gamma_{2\sigma_y^2}(y-Y(t))\,dx\,dy\\
&\quad= X(t)\bar{a}(t,X(t),Y(t))+2\sigma_x^2\partial_x\bar{a}(t,X(t),Y(t))+\sigma_x^2X(t)\partial_{xx}\bar{a}(t,X(t),Y(t))+\sigma_y^2X(t)\partial_{yy}\bar{a}(t,X(t),Y(t))+\mathcal{O}\Big(
\end{aligned}$$

Similarly,

$$\begin{aligned}
&\iint_{\mathbb{R}^2} y\bar{a}(t,x,y)n(t,x,y)\,dx\,dy \sim \iint_{\mathbb{R}^2} y\bar{a}(t,x,y)\Gamma_{2\sigma_x^2}(x-X(t))\Gamma_{2\sigma_y^2}(y-Y(t))\,dx\,dy\\
&\quad= Y(t)\bar{a}(t,X(t),Y(t))+2\sigma_y^2\partial_y\bar{a}(t,X(t),Y(t))+\sigma_x^2Y(t)\partial_{xx}\bar{a}(t,X(t),Y(t))+\sigma_y^2Y(t)\partial_{yy}\bar{a}(t,X(t),Y(t))+\mathcal{O}\Big(|
\end{aligned}$$

We have

$$\begin{aligned}
&\iint_{\mathbb{R}^2} \bar{a}(t,x,y)n(t,x,y)\,dx\,dy \sim \iint_{\mathbb{R}^2} \bar{a}(t,x,y)\Gamma_{2\sigma_x^2}(x-X(t))\Gamma_{2\sigma_y^2}(y-Y(t))\,dx\,dy\\
&\quad= \iint_{\mathbb{R}^2} \Big(\bar{a}(t,X(t),Y(t))+(x-X(t))\partial_x\bar{a}(t,X(t),Y(t))+(y-Y(t))\partial_y\bar{a}(t,X(t),Y(t))+\frac{(x-X(t))^2}{2}\partial_{xx}\bar{a}(t,X\\
&\qquad+\frac{(y-Y(t))^2}{2}\partial_{yy}\bar{a}(t,X(t),Y(t))+(x-X(t))(y-Y(t))\partial_{xy}\bar{a}(t,X(t),Y(t))+\mathcal{O}(\|(x-X(t),y-Y(t))\|^3)\Big)\\
&\qquad\Gamma_{2\sigma_x^2}(x-X(t))\Gamma_{2\sigma_y^2}(y-Y(t))\,dx\,dy\\
&\quad= \bar{a}(t,X(t),Y(t))+\sigma_x^2\partial_{xx}\bar{a}(t,X(t),Y(t))+\sigma_y^2\partial_{yy}\bar{a}(t,X(t),Y(t))+\mathcal{O}\left(\|(\sigma_x,\sigma_y)\|^3\right).
\end{aligned}$$

and, if we use the shortened notation $\bar\rho := \bar\rho[\delta_{x=X(t)}\delta_{y=Y(t)}](t,X(t),Y(t),X(t),Y(t))$ and the derivatives of this quantity, we get

$$
\begin{aligned}
&\iint_{\mathbb{R}^2}\iint_{\mathbb{R}^2} x_1^+ n(t,x_1,y_1)n(t,x_2,y_2)\bar\rho[n(t,\cdot,\cdot)](t,x_1,y_1,x_2,y_2)\,dx_1\,dy_1\,dx_2\,dy_2\\
&\quad\sim \iint_{\mathbb{R}^2}\iint_{\mathbb{R}^2} x_1^+ \bar\rho[\Gamma_{2\sigma_x^2}(\cdot-X(t))\Gamma_{2\sigma_y^2}(\cdot-Y(t))](t,x_1,y_1,x_2,y_2)\\
&\qquad\qquad \Gamma_{2\sigma_x^2}(x_1-X(t))\Gamma_{2\sigma_y^2}(y_1-Y(t))\Gamma_{2\sigma_x^2}(x_2-X(t))\Gamma_{2\sigma_y^2}(y_2-Y(t))\,dx_1\,dx_2\,dy_1\,dy_2\\
&\quad= \iint_{\mathbb{R}^2}\iint_{\mathbb{R}^2} x_1^+\Big(\bar\rho+(x_1-X(t))\partial_{x_1}\bar\rho+(x_2-X(t))\partial_{x_2}\bar\rho+(y_1-Y(t))\partial_{y_1}\bar\rho+(y_2-Y(t))\partial_{y_2}\bar\rho\\
&\qquad+\frac{(x_1-X(t))^2}{2}\partial_{x_1x_1}\bar\rho+\frac{(x_2-X(t))^2}{2}\partial_{x_2x_2}\bar\rho+\frac{(y_1-Y(t))^2}{2}\partial_{y_1y_1}\bar\rho+\frac{(y_2-Y(t))^2}{2}\partial_{y_2y_2}\bar\rho\\
&\qquad+(x_1-X(t))(x_2-X(t))\partial_{x_1x_2}\bar\rho+(y_1-Y(t))(y_2-Y(t))\partial_{y_1y_2}\bar\rho\\
&\qquad+(x_1-X(t))(y_1-Y(t))\partial_{x_1y_1}\bar\rho+(x_2-X(t))(y_2-Y(t))\partial_{x_2y_2}\bar\rho\\
&\qquad+(x_1-X(t))(y_2-Y(t))\partial_{x_1y_2}\bar\rho+(x_2-X(t))(y_1-Y(t))\partial_{x_2y_1}\bar\rho+\mathcal{O}(\|(x-X(t),y-Y(t))\|^3)\Big)\\
&\qquad\Gamma_{2\sigma_x^2}(x_1-X(t))\Gamma_{2\sigma_y^2}(y_1-Y(t))\Gamma_{2\sigma_x^2}(x_2-X(t))\Gamma_{2\sigma_y^2}(y_2-Y(t))\,dx_1\,dy_1\,dx_2\,dy_2\\
&\quad=\bar\rho X(t)+2\sigma_x^2\partial_{x_1}\bar\rho+\sigma_x^2X(t)\partial_{x_1x_1}\bar\rho+\sigma_x^2X(t)\partial_{x_2x_2}\bar\rho+\sigma_y^2X(t)\partial_{y_1y_1}\bar\rho+\sigma_y^2X(t)\partial_{y_2y_2}\bar\rho+\mathcal{O}\left(\|(\sigma_x,\sigma_y)\|^3\right).
\end{aligned}
$$

We consider now the last factor of (2.2.18):

$$
\begin{aligned}
&\iint_{\mathbb{R}^2}\iint_{\mathbb{R}^2}\frac{x_1+x_2}{2}x_1^+\bar\rho[n(t,\cdot,\cdot)](t,x_1,y_1,x_2,y_2)n(t,x_1,y_1)n(t,x_2,y_2)\,dx_1\,dy_1\,dx_2\,dy_2\\
&\quad\sim\frac12\iint_{\mathbb{R}^2}\iint_{\mathbb{R}^2}(x_1^2+x_2x_1)\bar\rho[\Gamma_{2\sigma_x^2}(\cdot-X(t))\Gamma_{2\sigma_y^2}(\cdot-Y(t))](t,x_1,y_1,x_2,y_2)\\
&\qquad\qquad\Gamma_{2\sigma^2}(x_1-X(t))\Gamma_{2\sigma^2}(y_1-Y(t))\Gamma_{2\sigma^2}(x_2-X(t))\Gamma_{2\sigma^2}(y_2-Y(t))\,dx_1\,dy_1\,dx_2\,dy_2\\
&\quad=(X(t)^2+\sigma_x^2)\bar\rho+3\sigma_x^2X(t)\partial_{x_1}\bar\rho+\sigma_x^2X(t)\partial_{x_2}\bar\rho\\
&\qquad+\sigma_x^2X^2\partial_{x_1x_1}\bar\rho+\sigma_x^2X^2\partial_{x_2x_2}\bar\rho+\sigma_y^2X^2\partial_{y_1y_1}\bar\rho+\sigma_y^2X^2\partial_{y_2y_2}\bar\rho+\mathcal{O}\left(\|(\sigma_x,\sigma_y)\|^3\right),
\end{aligned}
$$

as we prove in the next calculations:

$$
\begin{aligned}
&\iint_{\mathbb{R}^2}\iint_{\mathbb{R}^2} x_1^2\bar{\rho}[\Gamma_{2\sigma_x^2}(\cdot-X(t))\Gamma_{2\sigma_y^2}(\cdot-Y(t))](t,x_1,y_1,x_2,y_2)\\
&\qquad\Gamma_{2\sigma^2}(x_1-X(t))\Gamma_{2\sigma^2}(y_1-Y(t))\Gamma_{2\sigma^2}(x_2-X(t))\Gamma_{2\sigma^2}(y_2-Y(t))\,dx_1\,dy_1\,dx_2\,dy_2\\
&=\iint_{\mathbb{R}^2}\iint_{\mathbb{R}^2} x_1^2\Big(\bar{\rho}+(x_1-X(t))\partial_{x_1}\bar{\rho}+(x_2-X(t))\partial_{x_2}\bar{\rho}+(y_1-Y(t))\partial_{y_1}\bar{\rho}+(y_2-Y(t))\partial_{y_2}\bar{\rho}\\
&\quad+\frac{(x_1-X(t))^2}{2}\partial_{x_1x_1}\bar{\rho}+\frac{(x_2-X(t))^2}{2}\partial_{x_2x_2}\bar{\rho}+\frac{(y_1-Y(t))^2}{2}\partial_{y_1y1}\bar{\rho}+\frac{(y_2-Y(t))^2}{2}\partial_{y_2y_2}\bar{\rho}\\
&\quad+(x_1-X(t))(x_2-X(t))\partial_{x_1x_2}\bar{\rho}+(y_1-Y(t))(y_2-Y(t))\partial_{y_1y_2}\bar{\rho}\\
&\quad+(x_1-X(t))(y_1-Y(t))\partial_{x_1y_1}\bar{\rho}+(x_2-X(t))(y_2-Y(t))\partial_{x_2y_2}\bar{\rho}\\
&\quad+(x_1-X(t))(y_2-Y(t))\partial_{x_1y_2}\bar{\rho}+(x_2-X(t))(y_1-Y(t))\partial_{x_2y_1}\bar{\rho}+\mathcal{O}(\|(x-X(t),y-Y(t))\|^3)\Big)\\
&\quad\Gamma_{2\sigma_x^2}(x_1-X(t))\Gamma_{2\sigma_y^2}(y_1-Y(t))\Gamma_{2\sigma_x^2}(x_2-X(t))\Gamma_{2\sigma_y^2}(y_2-Y(t))\,dx_1\,dy_1\,dx_2\,dy_2\\
&=(X(t)^2+2\sigma_x^2)\bar{\rho}+4\sigma_x^2X(t)\partial_{x_1}\bar{\rho}+\sigma_x^2X(t)^2\partial_{x_1x_1}\bar{\rho}+\sigma_x^2X(t)^2\partial_{x_2x_2}\bar{\rho}+\sigma_y^2X(t)^2\partial_{y_1y1}\bar{\rho}\\
&\quad+\sigma_y^2X(t)^2\partial_{y_2y_2}\bar{\rho}+\mathcal{O}\left(\|(\sigma_x,\sigma_y)\|^3\right),
\end{aligned}
$$

where we noticed that

$$
\begin{aligned}
&\partial_{x_1x_1}\bar{\rho}\int_{\mathbb{R}} x_1^2\frac{(x_1-X(t))^2}{2}\Gamma_{2\sigma_x^2}(x_1-X(t))\,dx_1\\
&\quad=\partial_{x_1x_1}\bar{\rho}\left(\sigma_x^2+\frac{1}{2}\int_{\mathbb{R}}x^4\Gamma_{2\sigma_x^2}(x)\,dx\right)=\sigma_x^2\partial_{x_1x_1}\bar{\rho}+\mathcal{O}\left(\|(\sigma_x,\sigma_y)\|^3\right).
\end{aligned}
$$

Also,

$$
\begin{aligned}
&\iint_{\mathbb{R}^2}\iint_{\mathbb{R}^2} x_1x_2\bar\rho[\Gamma_{2\sigma_x^2}(\cdot-X(t))\Gamma_{2\sigma_y^2}(\cdot-Y(t))](t,x_1,y_1,x_2,y_2)\\
&\qquad\Gamma_{2\sigma^2}(x_1-X(t))\Gamma_{2\sigma^2}(y_1-Y(t))\Gamma_{2\sigma^2}(x_2-X(t))\Gamma_{2\sigma^2}(y_2-Y(t))\,dx_1\,dy_1\,dx_2\,dy_2\\
&=\iint_{\mathbb{R}^2}\iint_{\mathbb{R}^2} x_1x_2\Big(\bar\rho+(x_1-X(t))\partial_{x_1}\bar\rho+(x_2-X(t))\partial_{x_2}\bar\rho+(y_1-Y(t))\partial_{y_1}\bar\rho+(y_2-Y(t))\partial_{y_2}\bar\rho\\
&\quad+\frac{(x_1-X(t))^2}{2}\partial_{x_1x_1}\bar\rho+\frac{(x_2-X(t))^2}{2}\partial_{x_2x_2}\bar\rho+\frac{(y_1-Y(t))^2}{2}\partial_{y_1y_1}\bar\rho+\frac{(y_2-Y(t))^2}{2}\partial_{y_2y_2}\bar\rho\\
&\quad+(x_1-X(t))(x_2-X(t))\partial_{x_1x_2}\bar\rho+(y_1-Y(t))(y_2-Y(t))\partial_{y_1y_2}\bar\rho\\
&\quad+(x_1-X(t))(y_1-Y(t))\partial_{x_1y_1}\bar\rho+(x_2-X(t))(y_2-Y(t))\partial_{x_2y_2}\bar\rho\\
&\quad+(x_1-X(t))(y_2-Y(t))\partial_{x_1y_2}\bar\rho+(x_2-X(t))(y_1-Y(t))\partial_{x_2y_1}\bar\rho+\mathcal{O}(\|(x-X(t),y-Y(t))\|^3)\Big)\\
&\quad\Gamma_{2\sigma^2}(x_1-X(t))\Gamma_{2\sigma^2}(y_1-Y(t))\Gamma_{2\sigma^2}(x_2-X(t))\Gamma_{2\sigma^2}(y_2-Y(t))\,dx_1\,dy_1\,dx_2\,dy_2\\
&=X(t)^2\bar\rho+2\sigma_x^2X(t)\partial_{x_1}\bar\rho+2\sigma_x^2X(t)\partial_{x_2}\bar\rho\\
&\quad+\sigma_x^2X(t)^2\partial_{x_1x_1}\bar\rho+\sigma_x^2X(t)^2\partial_{x_2x_2}\bar\rho+\sigma_y^2X(t)^2\partial_{y_1y_1}\bar\rho+\sigma_y^2X(t)^2\partial_{y_2y_2}\bar\rho+\mathcal{O}\left(\|(\sigma_x,\sigma_y)\|^3\right).
\end{aligned}
$$

And we can finally consider now the last factor of (2.2.19):

$$
\begin{aligned}
&\iint_{\mathbb{R}^2}\iint_{\mathbb{R}^2}\frac{y_1+y_2}{2}x_1^+n(t,x_1,y_1)n(t,x_2,y_2)\bar\rho[n(t,\cdot,\cdot)](t,x_1,y_1,x_2,y_2)\,dx_1\,dy_1\,dx_2\,dy_2\\
&\sim\frac12\iint_{\mathbb{R}^2}\iint_{\mathbb{R}^2}(y_1x_1+y_2x_1)\bar\rho[\Gamma_{2\sigma_x^2}(\cdot-X(t))\Gamma_{2\sigma_y^2}(\cdot-Y(t))](t,x_1,y_1,x_2,y_2)\\
&\qquad\Gamma_{2\sigma^2}(x_1-X(t))\Gamma_{2\sigma^2}(y_1-Y(t))\Gamma_{2\sigma^2}(x_2-X(t))\Gamma_{2\sigma^2}(y_2-Y(t))\,dx_1\,dy_1\,dx_2\,dy_2\\
&=X(t)Y(t)\bar\rho+2\sigma_x^2Y(t)\partial_{x_1}\bar\rho+\sigma_y^2X(t)\partial_{y_1}\bar\rho+\sigma_y^2X(t)\partial_{y_2}\bar\rho\\
&\quad+\sigma_x^2X(t)Y(t)\partial_{x_1x_1}\bar\rho+\sigma_x^2X(t)Y(t)\partial_{x_2x_2}\bar\rho+\sigma_y^2X(t)Y(t)\partial_{y_1y_1}\bar\rho+\sigma_y^2X(t)Y(t)\partial_{y_2y_2}\bar\rho+\mathcal{O}\left(\|(\sigma_x,\sigma_y)\|^3\right),
\end{aligned}
$$

since

$$
\begin{aligned}
&\iint_{\mathbb{R}^2}\iint_{\mathbb{R}^2} y_1x_1\bar{\rho}[\Gamma_{2\sigma_x^2}(\cdot-X(t))\Gamma_{2\sigma_y^2}(\cdot-Y(t))](t,x_1,y_1,x_2,y_2)\\
&\qquad\Gamma_{2\sigma^2}(x_1-X(t))\Gamma_{2\sigma^2}(y_1-Y(t))\Gamma_{2\sigma^2}(x_2-X(t))\Gamma_{2\sigma^2}(y_2-Y(t))\,dx_1\,dx_2\,dy_1\,dy_2\\
&=\iint_{\mathbb{R}^2}\iint_{\mathbb{R}^2} x_1y_1\Big(\bar{\rho}+(x_1-X(t))\partial_{x_1}\bar{\rho}+(x_2-X(t))\partial_{x_2}\bar{\rho}+(y_1-Y(t))\partial_{y_1}\bar{\rho}+(y_2-Y(t))\partial_{y_2}\bar{\rho}\\
&\quad+\frac{(x_1-X(t))^2}{2}\partial_{x_1x_1}\bar{\rho}+\frac{(x_2-X(t))^2}{2}\partial_{x_2x_2}\bar{\rho}+\frac{(y_1-Y(t))^2}{2}\partial_{y_1y1}\bar{\rho}+\frac{(y_2-Y(t))^2}{2}\partial_{y_2y_2}\bar{\rho}\\
&\quad+(x_1-X(t))(x_2-X(t))\partial_{x_1x_2}\bar{\rho}+(y_1-Y(t))(y_2-Y(t))\partial_{y_1y_2}\bar{\rho}\\
&\quad+(x_1-X(t))(y_1-Y(t))\partial_{x_1y_1}\bar{\rho}+(x_2-X(t))(y_2-Y(t))\partial_{x_2y_2}\bar{\rho}\\
&\quad+(x_1-X(t))(y_2-Y(t))\partial_{x_1y_2}\bar{\rho}+(x_2-X(t))(y_1-Y(t))\partial_{x_2y_1}\bar{\rho}+\mathcal{O}(\|(x-X(t),y-Y(t))\|^3)\Big)\\
&\quad\Gamma_{2\sigma^2}(x_1-X(t))\Gamma_{2\sigma^2}(y_1-Y(t))\Gamma_{2\sigma^2}(x_2-X(t))\Gamma_{2\sigma^2}(y_2-Y(t))\,dx_1\,dy_1\,dx_2\,dy_2\\
&=X(t)Y(t)\bar{\rho}+2\sigma_x^2Y(t)\partial_{x_1}\bar{\rho}+2\sigma_y^2X(t)\partial_{y_1}\bar{\rho}+\sigma_x^2X(t)Y(t)\partial_{x_1x_1}\bar{\rho}\\
&\quad+\sigma_x^2X(t)Y(t)\partial_{x_2x_2}\bar{\rho}+\sigma_y^2X(t)Y(t)\partial_{y_1y1}\bar{\rho}+\sigma_y^2X(t)Y(t)\partial_{y_2y_2}\bar{\rho}+\mathcal{O}\left(\|(\sigma_x,\sigma_y)\|^3\right),
\end{aligned}
$$

and the similarly when $y_2$ replaces $y_1$.

Bringing all these expressions together, we obtain

$$
\begin{aligned}
\frac{d}{dt}X(t) &= -\Big(X(t)a(t,X(t),Y(t)) + 2\sigma_x^2\partial_x\bar{a}(t,X(t),Y(t)) + \sigma_x^2X(t)\partial_{xx}\bar{a}(t,X(t),Y(t)) + \sigma_y^2X(t)\partial_{yy}\bar{a}(t,X(t),Y(t)) \\
&\quad + \frac{\bar{a}(t,X(t),Y(t)) + \sigma_x^2\partial_{xx}\bar{a}(t,X(t),Y(t)) + \sigma_y^2\partial_{yy}\bar{a}(t,X(t),Y(t))}{\bar{\rho}X(t) + 2\sigma_x^2\partial_{x_1}\bar{\rho} + \sigma_x^2X(t)\partial_{x_1x_1}\bar{\rho} + \sigma_x^2X(t)\partial_{x_2x_2}\bar{\rho} + \sigma_y^2X(t)\partial_{y_1y_1}\bar{\rho} + \sigma_y^2X(t)\partial_{y_2y_2}\bar{\rho}} \\
&\quad \Big((X(t)^2+\sigma_x^2)\bar{\rho} + 3\sigma_x^2X(t)\partial_{x_1}\bar{\rho} + \sigma_x^2X(t)\partial_{x_2}\bar{\rho} \\
&\quad + \sigma_x^2X^2\partial_{x_1x_1}\bar{\rho} + \sigma_x^2X^2\partial_{x_2x_2}\bar{\rho} + \sigma_y^2X^2\partial_{y_1y_1}\bar{\rho} + \sigma_y^2X^2\partial_{y_2y_2}\bar{\rho}\Big) + \mathcal{O}\left(\|(\sigma_x,\sigma_y)\|^3\right) \\
&= -X(t)\bar{a}(t,X(t),Y(t)) - 2\sigma_x^2\partial_x\bar{a}(t,X(t),Y(t)) - \sigma_x^2X(t)\partial_{xx}\bar{a}(t,X(t),Y(t)) - \sigma_y^2X(t)\partial_{yy}\bar{a}(t,X(t),Y(t)) \\
&\quad + \bar{a}(t,X(t),Y(t))X(t)\frac{1 + \sigma_x^2\frac{\partial_{xx}\bar{a}(t,X(t),Y(t))}{\bar{a}(t,X(t),Y(t))} + \sigma_y^2\frac{\partial_{yy}\bar{a}(t,X(t),Y(t))}{\bar{a}(t,X(t),Y(t))}}{1 + 2\sigma_x^2\frac{\partial_{x_1}\bar{\rho}}{\bar{\rho}X(t)} + \sigma_x^2\frac{\partial_{x_1x_1}\bar{\rho}}{\bar{\rho}} + \sigma_x^2\frac{\partial_{x_2x_2}\bar{\rho}}{\bar{\rho}} + \sigma_y^2\frac{\partial_{y_1y_1}\bar{\rho}}{\bar{\rho}} + \sigma_y^2\frac{\partial_{y_2y_2}\bar{\rho}}{\bar{\rho}}} \\
&\quad \Big(1 + \frac{\sigma_x^2}{X(t)^2} + 3\sigma_x^2\frac{\partial_{x_1}\bar{\rho}}{X(t)\bar{\rho}} + \sigma_x^2\frac{\partial_{x_2}\bar{\rho}}{X(t)\bar{\rho}} \\
&\quad + \sigma_x^2\frac{\partial_{x_1x_1}\bar{\rho}}{\bar{\rho}} + \sigma_x^2\frac{\partial_{x_2x_2}\bar{\rho}}{\bar{\rho}} + \sigma_y^2\frac{\partial_{y_1y_1}\bar{\rho}}{\bar{\rho}} + \sigma_y^2\frac{\partial_{y_2y_2}\bar{\rho}}{\bar{\rho}}\Big) + \mathcal{O}\left(\|(\sigma_x,\sigma_y)\|^3\right) \\
&= -X(t)\bar{a}(t,X(t),Y(t)) - 2\sigma_x^2\partial_x\bar{a}(t,X(t),Y(t)) - \sigma_x^2X(t)\partial_{xx}\bar{a}(t,X(t),Y(t)) - \sigma_y^2X(t)\partial_{yy}\bar{a}(t,X(t),Y(t)) \\
&\quad + \bar{a}(t,X(t),Y(t))X(t)\left(1 + \sigma_x^2\frac{\partial_{xx}\bar{a}(t,X(t),Y(t))}{\bar{a}(t,X(t),Y(t))} + \sigma_y^2\frac{\partial_{yy}\bar{a}(t,X(t),Y(t))}{\bar{a}(t,X(t),Y(t))}\right) \\
&\quad \left(1 - 2\sigma_x^2\frac{\partial_{x_1}\bar{\rho}}{\bar{\rho}X(t)} - \sigma_x^2\frac{\partial_{x_1x_1}\bar{\rho}}{\bar{\rho}} - \sigma_x^2\frac{\partial_{x_2x_2}\bar{\rho}}{\bar{\rho}} - \sigma_y^2\frac{\partial_{y_1y_1}\bar{\rho}}{\bar{\rho}} - \sigma_y^2\frac{\partial_{y_2y_2}\bar{\rho}}{\bar{\rho}}\right) \\
&\quad \Big(1 + \frac{\sigma_x^2}{X(t)^2} + 3\sigma_x^2\frac{\partial_{x_1}\bar{\rho}}{X(t)\bar{\rho}} + \sigma_x^2\frac{\partial_{x_2}\bar{\rho}}{X(t)\bar{\rho}} \\
&\quad + \sigma_x^2\frac{\partial_{x_1x_1}\bar{\rho}}{\bar{\rho}} + \sigma_x^2\frac{\partial_{x_2x_2}\bar{\rho}}{\bar{\rho}} + \sigma_y^2X^2\frac{\partial_{y_1y_1}\bar{\rho}}{\bar{\rho}} + \sigma_y^2X^2\frac{\partial_{y_2y_2}\bar{\rho}}{\bar{\rho}}\Big) + \mathcal{O}\left(\|(\sigma_x,\sigma_y)\|^3\right) \\
&= -X(t)\bar{a}(t,X(t),Y(t)) - 2\sigma_x^2\partial_x\bar{a}(t,X(t),Y(t)) - \sigma_x^2X(t)\partial_{xx}\bar{a}(t,X(t),Y(t)) - \sigma_y^2X(t)\partial_{yy}\bar{a}(t,X(t),Y(t)) \\
&\quad + \bar{a}(t,X(t),Y(t))X(t) + \Big(\sigma_x^2X(t)\partial_{xx}\bar{a}(t,X(t),Y(t)) + \sigma_y^2X(t)\partial_{yy}\bar{a}(t,X(t),Y(t))\Big) \\
&\quad + \Big(-2\sigma_x^2\bar{a}(t,X(t),Y(t))\frac{\partial_{x_1}\bar{\rho}}{\bar{\rho}} - \sigma_x^2\bar{a}(t,X(t),Y(t))X(t)\frac{\partial_{x_1x_1}\bar{\rho}}{\bar{\rho}} - \sigma_x^2\bar{a}(t,X(t),Y(t))X(t)\frac{\partial_{x_2x_2}\bar{\rho}}{\bar{\rho}} \\
&\qquad - \sigma_y^2\bar{a}(t,X(t),Y(t))X(t)\frac{\partial_{y_1y_1}\bar{\rho}}{\bar{\rho}} - \sigma_y^2\bar{a}(t,X(t),Y(t))X(t)\frac{\partial_{y_2y_2}\bar{\rho}}{\bar{\rho}}\Big) \\
&\quad + \Big(\bar{a}(t,X(t),Y(t))\frac{\sigma_x^2}{X(t)} + 3\sigma_x^2\bar{a}(t,X(t),Y(t))\frac{\partial_{x_1}\bar{\rho}}{\bar{\rho}} + \sigma_x^2\bar{a}(t,X(t),Y(t))\frac{\partial_{x_2}\bar{\rho}}{\bar{\rho}} \\
&\qquad + \sigma_x^2\bar{a}(t,X(t),Y(t))X(t)\frac{\partial_{x_1x_1}\bar{\rho}}{\bar{\rho}} + \sigma_x^2\bar{a}(t,X(t),Y(t))X(t)\frac{\partial_{x_2x_2}\bar{\rho}}{\bar{\rho}} \\
&\qquad + \sigma_y^2\bar{a}(t,X(t),Y(t))X(t)\frac{\partial_{y_1y_1}\bar{\rho}}{\bar{\rho}} + \sigma_y^2\bar{a}(t,X(t),Y(t))X(t)\frac{\partial_{y_2y_2}\bar{\rho}}{\bar{\rho}}\Big) + \mathcal{O}\left(\|(\sigma_x,\sigma_y)\|^3\right) \\
&= 2\sigma_x^2\left[-\partial_x\bar{a}(t,X(t),Y(t)) + \bar{a}(t,X(t),Y(t))\frac{\partial_{x_1}\bar{\rho}}{2\bar{\rho}} + \bar{a}(t,X(t),Y(t))\frac{1}{2X(t)} + \bar{a}(t,X(t),Y(t))\frac{\partial_{x_2}\bar{\rho}}{2\bar{\rho}}\right] + \mathcal{O}\left(\|(\sigma_x\right. \\
&= 2\sigma_x^2\left[-\partial_x\bar{a}(t,X(t),Y(t)) + \frac{\bar{a}(t,X(t),Y(t))}{2X(t)} + \bar{a}(t,X(t),Y(t))\frac{\partial_{x_1}\bar{\rho}}{\bar{\rho}}\right] + \mathcal{O}\left(\|(\sigma_x,\sigma_y)\|^3\right).
\end{aligned}
$$

where the last equality uses the symmetry of $\bar{\rho}$. Similarly for $Y(t)$,

$$
\begin{aligned}
\frac{d}{dt}Y(t) = &-\Big(Y(t)\bar{a}(t,X(t),Y(t)) + 2\sigma_y^2\partial_y\bar{a}(t,X(t),Y(t)) + \sigma_x^2 Y(t)\partial_{xx}\bar{a}(t,X(t),Y(t)) + \sigma_y^2 Y(t)\partial_{yy}\bar{a}(t,X(t),Y(t)\\
&+ \frac{\bar{a}(t,X(t),Y(t)) + \sigma_x^2\partial_{xx}\bar{a}(t,X(t),Y(t)) + \sigma_y^2\partial_{yy}\bar{a}(t,X(t),Y(t))}{\bar{\rho}X(t) + 2\sigma_x^2\partial_{x_1}\bar{\rho} + \sigma_x^2 X(t)\partial_{x_1x_1}\bar{\rho} + \sigma_x^2 X(t)\partial_{x_2x_2}\bar{\rho} + \sigma_y^2 X(t)\partial_{y_1y_1}\bar{\rho} + \sigma_y^2 X(t)\partial_{y_2y_2}\bar{\rho}}\\
&\Big(X(t)Y(t)\bar{\rho} + 2\sigma_x^2 Y(t)\partial_{x_1}\bar{\rho} + \sigma_y^2 X(t)\partial_{y_1}\bar{\rho} + \sigma_y^2 X(t)\partial_{y_2}\bar{\rho}\\
&+ \sigma_x^2 X(t)Y(t)\partial_{x_1x_1}\bar{\rho} + \sigma_x^2 X(t)Y(t)\partial_{x_2x_2}\bar{\rho} + \sigma_y^2 X(t)Y(t)\partial_{y_1y_1}\bar{\rho} + \sigma_y^2 X(t)Y(t)\partial_{y_2y_2}\bar{\rho}\Big) + \mathcal{O}\left(\|(\sigma_x,\sigma_y)\|^3\right)\\
= &-Y(t)\bar{a}(t,X(t),Y(t)) - 2\sigma_y^2\partial_y\bar{a}(t,X(t),Y(t)) - \sigma_x^2 Y(t)\partial_{xx}\bar{a}(t,X(t),Y(t)) - \sigma_y^2 Y(t)\partial_{yy}\bar{a}(t,X(t),Y(t))\\
&+ Y(t)\bar{a}(t,X(t),Y(t))\left(1 + \sigma_x^2\frac{\partial_{xx}\bar{a}(t,X(t),Y(t))}{\bar{a}(t,X(t),Y(t))} + \sigma_y^2\frac{\partial_{yy}\bar{a}(t,X(t),Y(t))}{\bar{a}(t,X(t),Y(t))}\right)\\
&\left(1 - 2\sigma_x^2\frac{\partial_{x_1}\bar{\rho}}{\bar{\rho}X(t)} - \sigma_x^2\frac{\partial_{x_1x_1}\bar{\rho}}{\bar{\rho}} - \sigma_x^2\frac{\partial_{x_2x_2}\bar{\rho}}{\bar{\rho}} - \sigma_y^2\frac{\partial_{y_1y_1}\bar{\rho}}{\bar{\rho}} - \sigma_y^2\frac{\partial_{y_2y_2}\bar{\rho}}{\bar{\rho}}\right)\\
&\left(1 + 2\sigma_x^2\frac{\partial_{x_1}\bar{\rho}}{X(t)\bar{\rho}} + \sigma_y^2\frac{\partial_{y_1}\bar{\rho}}{Y(t)\bar{\rho}} + \sigma_y^2\frac{\partial_{y_2}\bar{\rho}}{Y(t)\bar{\rho}} + \sigma_x^2\frac{\partial_{x_1x_1}\bar{\rho}}{\bar{\rho}} + \sigma_x^2\frac{\partial_{x_2x_2}\bar{\rho}}{\bar{\rho}} + \sigma_y^2\frac{\partial_{y_1y_1}\bar{\rho}}{\bar{\rho}} + \sigma_y^2\frac{\partial_{y_2y_2}\bar{\rho}}{\bar{\rho}}\right) + \mathcal{O}\left(\|(\sigma_x,\sigma_y)\|^3\right)\\
= &-Y(t)\bar{a}(t,X(t),Y(t)) - 2\sigma_y^2\partial_y\bar{a}(t,X(t),Y(t)) - \sigma_x^2 Y(t)\partial_{xx}\bar{a}(t,X(t),Y(t)) - \sigma_y^2 Y(t)\partial_{yy}\bar{a}(t,X(t),Y(t))\\
&+ Y(t)\bar{a}(t,X(t),Y(t)) + \sigma_x^2 Y(t)\partial_{xx}\bar{a}(t,X(t),Y(t)) + \sigma_y^2 Y(t)\partial_{yy}\bar{a}(t,X(t),Y(t))\\
&- 2\sigma_x^2 Y(t)\bar{a}(t,X(t),Y(t))\frac{\partial_{x_1}\bar{\rho}}{\bar{\rho}X(t)} - \sigma_x^2 Y(t)\bar{a}(t,X(t),Y(t))\frac{\partial_{x_1x_1}\bar{\rho}}{\bar{\rho}} - \sigma_x^2 Y(t)\bar{a}(t,X(t),Y(t))\frac{\partial_{x_2x_2}\bar{\rho}}{\bar{\rho}}\\
&- \sigma_y^2 Y(t)\bar{a}(t,X(t),Y(t))\frac{\partial_{y_1y_1}\bar{\rho}}{\bar{\rho}} - \sigma_y^2 Y(t)\bar{a}(t,X(t),Y(t))\frac{\partial_{y_2y_2}\bar{\rho}}{\bar{\rho}}\\
&+ 2\sigma_x^2 Y(t)\bar{a}(t,X(t),Y(t))\frac{\partial_{x_1}\bar{\rho}}{X(t)\bar{\rho}} + \sigma_y^2\bar{a}(t,X(t),Y(t))\frac{\partial_{y_1}\bar{\rho}}{\bar{\rho}} + \sigma_y^2\bar{a}(t,X(t),Y(t))\frac{\partial_{y_2}\bar{\rho}}{\bar{\rho}}\\
&+ \sigma_x^2 Y(t)\bar{a}(t,X(t),Y(t))\frac{\partial_{x_1x_1}\bar{\rho}}{\bar{\rho}} + \sigma_x^2 Y(t)\bar{a}(t,X(t),Y(t))\frac{\partial_{x_2x_2}\bar{\rho}}{\bar{\rho}} + \sigma_y^2 Y(t)\bar{a}(t,X(t),Y(t))\frac{\partial_{y_1y_1}\bar{\rho}}{\bar{\rho}}\\
&+ \sigma_y^2 Y(t)\bar{a}(t,X(t),Y(t))\frac{\partial_{y_2y_2}\bar{\rho}}{\bar{\rho}} + \mathcal{O}\left(\|(\sigma_x,\sigma_y)\|^3\right)\\
= &\,2\sigma_y^2\left[-\partial_y\bar{a}(t,X(t),Y(t)) + \bar{a}(t,X(t),Y(t))\frac{\partial_{y_1}\bar{\rho}}{2\bar{\rho}} + \bar{a}(t,X(t),Y(t))\frac{\partial_{y_2}\bar{\rho}}{2\bar{\rho}}\right] + \mathcal{O}\left(\|(\sigma_x,\sigma_y)\|^3\right)\\
= &\,2\sigma_y^2\left[-\partial_y\bar{a}(t,X(t),Y(t)) + \bar{a}(t,X(t),Y(t))\frac{\partial_{y_1}\bar{\rho}}{\bar{\rho}}\right] + \mathcal{O}\left(\|(\sigma_x,\sigma_y)\|^3\right).
\end{aligned}
$$

We therefore recover (2.2.20)-(2.2.21), noticing that $\frac{\partial_{x_1}\bar{\rho}}{\bar{\rho}}$ can be replaced in the equations above by $\frac{\partial_x\hat{\rho}[t,X(t),Y(t)](t,X(t),Y(t)}{\hat{\rho}[t,X(t),Y(t)](t,X(t),Y(t)}$, and similarly $\frac{\partial_{y_1}\bar{\rho}}{\bar{\rho}}$ can be replaced in the equations above by $\frac{\partial_y\hat{\rho}[t,X(t),Y(t)](t,X(t),Y(t)}{\hat{\rho}[t,X(t),Y(t)](t,X(t),Y(t)}$.

CHAPTER 3

# Chapter 3: Modeling Phenotypic Structure and Plasticity under Climate Shifts in a Tree Population

**Abstract**

This study investigates the evolutionary dynamics of a tree population focusing on two phenotypic traits: the breeding values of daily seed production and the threshold temperature for dormancy, which determines the plastic trait of dormancy timing. These phenological traits are critical for understanding how trees adapt to rapid environmental change. Using a macroscopic model describing the mean traits dynamics of a structured population model, we explore the evolutionary trajectories of theses traits and analyse their adaptive responses to temperature and precipitation shifts. By simulating these scenarios, the study reveals that phenotypic plasticity in dormancy and absence of intrinsic mortality can hinder adaptation to new climatic conditions, emphasizing the importance of amplitude of environmental shifts in the adaptation process. The results underscore the role of co-evolution in enhancing adaptive capacities, providing insights into the resilience of tree populations facing rapid climate change.

## 3.1 Introduction

Phenotypic plasticity is a fundamental concept in biology that refers to the ability of a single genotype to produce different phenotypes in response to varying environmental conditions (Scheiner 1993). Unlike traits determined solely by genetic factors, phenotypic plasticity allows organisms to adapt to changing environmental signals throughout their development or lifespan. This phenomenon is observed across a wide range of taxa, including plants, animals, and microorganisms (Bradshaw 1965).

Plasticity can manifest in diverse traits such as morphology, physiology, behavior, and life history strategies. Various biotic and abiotic factors, including environmental, chemical, social, or hormonal cues, can induce phenotypic plasticity (Turcotte and Levine 2016). Phenology, which studies the timing of developmental events like bud burst and flowering, is a critical factor in determining the geographic range of tree species. Phenological traits, which determine the timing of various phases in a plant's life cycle—such as bud burst, flowering, fruiting, and leaf fall—are highly plastic. This plasticity allows plants to adapt flexibly to changing environmental conditions, including variations in temperature, precipitation, and day length. The plasticity of phenological traits enables plants to optimize their growth and reproductive success in response to fluctuating climates, thereby enhancing their ability to survive and thrive in diverse environments. This adaptability is crucial for coping with the impacts of climate change, as shifts in phenology can influence ecological interactions, such as plant-pollinator relationships and competition among species. The phenology or temporal control of the life cycle is presumed to provide adaptive strategies to avoid harsh environments for seedling establishment or seed development (Schwartz et al. 2003). This insight is crucial for assessing the impacts of global warming on plant distributions and the spread of invasive species (Chuine and Beaubien 2001).

Phenological plasticity is hence an important mechanism that may allow populations to cope with environmental threat. For instance, several studies have examined the evolutionary strategies of seed dormancy in response to environmental factors such as temperature and precipitation. For instance, (Penfield and MacGregor 2017) discussed the broad mechanisms of seed dormancy and germination regulation, emphasizing the significant impact of temperature on these processes. This work highlights the adaptive nature of dormancy as a response to environmental conditions. Additionally, phenotypic plasticity and adaptive evolution play significant roles in advancing the flowering phenology of plants in response to climate change. A study found strong directional selection favoring earlier flowering in

contemporary environments, indicating that these two mechanisms help plants adjust their reproductive timing to cope with changing climatic conditions (J. T. Anderson et al. 2012). Moreover, research on the impact of climate change on the phenology of vernal herb species in temperate forests showed that elevated temperatures advanced the timing of flowering events, while decreased precipitation accelerated the end of the flowering period, resulting in a shortened flowering season (Nam and Kim 2020). The impact of rising temperatures on flowering time demonstrated significant variations in flowering dates with lower-latitude populations exhibiting greater plasticity in warmer conditions compared to higher-latitude populations (Richardson et al. 2017).
However, while phenotypic plasticity can facilitate short-term adaptation, genetic adaptation might be necessary for long-term persistence (Gratani 2014). Indeed, a study showed that phenological plasticity will not help all species adapt to climate change (Duputié et al. 2015).

Two key aspects of the phenology of trees are seed production and dormancy, both of which are highly dependent on external conditions and are crucial for tree survival. While dormancy has attracted considerable interest in the scientific community, the interplay between dormancy and the number of daily seeds produced is still poorly understood. It is essential to investigate their adaptive capacities and interactions under severe environmental perturbations. For instance, a study showed that seed dormancy and germination are highly diverse and adaptive traits influenced by ecological and environmental factors. It highlights the evolutionary significance of these traits, showing how they have developed in response to various environmental pressures and have contributed to the survival and distribution of plant species across different biogeographical regions (C. C. Baskin and J. M. Baskin 1998). Research indicates that precipitation patterns can shape seed dormancy strategies across different geographic regions. For instance, in seasonally moist tropical forests, species exhibit a range of dormancy mechanisms that correlate with the timing of rainfall. This alignment ensures that germination occurs during favorable conditions, maximizing seedling survival and growth (Condit, Hubbell, and Foster 1996; Dalling, Swaine, and Garwood 1997). Moreover, studies on evolutionary trade-offs in dormancy phenology have explored how plants balance reproductive timing with environmental constraints. For example, the 'physiological constraints hypothesis' suggests that dormancy phenology occurs at transitions between favorable and unfavorable conditions, such as shifts in precipitation. This timing helps plants optimize reproductive success and resource use, particularly in environments with seasonal water availability (Condit, Hubbell, and Foster 1996).

Moreover, the interplay between seed dormancy and size as adaptive responses to varying environmental conditions has been explored, showing that when only dormancy evolves, it faces counter-selection with temperature shifts accelerating this process. However, the co-evolution of both traits results in reduced variations but faster evolution, especially in response to temperature shifts. Dormancy is counter-selected due to stable dynamics, while small seeds are favored due to the trade-off between size and number (Y. Liu et al. 2017). Studies have shown that temperature and water supply are critical drivers of seed dormancy and germination, with climate change altering these environmental cues and potentially affecting the initiation and break of dormancy (Walck et al. 2011).

Given the concerning threat of climate change, it is increasingly crucial to elucidate whether and how species will be affected and adapt to new environmental conditions. Specifically, given the high life expectancy of trees and the increasing rate of environmental change, these populations are likely to encounter several extreme events, increasing the risk of maladaptation or extinction.

In this work, we will consider the evolutionary dynamics of the mean number of seeds produced and temperature dormancy of a tree population derived from a mechanistic model that depends on temperature and precipitation variations considering threshold traits. The concept of threshold traits is well established in quantitative genetics, but the properties of threshold traits in phenotypic plasticity compared to continuously distributed traits are less commonly considered. Threshold traits often operate on a latent liability scale rather than being directly observable phenotypes (Reid and Acker 2022).In this work, the phenotypic traits under study are the breeding values for the daily number of seeds produced and the threshold temperature for dormancy, above which tree individuals become dormant and cease to die and reproduce. The latter trait represents the latent trait determining the dormancy timing of the trees, which is considered a plastic trait.

We will explore the evolutionary dynamics of these two traits using a macroscopic model derived from chapter 2. This model describes the mean traits of a structured population of trees. Our analysis will begin by investigating the steady-states of the system under constant environmental conditions. Subsequently, we will examine the adaptation of these phenotypic traits separately and then together in response to a temperature shift, a precipitation shift, and a combination of both. This investigation will consider the pre-shift steady-states as the initial conditions for the new environment assuming that the population is at its equilibrium when the shifts occur. This allow to determine if and how the traits will adapt to the new environment and elucidate the roles of phenotypic plasticity and co-evolution.

## 3.2 Models and methods

We describe the evolutionary dynamics of the mean traits within a tree population, as derived from an integrodifferential model (Chapter 2). This model represents two key variables: the daily number of seeds produced $x$ and the critical temperature $y$ above which the population becomes dormant, ceasing both reproduction and mortality. We assume that $x$ seeds are produced exclusively by mature individuals when water is available and the population is active, which occurs when the temperature remains below $y$. Conversely, individuals die at a rate proportional to the temperature when water is lacking and the population is not in a state of dormancy. To capture the dynamics of the mean traits of the population, denoted as $X$ and $Y$, we employed the following ordinary differential equations (ODEs), which were derived from the original model describing population dynamics:

$$\frac{d}{dt}\begin{pmatrix} X \\ Y \end{pmatrix} = \begin{pmatrix} 2\sigma_X^2 \\ 2\sigma_Y^2 \end{pmatrix} \begin{pmatrix} -\partial_x a(t,X(t),Y(t)) + a(t,X(t),Y(t))\frac{\partial_{x_1}\rho}{\rho} + \frac{a(t,X(t),Y(t))}{2X(t)} \\ -\partial_y a(t,X(t),Y(t)) + a(t,X(t),Y(t))\frac{\partial_{y_1}\rho}{\rho} \end{pmatrix} \tag{3.2.1}$$

Where the parameters $\sigma_X^2$ and $\sigma_Y^2$ denote the phenotypic variances of traits $X$ and $Y$ , respectively. The mortality functions $a$ is the average death rate proportional to the temperature during the period where the water is lacking while the individuals remain active over a season. The mortality function is defined as:

$$a(t,x,y) = \int_0^1 \gamma T^\circ(t,s)\phi_{plast}(s,y)\,(1-\phi_{water}(s,x))\,ds$$

Here, $\phi_{plast}$ indicates whether individuals are dormant based on their trait $Y$ at time $s \in [0,1]$, and is given by:

$$\phi^{plast}(t,s,y) = e^{-\beta\int_0^s 1_{T^\circ(t,\sigma)>y}\,d\sigma}$$

Similarly, $\phi_{water}$ indicates the availability of water for individuals with trait $X$ at the time $s \in [0,1]$, and is defined as :

$$\phi^{water}(t,s,x) = \begin{cases} 1 \text{ if } s \geq s_0 \text{ and } (1+\alpha x_+)(s-s_0) + \beta\int_{s_0}^s (T^\circ(t,\tau))_+\,d\tau \leq P(t), \\ 0 \text{ otherwise.} \end{cases}$$

Where $P(t)$ represents the precipitations over the year $t \in \mathbb{R}_+$ and $T^\circ(t,s)$ denotes the temperature variation at time $s \in [0,1]$ during the year $t \in \mathbb{R}_+$. Climate change is incorporated into the model through these two functions, by assuming either an increase in temperature over time, a decrease in precipitation, or changes in both.

The function $\rho$ represents the preferential mating and is defined by :

$$\rho(t,x_1,x_2,y_1,y_2) = \int_0^1 \phi_{plast}(s,y_1)\phi_{plast}(s,y_2)\phi_{water}(s,x_1)\phi_{water}(s,x_2)\,ds$$

The two first terms in the equations of the system 3.2.1 correspond to the fitness gradient of the two traits. The second terms are related to the preferential mating hypothesis from the original model (chapter 2). The last term in the equation of $X$ results from the control of the population size, assumed to be constant.

Moreover, we make the following time-scale separation assumptions to tally with biological characteristics of tree populations and also simplify our analysis :

- **Intrinsic Mortality:** We show that intrinsic mortality can be neglected, as it only allows for very slow evolution. However, evolution occurs much more rapidly if mortality only induced by water scarcity accelerates generational turnover. The primary notion here is that intrinsic mortality causes a slow adaptation of trees towards their optimal traits, but this process is too gradual to be significant. With a very high life expectancy, adaptation principle mainly relies on maladaptation to environmental conditions.

- **Abrupt Climatic Changes:** Given the high life expectancy of trees, climate change is perceived as a sudden shift. We simplify this to an abrupt transition from one climatic condition (to which the population was initially adapted) to another, characterized by higher temperatures, lower precipitation, or both. In practical terms, this involves considering initial values for $X(0)$ and $Y(0)$ that are optimal (on the "line of optimality") for past climatic conditions but become suboptimal for $t \geq 0$.

## 3.3 Numerical methods

In this section, we detail the methods used to obtain the numerical results for analyzing the evolutionary dynamics of seed production and dormancy temperature. This study was conducted in two main steps: first, the initialization of steady-states under constant environmental conditions, and second, the introduction of a perturbation as a climate change effect.

For the first step, the analysis was divided into three subsections. The first subsection examined the evolution of the number of seeds $X$ alone with a fixed dormancy temperature $Y$ considered as a parameter. The second subsection reversed this scenario, focusing on the evolution of dormancy temperature with a fixed daily number of seeds produced. The final subsection explored the co-evolution of both traits.

To analyze the evolution of seed production under stable environmental conditions with a fixed dormancy temperature, we simulated the system described by equation 3.4.1 using a phenotypic variance $\sigma_X^2 = 1$ and arbitrarily choosing the parameter set $\alpha = 1, \beta = 1, \gamma = 2$. We assume that the reproduction season starts at the beginning of the year to simplify the analysis. This assumption was made because the start of the reproduction season is not the primary focus of this study. We defined the annual temperature variations by :

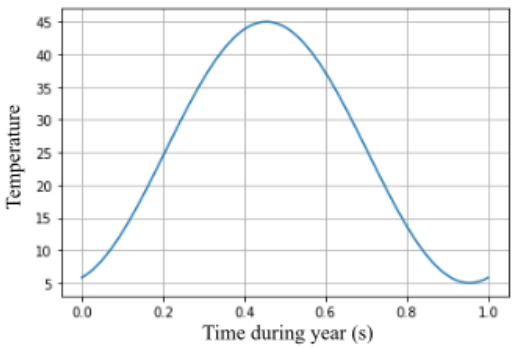



Fig. S1: Annual temperature variation

The functions appearing in the dynamical equation of $X$ 3.4.1 are defined as follows :

Let $S(x)$ be the moment at which water runs out for the production or $x$ seeds, which according to the function $\phi_{water}$ means :

$$(1+\alpha x)(S(x)-s_0)+\beta\int_{s_0}^{S(x)} T^\circ(\tau)_+\,d\tau = P_{max},$$

then we derive with respect to $x$,

$$\alpha(S(x)-s_0)+(1+\alpha x)S'(x)+\beta S'(x)T^\circ(S(x))_+ = 0,$$

that is $S'(x) = -\frac{\alpha(S(x)-s_0)}{1+\alpha x+\beta T^\circ(S(x))}$.

Therefore we have the variation of the mortality function with respect to $x$,

$$\begin{aligned}\partial_x a(x) &= \int_0^1 \phi^{plast}(s,Y)\gamma T^\circ(s)\left(1-\partial_x\phi^{water}(s,x)\right)ds\\ &= -\phi^{plast}(S(x),Y)\gamma T^\circ(S(x))S'(x)\\ &= \phi^{plast}(S(x),Y)\gamma T^\circ(S(x))\frac{\alpha(S(x)-s_0)}{1+\alpha x+\beta T^\circ(S(x))},\end{aligned}$$

And similarly, the variation in the preferential mating function with the respect to the trait of one parent, but given the asymmetry of the function $\rho$, we see only the partial derivative of the first vaiable $x_1$ :

$$\begin{aligned}\partial_{x_1}\rho(x_1,x_2) &= \int_0^1 \partial_{x_1}\phi^{water}(s,x_1)\phi^{water}(s,x_2)\phi^{plast}(s,Y)\,ds\\ &= \frac{\alpha(S(x_1)-s_0)}{1+\alpha x_1+\beta T^\circ(S(x_1))}\phi^{water}(S(x_1),x_2)\phi^{plast}(S(x_1),y)\end{aligned}$$

We then considered two different fixed dormancy temperatures, $Y$ to observe their effects on the evolutionary outcome of seed production $X$. This approach assumes that the water supply is least abundant during the reproduction period when the temperature reaches $Y$ as it decreases throughout the year. The function of water availability $\phi_{water}$ at this moment for selected $Y$ values, in terms of the number of seeds produced, is illustrated as follows:

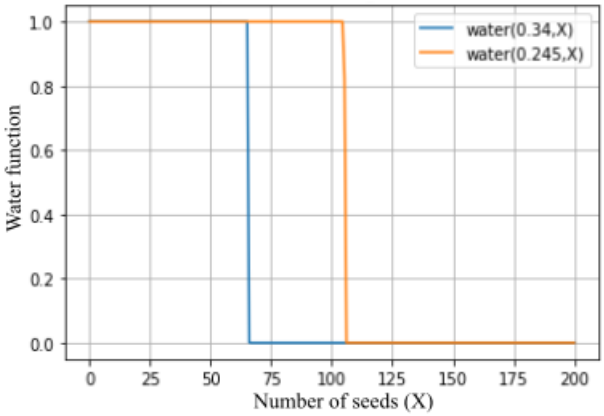



Fig. S2: Water availability function for the production of $X$ seeds at the moment when the temperature reaches $Y = 30$ (orange) and $Y = 40$ (blue).

Where we expect the value of $X$ at which the function drops to 0 to be the optimal strategy to maximize the seed production. We then simulated the the ODE system 3.4.1 for various initial conditions $\in [0, 200]$ for both selected temperature dormancy values $Y$ to obtain the trajectory of evolution of the number of seeds under a constant environment and identify the steady-state that will later be considered as the initial condition before the environmental perturbation.

Similarly, we repeat the analysis for the dynamical system 3.4.2 of evolution of dormancy temperature $Y$ with two different fixed numbers of seeds $X = 30$ and $X = 50$ and the following parameter set $\alpha = \beta = \gamma = 1$ and $P_{max} = 20$. The functions appearing in the equation 3.4.2 are defined as follow :

Let $S(y)$ the moment at which the yearly temperature reaches $y$ (moment at which the population with trait $y$ becomes dormant) :

$$T^{\circ}(S(y)) = y$$

We derive with respect to $y$

$$S'(y) = \frac{1}{\partial_s T^{\circ}(S(y))}$$

then the variation of the mortality function with respect to $y$ is,

$$\begin{aligned}\partial_y a(y) &= \int_0^1 \partial_y \phi^{plast}(s,y)\gamma T^\circ(s)\left(1-\phi^{water}(s,X)\right) ds \\ &= S'(y)\gamma T^\circ(S(y))(1-\phi^{water}(S(y),X)) \\ &= \gamma \frac{T^\circ(S(y))}{\partial_s T^\circ(S(y))}(1-\phi^{water}(S(y),X))\end{aligned}$$

$$\begin{aligned}\partial_{y_1}\rho(y_1,y_2) &= \int_0^1 \partial_{y_1}\phi^{plast}(s,y_1)\phi^{plast}(s,y_2)\phi^{water}(s,X)\, ds \\ &= \frac{1}{\partial_s T^\circ(S(y_1))}\phi^{plast}(S(y_1),y_2)\phi^{water}(S(y_1),X)\end{aligned}$$

Considering now the water availability function $\phi_{water}$ for the production of the selected $X$ numbers of seeds throughout the year $s \in [0,1]$ :

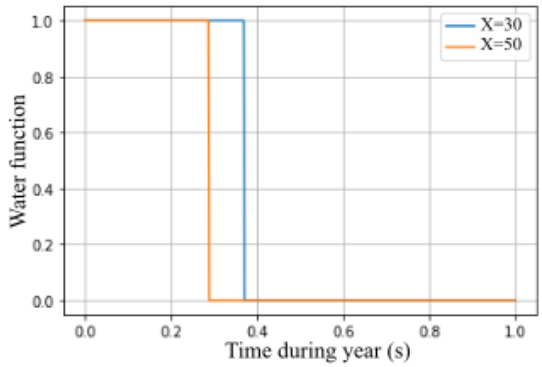



Fig. S3: Water availability function through the year $s \in [0,1]$ for the production of $X = 30$ seeds (blue) and $X = 50$ seeds (orange).

We simulated the ODE system 3.4.2 for various initial conditions for dormancy temperature $Y_0 \in [0,50]$ for both selected number of seeds values $X$ to obtain the trajectory of evolution of the dormancy temperature under constant environment. This allowed us to identify the steady-state, which we later used as the initial condition before introducing the environmental perturbation.

we repeated the analysis for the co-evolution scenario. We first determined the expected equilibria of the system 3.2.1 by finding the roots of the equations. Then, we used the Python function quiver to

illustrate the vector field of the system, initially setting $\sigma_X^2$ then $\sigma_Y^2$ to zeros. This approach helped us understand their influence on the evolutionary dynamics and specifically the direction of selective pressure on $X$ and $Y$.

For the second part of the study, we include climate change effects, specifically shifts in temperature and precipitation. In each scenario, we either increase the annual temperature, decrease the maximum water supply, or both, and then repeat the analysis to simulate how $X$ and $Y$ evolve under these new conditions. The initial conditions $(X_0, Y_0)$ are based on the previous steady-states identified earlier, assuming the traits were at their equilibrium before the shift. This method allows to explore the impact of each environmental change separately and together on the evolution of the number of seeds, dormancy temperature, and their combined evolution. We also consider different amplitudes of these shifts to study the traits' ability to adapt. Our focus is on the position of the new optimal strategy after the environmental change compared to the previous one, and whether the traits can evolve from the former steady-state to the new optimal strategy.

## 3.4 Results

### 3.4.1 Initialisation : Evolution of number of seeds $X$ and dormancy temperature $Y$ before a climate change

Before considering the effects of climate change, we first study the scenario where the annual environmental conditions remain constant, in order to obtain the steady-states of the number of seeds and temperature dormancy. We then consider these states as the initial conditions before introducing the environmental perturbations.

We divide this study into three parts. First, we examine the evolution of $X$ (the number of seeds) with a fixed dormancy temperature to assess its effects on seed production. Second, we investigate the opposite scenario, where the dormancy temperature $Y$ evolves while the number of seeds produced remains constant. Lastly, we focus on the co-evolution of $X$ and $Y$ to evaluate the resulting strategies.

#### 4.1.1 Effects of fixed dormancy temperature on the evolution of seed production

In this scenario, we examine the evolutionary dynamics of daily seed production $X$ over a season under constant environment, meaning constant annual temperature variation and precipitation quantity. Additionally, we treat the dormancy temperature $Y$ as a fixed parameter to evaluate its impact on

the evolutionary behavior of $X$ . In this context, the reproduction season is defined as ending when the temperature reaches $Y$ . We anticipate that the optimal strategy for seed production would be to maximize $X$ at this critical moment, which coincides with the point at which the water availability function $\phi_{water}$ transitions from 1 to 0.

In the context of no climate change, the model becomes as following :

$$\frac{d}{dt}X(t) = 2\sigma_X^2\left(-\partial_x a(X(t)) + a(X(t))\frac{\partial_{x_1}\rho(X(t),X(t))}{\rho(X(t),X(t))} + \frac{a(X(t))}{2X(t)}\right) \tag{3.4.1}$$

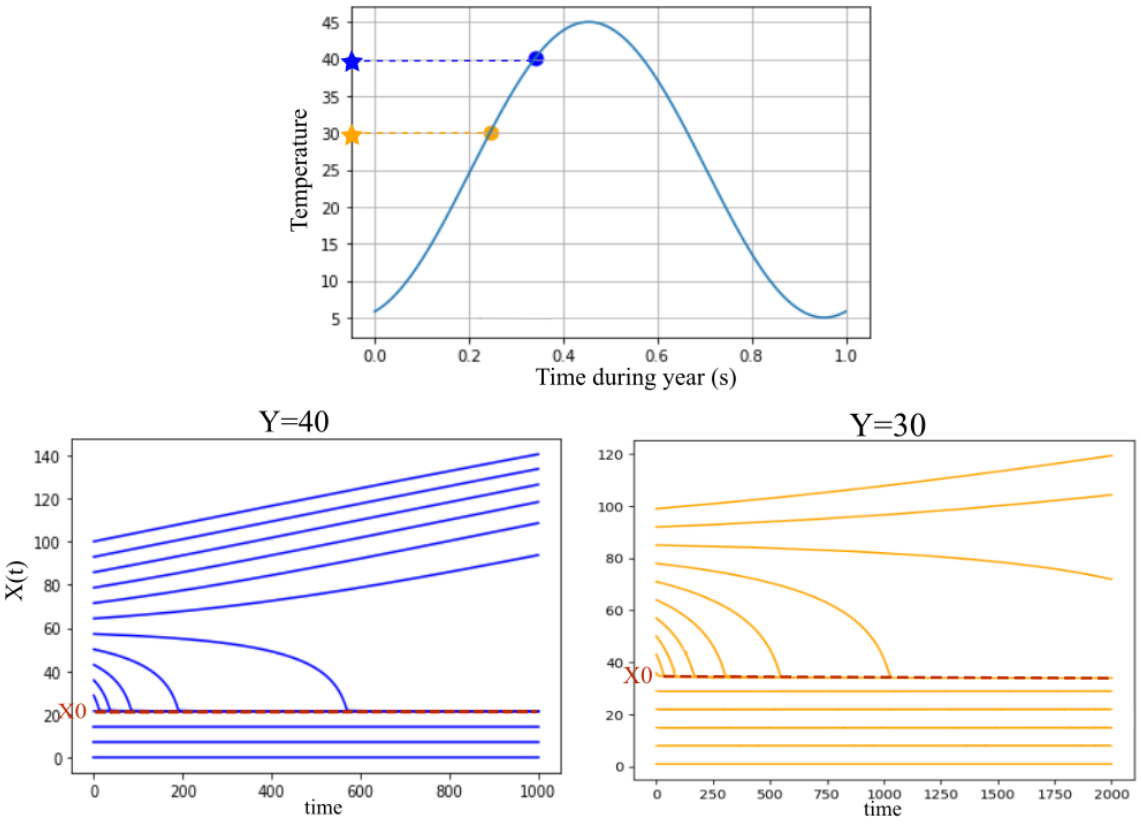



Fig. S1: **Evolution of number of seeds $X$ for 2 fixed temperature dormancy under constant environment**
**Top :** Temperature variations over a year (season) with two different chosen values for dormancy temperatures $Y = 30$ (orange dot) and $Y = 40$ (blue dot).
**Middle up:** Functions $\phi_{water}(s_{y_1}, X)$ and $\phi_{water}(s_{y_2}, X)$ for **Bottom :** Trajectories of the solution of 3.4.1 for different initial conditions for **left :** $Y = 40$ and **right :** $Y = 30$. The dotted lines represent the steady-states, denoted $X_0$, that we will consider later as an initial condition before the climate change perturbations.
*Parameters* : $\alpha = 3$, $\beta = 1$, $\gamma = 2$, $P_m = 30$, $T_m = 25$ and $s_0 = 0$.

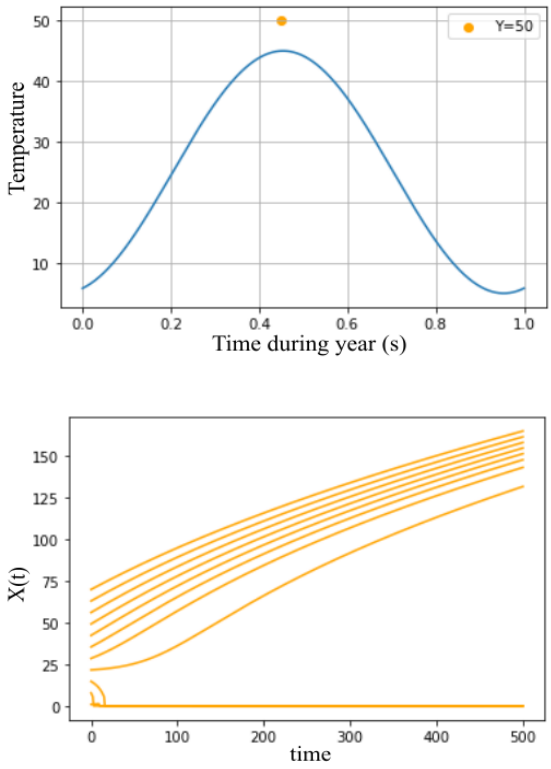



Fig. S2: **Evolution of number of seeds $X$ for a fixed temperature dormancy higher than the annual maximal temperature (no dormancy) under constant environment**
**Top :** Temperature variations over a year (season) with a chosen values for dormancy temperatures $Y = 50$ (orange dot) .
**Middle up:** Functions $\phi_{water}(s_{y_1}, X)$ and $\phi_{water}(s_{y_2}, X)$ for **Bottom :** Trajectories of the solution of 3.4.1 for different initial conditions for $Y = 50$.
*Parameters* : $\alpha = 3$, $\beta = 1$, $\gamma = 2$, $P_m = 30$, $T_m = 25$ and $s_0 = 0$.

Based on our findings illustrated in the preceding results from Fig. S2, we note that when the evolution of seed production occurs within the context of a fixed temperature dormancy, the scenario effectively transitions to one where the point at which the temperature reaches $Y$ represents the end of the year (or reproduction season). Within this framework, the outcomes indicate the emergence of three distinct evolutionary strategies governing seed production dynamics within tree populations : When the initial trait is below the threshold $X_0$ where water availability is constant, thereby preventing population mortality, no discernible selection pressure is exerted, and the number of seeds remains static at its initial value.

Conversely, when the initial condition exceeds this threshold and extends up to a certain limit, an alternative strategy emerges where the trait evolves towards that critical threshold. This critical threshold represents the maximum attainable number of seeds that can be produced while avoiding mortality until reaching the dormancy temperature $Y$. This strategy involves producing seeds at an optimized, moderate rate, ensuring a balance between seed production and resource consumption. This leads to sustainable reproduction over a longer period.

In contrast, when the initial trait overcomes another elevated threshold, an additional, unstable strategy manifests where the number of seeds keeps increasing. This strategy involves producing a large number of seeds within a condensed timeframe, resulting in the swift depletion of accessible resources. Under such circumstances, the prospect of long-term survival becomes uncertain, given the inherent initial high seed production requiring intense and fast water consumption. The strategy aims at maximizing the number of seeds, known as evolutio of semelparity, recognizing mortality as an inevitable outcome.

Moreover, in the specific case where the selected dormancy temperature exceeds the annual maximum temperature (as shown in Fig. S3), the population remains active throughout the year, rendering plasticity inconsequential. Under these conditions, the optimal strategy for seed production shifts to maximizing the number of seeds produced at the end of the year when water availability is at its lowest. However, it is observed that this optimal number of seeds can be very small or nearly zero. Consequently, the alternative strategy of uncontrolled increase of seed production becomes favored across a wide range of initial conditions. This scenario implies that mortality becomes almost inevitable, prompting individuals to invest all their resources at once by producing the maximum possible number of seeds.

### 4.1.2 Effects of fixed seed production on the evolution of the dormancy temperature

In this section, we examine the inverse scenario previously explored. We analyze the evolutionary dynamics of the dormancy temperature, denoted as $Y$, over a seasonal period with constant annual temperature and precipitation. Additionally, we consider the daily seed production, denoted as $X$, as a fixed parameter. Our focus is on the evolutionary outcomes of dormancy. Given the constant seed production rate, the point at which water availability becomes insufficient to produce $X$ seeds is predetermined. We expect that $Y$ will evolve towards the temperature at that critical moment to optimize reproduction and minimize mortality.

The model describing the evolutionary dynamics of $Y$ becomes:

$$\frac{d}{dt}Y(t) = 2\sigma_Y^2 \left( -\partial_x a(X(t)) + a(Y(t)) \frac{\partial_{x_1}\rho(X(t), X(t))}{\rho(X(t), X(t))} \right) \tag{3.4.2}$$

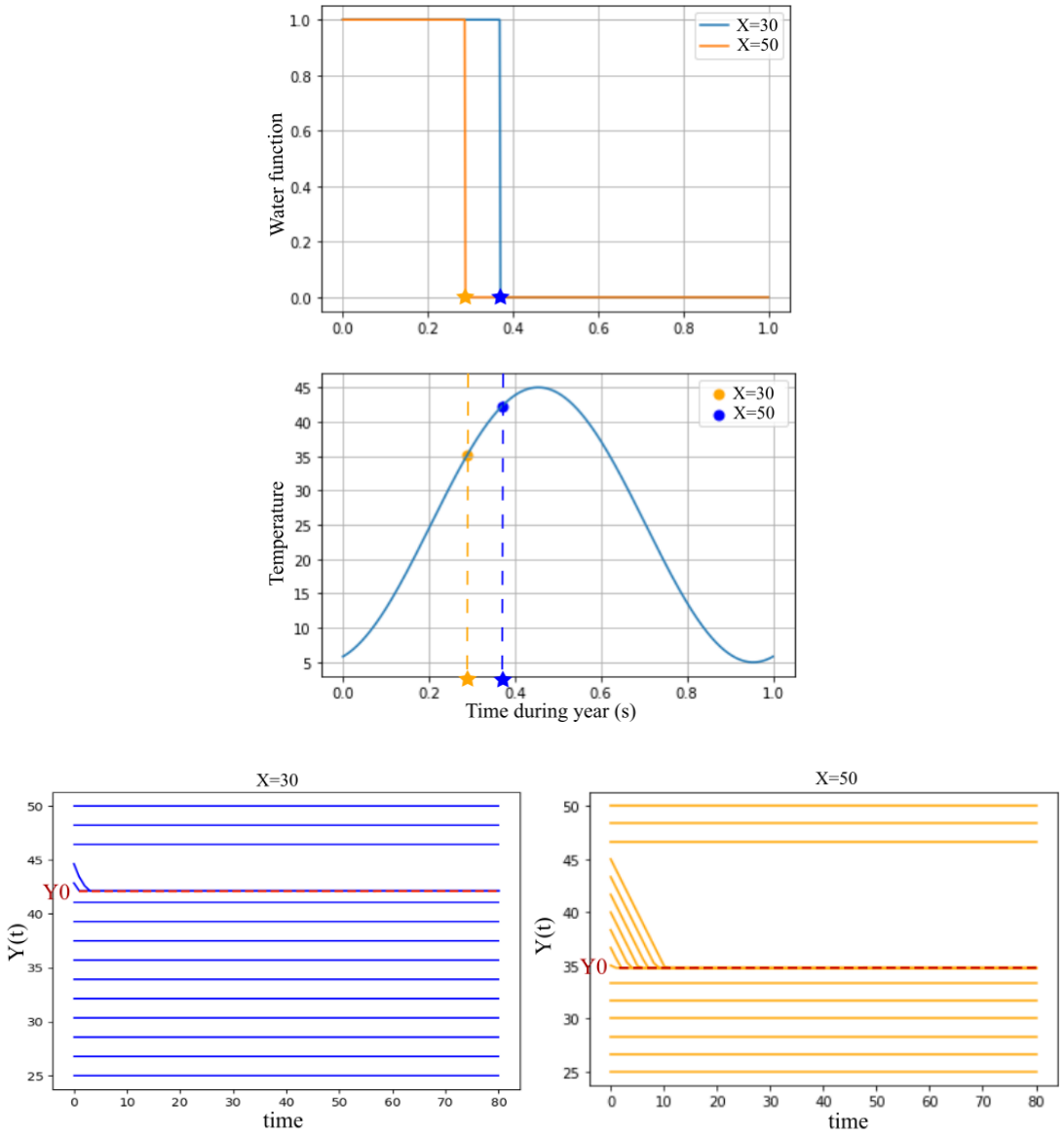



Fig. S3: **Evolution of temperature dormancy $Y$ for 2 fixed numbers of seeds under constant environment**

**Top :** Function $\phi_{water}(s,x)$ of water availability for the production of two fixed number of seeds $X = 30$ (blue) and $X = 50$ (orange) throughout the year $s \in [0,1]$.

**Middle :** Temperature variations along the year $s \in [0,1]$ with the time at which the water runs out for the production of $X = 30$ seeds (blue star) (respectively $X = 50$ (orange star)) and the corresponding temperature (blue dot) (respectively (orange dot)).

**Bottom :** Trajectories of the solution of 3.4.2 for different initial conditions for **left :** $X = 30$ and **right :** $X = 50$. The dotted lines represent the steady-state, denoted as $Y_0$, that we will consider later as an initial conditions before climate change perturbations.

*Parameters* : $\alpha = 1$, $\beta = 1$, $\gamma = 1$, $P_m = 20$, $T_m = 25$, $s_0 = 0$ and $x = 50$.

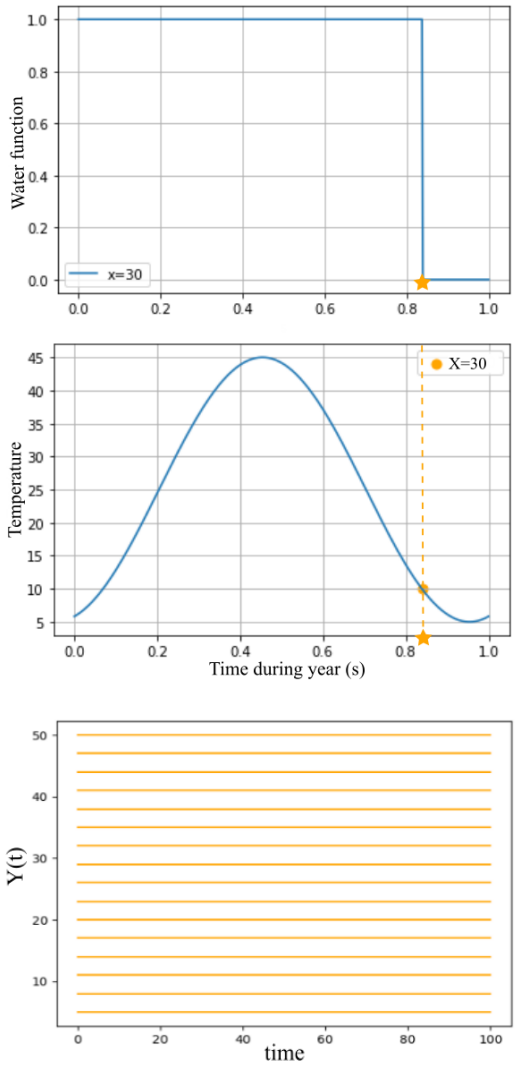



Fig. S4: **Evolution of temperature dormancy $Y$ with a fixed number of seeds under constant environment**
**Top :** Function $\phi_{water}(s,x)$ of water availability for the production of the fixed number of seeds $X$ throughout the year $s \in [0,1]$.
**Middle :** Temperature variations along the year $s \in [0,1]$ with the time at which the water runs out for the production of $X$ seeds (orange star) and the corresponding temperature (orange dot).
**Bottom :** Trajectories of the solution of 3.4.2 for different initial conditions.
*Parameters* : $\alpha = 1$, $\beta = 1$, $\gamma = 2$, $P_m = 50$, $T_m = 25$ and $s_0 = 0$.

Based on our results presented in Figures S4 and S5 regarding the evolution of dormancy temperature $Y$ with a fixed daily number of seeds produced $X$, we observe an evolutionary dynamic analogous to the reversed scenario analyzed in the previous section concerning seed evolution. In this context, three distinct behaviors emerge depending on the initial condition. When the number of seeds $X$ is fixed, their production is feasible only up to a specific point when water becomes scarce. At this critical juncture, the temperature reaches a particular threshold value. If the initial dormancy temperature $Y_0$ is below this threshold, there is no selective pressure on the dormancy temperature since water remains consistently available.

Conversely, if the initial condition lies between this threshold and the annual maximum temperature, $Y$ evolves towards the critical threshold temperature. This evolution represents an optimal strategy, maximizing seed production $X$ for as long as possible before water scarcity ensues, thereby ensuring optimal productivity and avoiding mortality.

However, we observe that if the initial condition exceeds the maximum yearly temperature, no selection occurs, and $Y$ remains at its initial value. This nuanced dynamic highlights the importance of initial conditions in determining the evolutionary trajectory and the optimal strategies for seed production in response to environmental constraints.

Furthermore, as observed in Fig.S5, when water depletion occurs after the temperature has reached its annual maximum, there is an absence of selective pressure on the dormancy temperature $Y$. This phenomenon can be attributed to the fact that the critical period for selection, which hinges on the availability of water, has already passed by the time the maximum temperature is attained. Consequently, any evolutionary adaptations that might have occurred to optimize seed production under fluctuating water availability are rendered moot. The temperature threshold necessary for driving the evolution of dormancy traits is no longer a factor, leading to a stabilization of $Y$ at its initial value.

### 4.1.3 Outcomes from the co-evolution of seed production and dormancy temperature

After exploring evolutionary outcomes of the daily number of seeds produced $X$ and dormancy temperature $Y$ separately, we now go back to our original 2D model in the context of fixed environment conditions, thereby excluding the effects of global climate change :

$$\frac{d}{dt}\begin{pmatrix} X \\ Y \end{pmatrix} = \begin{pmatrix} 2\sigma_X^2 \\ 2\sigma_Y^2 \end{pmatrix} \begin{pmatrix} -\partial_x a(X(t),Y(t)) + a(X(t),Y(t))\frac{\partial_{x_1}\rho(X(t),X(t),Y(t),Y(t))}{\rho(X(t),X(t),Y(t),Y(t))} + \frac{a(X(t),Y(t))}{2X(t)} \\ -\partial_y a(X(t),Y(t)) + a(X(t),Y(t))\frac{\partial_{y_1}\rho(X(t),X(t),Y(t),Y(t))}{\rho(X(t),X(t),Y(t),Y(t))} \end{pmatrix} \tag{3.4.3}$$

From our results on the co-evolution of $X$ and $Y$ Fig. S5, we observe the emergence of two distinct evolutionary strategies primarily driven by the respective rates of evolution of $X$ and $Y$, determined by their phenotypic variances $\sigma_X^2$ and $\sigma_Y^2$. When $\sigma_Y$ is negligible, the evolutionary dynamics of $X$ for moderate initial conditions tend towards a stable equilibrium with smaller values along the optimal

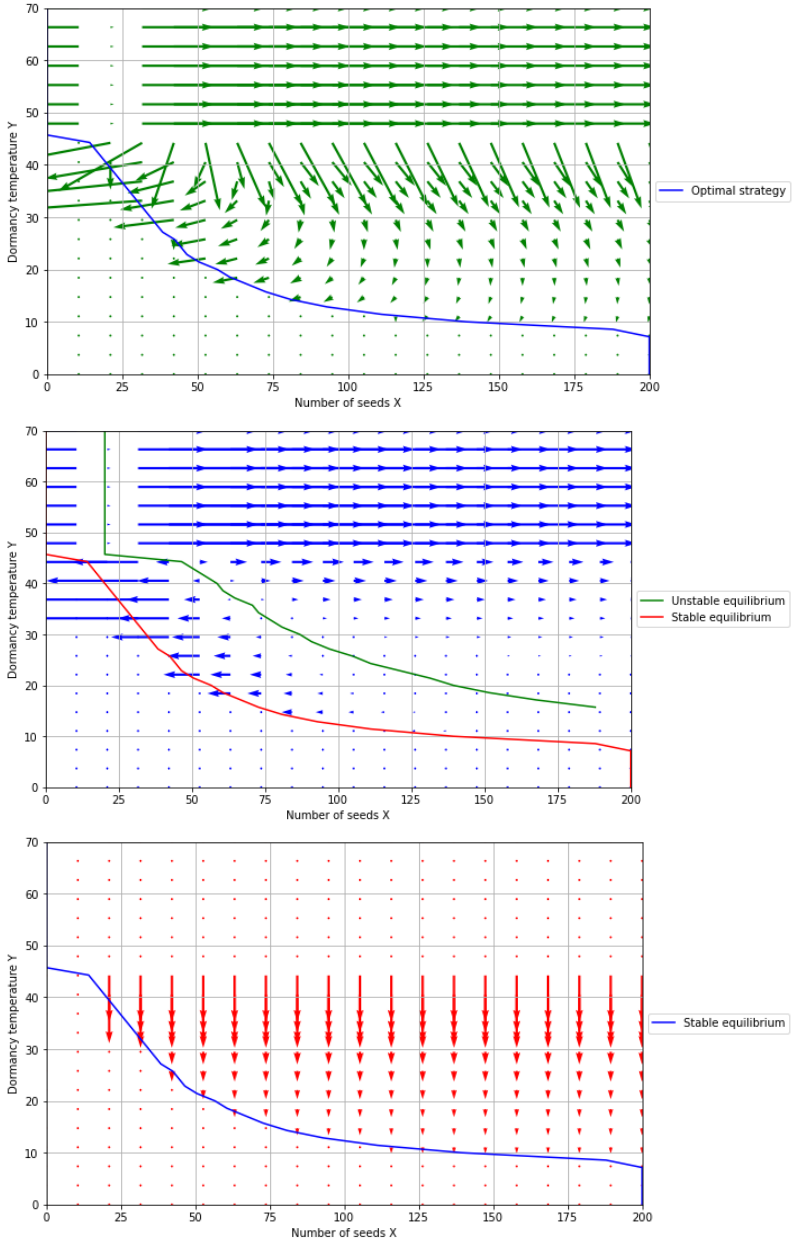



Fig. S5: **Co-evolution of number of seeds $X$ and temperature dormancy $Y$ under constant environment**

**Top :** Vector field of $(X,Y)$ from the full model 3.2.1 where the blue line is the expected steady-state representing the optimal strategy. We will later consider these values as initial conditions before the climate change perturbations.

**Middle :** Vector field of $X$ for each fixed dormancy trait $Y$ ($\sigma_Y^2$ of order 0). The red curve represents the optimal number of seeds $X$ to be produced at the moment where temperature reaches $Y$. The green curve represents the unstable equilibria

**Bottom :** Vector field of $Y$ for each fixed number of seeds trait $X$. The red curve is the expected steady-state which represents the temperature at the moment where water runs out to produce each number $X$ of seeds.

*Parameters* : $\alpha = 3$, $\beta = 1$, $\gamma = 2$, $P_m = 30$, $T_m = 25$, $s_0 = 0$ and $\sigma_X^2 = 20$ $\sigma_Y^2 = 1$.

strategy line. Conversely, when $\sigma_X$ is negligible, the evolution of $Y$ primarily leads to lower dormancy temperatures.

Although the respective evolutionary rates of $X$ and $Y$ do not affect the expected optimal strategy, they significantly influence the co-evolutionary process, reflecting the two possible extreme outcomes. Firstly, one evolutionary strategy occurs when the dynamics of $X$ dominate. This involves producing fewer seeds over a longer period, favoring smaller values of $X$ and larger values of $Y$, essentially evolving towards the left side of the optimal strategy curve (Figure S5). This strategy allows the population to maintain a steady reproductive output over an extended period, which can be advantageous in environments where resources are moderately available and stable over time.
Conversely, when the selective pressure on $Y$ dominates, the second strategy involves increasing the number of seeds produced $X$ while decreasing the dormancy temperature $Y$. This approach results in the population producing a large number of seeds over a shorter period and entering dormancy earlier in the season. This strategy can be particularly beneficial in environments where resources are abundant for short periods but become scarce quickly, necessitating rapid reproduction followed by dormancy to survive adverse conditions.

These results were obtained while neglecting intrinsic mortality and where trees individuals died only in the absence of water supply. This prevented the evolution towards the optimal strategy when the initial conditions $(X_0, Y_0)$ were too small, because the population doesn't experience any pressure at these values. However, when adding an intrinsic mortality parameter, it can enhance evolution towards the stable equilibrium from everywhere, as observed in Fig. S1.

### 3.4.2 Evolution of number of seeds $X$ and dormancy temperature $Y$ with climate change : Temperature shift

#### 4.2.1 Effects of temperature shift on the evolution of the number of seeds $X$ and dormancy temperature $Y$ separately

In this section, our aim is to integrate the influence of climate change, particularly temperature shifts, on the evolutionary dynamics of the number of seeds $X$. Given the long lifespan of trees, climate change is considered an abrupt perturbation. We revisit the evolutionary model (3.4.1) for the number of seeds $X$ in conjunction with fixed-temperature dormancy $Y$ to analyze the impact of a sudden

temperature rise on seed production, assuming the system is in equilibrium before the temperature shift. Under the assumption of fixed temperature dormancy, an increase in annual temperature would lead to an earlier onset of dormancy as the temperature reaches the threshold $Y$ sooner.

Next, we explore the impact of an abrupt rise in annual temperature on the evolution of dormancy temperature $Y$ under constant precipitation conditions and a fixed daily seed production $X$. An increase in temperature results in a higher critical temperature at which water becomes scarce. Since temperature has minimal effect on the total water quantity, the point at which it becomes unfeasible to produce $X$ seeds remains roughly constant. Therefore, the optimal dormancy strategy would adjust to align with the new elevated critical temperature.

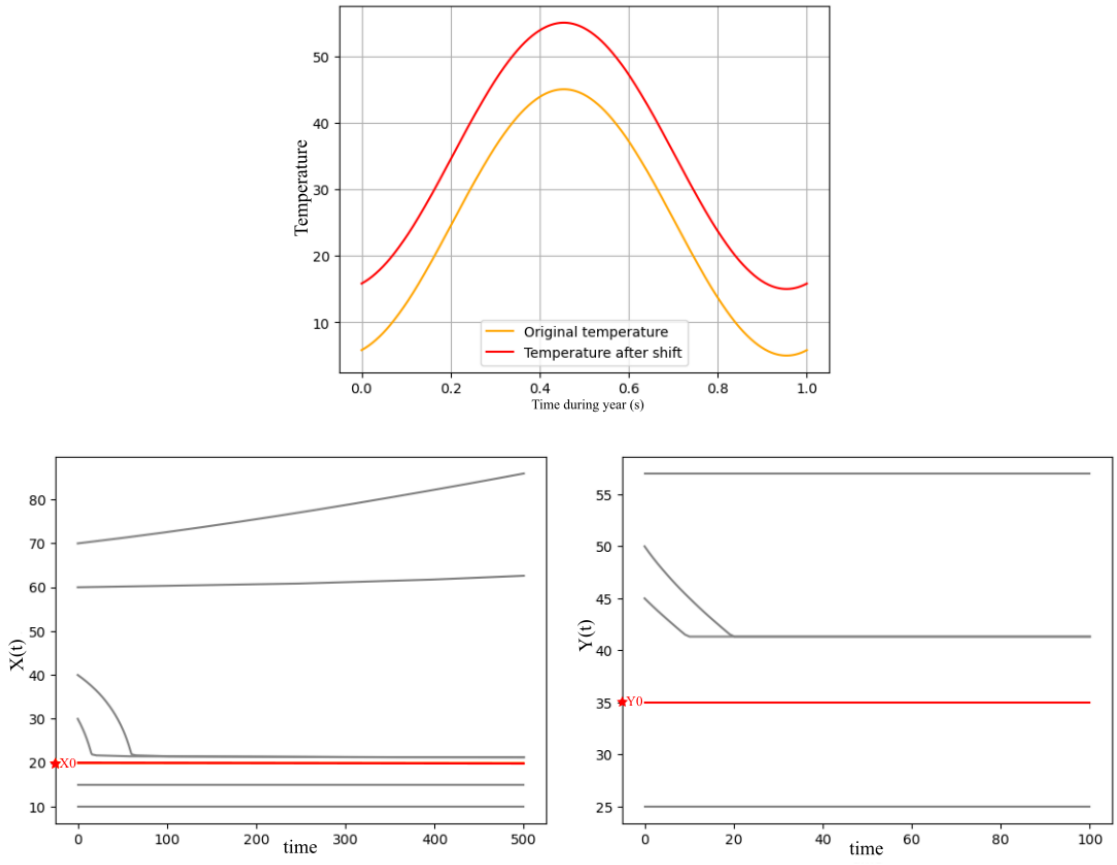



Fig. S6: **Top :** Yearly temperature variations before (orange) and after an abrupt shift increase by 10° (red).
**Bottom : Left :** Trajectories of number of seeds $X$ over time with a fixed dormancy temperature, after the temperature shift from different initial values, where is highlighted (red line) the pre-shift steady-state under former conditions which represents the initial condition of interest $X_0 \approx 20$. *Parameters* : $\alpha = 3$, $\beta = 1$, $\gamma = 2$ and $P_{max} = 30$
**Right :** Trajectories of the dormancy temperature $Y$ over time with a fixed number of seeds, after the temperature shift from different initial values, where highlighted (red line) is the pre-shift steady-state under former conditions which represents the initial condition of interest $Y_0 \approx 35$. *Parameters* : $\alpha = 1$, $\beta = 1$, $\gamma = 1$, $P_{max} = 20$ and $x = 50$.

The findings illustrated in Figure S6 indicate that following an increase in annual temperature

subsequent to the attainment of a unique stable equilibrium by the population, as discussed in the preceding section unaffected by climate change, the subsequent optimal number of seeds $X$ – defined as the maximum achievable seed production under the prevailing water conditions when temperature reaches the dormancy threshold $Y$ – exhibits an increase compared to its prior state. The earlier onset of dormancy, facilitated by the temperature rise, corresponds to a period of augmented water availability, thereby enabling the potential for increased seed production albeit within a reduced temporal window. Nevertheless, as elucidated in the earlier analysis, in scenarios where initial values ($X_0$) are inferior to the optimal level, no selective pressures are operative. Given our assumption that the initial seed quantity ($X_0$) coincides with the former equilibrium (optimal $X$), which is lower than the new optimal value, no adjustments occur, thereby maintaining the seed production at the pre-existing steady state. This observation underscores that in the absence of intrinsic mortality, where mortality is solely influenced by water scarcity, a shift in annual temperature fails to influence the evolutionary trajectory of seed quantity $X$, which is unable to align with the new optimal strategy.

These results also indicate that an abrupt increase in temperature does not alter the evolutionary dynamics of dormancy temperature $Y$ when the number of seeds produced $X$ is fixed, similar to the observations made regarding the evolution of $X$ alone. We assume that $Y$ initially resides at its former unique stable equilibrium, representing the optimal dormancy strategy of the critical temperature reached when water availability becomes insufficient to produce $X$ seeds. This threshold is evidently lower than the new critical temperature following the shift. Consequently, as discussed in the previous section concerning conditions without climate change, no selection pressure is exerted.

### 4.2.2 Effects of temperature shift on the co-evolution $X$ and $Y$

Finally, we consider the full model for co-evolution of number of seeds $X$ and dormancy temperature $Y$ after a temperature shift. As we have seen in the previous sections of the impact of a temperature shift on the evolution of $X$ and $Y$ separately, an increase in the temperature leads to the augmentation of the respective optimal strategies. However, when considering the initial conditions as the steady-states from the pre-shift environment, the traits fail to adapt.

As anticipated, considering the non-adaptability of $X$ and $Y$ to the post-temperature shift environment when initially starting from former steady-states, the same dynamics are observed in the co-evolution scenario. The two traits lack selective pressure when residing at the old environmental equilibrium in

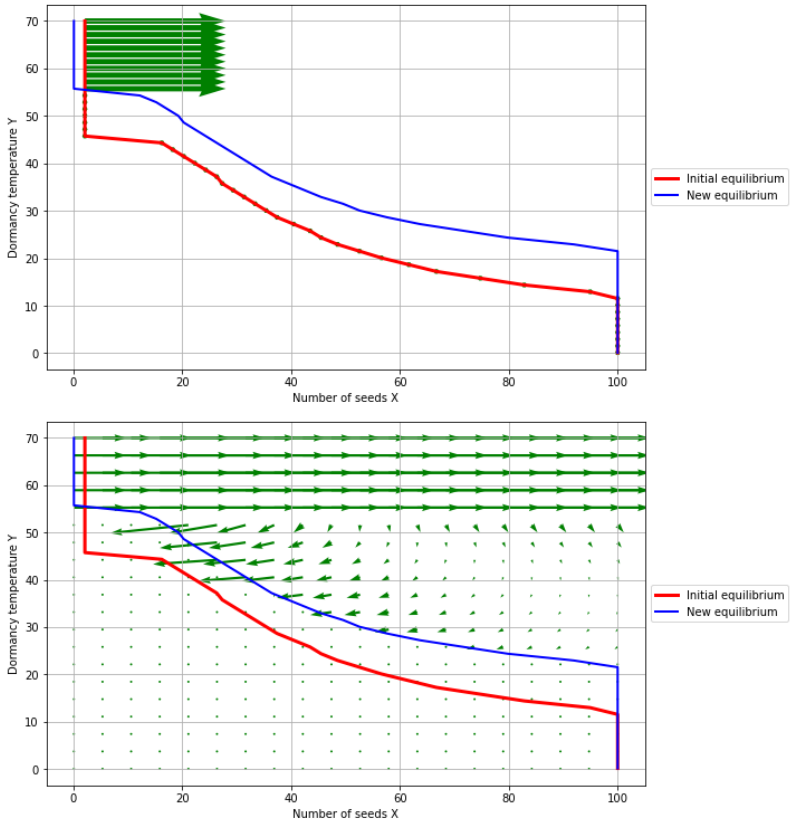



Fig. S7: **Co-evolution of number of seeds $X$ and dormancy temperature $Y$ after a temperature shift**
**Top :** Vector field for the co-evolution of $X$ and $Y$ after a temperature shift where the initial conditions considered correspond to the original steady states before the shift (red line). The new equilibria after the shift is represented in blue line.
**Bottom :** Same scenario with evolutionary trajectories from many initial values.
*Parameters* : $\alpha = 3$, $\beta = 1$, $\gamma = 2$, $P_{max} = 30$ and $y = 40$.

the absence of mortality pressure. Consequently, they do not evolve towards the new optimal strategy following the temperature shift.

### 3.4.3 Evolution of number of seeds $X$ and dormancy temperature $Y$ with climate change : Precipitation shift

#### 4.3.1 Effects of precipitation shift on the evolution of number of seeds $X$ with a fixed temperature dormancy

After examining the impact of a sudden temperature increase, we focus now on investigating the effects of an abrupt precipitation shift as a consequence of climate change. We begin by analyzing a model that considers the evolution of $X$ with a fixed dormancy temperature $Y$ and annual temperature variations. In a similar manner, an abrupt reduction in precipitation (water availability) is introduced once the number of seeds has reached the previous stable equilibrium, which then serves as the new initial condition. This equilibrium represents the optimal strategy for producing the maximum number of seeds when the temperature reaches $Y$. With the reduction in water availability, the new optimal value of $X$ at that time decreases.

Our findings from S8, show how the evolution of number of seeds may adapt to abrupt changes in precipitation but not to abrupt shifts in temperature. However, as observed in the studied examples S8, the magnitude of the shift in precipitation can significantly influence the evolutionary outcome regarding the number of seeds. As previously mentioned, the optimal post-shift strategy results in a smaller number of seeds than before. Consequently, when the magnitude of the shift is not excessively large, $X$ may adapt to the new environment and evolve toward a new stable equilibrium. Conversely, if the shift is too substantial, the previous steady-state (new initial point) may be excessively large, surpassing the critical point $X$ (unstable equilibrium). Beyond this critical point, the number of seeds may increase uncontrollably, indicating a transition where the trees occupy a different life cycle. This scenario aligns with a previously discussed strategy known as semelparity.

#### 4.3.2 Effects of precipitation shift on the evolution of dormancy temperature $Y$ with a fixed seed production

In this section, we examine the impact of alterations in precipitation, as a consequence of climate change, on the evolution of dormancy temperature $Y$, assuming a constant number of seed production $X$ and annual temperature variations. We further assume that the population initially resides at its

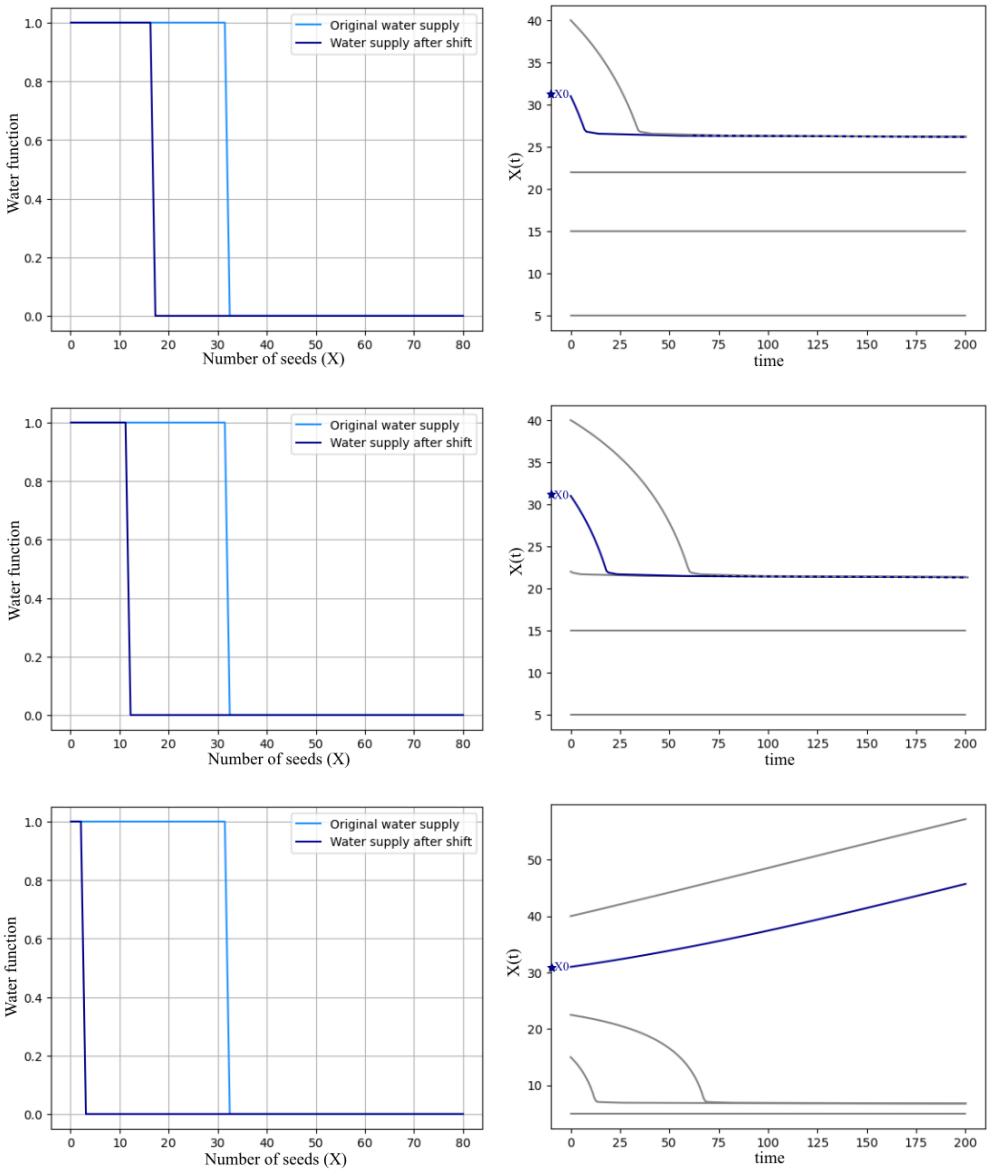



Fig. S8: **Evolution of number of seeds $X$ after a precipitation shift of different magnitudes with the pre-shift steady-state $X_0$**
**Left :** Functions of water availability $\phi_{water}$ at the moment when the temperature reaches the fixed dormancy temperature $Y = 40°$ for different values of $X$, before and after a precipitation shift where the water supply drops by **top :** $P_{max} = 30 \to 25$, **middle :** $P_{max} = 30 \to 20$ and **bottom :** $P_{max} = 40 \to 15$ leading to the possibility of producing fewer seeds.
**Right :** Trajectories of $X$ over time following a precipitation shift of varying magnitudes. The initial conditions, marked by blue stars, are derived from the pre-shift steady states. After the shift, the number of seeds evolves towards a new stable equilibrium when the magnitude of the shift is moderate (top and middle). However, when the magnitude is excessively high (bottom), the number of seeds increases uncontrollably.
*Parameters* : $\alpha = 3$, $\beta = 1$, $\gamma = 2$ and $Y = 40$.

unique stable equilibrium, which corresponds to the temperature at the point when water becomes insufficient for the production of $X$ seeds. A precipitation shift is then introduced as an extreme event, altering the prevailing environmental conditions. A sudden reduction in water availability would result in an earlier depletion of water resources necessary for the daily production of $X$ seeds. Consequently, the new optimal strategy for dormancy $Y$, would involve initiating dormancy at a lower temperature to minimize mortality. This adaptation reflects the new post-shift conditions, where resource scarcity impacts the seeds at an earlier developmental stage. This strategic shift is critical for ensuring the survival and continued propagation of the population under altered climatic conditions.

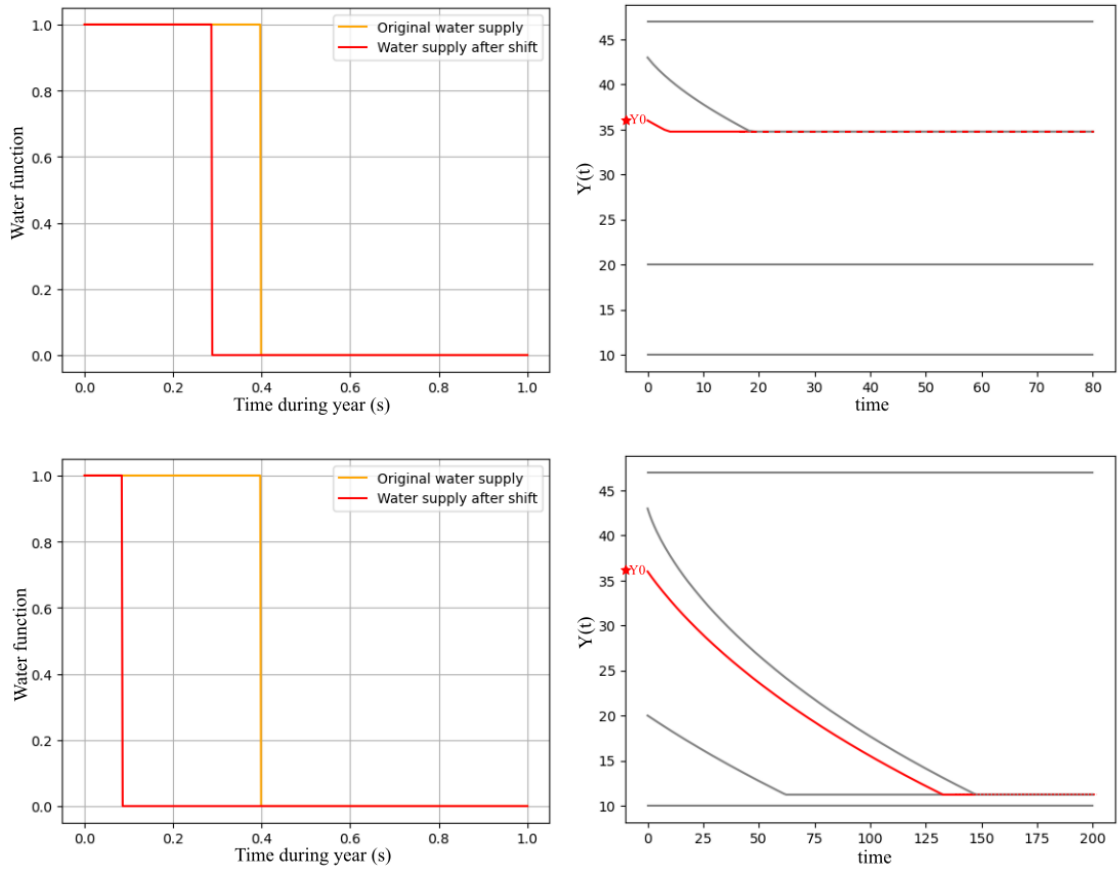



Fig. S9: **Evolution of dormancy temperature $Y$ after a precipitation shift of different magnitudes with the pre-shift steady-states $Y_0$**
**Top :** Functions of water availability $\phi_{water}$ for the production of a fixed number of seeds $X$ over the year, before and after a precipitation shift for two varying amplitudes (left and right).
**Bottom :** Trajectories of $Y$ over time following a precipitation shift of varying amplitudes. The initial conditions, marked by orange stars, are derived from the pre-shift steady states. After the shift, the dormancy temperature evolves towards a new stable equilibrium, corresponding to the temperature at which water becomes insufficient to produce $X$ seeds under the new conditions.
*Parameters :* $\alpha = 1$, $\beta = 1$, $\gamma = 1$ and $X = 50$

Our findings, as illustrated in Fig S9, demonstrate the capacity of temperature dormancy $Y$ to adapt to shifts in precipitation. This adaptation involves evolving towards the new optimal strategy, thereby reducing the reproductive period. While this adjustment may result in a decreased seed production

during a given season, it plays a crucial role in avoiding mortality under the severe conditions that follow a precipitation shift. By adopting this strategy, the population potentially avoids the risk of extinction despite the challenging environmental changes.

### 4.3.3 Effects of precipitation shift on the co-evolution of $X$ and $Y$

In the previous sections, we observed that a sudden shift in precipitation can independently influence the evolutionary trajectories of seed production $X$ and dormancy temperature $Y$. We now investigate the combined evolutionary outcomes of these traits in response to such climate change effects, considering their co-evolution when both traits are initially at their stable equilibrium, as identified in the results from Fig **??**. Such a perturbation would reduce the optimal strategies for both $X$ and $Y$, similar to the effects observed when each trait evolves separately. However, the magnitude of the precipitation shift could significantly impact the expected adaptations to the new equilibrium, potentially leading to varied evolutionary responses depending on the severity of the environmental change.

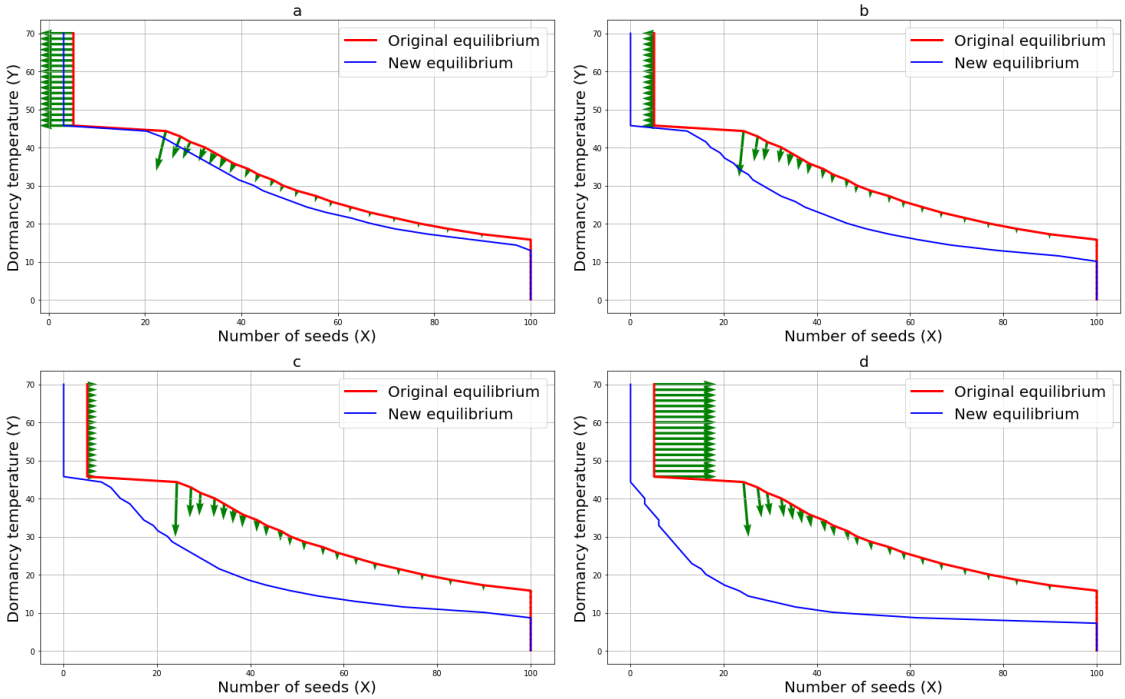



Fig. S10: **Co-evolution of number of seeds $X$ and dormancy temperature $Y$ after a precipitation shift of different magnitudes from the pre-shift steady-states** $(X_0, Y_0)$
Vector fields of the co-evolution of $X$ and $Y$ after a sudden precipitation shift when they are initially at their former steady-state (red line) for 4 different amplitudes of precipitation decrease. The blue lines represent the respective new expected stables strategies after the shift. a) $P_{max} = 40 \to 35$. b) $P_{max} = 40 \to 25$. c) $P_{max} = 40 \to 20$. d) $P_{max} = 40 \to 10$.
*Parameters :* $\alpha = 3$, $\beta = 1$, $\gamma = 2$, $\sigma_X^2 = 1$, $\sigma_Y^2 = 1$ and $s_0 = 0$.

Previous studies have highlighted the significant interplay between dormancy, seedling fitness, and water availability. For example, a research investigated how the timing of seed production affects seedling fitness in tropical live oak within Costa Rican dry forests. The study found that trees exhibited higher fitness when seeds were produced, dispersed, and germinated late in the wet season, underscoring the influence of precipitation patterns on shaping seed production and dormancy traits (Center et al. 2016).

Our results in Fig S10 corroborate these findings, demonstrating that when a precipitation shift is relatively small, the co-evolution of $X$ (seed production) and $Y$ (dormancy temperature) primarily results in earlier dormancy, with selective pressure having minimal impact on the number of seeds produced. This indicates that following an abrupt but slight reduction in water availability, a population can still adjust its reproductive period, thereby reducing the cost associated with seed production, similar to the evolutionary response observed when only $X$ evolved. It appears that the strategy of producing a smaller but comparable number of seeds within a shorter period is favored after a precipitation shift. This outcome aligns with the results discussed in the section on the evolution of dormancy temperature $Y$ alone.

However, our results indicate that as the magnitude of the precipitation shift increases, we observe a return to a scenario where the number of seeds begins to rise, leading to a change in the life cycle, as discussed in the section on the evolution of $X$ alone. In this context, if the initial conditions (former steady-state) of $Y$ are below the yearly maximum temperature and thus permit selective pressure on the dormancy temperature, the evolution of $Y$ to lower values prevents the number of seeds from increasing uncontrollably. This adaptive response ensures that $X$ adjusts to the new optimal strategy, albeit towards higher values, thereby stabilizing the population dynamics under the altered environmental conditions.

### 3.4.4 Evolution of number of seeds $X$ and dormancy temperature $Y$ under climate change : Temperature increase and precipitation decrease

In this section, we examine the simultaneous impact of sudden shifts in both temperature and precipitation on the co-evolution of seed production $X$ and dormancy temperature $Y$. Previous analyses have demonstrated that changes in precipitation exert a more substantial influence on the evolutionary trajectories of $X$ and $Y$. These traits have shown the potential to adapt to new conditions following a precipitation shift. Conversely, temperature shifts alone did not significantly affect the

evolutionary dynamics of $X$ and $Y$, allowing them to maintain their pre-shift strategies, which could result in maladaptation to the altered environment. By investigating the combined effects of both climatic factors, we aim to understand the complex interactions and potential adaptive responses of these traits under multifaceted environmental changes. This comprehensive analysis is essential for predicting how plant populations might cope with the synergistic impacts of climate change.

Our results indicate that the balance between precipitation and temperature shifts plays a crucial role in determining evolutionary outcomes. Specifically, the opposing effects of these perturbations on optimal strategies are noteworthy: an increase in temperature tends to favor higher optimal trait values, while a decrease in precipitation tends to favor lower optimal trait values. Thus, the combined effect of temperature and precipitation shifts on the co-evolution of $X$ and $Y$ depends on the relative amplitudes of these changes. If the temperature increase is more pronounced, it might prevent the selective pressure, whereas a more significant decrease in precipitation would push the traits towards lower values. The direction and extent of the post-shift optimal strategies will ultimately be determined by the interplay between these two opposing forces, highlighting the complexity of adaptive responses in the face of simultaneous climate change factors.

We observe in Fig. S11, first line, that a small shift in precipitation combined with a very small shift in temperature (Fig. S11 a) allows the adaptation of traits $X$ and $Y$ to the new optimal strategy across a wide range of values, provided that this new equilibrium is located below the initial strategy. However, when the temperature shift becomes too large (Fig. S11 b), the new strategy shifts above the former one, and the traits cease to evolve. In this scenario, only populations with an initial dormancy temperature higher than the new maximum yearly temperature experience an increase in the number of seeds $X$ (since the selection pressure no longer acts on $Y$). This is because the new optimal strategy is further from the initial condition, leading to an uncontrolled increase in seed production.

A similar behavior occurs in Fig. S11, second line, where a smaller increase in the magnitude of the temperature shift (from c to d in Fig. S11) still permits the adaptation of traits within a certain range. Additionally, we observe in Fig. S11, third line, that a slight increase in the temperature shift combined with a significant precipitation shift markedly affects the speed of evolution of $X$ and $Y$. Finally, when the magnitude of the precipitation shift is very high with a small temperature shift (Fig. S11 g), the effect of diminishing water supply dominates the dynamics. In this scenario, the number of seeds initially increases but is restrained by the evolution of $Y$ towards smaller values, guiding the traits towards the new optimal strategy, as already observed in the section of co-evolution

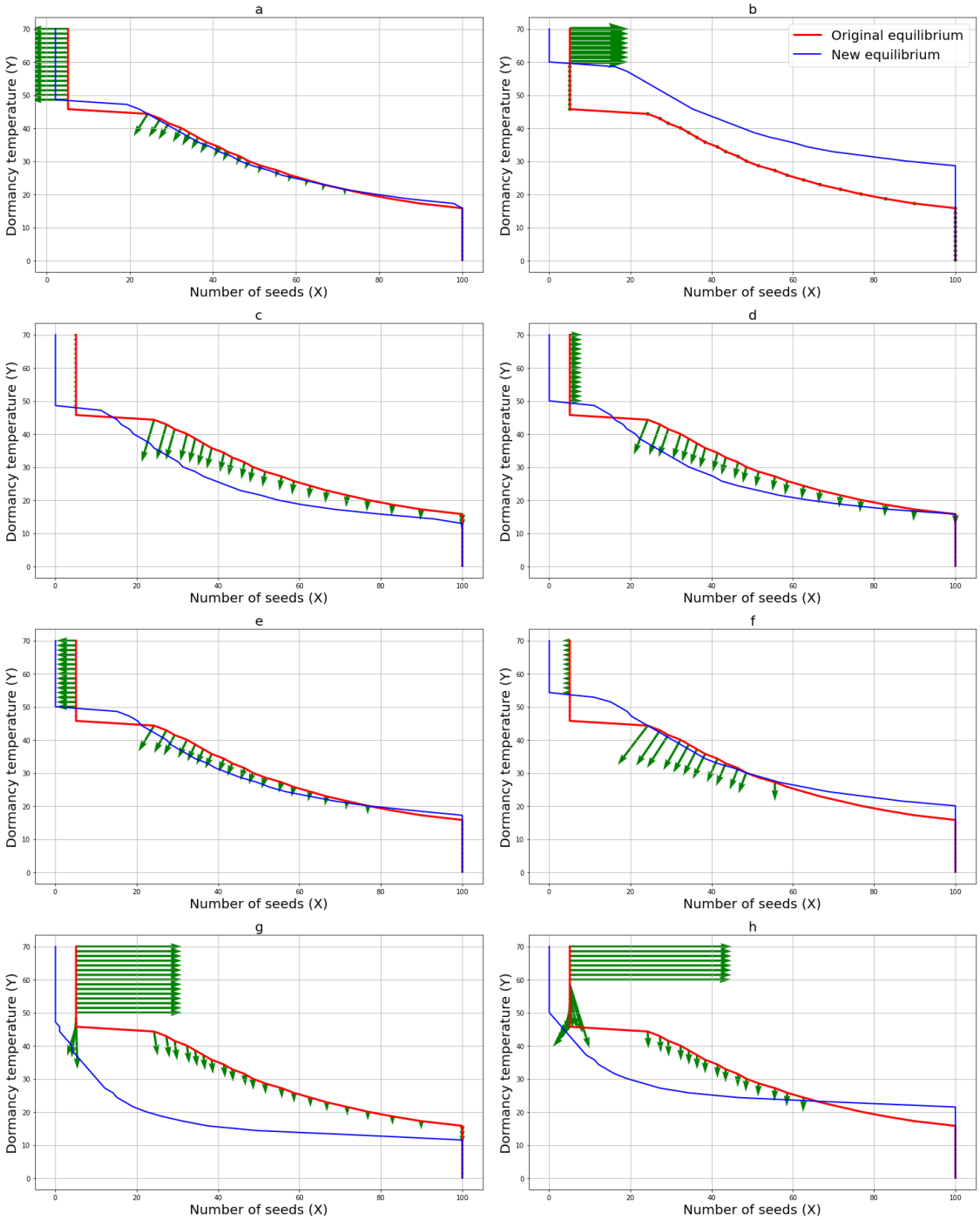



Fig. S11: **Co-evolution of number of seeds $X$ and dormancy temperature $Y$ after a temperature and precipitation shift of different magnitudes from the pre-shift steady-states** $(X_0, Y_0)$
Vector fields of $(X,Y)$ after a shift in both temperature and precipitation when starting from their former stable equilibrium (red line). The blue line represents the post-shift stable strategy.
The amplitude of the shift in precipitation is the same in both columns but increases from one line to another. Whereas the magnitude of the shift in temperature increases from the left to the right column. The extremes are **a)** low shift amplitudes in both perturbations and **h)** high shift amplitudes in both perturbations.

with only a precipitation shift. For a small range of high initial values $Y_0$, the past and new strategies are close, leading to a decrease in the number of seeds.

Interestingly, when both the temperature shift and the precipitation shift are very high (Fig. S11 h), a similar scenario occurs, except for high values of $X$, where the temperature shift becomes dominant, leading to a higher new equilibrium and preventing adaptation. Moreover, for initial dormancy temperature values between the past and new maximum annual temperatures, selection reduces $Y$ but can either increase or decrease the number of seeds depending on the distance between the two optimal strategies.

## 3.5 Discussion

| Scenario/Evolution | Evolution of $X$ only | Evolution of $Y$ only | Co-evolution of $X$ and $Y$ |
|---|---|---|---|
| Constant environment | 3 evolutionary outcomes:<br>-No evolution when $X_0$ too small<br>-Evolution towards optimum.<br>-Evolution towards high $X$. | 2 evolutionary outcomes:<br>-No evolution when $Y_0$ too small or above maximum temperature.<br>-Evolution towards optimum. | Evolution to 2 strategies:<br>- High seeds low dormancy.<br>-Low seeds high dormancy. |
| Temperature shift | No adaptation from former steady-state. | No adaptation from former steady-state. | No adaptation from former steady-state. |
| Precipitation shift | Adaptation to new optimum up to a certain amplitude then change of life cycle. | Always adapts to new optimum even when the shift is high. | Always adapts but to higher $X$ when shift is high. |
| Temperature and precipitation shift | — | — | Adaptation depends on the position of new optimum and balance between shifts. |

Table 3.1: Summary of evolutionary outcomes of number of seeds $X$ and dormancy temperaure $Y$ under different scenarios.

This study highlights the differential adaptability of seed production and dormancy temperature traits in response to shifts in precipitation and temperature, providing crucial insights into their evolutionary dynamics under climate change scenarios.

Our results demonstrate that both traits exhibit greater adaptability to changes in precipitation than to shifts in temperature. This disparity can be attributed to the plastic nature of dormancy, which prevents adaptation by inducing dormancy and thus preventing mortality and inhibiting further

evolutionary changes. There are studies indicating that the number of seeds produced by plants may not readily adapt to abrupt changes in climate, particularly temperature increases. For instance, authors discuss how climate change can potentially lead to a mismatch between seed production and environmental conditions, affecting seed dormancy, germination, and population dynamics, thereby limiting plant adaptation (Walck et al. 2011). Additionally, it was found that trees in semi-arid ecosystems show stronger responses to reduced precipitation than to increased temperature. Reduced precipitation delayed needle emergence, decreased photosynthesis, and induced morphological changes, suggesting a higher sensitivity to drought stress over atmospheric warming (Grossiord et al. 2017). The potential effects of climate change on plant phenology was also discussed in (Frank et al. 2017; Springate and Kover 2014), suggesting that rapid shifts in temperature may lead to maladaptation in plants, including mismatched dormancy periods.

The impact of shifts in precipitation on tree dormancy has been documented in several studies. Specifically, a study showed for instance, that young trees are more sensitive to water limitation than to temperature (Smithers and North 2020). Moreover, authors found that various stress factors, including changes in precipitation, lead to earlier dormancy dates across temperate deciduous forest communities (Xie, X. Wang, and Silander Jr 2015). Another study confirmed an evolutionary shift towards earlier flowering in response to drought (Hamann, Weis, and Franks 2018). Moreover, an investigation in plant communities in Australia, showed that climate shapes the length of flowering periods, leading to shorter durations in response to changes in precipitation patterns (Stephens et al. 2021).

The absence of intrinsic mortality in our model highlights an important aspect: without a mortality factor and with phenotypic plasticity in dormancy preventing reproduction, the traits do not experience strong selective pressure to adapt in many scenarios. This finding underscores the critical role mortality as a driving force in the adaptation of these traits. Fig. S1 show that with an additional intrinsic mortality, the traits are able to adapt to a temperature shift by evolving towards the new optimal strategy.

It is important to note that the plasticity considered in this study is not adaptive. Here the dormancy timing is fixed; meaning that whenever the temperature reaches the trait $Y$, all individuals with this trait become dormant. Adaptive plasticity may add flexibility with potentially allowing a proportion of individuals to keep reproducing, therefore enhancing adaptation. Indeed, a study discusses how

adaptive phenotypic plasticity enhances an organism's fitness in response to environmental changes, while non-adaptive plasticity does not confer such benefits. The authors discuss how adaptive plasticity can facilitate rapid adaptation by allowing organisms to cope with environmental variability (Ghalambor et al. 2007).

Precipitation shifts significantly influenced the evolutionary trajectories, with the amplitude of the shift being particularly crucial for the number of seeds produced. Indeed, a study examining seed germination and reproductive strategies in desert annuals suggests that seed production in these plants is more responsive to changes in precipitation, which directly affects water availability, while temperature shifts may not have a similarly immediate impact on seed number adaptation (Clauss and Venable 2000). Another study explored how desert annuals adapt their seed production strategies to variable precipitation. It suggests that the magnitude of precipitation shifts influences the extent to which seed production can adapt, with larger shifts presenting greater challenges for evolutionary adjustment (Mu et al. 2021). Even when it come to plastic traits, the effectiveness of plasticity depends on the rate and magnitude of environmental change. If changes occur too rapidly or are too extreme, plasticity alone may not suffice, and populations may face increased risk of extinction (Chevin, Lande, and Mace 2010).

When dormancy temperature co-evolves with seed production, it enhances the population's adaptability even under high amplitude precipitation shifts, proving beneficial overall. This co-evolution stabilizes population dynamics and improves resilience against environmental changes. This finding is consistent with previous studies that suggest the co-evolution of various traits can enhance adaptation to climate threats. For example, a study demonstrated how the co-evolution and adaptation of weed species, including dormancy and seed production traits, enable their survival under changing climatic conditions, such as shifts in precipitation and drought (Clements and V. L. Jones 2021). Another study examined the relationship between seed mass, fruit type, and precipitation, highlighting how the co-evolution of these traits facilitates adaptation to different climatic conditions (Yu et al. 2021).

Moreover, the co-evolution of seed production and dormancy temperature results in two extreme stable strategies, depending on their respective evolutionary rates. Selective pressure on dormancy tends to favor short reproduction periods with high daily seed production, while the evolution of seed number favors spreading seed production over a longer period by selecting for fewer seeds. The strategy involving producing a large number of seeds rapidly, typically in response to more favorable

conditions or during "mast" years, which are characterized by a high production of seeds has been documented on previous studies (Hodgson et al. 2020; Yousaf et al. 2016).
These two strategies are often discussed in the context of iteroparity (repeated reproduction) and semelparity (single, massive reproductive event). Iteroparous species, which produce fewer seeds continuously over time, can better cope with variable and unpredictable environments by spreading the risk and ensuring some reproductive success even in adverse conditions. In contrast, semelparous species put all their resources into one large reproductive event, which can be advantageous in stable environments where the timing of conditions is more predictable (Varpe and Ejsmond 2018).

However, the evolutionary outcomes span a spectrum between these extremes, influenced by the balance between selective pressures. A study highlighted that semelparity (one-time reproduction) and iteroparity (repeated reproduction) are not distinct, binary categories but exist on a continuum. Empirical data showed that many species exhibit a range of reproductive strategies between these two extremes, depending on environmental conditions and life-history traits. This study also demonstrated how different environmental pressures can shift species along the semelparity-iteroparity spectrum (W. Hughes 2015).

In scenarios where both temperature and precipitation shifts occur simultaneously, the dominant factor exerts the primary selective pressure. If the temperature increase is more pronounced, it might prevent adaptation by maintaining higher optimal trait values. Conversely, a significant decrease in precipitation pushes the traits towards lower values. The balance between these two factors ultimately determines the direction and extent of the evolutionary outcomes, illustrating the complexity of adaptive responses to multifaceted climate change effects.

Interestingly, our study suggests that the introduction of mortality could act as a catalyst, encouraging and stimulating adaptation. In natural settings, management practices such as controlled tree cutting could simulate intrinsic mortality, thereby forcing the population to adapt more to changing conditions. This approach could help mitigate the risk of maladaptation or extinction in tree populations facing severe environmental perturbations. For instance, weeds exhibit a remarkable capacity to adapt to human management strategies and climate change through various evolutionary mechanisms (Clements and V. L. Jones 2021).

In conclusion, the study underscores that while plastic traits such as dormancy can enable species to survive extreme events and harsh conditions, they can also hinder adaptation to new environments, especially if these new conditions persist over long periods. It also highlights the importance of considering both temperature and precipitation shifts and the co-evolution of multiple traits when evaluating the adaptive capacities of tree populations. The interplay between these factors, environmental shifts, and their respective magnitudes plays a crucial role in shaping evolutionary trajectories. Further research incorporating intrinsic mortality and other ecological interactions would provide deeper insights into the adaptive mechanisms of trees under climate change.

## 3.6 Appendix

### 3.6.1 Co-evolution of $X$ and $Y$ before and after a temperature shift with intrinsic mortality

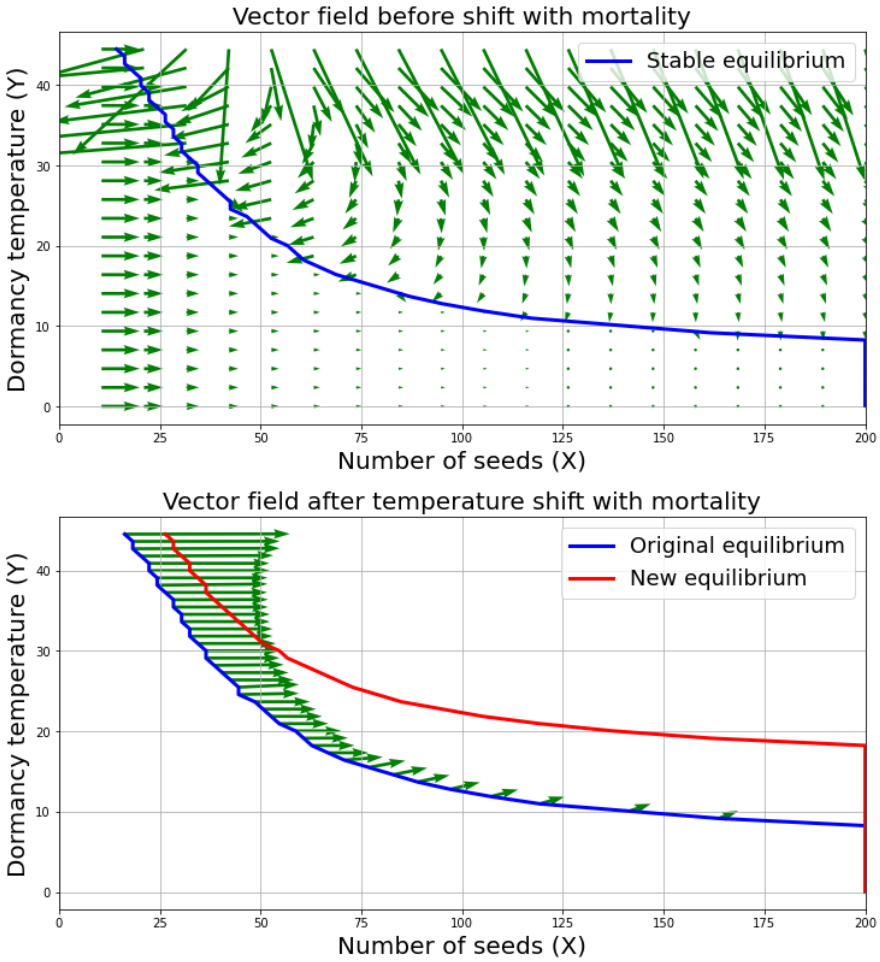



Fig. S1: **Top:** Vector field for co-evolution of number of seeds $X$ and dormancy temperature with an additional intrinsic mortality.
**Bottom:** Vector field after a temperature shift, from the initial values corresponding to the former steady-states (blue line). Red line represent the new optimal strategy (stable equilibrium) after the shift.
*Parameters:* $\alpha = 3$, $\beta = 1$, $\gamma = 2$, $\sigma_X^2 = 1$, $\sigma_Y^2 = 1$, $s_0 = 0$, *and* $m = 2$ *(intrinsic mortality).*

# Bibliography


Alfaro, Matthieu and Rémi Carles (2014). "Explicit solutions for replicator-mutator equations: extinction versus acceleration". In: *SIAM Journal on Applied Mathematics* 74.6, pp. 1919–1934.

Anderson, Jill T (2016). "Plant fitness in a rapidly changing world". In: *New Phytologist* 210.1, pp. 81–87.

Anderson, Jill T et al. (2012). "Phenotypic plasticity and adaptive evolution contribute to advancing flowering phenology in response to climate change". In: *Proceedings of the Royal Society B: Biological Sciences* 279.1743, pp. 3843–3852.

Anderson, Stefan (1990). "The relationship between seed dormancy, seed size and weediness, in Crepis tectorum (Asteraceae)". In: *Oecologia* 83, pp. 277–280.

Aspelmeier, Stella and Christoph Leuschner (2006). "Genotypic variation in drought response of silver birch (Betula pendula Roth): leaf and root morphology and carbon partitioning". In: *Trees* 20.1, pp. 42–52.

Baskin, Carol C and Jerry M Baskin (1998). *Seeds: ecology, biogeography, and, evolution of dormancy and germination*. Elsevier.

Bewley, J Derek, Kent Bradford, Henk Hilhorst, et al. (2012). *Seeds: physiology of development, germination and dormancy*. Springer Science & Business Media.

Bolley, François and JOSÉ A Carrillo (2007). "Tanaka theorem for inelastic Maxwell models". In: *Communications in mathematical physics* 276, pp. 287–314.

Bradshaw, Anthony D (1965). "Evolutionary significance of phenotypic plasticity in plants". In: *Advances in genetics* 13, pp. 115–155.

Calvez, Vincent, Thomas Lepoutre, and David Poyato (2024). "Ergodicity of the Fisher infinitesimal model with quadratic selection". In: *Nonlinear Analysis* 238, p. 113392.

Center, Alyson et al. (2016). "Seed production timing influences seedling fitness in the tropical live oak Quercus oleoides of Costa Rican dry forests". In: *American journal of botany* 103.8, pp. 1407–1419.

Champagnat, Nicolas and Sylvie Méléard (2007). “Invasion and adaptive evolution for individual-based spatially structured populations”. In: *Journal of Mathematical Biology* 55, pp. 147–188.

Chevin, Luis-Miguel, Sinéad Collins, and François Lefèvre (2013). “Phenotypic plasticity and evolutionary demographic responses to climate change: taking theory out to the field”. In: *Functional Ecology* 27.4, pp. 967–979.

Chevin, Luis-Miguel, Russell Lande, and Georgina M Mace (2010). “Adaptation, plasticity, and extinction in a changing environment: towards a predictive theory”. In: *PLoS biology* 8.4, e1000357.

Chuine, Isabelle and Elisabeth G Beaubien (2001). “Phenology is a major determinant of tree species range”. In: *Ecology Letters* 4.5, pp. 500–510.

Clauss, MJ and DL Venable (2000). “Seed germination in desert annuals: an empirical test of adaptive bet hedging”. In: *The American Naturalist* 155.2, pp. 168–186.

Clements, David R and Vanessa L Jones (2021). “Ten ways that weed evolution defies human management efforts amidst a changing climate”. In: *Agronomy* 11.2, p. 284.

Condit, Richard, Stephen P Hubbell, and Robin B Foster (1996). “Changes in tree species abundance in a neotropical forest: impact of climate change”. In: *Journal of tropical ecology* 12.2, pp. 231–256.

Constant, Théo et al. (2024). “Evolutionary trade-offs in dormancy phenology”. In: *Elife* 12, RP89644.

Dalling, JW, MD Swaine, and Nancy C Garwood (1997). “Soil seed bank community dynamics in seasonally moist lowland tropical forest, Panama”. In: *Journal of tropical ecology* 13.5, pp. 659–680.

Das, Adrian J, Nathan L Stephenson, and Kristin P Davis (2016). “Why do trees die? Characterizing the drivers of background tree mortality”. In: *Ecology* 97.10, pp. 2616–2627.

Dekens, Léonard (2022). “Evolutionary dynamics of complex traits in sexual populations in a heterogeneous environment: how normal?” In: *Journal of Mathematical Biology* 84.3, p. 15.

Dekens, Léonard, Sarah P Otto, and Vincent Calvez (2022). “The best of both worlds: combining population genetic and quantitative genetic models”. In: *Theoretical Population Biology* 148, pp. 49–75.

Desvillettes, Laurent et al. (2008). “On selection dynamics for continuous structured populations”. In: *Communications in Mathematical Sciences* 6.3, pp. 729–747.

Duputié, Anne et al. (2015). “Phenological plasticity will not help all species adapt to climate change”. In: *Global change biology* 21.8, pp. 3062–3073.

Fisher, RA (1930). “The genetical theory of natural selection.” In.

Flores, Bernardo M et al. (2024). “Critical transitions in the Amazon forest system”. In: *Nature* 626.7999, pp. 555–564.

Frank, Aline et al. (2017). “Risk of genetic maladaptation due to climate change in three major European tree species”. In: *Global Change Biology* 23.12, pp. 5358–5371.

Frouvelle, Amic and Cécile Taing (2023). “On the Fisher infinitesimal model without variability”. In: *arXiv preprint arXiv:2307.12735*.

Ghalambor, Cameron K et al. (2007). “Adaptive versus non-adaptive phenotypic plasticity and the potential for contemporary adaptation in new environments”. In: *Functional ecology* 21.3, pp. 394–407.

Gratani, Loretta (2014). “Plant phenotypic plasticity in response to environmental factors”. In: *Advances in botany* 2014.

Gremer, Jennifer R and D Lawrence Venable (2014). “Bet hedging in desert winter annual plants: optimal germination strategies in a variable environment”. In: *Ecology letters* 17.3, pp. 380–387.

Grossiord, Charlotte et al. (2017). “Precipitation, not air temperature, drives functional responses of trees in semi-arid ecosystems”. In: *Journal of Ecology* 105.1, pp. 163–175.

Guerand, J, M Hillairet, and S Mirrahimi (2023). “A moment-based approach for the analysis of the infinitesimal model in the regime of small variance”. In: *arXiv preprint arXiv:2309.09567*.

Haldane, John Burdon (1990). *The causes of evolution*. Vol. 5. Princeton University Press.

Hamann, Elena, Arthur E Weis, and Steven J Franks (2018). “Two decades of evolutionary changes in Brassica rapa in response to fluctuations in precipitation and severe drought”. In: *Evolution* 72.12, pp. 2682–2696.

Hamrick, James L (2004). “Response of forest trees to global environmental changes”. In: *Forest ecology and management* 197.1-3, pp. 323–335.

Hodgson, John G et al. (2020). “Seed size, number and strategies in annual plants: a comparative functional analysis and synthesis”. In: *Annals of Botany* 126.7, pp. 1109–1128.

Hoffmann, Ary A and Carla M Sgrò (2011). “Climate change and evolutionary adaptation”. In: *Nature* 470.7335, pp. 479–485.

Hughes, William (2015). “Empirical evidence for the continuity of semelparity and iteroparity”. PhD thesis. Carleton University.

Jaganathan, Ganesh K and Matthew Biddick (2021). “Experimental warming hastens physical dormancy break and germination in tropical Fabaceae”. In: *Frontiers in Plant Science* 12, p. 782706.

Jump, Alistair S and Josep Peñuelas (2005). “Running to stand still: adaptation and the response of plants to rapid climate change”. In: *Ecology letters* 8.9, pp. 1010–1020.

Kirkpatrick, Mark and Nicholas H Barton (1997). “Evolution of a species’ range”. In: *The American Naturalist* 150.1, pp. 1–23.

Klupczyńska, Ewelina A and Tomasz A Pawłowski (2021). “Regulation of seed dormancy and germination mechanisms in a changing environment”. In: *International journal of molecular sciences* 22.3, p. 1357.

Kremer, Antoine and Andrew L Hipp (2020). “Oaks: an evolutionary success story”. In: *New Phytologist* 226.4, pp. 987–1011.

Laude, Horton M (1953). “The nature of summer dormancy in perennial grasses”. In: *Botanical gazette* 114.3, pp. 284–292.

Laurance, William F et al. (2004). “Inferred longevity of Amazonian rainforest trees based on a long-term demographic study”. In: *Forest Ecology and Management* 190.2-3, pp. 131–143.

Lipiec, Jerzy et al. (2013). “Effect of drought and heat stresses on plant growth and yield: a review.” In: *International Agrophysics* 27.4.

Lorz, Alexander, Sepideh Mirrahimi, and Benoıt Perthame (2011). “Dirac mass dynamics in multidimensional nonlocal parabolic equations”. In: *Communications in Partial Differential Equations* 36.6, pp. 1071–1098.

Măgălie, Andreea et al. (2023). “Optimal dormancy strategies in fluctuating environments given delays in phenotypic switching”. In: *Journal of theoretical biology* 561, p. 111413.

Maron, John L and Elizabeth Crone (2006). “Herbivory: effects on plant abundance, distribution and population growth”. In: *Proceedings of the Royal Society B: Biological Sciences* 273.1601, pp. 2575–2584.

Matesanz, Silvia, Ernesto Gianoli, and Fernando Valladares (2010). “Global change and the evolution of phenotypic plasticity in plants”. In: *Annals of the New York Academy of Sciences* 1206.1, pp. 35–55.

McDowell, Nate et al. (2008). “Mechanisms of plant survival and mortality during drought: why do some plants survive while others succumb to drought?” In: *New phytologist* 178.4, pp. 719–739.

Mediavilla, Sonia et al. (2019). “Foliar plasticity related to gradients of heat and drought stress across crown orientations in three Mediterranean Quercus species”. In: *PLoS One* 14.10, e0224462.

Menzel, Annette et al. (2006). “European phenological response to climate change matches the warming pattern”. In: *Global change biology* 12.10, pp. 1969–1976.

Mu, Xiao-Han et al. (2021). “Population dynamics and life history response to precipitation changes for a desert ephemeral plant with biseasonal germination”. In: *Frontiers in Plant Science* 12, p. 625475.

Munguía-Rosas, Miguel A et al. (2011). “Meta-analysis of phenotypic selection on flowering phenology suggests that early flowering plants are favoured”. In: *Ecology letters* 14.5, pp. 511–521.

Nam, Bo Eun and Jae Geun Kim (2020). “Flowering season of vernal herbs is shortened at elevated temperatures with reduced precipitation in early spring”. In: *Scientific Reports* 10.1, p. 17494.

ONF (2024). *Observation massive de dépérissement forestier en Guyane*. URL: https://www.reserve-trinite.fr/observation-massive-de-deperissement-forestier-en-guyane/ (visited on 05/17/2024).

Patout, Florian (2023). “The cauchy problem for the infinitesimal model in the regime of small variance”. In: *Analysis & PDE* 16.6, pp. 1289–1350.

Penfield, Steven and Dana R MacGregor (2017). “Effects of environmental variation during seed production on seed dormancy and germination”. In: *Journal of experimental botany* 68.4, pp. 819–825.

Penman, Howard Latimer (1948). “Natural evaporation from open water, bare soil and grass”. In: *Proceedings of the Royal Society of London. Series A. Mathematical and Physical Sciences* 193.1032, pp. 120–145.

Philippi, Thomas (1993). “Bet-hedging germination of desert annuals: beyond the first year”. In: *The American Naturalist* 142.3, pp. 474–487.

Pulvirenti, Ada and Giuseppe Toscani (2004). “Asymptotic properties of the inelastic Kac model”. In: *Journal of statistical physics* 114, pp. 1453–1480.

Raoul, Gaël (2017). “Macroscopic limit from a structured population model to the Kirkpatrick-Barton model”. In: *arXiv preprint arXiv:1706.04094*.

Ravn, Jacob et al. (2022). “Phenotypic plasticity enables considerable acclimation to heat and drought in a cold-adapted boreal forest tree species”. In: *Frontiers in Forests and Global Change* 5, p. 1075787.

Reid, Jane M and Paul Acker (2022). “Properties of phenotypic plasticity in discrete threshold traits”. In: *Evolution* 76.2, pp. 190–206.

Richardson, Bryce A et al. (2017). “Will phenotypic plasticity affecting flowering phenology keep pace with climate change?” In: *Global change biology* 23.6, pp. 2499–2508.

Rizza, F et al. (2004). “Use of a water stress index to identify barley genotypes adapted to rainfed and irrigated conditions”. In: *Crop science* 44.6, pp. 2127–2137.

Rouzine, Igor M, John Wakeley, and John M Coffin (2003). “The solitary wave of asexual evolution”. In: *Proceedings of the National Academy of Sciences* 100.2, pp. 587–592.

Scheiner, Samuel M (1993). “Genetics and evolution of phenotypic plasticity”. In: *Annual review of ecology and systematics* 24.1, pp. 35–68.

Schwartz, Mark Donald et al. (2003). *Phenology: an integrative environmental science*. Vol. 39. Springer.

Sinclair, Thomas R, N Michelle Holbrook, and Maciej A Zwieniecki (2005). “Daily transpiration rates of woody species on drying soil”. In: *Tree physiology* 25.11, pp. 1469–1472.

Smithers, Brian V and Malcolm P North (2020). “Mechanisms of species range shift: germination and early survival of Great Basin bristlecone pine and limber pine”. In: *Plant and Soil* 457, pp. 167–183.

Sniegowski, Paul D and Philip J Gerrish (2010). “Beneficial mutations and the dynamics of adaptation in asexual populations”. In: *Philosophical Transactions of the Royal Society B: Biological Sciences* 365.1544, pp. 1255–1263.

Springate, David A and Paula X Kover (2014). “Plant responses to elevated temperatures: a field study on phenological sensitivity and fitness responses to simulated climate warming”. In: *Global Change Biology* 20.2, pp. 456–465.

Stephens, Ruby E et al. (2021). “Climate shapes flowering periods across plant communities”. In: *bioRxiv*, pp. 2021–10.

Thornthwaite, Charles Warren (1948). “An approach toward a rational classification of climate”. In: *Geographical review* 38.1, pp. 55–94.

Tsimring, Lev S, Herbert Levine, and David A Kessler (1996). “RNA virus evolution via a fitness-space model”. In: *Physical review letters* 76.23, p. 4440.

Turcotte, Martin M and Jonathan M Levine (2016). “Phenotypic plasticity and species coexistence”. In: *Trends in ecology & evolution* 31.10, pp. 803–813.

Valladares, Fernando et al. (2000). “Plastic phenotypic response to light of 16 congeneric shrubs from a Panamanian rainforest”. In: *Ecology* 81.7, pp. 1925–1936.

Varpe, Øystein and Maciej J Ejsmond (2018). “Semelparity and iteroparity”. In: *Natural history of crustacea* 5, pp. 97–124.

Vegis, Anseklis (1964). “Dormancy in higher plants”. In: *Annual review of plant physiology* 15.1, pp. 185–224.

Venable, D Lawrence and Lawrence Lawlor (1980). "Delayed germination and dispersal in desert annuals: escape in space and time". In: *Oecologia* 46, pp. 272–282.

Volaire, Florence and Mark Norton (2006). "Summer dormancy in perennial temperate grasses". In: *Annals of botany* 98.5, pp. 927–933.

Vukialau-Taoi, M, L Lili, and W Bolatolu (2023). "DIFFERENTIAL EFFECTS OF PRECIPITATION AND TEMPERATURE ON SEED PHENOLOGY AND SEED PRODUCTION IN AGATHIS MACROPHYLLA IN FIJI". In: *Journal of Tropical Forest Science* 35.2, pp. 157–167.

Wagner, David L and Roy G Van Driesche (2010). "Threats posed to rare or endangered insects by invasions of nonnative species". In: *Annual review of entomology* 55, pp. 547–568.

Wakeley, John (2005). "The limits of theoretical population genetics". In: *Genetics* 169.1, pp. 1–7.

Walck, Jeffrey L et al. (2011). "Climate change and plant regeneration from seed". In: *Global change biology* 17.6, pp. 2145–2161.

West-Eberhard, Mary Jane (2003). *Developmental plasticity and evolution*. Oxford University Press.

Wright, Sewall (1935). "The analysis of variance and the correlations between relatives with respect to deviations from an optimum". In: *Journal of Genetics* 30, pp. 243–256.

Xie, Yingying, Xiaojing Wang, and John A Silander Jr (2015). "Deciduous forest responses to temperature, precipitation, and drought imply complex climate change impacts". In: *Proceedings of the National Academy of Sciences* 112.44, pp. 13585–13590.

Yousaf, Zubaida et al. (2016). "Postharvesting techniques and maintenance of seed quality". In: *New Challenges in Seed Biology-Basic and Translational Research Driving Seed Technology*, pp. 114–135.

Yu, Shunli et al. (2021). "Shift of seed mass and fruit type spectra along longitudinal gradient: high water availability and growth allometry". In: *Biogeosciences* 18.2, pp. 655–667.

Zhang, Qindi et al. (2023). "Climatic Warming-Induced Drought Stress Has Resulted in the Transition of Tree Growth Sensitivity from Temperature to Precipitation in the Loess Plateau of China". In: *Biology* 12.10, p. 1275.

Chapter 4

# Discussion

## 4.1 Main Results

### 4.1.1 Evolution is Double-Edged

We have addressed in the introduction the question of whether evolution could save the day under the threat of global change. We have seen throughout this manuscript that while evolution can allow the adaptation and survival of certain populations in ecosystems under environmental stress, it is not always the case.

Indeed, in **chapter 1**, we observed the paradoxical situation of evolutionary suicide. This arises when adaptation that increases individuals fitness in the short term, ultimately leads to negative consequences that reduce the overall viability of the population in the long term (Ferriere 2000; Dieckmann, Marrow, and Law 1995). The evolution of the submerged macrophytes to extinction occurred within a bistability region under adverse conditions, after oscillations became very high until the population cycles between high and low densities. When the low density size became close to zero, individuals failed to grow again, leading to the extinction of the population.

In reality, such phenomena can occur through demographic stochasticity, where populations facing declines and reaching low densities are at higher risk of extinction (Gomulkiewicz, Holt, and Barfield 1999). Another potential scenario is genetic drift, because it has more significant impact in small populations because random events can cause bigger changes in allele frequencies (Willi et al. 2007). Moreover, in small populations genetic drift can overpower natural selection, leading to the fixation of

neutral or even deleterious alleles (Gabriel and Bürger 1994; Cowperthwaite, Bull, and Meyers 2006). But even natural selection can also contribute to such fatal outcomes. Since natural selection operates on individuals, the environmental change as well as interactions with other species can turn out to be too harmful for the population to survive. Darwin (1859,1871) had already observed that natural selection might favor traits that eventually can prove to be harmful to the individuals (Parvinen 2005). There are only few examples of evolutionary suicide, but as Webb 2003a stated, it is difficult to study in nature simply because it is difficult to observe anything about extinct populations.

The theory behind evolutionary suicide suggests that a bifurcation in population dynamics is a necessary condition, and it has to be discontinuous (Gyllenberg, Parvinen, and Dieckmann 2002). Also Webb 2003a proposed a classification of different bifurcations for evolutionary suicide. In our study, evolutionary suicide also happened when critical shifts where possible and where the extinction of the submerged macrophytes was an alternative stable state. Although such outcomes occurred after the diversification of the population with a wide range of traits coexisting, while the bistability arose when the submerged population was monomorphic. However, the wide oscillations between high and low density preceding the extinction suggest the potential presence of the positive feedback mechanism that leads to abrupt shifts.

Despite the great variety of species present today, we know that an even greater number of species have gone extinct. Evolutionary suicide could be a possible explanation for this. A potential mechanism leading to evolutionary suicide, is the neutral theory of evolution, proposed by Kimura in the late 60s (Kimura 1979), stating that the majority of evolutionary changes at the molecular level are caused by genetic drift of neutral mutations. According to this theory, most genetic variation is due to the randim fixation of neutral mutations rather than the result of ongoing selection. This could explain the high levels of genetic variations observed within populations on one hand. On another hand, the random fixation of neutral mutations can alter the genetic background of a population which contributed to maladaptative genetic combinations. Also, the accumulation of neutral mutations can allow populations to drift across flat regions of the fitness landscape (areas of the fitness landscape where the fitness values of different phenotypes or genotypes are very similar or nearly equal), potentially leading them into evolutionary traps where adaptive changes are harmful in the long run. By considering the interactions between neutral processes and selective forces, we can perhaps gain more insights on the dynamics that lead to evolutionary suicide.

In **chapter 3**, I explored the evolutionary dynamics and adaptive capacitites of two phenotypic traits within a tree population facing environmental shifts, notably in temperature and precipitation. The results showed that without an intrinsic mortality acting upon the population, and dormancy preventing reproduction, the phenotypic traits didn't adapt to the new environment in a wide range of scenarios. Although dormancy allows individuals to survive through adverse conditions such as extreme temperatures and drought (Finch-Savage and Leubner-Metzger 2006; Aragón-Gastélum et al. 2018; Jurado and J. Flores 2005), it can also hinder or slow down the adaptation to changing environment (Vidigal et al. 2016). Specifically, if a significant proportion of a population is dormant, beneficial mutations and adaptive traits may spread more slowly or not at all through the population. Moreover, very long dormancy periods means less generations over time, which may reduce the speed of adaptation to new environmental stress. It is important to note that the trait we considered was related to the timing of dormancy, which is subject to phenotypic plasticity. However, in our study we didn't assume an adaptive plasticity. I will discuss this more in detail later.

Additionally, I found that one of the traits failed to adapt to high amplitude shifts. Indeed, when the environmental change occurs too quickly and extremely, there may not be enough time for beneficial mutations to spread and for the traits to track the new optimal strategy. This may lead to a mismatch between the population' traits and the new environment (Shibata et al. 2020). In our study, this led to a potential change of ecological niche where the seed production of the tree individuals exploded. This can be explained by the speciation phenomena, where the environmental shift can drive the population to split into two distinct groups that specialize in different niches. A study found that physiological dormancy is associated with higher rates of lineage diversification, primarily through increased speciation rates (Willis et al. 2014).
In our studied case, individuals that failed to adapt rapidly, could adopt a different strategy of high seed production to ensure their offspring's survival, leading to genetic divergence. As these traits become more present, this can lead to the emergence of a new species.

### 4.1.2 Impact of Co-evolution on Species Stability and Adaptation

A crucial notion studied in this thesis is co-evolution. Co-evolution refers to the reciprocal evolutionary influence of two or more species or traits. The results obtained in this work illustrate how co-evolution may shape and drive adaptive processes.

In **chapter 1**, I considered the co-evolution of floating and submerged macrophytes. Although this co-evolution didn't qualitatively affect the overall evolutionary outcomes, it exerted a stabilizing effect on the dynamics by preventing oscillations. Co-evolution, leading to reciprocal adaptations, can influence the dynamics and balance the interactions between species, therefore preventing fluctuations. Moreover, despite the antagonistic relationship between floating and submerged plants, their co-evolution delayed the evolutionary suicide of submerged macrophytes. By stabilizing the dynamics, co-evolution allowed the submerged plants to survive a bit longer, even under hostile environment of excessive nutrient diffusion. In general, co-evolution may contribute to the stability of ecosystems by balancing competitive interactions and promoting cooperative behaviours. This can result in more resilient communities that are better equipped to face environmental change. For instance, the co-evolution of competitive species in freshwater ecosystems can lead to diverse and stable communities with complex trophic interactions. Co-evolution can also enhance genetic variance as we have seen in some scenarios where floating macrophytes diversified which helped maintaining both species with rich phenotypic pool and high population sizes.
According to many investigations, it seems that co-extinctions are quite rare phenomena (Bronstein, Dieckmann, and Ferrière 2004). But surely, an absence of proof isn't a proof of absence. However, if it is indeed the case, it can be explained by the fact that co-evolving species may be more resilient to environmental change. An obvious example of this is mutualism, but this can be expanded to other types of ineractions.

In **chapter 3**, I considered the case of co-evolution of two different traits within a population of trees, where we have also seen the important role of co-evolution. The main observation in the matter, is that co-evolution allowed the adaptation to environmental shifts of a trait that would have failed to adapt when evolving alone. In some cases, the simultaneous evolution of dormancy and seed production, prevented the change of ecological niche observed when the number of seeds evolved alone, therefore enhancing the rapid evolution towards the optimal strategy under the new environment. This shows that co-evolution can mitigate the negative effects of certain adaptations.

When populations face multiple environmental stressors simultaneously, co-evolutionary interactions can result in divergent evolutionary paths across different environments. This process can enhance the ability of species to adapt to multiple stressors by promoting genetic diversity and local adaptations, allowing species to better cope with varying environmental challenges Laine 2009. Co-evolution

can foster genetic diversity (John N Thompson et al. 2013; Laine 2009), therefore facilitating rapid adaptation which helps the populations to keep pace with fast changing conditions. A study revealed the genetic characteristics that may contribute to the oak tree's long lifespan, shedding light on how co-evolution has shaped these features over time (Mesny, Hacquard, and Thomma 2023).

### 4.1.3 Making Sense of Mechanistic Eco-Evolutionary Models

In this thesis, I employed mechanistic models of varying complexity to describe the eco-evolutionary dynamics of ecosystems under environmental stress. In **Chapter 1**, I extended the models used in (Marten Scheffer, Szabo, et al. 2003a; Aragón-Gastélum et al. 2018) to propose a more realistic and comprehensive model of macrophyte dynamics in shallow lakes, incorporating elements such as competition, trade-offs, phenotypic structure, and its evolution. The goal was to study and understand the evolutionary outcomes of species within an ecosystem exhibiting bistability due to positive feedback mechanisms. To achieve this, I used Adaptive Dynamics and Quantitative Genetics approaches, resulting in a diverse range of evolutionary outcomes, including diversification, oscillations, and extinction.

These models, while not capturing every interaction among species in shallow lakes, provide significant insights into the potential evolutionary behaviors of floating and submerged macrophytes. Adaptive Dynamics (AD) was used to model monomorphic populations evolving with assumptions of small and rare mutations, while Quantitative Genetics (QG) considered trait distributions with high initial genetic variance, focusing only on the role of selection. These approaches allowed for a deeper understanding of how macrophytes might evolve under different scenarios, highlighting the complexity and variability of evolutionary processes in bistable ecosystems.

In **Chapter 2**, I again used the Quantitative Genetics (QG) approach to model the annual dynamics of a tree population characterized by two phenotypic traits. This model incorporated elements such as sexual reproduction, selection, mutations, environmental variations, and mortality. Although analytically challenging, we simplified the model using an approach based on previous findings, focusing on macroscopic quantities that capture the essential population dynamics. This demonstrated that even complex models integrating multifaceted dynamics can be studied and described using well-established theoretical frameworks.

Building on this, the simplified macroscopic model obtained allowed to explored the evolutionary dynamics and adaptation of the population's mean traits under climate change in **Chapter 3**. This provided a deeper understanding of the potential evolutionary responses of tree populations to environmental shifts, highlighting the intricate relationship between phenotypic traits and adaptive capacity in the face of changing climates.

This showed that while adding multiple layers of complexity to mathematical models—like sexual reproduction, multiple traits, assortative mating, and various environmental factors—can make them intractable and difficult to study, one must not fear challenging and complex models, nor be intimidated by seemingly daunting equations. Such models often carry hidden feasibility through potential simplification assumptions or previous results that allow their study. While many biologists criticize the excessive simplifications of models as unrealistic, numerous simplified models were proven to be justified and reliable. At the same time, ongoing efforts to incorporate additional complexities on multiple scales are showing promise and providing deeper insights into biological phenomena.

## 4.2 Limitations and Perspectives

### 4.2.1 The Need for Empirical Validation

In 1932, J.B.S. Haldane wrote in one of his articles : *"At present, one can say that the mathematical theory of evolution is somewhat in a difficult position; too much mathematics to interest biologists, and not enough mathematics to interest mathematicians. Nevertheless, one can reasonably suppose that in the next half century it will find its place as a respectable branch of applied mathematics."*. Today, almost a century later, we can affirm that his predictions were correct. After decades of research, theoretical models where the first to attempt to link ecological and evolutionary dynamics by modeling their feedback and interactions (Govaert et al. 2019). These models enable us to simplify the subtleties of nature into understandable and testable hypotheses, allowing predictions about population dynamics and evolutionary outcomes, species interactions, and ecosystem responses to environmental changes. For instance, the different findings of this present work including predictions of how species would evolve under various environmental pressures, can be valuable for conservation biology.

We have seen how such models provide a framework for better understanding complex interactions

and responses within ecosystems. As the physicist Richard Feynman once quoted : *"Mathematics is a way of reasoning, it's a tool that enables to go further in our understanding"*. However, it is important to keep in mind that is it indeed just tool, and tools are not infallible. Mathematical language as symbolic logic is a human prowess, but nature and its complexity can go beyond our scope. We are merely able describe nature, let alone explain and predict its behaviour with certainty, something that A. Einstein formulated as : *"As far as the laws of maths refer to reality, they are not certain; and as far as they are certain, they do not refer to reality"*.

To address these limitations, it is crucial to validate models and their underlying assumptions by going back to our starting point : observations and experiments. Because experience is the only way that knowledge of anything outside ourselves arises. Models are only reliable once validated empirically. Observational data and experimental results provide the necessary feedback to refine models, correct inaccuracies, and update assumptions. This iterative process of validation helps to bridge the gap between theoretical predictions and empirical reality, enhancing the robustness and applicability of mathematical models in ecology and evolution. An analogy can be made with one definition of the truth, attributed to the philosopher G.W.H Hegel that I admire, who wrote : *"The truth in philosophy means that concept and external reality correspond."* Many studies highlighted the importance of validation in models of evolutionary ecology to ensure that the results have relevance to reality (Maley 1998; Barros et al. 2023; Lotterhos, Moore, and Stapleton 2018).

In this thesis, I only considered mathematical models and frameworks that have been proven reliable. Nonetheless, this work represents just one step in the scientific process and further validation is required. The study conducted in **chapter 1** on evolutionary dynamics of macophytes in shallow lakes can be be validated through extensive genetic, ecological, and phenotypic data. Phenotypes such as growth depth are measurable and quantifiable through field observations and experimental setups. For instance, growth depth can be assessed by measuring the maximum rooting depth or canopy height of macrophytes across different environmental gradients in shallow lakes. Studies have shown that such integrated approaches can effectively validate evolutionary hypotheses. For example, (Santamaría 2002) demonstrated how environmental and genetic factors influence macrophyte growth forms in aquatic ecosystems, while (Riis and Biggs 2003) quantified the phenotypic plasticity of macrophytes in response to varying water depths. Similarly, phenotypes related to plant phenology such as leaf emergence timing and dormancy cam be measured through long-term field observations,

controlled experiments, and remote sensing technologies. For instance, the timing of leaf emergence and senescence can be tracked annually to study phenological response to climate change.
Furthermore, validating results such as the finding of **chapter 3** that dormancy and absence of intrinsic mortality slow down or prevent adaptation can have practical applications in forest management. For instance, actively managing tree populations by selective cutting could provoke better adaptation to environmental changes. This proactive approach could enhance genetic diversity and phenotypic plasticity, leading to more resilient forest ecosystems.

In summary, the assumptions made and the results obtained still need to be tested and validated or refuted with data analysis, to advance further and apply this acquired knowledge and understanding in practical ways. Because after all, empirical problems ultimately require empirical solutions.

### 4.2.2 Considering Adaptive Phenotypic Plasticity

In **Chapters 2 and 3**, we explored phenotypic plasticity of dormancy in tree populations. Our findings indicated that dormancy could hinder adaptation by preventing reproduction. However, our model did not incorporate adaptive plasticity, as the timing of dormancy response which was triggered by reaching a temperature threshold, was fixed. It is well established that adaptive plasticity enables organisms to cope with varying environmental conditions, thus enhancing their survival and reproductive success. It is also known that different species of plants or trees exhibit varying levels of plasticity. For instance, trees from hotter, southern populations exhibit up to four times greater phenotypic plasticity compared to northern, frost-adapted populations in response to warmer spring temperatures, indicating a strong adaptive response to warmer springs (Cooper et al. 2019). Another study found that trait plasticity was positively related to the precipitation variability of origin, suggesting an adaptive role of plasticity. This means that *Arabidopsis thaliana* populations from regions with higher climatic variability showed greater plasticity, which could be an adaptive response to their environment ((Scheepens, Deng, and Bossdorf 2018).
In plants, for example, adaptive plasticity serves as a primary defense against environmental changes, allowing them to adjust and maintain fitness (Brooker et al. 2021). This type of plasticity aligns populations closer to a new phenotypic optimum, facilitating more effective directional selection. Adaptive plasticity is likely to boost fitness and support adaptive evolution on ecological timescales in new environments (Ghalambor et al. 2007). In contrast, non-adaptive plasticity does not move the population towards an optimum and can even be maladaptive, potentially hindering adaptive

evolution (Ghalambor et al. 2007), as observed in certain scenarios in Chapter 3. Adaptive plasticity promotes rapid evolutionary changes by adjusting traits in response to environmental pressures, leading to fast adaptation and the evolution of new traits. For example, a study demonstrated the adaptive value of phenotypic plasticity in tree phenology, showing that plastic responses help trees cope with varying climatic conditions along elevational gradients (Gauzere et al. 2020). Moreover, adaptive plasticity helps populations cope with sudden environmental changes by allowing immediate phenotypic adjustments. This plasticity can reduce the effective magnitude of environmental shifts, providing a temporary buffer that enables the population to maintain positive growth rates until genetic adaptations occur (Chevin and Lande 2010).

Our results of **chapter 3** showed that in certain scenarios dormancy as a plastic could evolve towards a strategy that would later hinder the adaptation to a new environment by preventing reproduction. Adaptive plasticity—where dormancy timing is not fixed—could indeed facilitate better adaptation. Adaptive plasticity allows trees to modify their dormancy response to environmental cues, thereby allowing a part of the population to stay active and maintain selective pressures. This would improve their chances of survival and reproduction under changing conditions. A study discusses how organisms adapt to extreme environments through the evolution of phenotypic plasticity and genetic assimilation (Lande 2009) while another work shows that if plastic responses mask genetic variation from selection, they could slow down genetic adaptation, emphasizing that moderate levels of plasticity can be particularly beneficial for evolutionary adaptation (T. D. Price, Qvarnström, and Irwin 2003).

Overall, this shows that it is crucial to integrate adaptive phenotypic plasticity in future research as it is a vital mechanism that allows population to flexibly and better adapt in an often unpredictable world. Understanding and leveraging this plasticity is crucial for both evolutionary biology and the conservation of biodiversity, particularly in the context of rapid environmental changes.

### 4.2.3 Including Stochasticity

In this thesis, I only considered deterministic models (ODEs and PDEs) to study eco-evolutionary dynamics of ecosystems. Although the use of such models is justified for large populations since many studies have shown the convergence of stochastic processes to deterministic models when the populations became large (Champagnat, Ferrière, and Méléard 2006). Therefore, these models are inadequate for small populations where random demographic events (e.g., individual birth and death events)

(Dunlop, Heino, and Dieckmann 2009) significantly influence population dynamics. Deterministic models do not capture these effects well. This study (Dunlop, Heino, and Dieckmann 2009) highlights the significance of individual-level interactions in shaping eco-evolutionary dynamics. The authors advocate for the use of demo-genetic agent-based models, which incorporate genetic heterogeneity and interindividual interactions, to better understand population dynamics. These models provide a more detailed and realistic framework (Lamarins et al. 2022). Moreover, deterministic models may not adequately account for stochastic environmental changes, such as random fluctuations, which can drastically alter ecological and evolutionary dynamics. While examining seasonal environmental fluctuations influence species coexistence and diversity, authors used eco-evolutionary models to show that environmental variability can affect species diversity and community structure (C. T. Kremer and Klausmeier 2017). In **chapter 3,** we considered constant annual temperature variations and water supply before and after a sudden shift. But in reality, environmental conditions vary year by year, and stochastic events like droughts or floods can drastically affect population sizes. Additionally, deterministic models assume a constant mutation rate and predict evolutionary trajectories accordingly. While mutations occur randomly, and rare beneficial mutations can have important effects on evolutionary outcomes. Models incorporating stochasticity better capture the role of heritable trait variation in eco-evolutionary dynamics, influencing how trait distributions change over time (DeLong and Gibert 2016; Doulcier et al. 2020)

In summary, including stochasticity in eco-evolutionary models is crucial for several reasons; including enhancing the realism, accuracy, and predictive power of these models.

## 4.3 Conclusion

This thesis builds on previous theoretical and mathematical frameworks to investigate the intricate eco-evolutionary dynamics of ecosystems under the threat of global changes, such as regime shifts and environmental perturbations. It emphasizes the roles of co-evolution, phenotypic plasticity, and environmental pressures in shaping evolutionary outcomes. The research highlights the critical interplay between these factors and provides valuable insights into the adaptive capacities of species and ecosystems.

Overall, this thesis bridges the gap between mathematical modeling and ecology and evolution. It demonstrates the usefulness and importance of mathematical models in describing specific eco-

evolutionary dynamics of different species. By integrating detailed mechanistic models with evolutionary approaches, the research provides a better understanding of species' responses to environmental stressors and their adaptive capacities under various scenarios. The findings can have practical implications for ecosystem conservation strategies, highlighting the need to consider multiple interacting traits and species to enhance adaptive responses in changing environments.

# Bibliography


Aragón-Gastélum, José Luis et al. (2018). "Potential impact of global warming on seed bank, dormancy and germination of three succulent species from the Chihuahuan Desert". In: *Seed Science Research* 28.4, pp. 312–318.

Ardichvili, Alice Nadia, Nicolas Loeuille, and Vasilis Dakos (2023). "Evolutionary emergence of alternative stable states in shallow lakes". In: *Ecology Letters* 26.5, pp. 692–705.

Barros, Ceres et al. (2023). "Empowering ecological modellers with a PERFICT workflow: Seamlessly linking data, parameterisation, prediction, validation and visualisation". In: *Methods in Ecology and Evolution* 14.1, pp. 173–188.

Bronstein, Judith L, Ulf Dieckmann, and Régis Ferrière (2004). "Coevolutionary dynamics and the conservation of mutualisms". In: *Evolutionary conservation biology* 4, p. 305.

Brooker, Rob et al. (2021). "Adaptive plasticity–its definition, measurement, and importance". In.

Chevin, Luis-Miguel and Russell Lande (2010). "When do adaptive plasticity and genetic evolution prevent extinction of a density-regulated population?" In: *Evolution* 64.4, pp. 1143–1150.

Cooper, Hillary F et al. (2019). "Genotypic variation in phenological plasticity: Reciprocal common gardens reveal adaptive responses to warmer springs but not to fall frost". In: *Global change biology* 25.1, pp. 187–200.

Cowperthwaite, Matthew C, James J Bull, and Lauren Ancel Meyers (2006). "From bad to good: Fitness reversals and the ascent of deleterious mutations". In: *PLoS computational biology* 2.10, e141.

DeLong, John P and Jean P Gibert (2016). "Gillespie eco-evolutionary models (GEM s) reveal the role of heritable trait variation in eco-evolutionary dynamics". In: *Ecology and evolution* 6.4, pp. 935–945.

Doulcier, Guilhem et al. (2020). "Eco-evolutionary dynamics of nested Darwinian populations and the emergence of community-level heredity". In: *Elife* 9, e53433.

Dunlop, Erin S, Mikko Heino, and Ulf Dieckmann (2009). “Eco-genetic modeling of contemporary life-history evolution”. In: *Ecological Applications* 19.7, pp. 1815–1834.

Finch-Savage, William E and Gerhard Leubner-Metzger (2006). “Seed dormancy and the control of germination”. In: *New phytologist* 171.3, pp. 501–523.

Gabriel, Wilfried and Reinhard Bürger (1994). “Extinction risk by mutational meltdown: synergistic effects between population regulation and genetic drift”. In: *Conservation genetics*, pp. 69–84.

Gauzere, Julie et al. (2020). “Where is the optimum? Predicting the variation of selection along climatic gradients and the adaptive value of plasticity. A case study on tree phenology”. In: *Evolution letters* 4.2, pp. 109–123.

Gomulkiewicz, Richard, Robert D Holt, and Michael Barfield (1999). “The effects of density dependence and immigration on local adaptation and niche evolution in a black-hole sink environment”. In: *Theoretical population biology* 55.3, pp. 283–296.

Govaert, Lynn et al. (2019). “Eco-evolutionary feedbacks—Theoretical models and perspectives”. In: *Functional Ecology* 33.1, pp. 13–30.

Gyllenberg, Mats, Kalle Parvinen, and Ulf Dieckmann (2002). “Evolutionary suicide and evolution of dispersal in structured metapopulations”. In: *Journal of mathematical biology* 45, pp. 79–105.

Josephs, Emily B et al. (2021). “Adaptive and maladaptive expression plasticity underlying herbicide resistance in an agricultural weed”. In: *Evolution Letters* 5.4, pp. 432–440.

Jurado, Enrique and Joel Flores (2005). “Is seed dormancy under environmental control or bound to plant traits?” In: *Journal of Vegetation Science* 16.5, pp. 559–564.

Kimura, Motoo (1979). “The neutral theory of molecular evolution”. In: *Scientific American* 241.5, pp. 98–129.

Kremer, Colin T and Christopher A Klausmeier (2017). “Species packing in eco-evolutionary models of seasonally fluctuating environments”. In: *Ecology Letters* 20.9, pp. 1158–1168.

Laine, Anna-Liisa (2009). “Role of coevolution in generating biological diversity: spatially divergent selection trajectories”. In: *Journal of experimental botany* 60.11, pp. 2957–2970.

Lamarins, Amaıa et al. (2022). “Importance of interindividual interactions in eco-evolutionary population dynamics: The rise of demo-genetic agent-based models”. In: *Evolutionary applications* 15.12, pp. 1988–2001.

Lande, Russell (2009). “Adaptation to an extraordinary environment by evolution of phenotypic plasticity and genetic assimilation”. In: *Journal of evolutionary biology* 22.7, pp. 1435–1446.

Lotterhos, Kathleen E, Jason H Moore, and Ann E Stapleton (2018). "Analysis validation has been neglected in the Age of Reproducibility". In: *PLoS Biology* 16.12, e3000070.

Maley, CC (1998). "Models in evolutionary ecology and the validation problem". In: *Artificial Life VI*. MIT Press Cambridge, MA, pp. 423–427.

Mesny, Fantin, Stéphane Hacquard, and Bart PHJ Thomma (2023). "Co-evolution within the plant holobiont drives host performance". In: *EMBO reports* 24.9, e57455.

Price, Trevor D, Anna Qvarnström, and Darren E Irwin (2003). "The role of phenotypic plasticity in driving genetic evolution". In: *Proceedings of the Royal Society of London. Series B: Biological Sciences* 270.1523, pp. 1433–1440.

Riis, Tenna and Barry JF Biggs (2003). "Hydrologic and hydraulic control of macrophyte establishment and performance in streams". In: *Limnology and oceanography* 48.4, pp. 1488–1497.

Santamaría, Luis (2002). "Why are most aquatic plants widely distributed? Dispersal, clonal growth and small-scale heterogeneity in a stressful environment". In: *Acta oecologica* 23.3, pp. 137–154.

Scheepens, JF, Ying Deng, and Oliver Bossdorf (2018). "Phenotypic plasticity in response to temperature fluctuations is genetically variable, and relates to climatic variability of origin, in Arabidopsis thaliana". In: *AoB Plants* 10.4, ply043.

Shibata, Mitsue et al. (2020). "Decadal changes in masting behaviour of oak trees with rising temperature". In: *Journal of Ecology* 108.3, pp. 1088–1100.

Thompson, John N et al. (2013). "Diversification through multitrait evolution in a coevolving interaction". In: *Proceedings of the National Academy of Sciences* 110.28, pp. 11487–11492.

Vidigal, Deborah S et al. (2016). "Altitudinal and climatic associations of seed dormancy and flowering traits evidence adaptation of annual life cycle timing in Arabidopsis thaliana". In: *Plant, cell & environment* 39.8, pp. 1737–1748.

Willi, Yvonne et al. (2007). "Genetic isolation of fragmented populations is exacerbated by drift and selection". In: *Journal of evolutionary biology* 20.2, pp. 534–542.

Willis, Charles G et al. (2014). "The evolution of seed dormancy: environmental cues, evolutionary hubs, and diversification of the seed plants". In: *New Phytologist* 203.1, pp. 300–309.

# French Synthesis

## 5.1 Contexte : La menace du changement global sur les écosystèmes

Il est maintenant largement reconnu, bien que pas universellement accepté, que le changement global est une réalité. Depuis des décennies, de nombreux indicateurs et recherches scientifiques ont souligné l'évidence de ce changement. Les premières mesures des concentrations de CO2 atmosphérique, comme celles établissant la courbe de Keeling, ont fourni des preuves sans équivoque de l'augmentation des niveaux de CO2 attribuable aux activités humaines (Keeling 1960). D'autres documents incluent la perte de glace accélérée du Groenland et de l'Antarctique, qui a contribué de manière significative à l'élévation du niveau de la mer (Rignot et al. 2011). Les analyses des températures de surface mondiales montrent également une tendance constante au réchauffement au cours du siècle dernier (Hansen et al. 2010). De nombreuses études ont mis en évidence les menaces potentielles pour la biodiversité et les écosystèmes. Par exemple, une étude fournit des preuves cohérentes à l'échelle mondiale des impacts du changement climatique sur divers systèmes naturels, liant les changements observés directement au réchauffement global (Parmesan and Yohe 2003).

Ces études soulignent le besoin urgent de sensibilisation et d'action pour faire face à ces changements. Bien que tous les facteurs environnementaux ne soient pas également prévisibles, il n'en reste pas moins que ces changements se produisent à des rythmes alarmants (Comiso et al. 2008; Velicogna 2009; J. Liu and Curry 2010). Par exemple, diverses études ont documenté l'augmentation constante des températures mondiales (Vinnikov et al. 1999; D. W. Thompson and Wallace 2001; Brohan et al. 2006) et la fréquence et la gravité accrues des sécheresses (Chiang, Mazdiyasni, and AghaKouchak 2021; Trenberth et al. 2014; Dai 2011).

Les changements environnementaux ne se limitent pas aux phénomènes naturels et climatiques. Les activités humaines jouent un rôle significatif dans la modification des conditions environnementales (Nelson et al. 2006). Une conséquence claire de l'Anthropocène est la pollution, qui exacerbe l'état déjà précaire des écosystèmes (Eriksen et al. 2014; Steffen, Broadgate, et al. 2015; Steffen, Crutzen,

McNeill, et al. 2007). Par exemple, une étude examine les variations spatio-temporelles des niveaux de azote et de phosphore dans un grand lac artificiel, et explore leurs relations avec les activités humaines. Les résultats mettent en évidence l'impact significatif des activités humaines sur l'enrichissement en nutriments et l'eutrophisation de l'eau dans le lac (Zhou et al. 2020).

Les altérations des conditions environnementales dues au changement global ont des conséquences significatives. Il existe des preuves inquiétantes que les impacts du changement global sur les écosystèmes, les espèces et la biodiversité sont graves. De nombreuses études ont souligné le déclin mondial de la biodiversité, pointant les taux alarmants d'extinction des espèces et de diminution des populations (Rosenberg et al. 2019; Stork 1997; Sala and Knowlton 2006; Malcolm and Markham 2000). Au-delà de la menace d'extinction, le changement global entraîne également des modifications des comportements écologiques (Steffen, Crutzen, McNeill, et al. 2007; Rockström et al. 2009) et la réorganisation des interactions entre les espèces et des structures des systèmes (Marten Scheffer 2020; Solé and Bascompte 2012).

L'augmentation du stress environnemental entraîne souvent des migrations et des invasions plus fréquentes, des changements de dominance des espèces et des modifications des activités de certaines espèces.

De plus, des exemples qui seront centraux dans ce travail sont liés au fait que l'augmentation des températures peut entraîner une floraison plus précoce des plantes, perturbant le timing des interactions avec les pollinisateurs (Raju 2018). Ou encore comment les changements de température accélèrent l'évolution de la dormance des graines dans les populations d'arbres, impactant la dormance (Y. Liu et al. 2017; Cheddadi et al. 2016). De même, les changements dans les régimes de précipitations peuvent affecter la disponibilité des ressources en eau, impactant la croissance et la survie des plantes (Zeppel, Wilks, and Lewis 2014; Miranda et al. 2009).

L'interaction complexe de ces facteurs montre l'importance de comprendre les impacts du changement global sur les écosystèmes et la biodiversité. En étudiant la dynamique des espèces et leurs interactions en réponse aux conditions environnementales changeantes, nous pouvons développer des stratégies pour promouvoir la conservation de la biodiversité. Cette thèse vise à contribuer à cette compréhension en explorant les dynamiques évolutives au sein des populations sous différentes conditions environnementales, fournissant des aperçus sur les capacités d'adaptation et les réponses potentielles de ces espèces au changement global.

À la lumière des changements globaux mentionnés ci-dessus et de leurs impacts sur les écosystèmes et les dynamiques écologiques, il est crucial de comprendre les différents mécanismes qui dictent

et caractérisent les réponses écologiques aux facteurs environnementaux. Cette entreprise revêt une importance significative, car elle permet d'anticiper ou de prédire les résultats écologiques au sein des écosystèmes, facilitant ainsi une meilleure préparation pour faire face aux conséquences de tels changements, ou idéalement, pour les prévenir. Une compréhension plus approfondie de ces mécanismes sous-jacents peut également améliorer la prise de décision en matière de gestion écologique.

L'un des outils les plus efficaces à cet effet est la modélisation mathématique. Tout au long de l'histoire, les humains ont utilisé le langage mathématique pour capturer les phénomènes observés et déduits du monde naturel. Cette approche sert à expliquer et à valider des hypothèses, à établir des connexions entre les variables et, en fin de compte, à prédire les résultats au sein d'un cadre structuré fondé sur la rationalité et la logique. En exploitant les modèles mathématiques, nous pouvons analyser systématiquement des systèmes écologiques complexes, offrant des aperçus critiques pour les stratégies de gestion et de conservation écologiques à court et à long terme.

### 5.1.1 Aperçu des modèles de dynamique des populations : Eco sans Evo

Dans cette introduction, je vais fournir un aperçu historique sélectif de certains modèles importants de dynamique des populations. Ces modèles visent à décrire les variations temporelles des populations d'espèces au sein d'écosystèmes spécifiques sous certaines hypothèses qui régissent ces variations. Notre attention se portera sur les modèles déterministes en temps continu, en particulier les équations différentielles ordinaires et partielles, car ce sont les types de modèles employés dans cette thèse.

L'un des premiers modèles en dynamique des populations a été proposé par Malthus en 1798 (Malthus 1798), connu sous le nom de modèle de croissance malthusienne. Ce modèle décrit une croissance exponentielle de la population basée sur le principe que les populations croissent à un taux proportionnel à leur taille.

Ces modèles décrivent la dynamique d'une seule population. En 1926, deux chercheurs, Lotka et Volterra (Lotka 1925; Volterra 1927), ont élargi cette approche en incorporant des interactions entre deux espèces différentes, spécifiquement dans un contexte prédateur-proie. Cela a conduit au développement du célèbre modèle de Lotka-Volterra, formulé comme un système d'équations différentielles pour capturer la dynamique entre les prédateurs et leurs proies.

Plus tard, en 1945, P.H. Leslie (Leslie 1945) a introduit un modèle utilisant des méthodes matricielles pour décrire la dynamique des populations structurées par âge. Cette approche a fourni une compréhension plus détaillée de la manière dont les différents groupes d'âge au sein d'une population

contribuent aux changements de population globaux. Ce modèle a ouvert la voie aux modèles de population structurés en général. Par exemple, les modèles structurés par stades étendent l'approche structurée par âge pour inclure d'autres caractéristiques telles que la taille ou le stade de développement. De plus, les équations de Lotka-Volterra ont également été étendues pour inclure la variation phénotypique parmi les individus. Je discuterai plus en détail de ce type de modèles dans la section des modèles évolutifs.

Un concept crucial dans les équations différentielles est la stabilité. Sous certaines hypothèses, les systèmes tendent à évoluer vers un point d'équilibre, lorsque la population ne connaît pas de croissance nette.

Cet équilibre peut être soit stable, ce qui signifie que la population converge de nouveau vers celui-ci après une petite perturbation, soit instable, auquel cas même une perturbation mineure peut entraîner des déviations significatives de l'équilibre initial. L'analyse de la stabilité permet de comprendre comment une population réagira à différentes perturbations environnementales ou biologiques.

Ce concept est fondamental dans la modélisation mathématique car il permet de prédire le comportement à long terme des systèmes et leurs résultats après des perturbations. Les modèles de systèmes dynamiques ont considérablement amélioré notre compréhension des trajectoires des populations et de l'impact de diverses hypothèses et paramètres Pielou 1981, permettant de meilleures prédictions écologiques pouvant informer la gestion et la conservation des écosystèmes (Fer et al. 2021; J. S. Clark et al. 2001; Bodner et al. 2021). De plus, ces outils théoriques ont été validés et ont gagné en crédibilité grâce à divers travaux expérimentaux (Mayer and Butler 1993; Tedeschi 2006).

Dans notre contexte, ces modèles ont également été appliqués pour étudier les effets des changements environnementaux sur la dynamique écologique. Par exemple, (Ives 1995) a montré que les interactions compétitives peuvent augmenter les effets néfastes des changements environnementaux sur la taille des populations des espèces. Un travail plus récent (Rinnan 2018) explore les impacts du changement climatique sur les écosystèmes grâce à la modélisation mathématique. Il se concentre sur la manière dont les changements climatiques modifient les interactions entre les espèces et les dynamiques de population, affectant la biodiversité et la stabilité des écosystèmes. L'étude souligne l'importance de comprendre ces dynamiques pour prédire et atténuer les conséquences écologiques du changement climatique.

Il existe plusieurs façons de modéliser les variations environnementales, y compris les changements progressifs et abrupts, généralement appelés perturbations de type "pression" et "impulsion".

## 5.2 Réponses écologiques aux changements globaux

### 5.2.1 Changements écologiques abruptes en réponse à des changements environnementaux progressifs

Les modèles de population ont été largement utilisés depuis leur introduction dans le domaine de l'écologie. Ils ont permis d'étudier les dynamiques des écosystèmes, y compris les transitions d'état, connues sous le nom de changements de régime, en réponse aux paramètres environnementaux. Ces changements de régime peuvent être progressifs et sont généralement décrits à l'aide d'équations déterministes simples, telles que l'équation logistique. Cependant, ces équations peuvent également inclure d'autres interactions, telles que des rétroactions positives décrites par des termes non linéaires, qui modifient les taux de croissance linéaires et à partir desquels émerge le concept de multiples équilibres Villa Martín et al. 2015. Un exemple notable de cela est lorsque deux équilibres stables existent, un phénomène connu sous le nom de bistabilité. Les rétroactions positives sont l'ingrédient clé de la multistabilité, et possiblement des transitions abruptes (ou critiques/catastrophiques).

La recherche menée par (Holling 1973a; May 1977a) a démontré que dans des conditions spécifiques, un écosystème peut passer abruptement d'un état stable à un autre état stable alternatif en réponse à des changements environnementaux progressifs (pression). Cette transition se produit lorsqu'un apport externe dépasse un certain seuil, provoquant le passage de l'écosystème à un état stable différent. Ce seuil critique, connu sous le nom de point de basculement, correspond mathématiquement à un point de bifurcation. Des études menées par (Erbach, Lutscher, and Seo 2013; Russo and Spiliotis 2016) ont montré que la plupart des points de basculement se manifestent sous forme de bifurcations en fourche, de bifurcations de Hopf sous-critiques ou de bifurcations en selle-noeud (pli). Inversement, lorsque le facteur de stress environnemental est réduit ou inversé, l'écosystème ne revient pas immédiatement à son état initial. Au lieu de cela, il reste dans l'état stable alternatif jusqu'à ce que le facteur de stress atteigne un autre point de basculement, généralement plus éloigné du premier. Ces connaissances sont cruciales pour comprendre les dynamiques des écosystèmes, car elles mettent en évidence la possibilité de transitions écologiques significatives et apparemment chaotiques résultant de petits changements progressifs des facteurs environnementaux. Ces découvertes soulignent également le caractère potentiellement irréversible de ces transitions (Marten Scheffer and Stephen R Carpenter 2003a; Suding and Hobbs 2009).

La réversibilité de ces transitions dépend largement de la distance entre les deux points de basculement

différents, une mesure connue sous le nom d'hystérésis (Holling 1973a), qui représente la différence entre les trajectoires de dégradation et de restauration. Ce concept permet de quantifier la résilience d'un écosystème (capacité de l'écosystème à absorber les changements et les perturbations sans passer à un état stable alternatif) et souligne l'importance de comprendre et de prédire les seuils critiques pour gérer et préserver la stabilité écologique.

Des exemples bien connus de changements de régime incluent l'eutrophisation des eaux douces, où les lacs passent d'un état d'eau claire à un état d'eau trouble, ce qui entraîne une diminution de la productivité de la pêche et la survenue de proliférations d'algues toxiques (Marten Scheffer, Hosper, et al. 1993; Stephen R Carpenter and Kinne 2003). Un autre exemple célèbre est la dégradation des terres arides, où les forêts sèches et les savanes se transforment en déserts et en sols nus, réduisant les services écosystémiques tels que la production agricole et le cycle de l'eau (Geist and Lambin 2004). De plus, un changement de régime spéculatif est la fonte de la calotte glaciaire du Groenland, où la fréquence et l'intensité des événements chauds peuvent faire passer la calotte glaciaire d'un état permanent à un état occasionnel (Greene et al. 2008). Les premiers développements de la compréhension des changements de régime ont été initialement critiqués pour leur manque de preuves empiriques ; cependant, au début des années 2000, des preuves suffisantes avaient été accumulées à partir de systèmes tels que les récifs coralliens et les lacs, confirmant l'existence de changements de régime (Marten Scheffer and Stephen R Carpenter 2003a; Marten Scheffer, S. Carpenter, et al. 2001a; Folke et al. 2004a).

Un exemple d'écosystèmes bistables étudiés dans la première partie de cette thèse est les lacs peu profonds, où l'eutrophisation peut déclencher une transition d'un état d'eau claire (illustré dans la Fig. 0.2.1), caractérisé par la dominance de la végétation submergée, à un état d'eau trouble, dominé par le phytoplancton (Marten Scheffer, Hosper, et al. 1993; Marten Scheffer, Szabo, et al. 2003a; Ibelings et al. 2007). Le changement de régime dans ce cas résulte de la rétroaction positive suivante : la présence de végétation stabilise l'état d'eau claire en réduisant la disponibilité des nutriments et en améliorant la stabilité des sédiments, tandis que l'absence de végétation favorise un état trouble par une augmentation du cycle des nutriments et de la remise en suspension des sédiments. Lorsque la concentration en nutriments dépasse un seuil, la croissance des microalgues explose, créant des proliférations d'algues. Celles-ci réduisent la pénétration de la lumière au fond du lac, ce qui diminue la capacité des plantes submergées à pousser et diminue ainsi la végétation. Cette rétroaction est illustrée dans la Fig. 0.2.1. Le principal facteur de l'eutrophisation est généralement l'accumulation de nutriments tels que l'azote et le phosphore (Stephen R Carpenter and Kinne 2003; Stephen R

Carpenter, Ludwig, and Brock 1999), bien que le changement climatique seul ait également été signalé comme une cause potentielle (Winder 2012).

### 5.2.2 Réponses écologiques aux changements environnementaux soudains

Les perturbations environnementales soudaines (impulsion) sont des perturbations à court terme et intenses qui peuvent avoir des impacts significatifs sur les écosystèmes. Par exemple, les ouragans sont un type de perturbation par impulsion qui peuvent altérer dramatiquement les écosystèmes côtiers. L'impact immédiat comprend la destruction physique des habitats, tels que les mangroves et les récifs coralliens, mais les conséquences peuvent entraîner des changements dans la composition des espèces et le cycle des nutriments à mesure que l'écosystème se rétablit (Patrick et al. 2020). Un autre exemple est l'incendie de forêt, qui agit comme une perturbation par impulsion dans les écosystèmes forestiers et de prairies. Les incendies de forêt peuvent rapidement changer le paysage en éliminant la végétation, en modifiant les propriétés du sol et en libérant de grandes quantités de carbone dans l'atmosphère. Les effets écologiques des incendies de forêt comprennent des changements dans la dominance des espèces, les espèces adaptées au feu prenant souvent l'avantage dans l'environnement post-perturbation (Brown and J. K. Smith 2000). De plus, les éruptions volcaniques représentent une autre forme de perturbation par impulsion, où le dépôt soudain de cendres et de lave peut dévaster la flore et la faune locales. Cependant, ces zones deviennent souvent des sites de succession écologique rapide, conduisant à l'établissement de nouvelles communautés écologiques au fil du temps (Dale et al. 2005).

Les changements environnementaux soudains peuvent également avoir un impact profond sur la phénologie, une autre notion importante étudiée dans ce travail, qui est l'étude des phénomènes naturels cycliques et saisonniers, en particulier en relation avec le climat et la vie végétale et animale. Ces changements peuvent modifier le calendrier des événements phénologiques clés, tels que la floraison, la fructification et la migration. Par exemple, une augmentation brusque de la température peut entraîner une floraison des plantes plus tôt que d'habitude, ce qui peut potentiellement entraîner des décalages avec la disponibilité des pollinisateurs. Cela peut entraîner une réduction du succès de la pollinisation et une diminution subséquente de la production reproductive des plantes, affectant finalement les populations de plantes et les espèces qui en dépendent (Dalpasso et al. 2023).

De même, des changements soudains dans les régimes de précipitations peuvent affecter le calendrier de la germination et de la croissance des graines chez les plantes, perturbant les relations écologiques établies. Par exemple, un changement vers des temps de germination plus précoces ou plus tardifs

peut entraîner des décalages de compétition entre les espèces végétales, modifiant la composition de la communauté et entraînant potentiellement des changements dans la distribution des espèces. Cela a été observé dans divers écosystèmes où les changements de précipitations ont un impact significatif sur les cycles de vie des plantes (Li et al. 2023).

Dans la deuxième partie de cette thèse, l'accent est mis sur l'étude des impacts des changements de température et de précipitations sur la phénologie des populations d'arbres. Étant donné leur longévité, souvent de plusieurs décennies à des siècles, les arbres peuvent percevoir des changements environnementaux qui semblent progressifs à l'échelle humaine comme abrupts. Par exemple, un changement rapide des régimes climatiques, tel qu'une augmentation des températures moyennes ou des changements dans les précipitations sur quelques décennies, peut être perçu par les arbres comme un changement abrupt. Cette soudaineté perçue peut induire un stress significatif sur les populations d'arbres, entraînant potentiellement des changements dans la composition des espèces et la structure de la forêt, certaines espèces d'arbres pouvant être incapables de s'adapter rapidement aux nouvelles conditions (Stanke et al. 2021).

## 5.3 Les Dynamiques Évolutives Peuvent-elles Sauver la Situation ?

### 5.3.1 Comprendre l'Évolution : Un Processus Biologique Fondamental

Face aux risques croissants auxquels sont confrontés de nombreux écosystèmes en raison des changements globaux, il devient évident que se limiter aux modèles écologiques et aux observations directes des dynamiques des écosystèmes pourrait s'avérer insuffisant. La vitesse et l'intensité de ces changements continuent d'accélérer, nécessitant une compréhension plus approfondie de leurs mécanismes sous-jacents et des stratégies d'atténuation efficaces. Cette urgence est exacerbée par le défi d'aligner les connaissances scientifiques avec des politiques d'action face aux intérêts diversifiés des parties prenantes.

L'évolution, telle que proposée par Charles Darwin, offre un outil puissant mais souvent négligé dans ce contexte. Darwin a défini l'évolution comme un processus graduel conduit par la sélection naturelle, où les espèces s'adaptent au fil du temps à travers des variations successives. Bien que traditionnellement considéré comme un processus lent, les avancées modernes révèlent que l'évolution peut se produire rapidement sous des pressions sélectives intenses, un phénomène observé dans diverses espèces, comme le papillon de nuit pendant la révolution industrielle et Spartina densiflora s'adaptant aux conditions induites par le changement climatique.

### 5.3.2 Adaptation aux Changements Environnementaux dans les Lacs et la Phénologie

Dans le domaine des écosystèmes aquatiques, les mécanismes d'adaptation tels que les changements génétiques, la plasticité phénotypique et les ajustements comportementaux jouent des rôles cruciaux. Par exemple, les plantes aquatiques dans les lacs développent diverses adaptations aux conditions fluctuantes telles que la profondeur de l'eau et la disponibilité des nutriments, facilitées par des mécanismes comme les banques de graines qui renforcent la diversité génétique et le potentiel d'adaptation rapide.

La phénologie—la synchronisation des événements biologiques tels que la floraison et la dormance—est un autre domaine critique où les dynamiques évolutives entrent en jeu. Les espèces montrent une plasticité en réponse aux changements climatiques, ajustant leurs calendriers de cycle de vie pour optimiser leur succès reproductif. Les espèces d'arbres dans diverses régions, du hêtre européen aux cerisiers japonais, présentent des réponses adaptatives aux changements de température, soulignant l'importance de la flexibilité évolutive dans le maintien de la stabilité des écosystèmes. Dans le domaine des écosystèmes aquatiques, les mécanismes d'adaptation tels que les changements génétiques, la plasticité phénotypique et les ajustements comportementaux jouent des rôles cruciaux. Par exemple, les plantes aquatiques dans les lacs développent diverses adaptations aux conditions fluctuantes telles que la profondeur de l'eau et la disponibilité des nutriments, facilitées par des mécanismes comme les banques de graines qui renforcent la diversité génétique et le potentiel d'adaptation rapide.

La phénologie—la synchronisation des événements biologiques tels que la floraison et la dormance—est un autre domaine critique où les dynamiques évolutives entrent en jeu. Les espèces montrent une plasticité en réponse aux changements climatiques, ajustant leurs calendriers de cycle de vie pour optimiser leur succès reproductif. Les espèces d'arbres dans diverses régions, du hêtre européen aux cerisiers japonais, présentent des réponses adaptatives aux changements de température, soulignant l'importance de la flexibilité évolutive dans le maintien de la stabilité des écosystèmes.

## 5.4 Théories et Modèles Actuels en Dynamiques Évolutives

### 5.4.1 Modèles de Génétique des Populations : Evo sans Eco

Depuis l'avènement de la théorie de l'évolution, les modèles mathématiques se sont multipliés dans le but de comprendre les mécanismes des processus évolutifs tels que la sélection naturelle, la dérive génétique, les mutations et le flux génique. Ces modèles visent également à prédire les résultats des

changements évolutifs au fil du temps et à tester des hypothèses de manière contrôlée et systématique. Voici un bref aperçu de certains modèles évolutifs fondamentaux.

Le voyage a commencé en 1931 avec le célèbre modèle Wright-Fisher (Wright 1931; Ronald Aylmer Fisher 1930), qui décrit la dérive génétique et les changements de fréquence allélique au sein d'une population finie. Ce modèle a été développé indépendamment par Sewall Wright et Ronald Fisher. L'année précédente, Fisher avait formulé le théorème fondamental de la sélection naturelle de Fisher (1930) (Ronald Aylmer Fisher 1930), qui stipule que le taux d'augmentation de la fitness de tout organisme à tout moment est égal à sa variance génétique de fitness à ce moment-là. En 1932, J.B.S. Haldane a introduit un modèle de sélection décrivant comment la sélection agit sur les allèles (Haldane 1932). En 1958, Patrick Moran a introduit un modèle de dérive génétique dans une population finie, qui, contrairement au modèle de Fisher, suppose des générations chevauchantes et une taille de population constante (Moran 1958).

Les modèles de génétique des populations sont utilisés pour prédire comment les changements génétiques surviennent au sein d'une population au fil du temps dans différentes situations. Ces modèles simplifient la dynamique en se concentrant sur un petit nombre d'allèles génétiques majeurs, tels que la couleur des yeux (Bürger 2020), au lieu de considérer tous les allèles à la fois. La génétique des populations classique étudie les changements de distribution génotypique sur de courtes périodes démographiques, mais ne prend pas en compte les dynamiques écologiques. Cependant, si la carte génotype-phénotype est connue, il est possible de lier la démographie aux dynamiques évolutives (Crow 2017).

En utilisant un modèle démographique stochastique, nous pouvons décrire comment les processus de naissance, de décès et de migration modifient les abondances de population, la variabilité phénotypique découlant de mutations génétiques aléatoires et de recombinaisons. Cette approche conduit aux modèles basés sur l'individu, où chaque individu est représenté par son génotype. Ces modèles sont à la pointe de la génétique des populations modernes, offrant un cadre détaillé et réaliste pour décrire la démographie et le changement évolutif.

En raison de la complexité de la génétique et de la nécessité de modèles mathématiques plus simples, les chercheurs ont développé des approches alternatives. Une telle méthode considère les phénotypes contrôlés par de nombreux gènes avec de faibles effets (Lang, Botstein, and Desai 2011). De plus, si les mutations sont rares à l'échelle démographique et que les observations sont effectuées sur une longue période évolutionnaire, l'utilisation de modèles démographiques asexués pour les populations sexuellement reproductrices peut être justifiée (Wissel and Stöcker 1991; Bürger 2000).

### 5.4.2 Dynamique Adaptative : Eco-Evo

Un article phare par (Champagnat, Ferrière, and Méléard 2006) utilisait un modèle stochastique individuel basé sur les naissances et les décès pour les populations se reproduisant asexuellement et tenait compte de divers phénomènes biologiques régissant la vie individuelle, tels que la sélection naturelle, les interactions non locales incluant la compétition pour les ressources, et les transmissions génétiques non fidèles impliquant des mutations. Les auteurs ont prouvé que, dans la limite des grandes populations, leur processus stochastique renormalisé converge vers une équation aux dérivées partielles déterministe (EDP) décrivant la dynamique de la distribution des traits.

De plus, dans la même étude, les auteurs (Champagnat, Ferrière, and Méléard 2006) ont obtenu une autre limite mathématique en prenant simultanément des limites de population grande et de mutation rare : un modèle de processus de saut. Ce modèle reflète l'heuristique selon laquelle l'occurrence des mutations est si rare qu'après l'apparition d'une mutation et lorsque le nombre de mutants atteint un certain seuil, les dynamiques écologiques du résident et du variant avec la mutation sont déterministes et atteignent un état stable avant qu'une autre mutation ne survienne. Ce processus de substitution des traits, modélisé par l'équation canonique, est un objet fondamental de la dynamique adaptative. Je détaillerai ce cadre tel qu'il a été utilisé dans le premier chapitre de ma thèse.

La dynamique adaptative, une approche développée par (Dieckmann and Law 1996a; Metz and S. A. H. Nisbet a. G. 1996; Geritz et al. 1997), trouve ses origines dans la théorie des jeux évolutionnistes où le concept de stratégie évolutivement stable a été introduit par (G. R. Price 1973; J. M. Smith 1974). Cette approche simplifie les détails génétiques en utilisant un argument de séparation des échelles de temps, justifiant l'utilisation de modèles démographiques asexués. En dynamique adaptative, la compétition entre les populations résidentes et mutantes est explicitement décrite par un modèle résident-mutant. Ce modèle, un système d'équations différentielles ordinaires (ODE), détaille les densités de population des populations résidentes et mutantes pour toute valeur de trait donnée, incorporant des effets dépendants de la fréquence et de la densité.

La notion de paysage adaptatif est au cœur de ce cadre. Les dynamiques évolutives à long terme d'un trait continu $x$ peuvent être visualisées comme une ascension sur un paysage de fitness $s(x)$, où les pics sur le paysage représentent des combinaisons de traits optimales avec une grande fitness, tandis que les vallées représentent une faible fitness (Wright 1931; Dieckmann and Law 1996a).

Les dynamiques évolutives décrites par cette équation suggèrent une augmentation continue de la fitness, atteignant potentiellement un maximum local sur le paysage de fitness.

Dans le cadre de la dynamique adaptative, les mutations se produisent de manière aléatoire, et les changements évolutifs sont représentés comme une séquence de substitutions de traits, représentées comme des marches aléatoires dans l'espace des traits. Le gradient de sélection est crucial, et Dieckmann and Law 1996a a appelé leur équation différentielle ordinaire (ODE) l'équation canonique de la dynamique adaptative. Cette équation décrit la trajectoire évolutive d'un trait continu sous l'influence de la mutation et de la sélection.

Un équilibre évolutif (ou point singulier) est défini comme une solution constante de l'équation canonique, c'est-à-dire un trait $\bar{x}$ auquel le gradient de sélection s'annule.

Nous notons que les équations canoniques de la dynamique adaptative peuvent conduire à un point de bifurcation, qui est un point critique dans l'espace des traits où une seule lignée évolutive peut se diviser en deux lignées distinctes. Ce phénomène se produit lorsque la sélection disruptive favorise la divergence des traits. À ce point de bifurcation, de nouveaux variants peuvent envahir et coexister avec les traits précédemment établis. Cela se produit lorsqu'un point singulier est convergent stable mais pas ESS.

Lors de l'étude de la dynamique évolutionnaire des stratégies unidimensionnelles dans le cadre de la dynamique adaptative, un graphique d'invasibilité par paires (Matsuda 1985; Van Tienderen and De Jong 1986) est un outil graphique précieux. Ces graphiques illustrent la fitness d'invasion basée sur les stratégies résidentes et mutantes. Les régions gris foncé dans les graphiques indiquent généralement les combinaisons de stratégies résidentes et mutantes où les mutants peuvent réussir à envahir (fitness d'invasion positive). En revanche, les régions gris clair indiquent des combinaisons où la fitness d'invasion est négative, suggérant des mutants délétères. Un résultat évolutif possible est le suicide évolutif, où l'évolution peut (avec de petites mutations) amener la stratégie de la population suffisamment proche de la limite d'extinction, qu'un mutant avec une stratégie en dehors de la région de faisabilité peut envahir, déplaçant la dynamique hors de l'attracteur résident, entraînant l'extinction de l'ensemble de la population, résidente et mutante (Parvinen 2005).

Dans l'ensemble, la Dynamique Adaptative fournit un cadre pour étudier les pressions sélectives à long terme qui déterminent le succès des mutations dans des contextes écologiques. Elle intègre les interactions écologiques et la dynamique des populations, visant à prédire les résultats évolutifs et à comprendre l'émergence de traits complexes. Cependant, elle présente des limitations importantes, nous en citerons seulement quelques-unes. Premièrement, la séparation des échelles de temps de la Dynamique Adaptative, en supposant que les dynamiques évolutives sont beaucoup plus lentes que les dynamiques de population, peut être irrelevante dans de nombreux cas, surtout depuis que les

preuves d'une évolution rapide s'accumulent (John N Thompson 1998; Hendry et al. 2000). De plus, la Dynamique Adaptative ne considère que les populations asexuées alors que la majorité des espèces se reproduisent sexuellement. La variation génétique n'est pas non plus prise en compte, et il n'y a pas de justification claire pour limiter l'utilisation des modèles de gradient de fitness aux scénarios où l'évolution se produit par le remplacement de mutations rares à effet mineur (Abrams 1992).

### 5.4.3 Génétique Quantitative

Face aux limitations du cadre de la dynamique adaptative, y compris ses hypothèses simplifiées, son détail génétique limité et son inapplicabilité aux populations sexuées, cette thèse adopte également une approche comparative : la génétique quantitative. La génétique quantitative modélise les effets de l'hérédité, de la sélection naturelle et des facteurs évolutifs sur la distribution phénotypique des populations. Ces phénotypes sont presque continûment distribués et peuvent être mesurés sur une échelle métrique. En supposant que toute la variabilité génétique possible est toujours présente dans la population, les mutations peuvent être négligées, permettant à l'évolution de la distribution des traits d'être gouvernée uniquement par l'hérédité et la sélection naturelle (Lande 1976).

Dans une partie de ce travail, le cadre de la génétique quantitative est utilisé pour considérer la reproduction sexuelle dans l'étude des populations d'arbres. La prise en compte de la reproduction sexuelle est pertinente pour plusieurs raisons. Tout d'abord, elle est plus réaliste et applicable à un large éventail d'espèces. En effet, de nombreuses espèces, y compris la plupart des plantes, des animaux et de nombreux microorganismes, se reproduisent sexuellement. De plus, elle maintient plus de variation génétique grâce au brassage génétique selon les lois de Mendel. L'hypothèse de base dans l'héritabilité des traits quantitatifs est que, au sein de chaque famille, les valeurs de reproduction des descendants suivent une distribution normale avec une variance constante, et une moyenne qui équivaut à la moyenne des valeurs de reproduction de leurs deux parents (Michael George Bulmer 1981), comme illustré dans la Fig. **??**. Ce modèle est connu sous le nom de modèle infinitésimal, reflétant sa dérivation des effets cumulatifs d'un nombre infini de gènes non liés contribuant au trait (Michael George Bulmer 1981; Barton, Etheridge, and Véber 2017; Turelli and Barton 1994). Le modèle infinitésimal est un pilier fondamental à la fois de la génétique des populations et de la génétique quantitative et a été utilisé pour de nombreuses applications (Verrier, Colleau, and Foulley 1991; Martinez, Bünger, and Hill 2000).

L'analyse mathématique des équations différentielles avec des opérateurs de reproduction sexuelle est un développement relativement récent dans le domaine, présentant plusieurs défis en raison de la

complexité ajoutée. Le travail séminaristique de Fisher a démontré que les effets additifs de multiples gènes, suivant chacun l'hérédité mendélienne, pourraient expliquer la variation continue des traits.

Parmi ses nombreuses contributions antérieures, le travail séminaristique de Fisher a démontré que les effets additifs de multiples gènes, suivant chacun l'hérédité mendélienne, pourraient expliquer la variation continue des traits. En appliquant le théorème central limite, Fisher a montré que la distribution des traits polygéniques serait approximativement normale (gaussienne) autour de la moyenne des traits parentaux. Un demi-siècle plus tard, Alan Bulmer en 1971 (Michael G. Bulmer 1971) a fourni un traitement mathématique détaillé et rigoureux du sujet. Le travail de Bulmer a significativement fait progresser la théorie mathématique et la compréhension de la génétique quantitative.

Sous le modèle infinitésimal, l'hypothèse d'équilibre de liaison est souvent faite pour simplifier l'architecture génétique du trait. L'équilibre de liaison signifie que les allèles à différents loci sont hérités indépendamment les uns des autres. Lorsque cette hypothèse est vérifiée (ce qui est courant en génétique quantitative), le modèle suppose une distribution gaussienne du trait. Ce cadre a été appliqué pour utiliser des quantités macroscopiques afin de décrire la dynamique des populations (Sepideh Mirrahimi and Raoul 2011; Sepideh Mirrahimi and Raoul 2013). Par exemple, dans Raoul 2021, l'auteur a proposé une méthode pour étudier l'adaptation des populations à reproduction sexuelle bien mélangées au fil du temps. Le principal résultat de cette étude est l'existence et l'unicité locale d'un état stable, qui est proche des distributions gaussiennes sous des hypothèses de faible sélection, où l'équation intégrale-différentielle peut asymptotiquement être décrite par la dynamique de la moyenne du trait et de la taille de la population.

Ces différents cadres mathématiques dans la modélisation évolutionnaire offrent diverses approches pour étudier les dynamiques évolutives et comprendre l'adaptation des espèces sous différentes hypothèses, en particulier dans le contexte du changement global. En exploitant ces cadres mathématiques diversifiés, nous pouvons mieux prévoir les réponses adaptatives des espèces au changement climatique, identifier les risques potentiels et développer des stratégies de conservation efficaces.

## 5.5 Chapitres et Questions

### 5.5.1 Chapitre 1 : Résultats évolutifs découlant de la bistabilité dans la dynamique des écosystèmes

Dans ce chapitre, j'explore les dynamiques éco-évolutives des macrophytes immergés et flottants dans les écosystèmes de lacs peu profonds bistables, en utilisant un modèle mécaniste de compétition pour les nutriments et la lumière, posant des questions scientifiques clés :

- Comment l'évolution rapide des traits impacte-t-elle la dynamique et la stabilité de ces écosystèmes ?
- Les rétroactions éco-évolutives peuvent-elles retarder ou avancer les points de basculement écologiques, potentiellement conduisant le système vers ou hors d'une zone de bistabilité ?
- Quel rôle joue la co-évolution dans ces dynamiques ?

Pour répondre à ces questions, je considère un modèle d'équations différentielles ordinaires de compétition entre macrophytes flottants et immergés pour les nutriments et la lumière, en extension d'un modèle utilisé dans (Marten Scheffer, Szabo, et al. 2003a). Ces deux espèces sont caractérisées par un trait phénotypique, représentant leur profondeur de croissance dans le lac, qui sous-tend leurs capacités d'accès aux ressources. Le modèle présente une rétroaction positive entre les deux espèces : les macrophytes flottants ont un avantage pour la lumière en raison de leur position en surface, d'où ils exercent un effet d'ombrage sur les macrophytes immergés et empêchent la pénétration de la lumière. En retour, les macrophytes immergés ont un meilleur accès aux nutriments, étant enracinés au fond, ce qui diminue la quantité de nutriments diffusés à la surface pour les macrophytes flottants. Ensuite, j'utilise les approches de la Dynamique Adaptative et de la Génétique Quantitative pour étudier les résultats évolutifs du trait phénotypique étudié. Cela fournit une approche comparative pour étudier d'une part une population résidente-mutante et d'autre part une distribution continue des traits à travers la colonne d'eau.

Les résultats montrent que l'évolution de la profondeur de croissance des macrophytes immergés peut avoir un impact sur la dynamique écologique et la stabilité du système en favorisant la diversification et en permettant la coexistence avec les macrophytes flottants compétitifs. De plus, cette évolution conduit également à des dynamiques complexes, incluant des oscillations évolutives et un "suicide évolutif", où le trait évolué conduit à l'extinction de l'espèce. Lorsque les macrophytes immergés évoluent vers des niveaux plus élevés en traversant des régions de bistabilité, ils subissent des oscillations de plus en plus grandes à mesure que la diffusion des nutriments augmente, conduisant

ultimement à l'extinction de la population. La co-évolution des macrophytes immergés et flottants produit un effet stabilisateur en prévenant les oscillations, en retardant le suicide évolutif et en favorisant ainsi une stabilité temporaire dans l'écosystème. Malgré cela, la co-évolution ne modifie pas de manière significative les résultats évolutifs globaux : l'effondrement de l'écosystème survient toujours sous des taux élevés de diffusion des nutriments.

### 5.5.2 Chapitre 2 : Dérivation d'un modèle macroscopique dans une population d'arbres

Dans ce chapitre, je définis un modèle mécaniste pour décrire la dynamique de la dormance et de la production de semences quotidiennes dans les populations d'arbres, en incluant différentes caractéristiques que nous estimons importantes. Le modèle prend en compte la reproduction sexuée, en distinguant entre les semences et les individus matures. Les populations sont caractérisées par deux traits phénotypiques (valeurs d'élevage déterminées par les génotypes des individus uniquement) : l'un est défini comme le nombre quotidien de semences produites, noté $x \in \mathbb{R}$, et l'autre comme la température seuil de dormance au-dessus de laquelle les individus deviennent dormants, arrêtant de mourir et de se reproduire, notée $y \in \mathbb{R}$. Ce dernier trait représente la valeur d'élevage (trait latent) qui détermine le trait plastique du timing annuel ; c'est-à-dire le moment où les individus passent à un état de dormance. Les traits représentant le nombre de semences produites $x$ et le seuil de température de dormance $y$ sont influencés par des facteurs environnementaux, y compris les variations de température annuelle et la disponibilité en eau. Pour un arbre individuel avec les traits $(x, y)$, je suppose qu'il devient dormant et cesse de mourir et de se reproduire lorsque la température atteint $y$. En dessous de ce seuil, la mortalité est conditionnée par le manque d'eau, c'est-à-dire que les individus ne meurent pas tant que toute l'eau n'est pas consommée. De même, la reproduction se produit uniquement lorsqu'il y a suffisamment d'approvisionnement en eau pour produire $x$ semences. Les traits moyens de la population sont notés $X(t)$ et $Y(t)$. La dynamique du modèle est illustrée dans la figure **??**. Dans cette partie, je m'intéresse à la question suivante :

- Comment dérivons-nous un modèle macroscopique décrivant la dynamique des traits moyens de la population $X(t)$ et $Y(t)$ ?

Le processus de simplification implique la dérivation d'un modèle intégral-différentiel annuel à partir d'un modèle d'année en année, sous l'hypothèse d'un faible taux de mortalité des individus matures ($\varepsilon \ll 1$). Sous des hypothèses de sélection faible, ce modèle réduit de distribution de traits est proche d'une distribution gaussienne centrée autour des traits moyens de la population. Cela offre une

approche pour décrire la dynamique globale de la population à travers la dynamique des traits moyens. J'ai ensuite dérivé un modèle macroscopique pour ces quantités, résultant en un système d'ODE simple. En se concentrant sur la production moyenne de semences et la température moyenne de dormance, le modèle macroscopique capture les dynamiques essentielles du système.
Le chapitre détaille comment le modèle mécaniste complexe se transforme en un modèle plus abordable. Cette approche aidera à révéler les stratégies adaptatives que les arbres peuvent utiliser pour équilibrer la production de semences et le timing de la dormance en réponse aux changements environnementaux abrupts.

### 5.5.3 Chapitre 3 : Modèle de population d'arbres : Évolution de la production de semences et de la dormance face aux changements climatiques

Ce chapitre présente une enquête détaillée sur les dynamiques évolutives des populations d'arbres, en mettant l'accent sur la production de semences et la dormance sous l'influence du changement climatique, en utilisant le modèle macroscopique dérivé dans le chapitre précédent et des simulations numériques.
Les principales questions abordées sont :

- Comment les changements environnementaux, en particulier les changements de température et de précipitations, impactent-ils les stratégies évolutives de production de semences et de dormance chez les arbres ?
- Quelles sont les réponses adaptatives de ces traits sous différents scénarios climatiques, et comment la plasticité phénotypique façonne-t-elle ces réponses ?

L'étude révèle que la plasticité phénotypique peut empêcher l'adaptation des traits aux changements de température par dormance et en raison de l'absence de mortalité intrinsèque. Cependant, les changements abrupts dans les précipitations influencent significativement à la fois la production de graines et la dormance, la magnitude de ces changements déterminant l'étendue de la réponse adaptative.
Les résultats montrent également que tandis que la dormance peut s'adapter à des changements importants dans les précipitations, la production de graines ne peut s'adapter qu'à une certaine amplitude de changement, au-delà de laquelle elles évoluent vers un nichoir biologique différent. Cependant, en explorant la coévolution de la production de graines et de la dormance, j'ai découvert que sous ce scénario, les deux traits pourraient évoluer vers la nouvelle stratégie optimale même

lorsque le changement de précipitations est élevé. Cette coévolution conduit à deux stratégies extrêmes stables selon les taux évolutifs des traits : une stratégie favorisant moins de graines sur une période plus longue et une autre favorisant une production rapide de graines suivie d'une dormance précoce. L'interaction entre les changements de température et de précipitations façonne finalement les résultats évolutifs, mettant en évidence les réponses adaptatives complexes nécessaires aux populations d'arbres pour faire face aux changements climatiques complexes. Les conclusions montrent que si la dormance permet la survie des espèces lors d'événements climatiques extrêmes, elle peut également entraver une adaptation rapide à de nouveaux environnements.

## 5.6 Discussion

### 5.6.1 Principaux Résultats

#### 6.1.1 L'Évolution est à Double Tranchant

Nous avons abordé dans l'introduction la question de savoir si l'évolution pourrait sauver la situation face à la menace du changement global. Tout au long de ce manuscrit, nous avons constaté que bien que l'évolution puisse permettre l'adaptation et la survie de certaines populations dans des écosystèmes soumis à des contraintes environnementales, ce n'est pas toujours le cas. En effet, dans **le chapitre 1**, nous avons observé la situation paradoxale du suicide évolutif. Celui-ci survient lorsque l'adaptation qui augmente la fitness individuelle à court terme conduit ultimement à des conséquences négatives réduisant la viabilité globale de la population à long terme (Ferriere 2000; Dieckmann, Marrow, and Law 1995). L'extinction des macrophytes submergés a eu lieu dans une région de bistabilité sous des conditions défavorables, après que les oscillations soient devenues très élevées jusqu'à ce que la population cycle entre des densités élevées et basses. Lorsque la taille à faible densité est devenue proche de zéro, les individus ont cessé de croître à nouveau, entraînant l'extinction de la population.

En réalité, de tels phénomènes peuvent survenir par la stochasticité démographique, où les populations confrontées à des déclins et atteignant de faibles densités sont plus à risque d'extinction (Gomulkiewicz, Holt, and Barfield 1999). Un autre scénario potentiel est la dérive génétique, qui a un impact plus important dans les petites populations car des événements aléatoires peuvent entraîner des changements plus importants dans les fréquences alléliques (Willi et al. 2007). De plus, dans les petites populations, la dérive génétique peut l'emporter sur la sélection naturelle, conduisant à la fixation d'allèles neutres

voire délétères (Gabriel and Bürger 1994; Cowperthwaite, Bull, and Meyers 2006). Même la sélection naturelle peut contribuer à de tels résultats fatals. Comme la sélection naturelle opère sur les individus, le changement environnemental ainsi que les interactions avec d'autres espèces peuvent s'avérer trop nuisibles pour que la population survive. Darwin (1859, 1871) avait déjà observé que la sélection naturelle pourrait favoriser des traits qui peuvent finalement se révéler nuisibles pour les individus (Parvinen 2005). Il y a seulement quelques exemples de suicide évolutif, mais comme Webb 2003a l'a souligné, il est difficile à étudier dans la nature simplement parce qu'il est difficile d'observer quoi que ce soit sur les populations éteintes.

La théorie derrière le suicide évolutif suggère qu'une bifurcation dans la dynamique des populations est une condition nécessaire, et elle doit être discontinue (Gyllenberg, Parvinen, and Dieckmann 2002). De plus, Webb 2003a a proposé une classification des différentes bifurcations pour le suicide évolutif. Dans notre étude, le suicide évolutif est également survenu lorsque des changements critiques étaient possibles et que l'extinction des macrophytes submergés constituait un état stable alternatif. Bien que de tels résultats surviennent après la diversification de la population avec une large gamme de traits coexistants, alors que la bistabilité est apparue lorsque la population submergée était monomorphe. Cependant, les vastes oscillations entre haute et basse densité précédant l'extinction suggèrent la présence potentielle d'un mécanisme de rétroaction positive menant à des changements abrupts.

Malgré la grande variété d'espèces présentes aujourd'hui, nous savons qu'un nombre encore plus grand d'espèces ont disparu. Le suicide évolutif pourrait être une explication possible pour cela. Un mécanisme potentiel conduisant au suicide évolutif est la théorie neutre de l'évolution, proposée par Kimura à la fin des années 60 (Kimura 1979), qui affirme que la majorité des changements évolutifs au niveau moléculaire sont causés par la dérive génétique de mutations neutres. Selon cette théorie, la variation génétique est principalement due à la fixation aléatoire de mutations neutres plutôt qu'au résultat d'une sélection en cours. Cela pourrait expliquer les niveaux élevés de variation génétique observés au sein des populations d'une part. D'autre part, la fixation aléatoire de mutations neutres peut altérer l'arrière-plan génétique d'une population, ce qui contribue à des combinaisons génétiques mal adaptatives. De plus, l'accumulation de mutations neutres peut permettre aux populations de dériver à travers des régions plates du paysage fitness (des zones du paysage fitness où les valeurs de fitness des différents phénotypes ou génotypes sont très similaires ou presque égales), les conduisant potentiellement dans des pièges évolutifs où les changements adaptatifs sont nocifs à long terme. En considérant les interactions entre les processus neutres et les forces sélectives, nous pouvons peut-être mieux comprendre les dynamiques qui conduisent au suicide évolutif.

Dans **le chapitre 3**, j'ai exploré les dynamiques évolutives et les capacités adaptatives de deux traits phénotypiques au sein d'une population d'arbres confrontée à des changements environnementaux, notamment en termes de température et de précipitations. Les résultats ont montré que sans mortalité intrinsèque agissant sur la population, et avec la dormance empêchant la reproduction, les traits phénotypiques n'ont pas réussi à s'adapter au nouvel environnement dans une large gamme de scénarios. Bien que la dormance permette aux individus de survivre à des conditions adverses telles que des températures extrêmes et la sécheresse (Finch-Savage and Leubner-Metzger 2006; Aragón-Gastélum et al. 2018; Jurado and J. Flores 2005), elle peut également entraver ou ralentir l'adaptation à un environnement changeant (Vidigal et al. 2016). Plus précisément, si une proportion significative d'une population est en dormance, les mutations bénéfiques et les traits adaptatifs peuvent se propager plus lentement voire pas du tout à travers la population. De plus, des périodes de dormance très longues signifient moins de générations au fil du temps, ce qui peut réduire la vitesse d'adaptation au stress environnemental. Il est important de noter que le trait que nous avons considéré était lié au moment de la dormance, qui est sujet à la plasticité phénotypique. Cependant, dans notre étude, nous n'avons pas supposé une plasticité adaptative. Je discuterai de cela plus en détail plus tard.

De plus, j'ai trouvé qu'un des traits n'a pas réussi à s'adapter à des changements d'amplitude élevée. En effet, lorsque le changement environnemental se produit trop rapidement et de manière extrême, il peut ne pas y avoir assez de temps pour que les mutations bénéfiques se propagent et que les traits suivent la nouvelle stratégie optimale. Cela peut conduire à un décalage entre les traits de la population et le nouvel environnement (Shibata et al. 2020). Dans notre étude, cela a conduit à un changement potentiel de niche écologique où la production de graines des individus d'arbres a explosé. Cela peut s'expliquer par le phénomène de spéciation, où le changement environnemental peut pousser la population à se diviser en deux groupes distincts spécialisés dans des niches différentes. Une étude a révélé que la dormance physiologique est associée à des taux plus élevés de diversification des lignées, principalement grâce à des taux de spéciation accrus (Willis et al. 2014). Dans notre cas étudié, les individus qui n'ont pas réussi à s'adapter rapidement ont pu adopter une stratégie différente de production élevée de graines pour assurer la survie de leur progéniture, conduisant à une divergence génétique. À mesure que ces traits deviennent plus présents, cela peut conduire à l'émergence d'une nouvelle espèce.

### 6.1.2 Impact de la Co-Évolution sur la Stabilité et l'Adaptation des Espèces

Une notion cruciale étudiée dans cette thèse est la co-évolution. La co-évolution fait référence à l'influence évolutive réciproque de deux espèces ou traits, voire plus. Les résultats obtenus dans ce travail illustrent comment la co-évolution peut façonner et stimuler les processus adaptatifs.

Dans **le chapitre 1**, j'ai examiné la co-évolution des macrophytes flottants et submergés. Bien que cette co-évolution n'ait pas affecté qualitativement les résultats évolutifs globaux, elle a exercé un effet stabilisateur sur la dynamique en prévenant les oscillations. La co-évolution, menant à des adaptations réciproques, peut influencer la dynamique et équilibrer les interactions entre espèces, prévenant ainsi les fluctuations. En dépit de la relation antagoniste entre les plantes flottantes et submergées, leur co-évolution a retardé le suicide évolutif des macrophytes submergés. En stabilisant la dynamique, la co-évolution a permis aux plantes submergées de survivre un peu plus longtemps, même dans un environnement hostile de diffusion excessive de nutriments. En général, la co-évolution peut contribuer à la stabilité des écosystèmes en équilibrant les interactions compétitives et en favorisant les comportements coopératifs. Cela peut aboutir à des communautés plus résilientes, mieux équipées pour faire face aux changements environnementaux. Par exemple, la co-évolution des espèces compétitives dans les écosystèmes d'eau douce peut conduire à des communautés diversifiées et stables avec des interactions trophiques complexes. La co-évolution peut également augmenter la variance génétique, comme nous l'avons observé dans certains scénarios où les macrophytes flottants se sont diversifiés, ce qui a aidé à maintenir les deux espèces avec un pool phénotypique riche et des tailles de population élevées.

Selon de nombreuses études, il semble que les co-extinctions soient des phénomènes assez rares (Bronstein, Dieckmann, and Ferrière 2004). Mais certes, une absence de preuve n'est pas une preuve d'absence. Cependant, si c'est effectivement le cas, cela peut s'expliquer par le fait que les espèces en co-évolution sont peut-être plus résilientes aux changements environnementaux. Un exemple évident en est le mutualisme, mais cela peut s'étendre à d'autres types d'interactions.

Dans **le chapitre 3**, j'ai étudié le cas de la co-évolution de deux traits différents au sein d'une population d'arbres, où nous avons également observé le rôle important de la co-évolution. L'observation principale dans ce domaine est que la co-évolution a permis l'adaptation aux changements environnementaux d'un trait qui aurait échoué à s'adapter s'il avait évolué seul. Dans certains cas, l'évolution simultanée de la dormance et de la production de graines a empêché le changement de niche écologique observé lorsque le nombre de graines a évolué seul, renforçant ainsi l'évolution rapide vers la stratégie

optimale sous le nouvel environnement. Cela montre que la co-évolution peut atténuer les effets négatifs de certaines adaptations.

Lorsque les populations font face simultanément à de multiples stress environnementaux, les interactions co-évolutives peuvent entraîner des voies évolutives divergentes à travers différents environnements. Ce processus peut améliorer la capacité des espèces à s'adapter à de multiples stress en favorisant la diversité génétique et les adaptations locales, permettant ainsi aux espèces de mieux faire face aux défis environnementaux variables (Laine 2009). La co-évolution peut favoriser la diversité génétique (John N Thompson et al. 2013; Laine 2009), facilitant ainsi une adaptation rapide qui aide les populations à suivre le rythme des conditions changeantes. Une étude a révélé les caractéristiques génétiques qui pourraient contribuer à la longue durée de vie du chêne, éclairant ainsi la manière dont la co-évolution a façonné ces traits au fil du temps (Mesny, Hacquard, and Thomma 2023).

Ces résultats et études illustrent l'impact important de la co-évolution sur les processus écologiques et évolutifs, soulignant son importance dans la compréhension et la modélisation des systèmes biologiques.

### 6.1.3 Comprendre les Modèles Éco-Évolutifs Mécanistes

Dans ce travail, j'ai utilisé des modèles mécanistes de complexité variable pour décrire les dynamiques éco-évolutives des écosystèmes sous stress environnemental. Dans **le chapitre 1**, j'ai étendu les modèles utilisés dans (Marten Scheffer, Szabo, et al. 2003a; Aragón-Gastélum et al. 2018) pour proposer un modèle plus réaliste et complet de la dynamique des macrophytes dans les lacs peu profonds, intégrant des éléments tels que la compétition, les compromis, la structure phénotypique et son évolution. L'objectif était d'étudier et de comprendre les résultats évolutifs des espèces au sein d'un écosystème présentant une bistabilité due à des mécanismes de rétroaction positive. Pour ce faire, j'ai utilisé des approches de Dynamique Adaptative et de Génétique Quantitative, conduisant à une gamme diversifiée de résultats évolutifs, y compris la diversification, les oscillations et l'extinction.

Ces modèles, bien qu'ils ne captent pas toutes les interactions entre espèces dans les lacs peu profonds, fournissent des perspectives importantes sur les comportements évolutifs potentiels des macrophytes flottants et submergés. La Dynamique Adaptative (AD) a été utilisée pour modéliser des populations monomorphes évoluant avec des hypothèses de mutations petites et rares, tandis que la Génétique Quantitative (QG) a considéré des distributions de traits avec une variance génétique initiale élevée, se concentrant uniquement sur le rôle de la sélection. Ces approches ont permis une compréhension approfondie de la façon dont les macrophytes pourraient évoluer dans différents scénarios, mettant en évidence la complexité et la variabilité des processus évolutifs dans les écosystèmes bistables.

Dans **le chapitre 2**, j'ai à nouveau utilisé l'approche de la Génétique Quantitative (QG) pour modéliser les dynamiques annuelles d'une population d'arbres caractérisée par deux traits phénotypiques. Ce modèle a intégré des éléments tels que la reproduction sexuée, la sélection, les mutations, les variations environnementales et la mortalité. Bien que cela soit analytiquement complexe, nous avons simplifié le modèle en utilisant une approche basée sur des résultats antérieurs, en nous concentrant sur des quantités macroscopiques capturant les dynamiques essentielles de la population. Cela a démontré que même des modèles complexes intégrant des dynamiques multifacettes peuvent être étudiés et décrits en utilisant des cadres théoriques bien établis.

Sur cette base, le modèle macroscopique simplifié obtenu a permis d'explorer les dynamiques évolutives et l'adaptation des traits moyens de la population face au changement climatique dans **le chapitre 3**. Cela a permis une compréhension plus approfondie des réponses évolutives potentielles des populations d'arbres aux changements environnementaux, mettant en lumière la relation complexe entre les traits phénotypiques et la capacité d'adaptation face aux climats changeants.

Cela a montré que l'ajout de plusieurs couches de complexité aux modèles mathématiques - comme la reproduction sexuée, les traits multiples, l'accouplement assortatif et divers facteurs environnementaux - peut les rendre inaccessibles et difficiles à étudier, mais il ne faut pas craindre les modèles complexes et les équations apparemment intimidantes. De tels modèles cachent souvent une faisabilité cachée grâce à des hypothèses de simplification potentielles ou à des résultats antérieurs qui permettent leur étude. Alors que de nombreux biologistes critiquent les simplifications excessives des modèles comme étant irréalistes, de nombreux modèles simplifiés ont été prouvés être justifiés et fiables. Parallèlement, les efforts continus pour incorporer des complexités supplémentaires à plusieurs échelles montrent des promesses et fournissent des insights plus profonds dans les phénomènes biologiques.

## 5.7 Conclusion

Cette thèse s'appuie sur des cadres théoriques et mathématiques antérieurs pour étudier les dynamiques éco-évolutives complexes des écosystèmes confrontés aux changements globaux, tels que les changements de régime et les perturbations environnementales. Elle met en avant les rôles de la co-évolution, de la plasticité phénotypique et des pressions environnementales dans la formation des résultats évolutifs. La recherche souligne l'interaction critique entre ces facteurs et offre des perspectives précieuses sur les capacités adaptatives des espèces et des écosystèmes. Dans l'ensemble, cette thèse comble le fossé entre la modélisation mathématique et l'écologie et l'évolution. Elle démontre l'utilité

et l'importance des modèles mathématiques pour décrire les dynamiques éco-évolutives spécifiques des différentes espèces. En intégrant des modèles mécanistiques détaillés avec des approches évolutives, la recherche permet de mieux comprendre les réponses des espèces aux stress environnementaux et leurs capacités adaptatives dans divers scénarios. Les résultats peuvent avoir des implications pratiques pour les stratégies de conservation des écosystèmes, en soulignant la nécessité de considérer plusieurs traits et espèces interagissant pour renforcer les réponses adaptatives dans des environnements changeants.